ISOLATION AND CHARACTERISATION OF SUPPRESSORS OF CONDITIONAL HISTONE MUTANTS

LEE SHU YI, LINDA

(B. Sci. (Hons.), NUS)

A THESIS SUBMITTED

FOR THE DEGREE OF

MASTER OF SCIENCE (RSH-SOM)

DEPARTMENT OF MICROBIOLOGY

NATIONAL UNIVERSITY OF SINGAPORE

2012

Acknowledgements

I would like to express my deep gratitude to the following people who have made this dissertation possible and because of whom my graduate experience will be cherished.

I have been fortunate to have Dr Norbert Lehming as my advisor, as he gave me freedom to explore various areas on my own and always provided timely guidance whenever I faltered. In addition, this project would not have been as smooth sailing as it had been without the help and friendship of Zhao Jin, Wee Leng, Keven, Gary, Edwin, Daniel, Mei Hui, Jia Hui and Agnes.

Most importantly, none of this would have been possible without the love and patience of my two buddies, my family and Kian Sim. They have been a constant source of love, concern, support and strength that encouraged me throughout this endeavour.

Thank you once again to all.

Table of contents

1. Introduction

2. Literature review

3. Materials and methods

4. Results

Chapter I Genomic library screening of histone H4 mutant strains Y51A, E53A and Y98A

Chapter II Characterisation of histone H4 tyrosine residues

Chapter III Directed screening of histone H4 mutant strain Y98A

5. Discussion

6. Conclusion and future studies

8. Appendices

List of abbreviations and symbols

Symbol	
Δ	Delta, knock out or deleted for
°C	degree Celsius
µl	Microlitre
µM	Micromoles per litre
Number	
3-AT	3-amino-1,2,4-triazole
5-FOA	5-fluoro-orotic acid
5-FU	5-fluorouracil
6AU-NAM (phenotype)	Sensitivity to 6-azauracil and nicotinamide
A	
A (Amino acid)	Alanine
A. thaliana	*Arabidopsis thaliana*
aa	Amino acid
AA	Antimycin A
AA (phenotype)	Sensitivity to antimycin A
ACT1	Actin
Ahc1	ADA HAT complex component 1
Amp	Ampicillin
Amp^R	Ampicillin resistant
APS	Ammonium persulphate
AT (phenotype)	Sensitivity to 3-amino-1,2,4-triazole
ATC1	Aip three complex
B	
BLAST	Basic local alignment search tool
bp	Base pair
BSA	Bovine serum albumin
C	
CCT6	Chaperonin-containing TCP-1
cDNA	Complementary DNA
ChIP	Chromatin immunoprecipitation
Chl	Chloramphenicol
Chl^R	Chloramphenicol resistant
CSE4	Chromosome segregation
$CuSO_4$	Copper sulphate

D

D (Amino acid)	Aspartic acid
D. melanogaster	*Drosophila melanogaster*
DNA	Deoxyribonucleic acid
DNMT	DNA methyltransferase

E

E (Amino acid)	Glutamic acid
E. coli	*Escherichia coli*
EAF7	Esa1-associated factor
EDTA	Ethylenediaminetetraacetic acid
ELM1	Elongated morphology
ELP3	Elongator protein 3
ESA1	Catalytic subunit of the histone acetyltransferase complex NuA4
EtOH	Ethanol
EUROSCARF	EUROpean *Saccharomyces cerevisiae* ARchive for Functional Analysis

F

F (Amino acid)	Phenylalanine
FA	Formaldehyde agarose
FS DNA	Fish sperm DNA

G

GAL4	Galactose metabolism
GCN4 / *GCN5*	General control nonderepressible
GNAT	Gcn5-related acetyltransferase

H

h	Hour (time)
H (Amino acid)	Histidine
HA	Haemagglutinin
HAT (enzyme)	Histone acetyltransferase
HAT1 / *HAT2*	Histone acetyltransferase
HDAC	Histone deacetylase
HDM	Histone demethylase
HHF1 / *HHF2*	Histone H Four
HHT1 / *HHT2*	Histone H Three
HHTF	Histone H Three and H Four
HIS3	Histidine
HKMT	Histone lysine methyltransferase
HMT	Histone methyltransferase
HPA1 / *HPA2* / *HPA3*	Histone and other protein acetyltransferase
HTA1 / *HTA2*	Histone H Two A
HTB1 / *HTB2*	Histone H Two B
HU (phenotype)	Sensitivity to hydroxyurea

K

K (Amino acid)	Lysine
KAR4	Karyogamy
kb	Kilobase
kDa	Kilodalton
kV	Kilovolt

L

L	Litre
L (Amino acid)	Leucine
LB	Luria-Bertani
LEU2	Leucine biosynthesis
LiAc	Lithium acetate
LiCl	Lithium chloride
LYS2	Lysine requiring

M

M	Moles per litre
M (Amino acid)	Methionine
MALDI-TOF	Matrix-assisted laser desorption ionisation time-of-flight
MCK1	Meiotic and centromere regulatory ser, tyr-kinase
MDa	Megadalton
MET3	Methionine requiring
mg	Milligram
min	Minute (time)
ml	Millilitre
mM	millimolar
MMS (phenotype)	Sensitivity to methyl-methanesulfonate
MOPS	3-[N-morpholino]propanesulfonic acid
MRPS18	Mitochondrial ribosomal protein, small subunit
MSC3	Meiotic sister-chromatid recombination
MYST	MOZ-Ybf2/Sas3-Sas2-Tip60

N

NaAc	Sodium acetate
NaOH	Sodium hydroxide
ng	Nanogram
nm	Nanometer

O

OD_{600}	Optical density measured at a wavelength of 600 nm
OMP	Orotidine-5'-phosphate
ORF	Open reading frame

P

PCAF	p300/CREB-binding protein associated factor
PCR	Polymerase chain reaction
PEG	Polyethylene glycol
PHD finger	Plant homeodomain finger
PLP1	Phosducin-like protein
PMSF	Phenylmethanesulphonylfluoride
PRMT	Protein arginine methyltransferase
PTM	Post-translational modification

R

R (Amino acid)	Arginine
RNA	Ribonucleic acid
RNAi	RNA interference
rpm	Revolutions per minute
RT	Reverse transcription
RTT109	Regulator of Ty1 transposition

S

s	Second (time)
S. cerevisiae	*Saccharomyces cerevisiae*
S. pombe	*Schizosaccharomyces pombe*
SAGA	Spt-Ada-Gcn5 acetyltransferase
SAS2 / *SAS3*	Something about silencing
SDS	Sodium dodecyl sulphate
SDS-PAGE	Sodium dodecyl sulphate polyacrylamide gel electrophoresis
SET	Su(var)3-9, Enhancer of zeste and Trithorax
SFG1	Superficial pseudohyphal growth
SIP5	Snf1 interacting protein
siRNA	Small interfering RNA
SKI8	Superkiller
SLH1	Synthetic lethal with Hnt1
SPS4	Sporulation specific transcript
Spt (phenotype)	Suppressor of Ty phenotype
SUF2	Suppression of frameshift mutation
SUMO	Small ubiquitin related modifier

T

T. gondii	*Toxoplasma gondii*
T. thermophila	*Tetrahymena thermophila*
TAF1	TATA-binding protein-associated factor
TBST	Tris-buffered Saline Tween-20
TEMED	N,N,N’,N’-tetramethyl-1,2-diaminoethane
TRP1	Tryptophan requiring
TS (phenotype)	Sensitivity to temperature

U

U (Amino acid)	Uracil
UMP	Uridine monophosphate
URA3	Uracil requiring
UV	Ultraviolet

W

W (Amino acid)	Tryptophan
WT	Wild type

Y

Y (Amino acid)	Tyrosine
YAP1	Yeast AP-1
YPDA	Yeast extract peptone dextrose adenine

List of tables

List of figures

Summary

Histone H4 is one of four core histone proteins that make up the nucleosome, the smallest building block of chromosomes. Alanine-scanning mutagenesis of histone H4 had determined that the three mutant proteins H4Y51A, H4E53A and H4Y98A conferred sensitivity to 3-aminotriazole (AT), antimycin A and high temperature when expressed in place of endogenous histone H4. Multi-copy phenotypic suppressor screens were performed and the histone acetyltransferases Gcn5, Hpa1 and Hpa2 were isolated as multi-copy suppressors of the AT sensitivity of the H4Y98A mutant strain. Chromatin immunoprecipitation studies carried out at the *HIS3* gene showed that the histidine starvation-induced histone eviction was reduced in the H4Y98A mutant strain and restored back to the WT levels upon the over-expression of Gcn5. By controlling all aspects of DNA biology, histones play an important role in human diseases, and the homologous human proteins of the isolated suppressors might become interesting drug targets in the future.

(149 words)

1. Introduction

1.1 Epigenetics

Epigenetics, by definition, is the study of all mitotically and meiotically heritable changes in phenotype that do not result from changes in the genomic deoxyribonucleic acid (DNA) nucleotide sequence (Petronis, 2010; Zhu and Reinberg, 2011). Several important cellular processes were found to be fundamentally regulated by epigenetic modifications, such as gene expression, DNA-protein interactions, suppression of transposable element mobility, cellular differentiation and embryogenesis. Thus, several major pathologies, including cancer, syndromes associated with chromosomal alterations and neurological diseases, often arise due to the occurrence of aberrant epigenetic modifications. Within cells, there are at least three mechanisms of epigenetic modifications that can interact and stabilise one another to lead to the expression or silencing of genes — DNA methylation, ribonucleic acid (RNA)-associated silencing and histone modifications (Egger et al., 2004).

1.1.1 DNA methylation

DNA methylation is one of the most-studied epigenetic modifications because it plays an important role in several key processes, such as genomic imprinting, X chromosome inactivation and suppression of repetitive element transcription and transposition (Jin et al., 2011), where it ensures the proper regulation of gene expression and stable gene silencing (Khavari et al., 2010; Kulis and Esteller, 2010). DNA methylation involves the covalent addition of a methyl group ($-CH_3$) to DNA, specifically at the carbon-5 position of the cytosine ring. DNA methyltransferases (DNMTs) establish and maintain the methylation pattern, which occurs generally within CpG dinucleotides where a cytosine nucleotide is linked by a phosphate

directly to a guanine nucleotide. DNA methylation is often associated with gene silencing as it blocks the binding of transcription factors and also promotes the recruitment of methyl-CpG-binding domain proteins, which then help to recruit histone-modifying complexes and chromatin-remodelling complexes (Khavari et al., 2010; Kulis and Esteller, 2010; Jin et al., 2011).

1.1.2 RNA-associated silencing

In living cells, RNA can have a regulatory effect on DNA and the expression profile of the genome (Morris, 2005). RNA may affect gene expression by causing the formation of heterochromatin or by triggering DNA methylation and histone modification (Egger et al., 2004). RNA-associated silencing is achieved through a RNA interference (RNAi)-based mechanism, which is mediated by small interfering RNAs (siRNAs) that can specifically direct epigenetic modifications to targeted loci to silence target genes (Egger et al., 2004; Morris, 2005).

1.1.3 Histone modifications

Histones are proteins, which together with non-histone chromosomal proteins, associate with DNA to form chromatin. Four core histones, H2A, H2B, H3 and H4, make up an octameric complex, around which 147 base pairs (bp) of double stranded super helical DNA winds to form the nucleosome (Millar and Grunstein, 2006). Initially, histones were regarded only as static, non-participating structural elements of the nucleosome for DNA packaging (Felsenfeld and McGhee, 1986). However, experimental evidence has shown histones to be dynamic and integral in regulating chromatin condensation and DNA accessibility, where histones can undergo multiple types of post-translational modifications. This is important for the regulation of all

aspects of DNA biology, including transcriptional activation or repression, homologous recombination, DNA repair or replication, cell cycle regulation and chromatin compaction in apoptosis.

1.2 Approaches utilised towards the study of epigenetics

1.2.1 Model organism *S. cerevisiae*

Saccharomyces cerevisiae (*S. cerevisiae*) or budding yeast has been used as the model eukaryotic organism in this study because of several characteristics — size, doubling time, accessibility, manipulation, genetics and conservation of mechanisms (Botstein et al., 1997; Botstein and Fink, 2011). *S. cerevisiae* is a small, unicellular eukaryote that has a relatively short doubling time and can be easily cultured. Transformation of *S. cerevisiae* is straightforward, which allows for the addition of new or foreign genes through vector introduction or homologous recombination. Similarly, haploid *S. cerevisiae* strains make it simple to generate gene knock out strains by the deletion of genes through homologous recombination, where gene deletion is a common genetic method for studying gene function. More importantly, *S. cerevisiae* genome sequence and data on the complete set of deletion strains is freely available on Saccharomyces Genome Database (http://www.yeastgenome.org/).

In relation to this study, *S. cerevisiae* is the model eukaryotic system for analysis of histone genetics and functions due to its simple gene organisation and ease of manipulation (Smith and Santisteban, 1998). The mechanisms of transcriptional regulation are relatively similar in most eukaryotic cells because many proteins involved in histone modification and chromatin assembly are evolutionarily conserved. Hence, the findings obtained from *S. cerevisiae* can be directly applied to

research in humans. In fact, histone H4 is the most highly conserved in evolution, with a difference of only eight amino acids out of 102 between *S. cerevisiae* and humans (Wolffe, 1995). The amino acid sequence identities between *S. cerevisiae* and humans are 92 % for histone H4, 90 % for histone H3, 71 % for histone H2A and 63 % for histone H2B (Huang et al., 2009). *S. cerevisiae* also allows for easy exchange of wild type histones with mutant histones, where this forms the basis of the multi-copy suppressor screen.

1.2.2 Alanine-scanning mutagenesis

In this study, the histone H4 mutants Y51A, E53A and Y98A were generated by site-directed mutagenesis, where the original amino acid residue was substituted with alanine. This technique is called alanine-scanning mutagenesis and is commonly employed during the characterisation of individual amino acid residues for protein function and the identification of connections between various components of the cellular pathway (Cunningham and Wells, 1989; Matsubara et al., 2007). Alanine mutations do not impose electrostatic or steric effects on a protein, as alanine does not undergo covalent modifications, will not alter the main chain conformation and eliminates side chains beyond the β carbon (Lefèvre et al., 1997). In addition, alanine is an abundant amino acid, where it is often found on either buried or exposed surfaces and in all varieties of secondary structures. Thus, alanine is often the replacement amino acid of choice.

1.2.3 Phenotype testing

Genetic mutations may lead to observable phenotypes, where phenotype testing is a basic tool of genetics (Hampsey, 1997). Primary phenotype tests like

complementation involves replacing the wild type allele with a mutant allele to determine whether the mutant allele is able to support cell growth. Conditional phenotypes can also be tested, such as heat sensitivity, cold sensitivity and sensitivity to certain chemicals or analogues like 3-amino-1,2,4-triazole (3-AT). Other possible phenotypes that can be tested include respiratory deficiency, nucleic acid metabolism defects using 6-Azauracil, nitrogen utilisation defects, carbon catabolite repression, cell cycle defects, mating defects, cell morphology and cell wall defects like flocculence. In this study, phenotype testing was focused on 3-AT sensitivity (AT), antimycin A sensitivity (AA) and temperature sensitivity (TS) phenotypes, which could arise due to transcriptional defects that may be a result of changes caused by histone mutations, reflecting defects in the activation and repression of gene expression.

1.2.3.1 Sensitivity to 3-AT

The *HIS3* gene codes for imidazoleglycerol phosphate dehydratase, which is an enzyme that catalyses the sixth step in the histidine synthesis pathway (Sinha et al., 2004). The chemical 3-AT is an analogue that competitively inhibits imidazoleglycerol phosphate dehydratase. When *S. cerevisiae* strains are plated onto histidine-depleted media containing 3-AT, the histidine starvation elicits a general control response (McCusker and Haber, 1988). This results in transcriptional activation of the *HIS3* gene and other amino acid biosynthetic genes, where this response is mediated by the positive regulatory transcription factor Gcn4 (Joo et al., 2011). Mutant strains that are unable to lead to the activation of these genes have impaired growth on histidine-depleted media containing 3-AT, as compared to wild type strains (refer to section 2.3.1.1).

1.2.3.2 Sensitivity to antimycin A

Gal4 and Gal80 are two regulatory proteins that affect the expression of the GAL genes, which enable cells to utilise galactose as a carbon source. In the presence of galactose, Gal4 binds to sites in the upstream activation sequence and activates transcription. In the presence of glucose, Gal4 is inactivated by the binding of Gal80. Mutant strains that have defects in the activation of the GAL genes have impaired growth on galactose media, as compared to wild type strains. Although *S. cerevisiae* does not exhibit Kluyver effect for galactose and can ferment galactose under anaerobic conditions, low ATP yield and a dramatic decrease of energy charge make *S cerevisiae* less able to induce a functional Leloir pathway for galactose utilisation under anaerobic conditions (van den Brink et al., 2009). Thus, growth defects of *S cerevisiae* are often more severe under anaerobic conditions because the cells need to utilise more galactose to sustain growth under anaerobic conditions as compared to under aerobic conditions. Anaerobic conditions are mimicked by the addition of antimycin A, which is an antibiotic that inhibits mitochondrial respiration by blocking the electron transport chain (Goffrini et al., 2002).

1.2.3.3 Sensitivity to temperature

Mutant strains that have growth defects at a relatively high temperature like 38°C may have mutations in genes that are essential for cell viability or cellular events, such as mRNA stability, transcription start site selection, translation initiation or cell cycle control (Hampsey et al., 1991).

1.2.4 Suppression

Suppression is another genetic tool commonly used to identify the functions of

proteins and functional interactions between proteins. There are two main types of suppression — suppression via over-expression of genes involved in affected pathway and suppression via extragenic mutation.

1.2.4.1 Suppression via over-expression of genes involved in affected pathway

The histone H4 mutants Y51A, E53A and Y98A were found to be conferred with phenotypic deficiencies. These phenotypic deficiencies most likely arose due to the disruption of normal genetic interactions, which include direct changes to protein interactions, loss of protein interactions and direct or indirect changes to gene expression levels (Smith and Santisteban, 1998). In order to suppress the phenotypic deficiencies of the histone H4 mutants such that they are restored to that of wild type, over-expression of genes involved in affected pathway were achieved through a multi-copy suppressor screen. Upon the isolation of the dosage suppressor, the specific gene involved in the defective genetic interaction could be identified.

In the event that the specific gene involved coded for an interacting protein, functional protein interactions and their relevance could be discovered. This is important as protein interactions form the basis of major cellular process, including gene transcription and protein translation. Two mechanisms of suppression may take place, where one involves the restoration of the mutation to wild type through the formation of novel contacts between interacting proteins, while the second involves the restoration of the original contact points between interacting proteins (Sujatha et al., 2001; Prelich, 2012).

If the specific gene involved coded for an enzyme responsible for the direct or indirect

regulation of gene expression levels, the pathway and its mechanisms could potentially be elucidated. In a multi-copy suppressor screen, suppression of the mutant phenotype is achieved either by direct dosage compensation of the affected enzymatic activity or by indirect changes in enzymatic activity of upstream factors. For example, the methylation of H4R3 by histone methyltransferase PRMT1 is essential for establishing or maintaining a wide range of subsequent chromatin modifications for transcriptional activation. Through the indirect activity of PRMT1, transcriptional activation was restored through an alternative chromatin modification (Huang et al., 2005).

1.2.4.2 Suppression via extragenic mutation

Extragenic mutation refers to a second mutation at a site distinct from the original mutation, where the second mutation is able to partially or completely suppress the phenotypic deficiencies of the original mutation. The identification of an extragenic suppressor may provide indirect information on the gene containing the original mutation, as the extragenic suppressor may code for an interacting protein (Phizicky and Fields, 1995). For example, the missense allele of ILV5 is able to rescue yme2-4 growth phenotypes through synthetic interactions with yme2-4 and suppression of mitochondrial DNA transfer to the nucleus (Park et al., 2006).

1.2.5 Chromatin immunoprecipitation (ChIP)

ChIP is a widely used technique to examine histone modifications, chromatin remodelling and other chromatin related processes that play crucial roles in gene regulation (Haring et al., 2007). Briefly, ChIP relies on antibodies that target specific histone modifications at loci-of-interest on the chromosome, i.e. selective enrichment

of a chromatin fraction containing the specific antigen. ChIP is highly versatile, where it may be used to compare the enrichment of a protein or protein modification at different loci, to map a protein or protein modification across a locus-of-interest or even to quantify a protein or protein modification at an inducible gene over a time course. Chromatin is extracted, fragmented and incubated with the antibody of choice. Chromatin fragments that bind to the antibody of choice are captured using protein A/G beads. DNA is isolated from the precipitate and analysed to determine the abundance of the loci-of-interest in the precipitated material. There are two general procedures to carry out ChIP experiments (Figure 1.1) — X-ChIP, where chromatin is crosslinked then fragmented by sonication, as well as N-ChIP, where native chromatin is not crosslinked and is fragmented by micrococcal nuclease digestion (O'Neill and Turner, 2003). The analysis of isolated DNA can be carried out using several methods, such as conventional PCR, quantitative real-time PCR, microarray analysis and slot blotting (Haring et al., 2007). In this study, X-ChIP coupled with quantitative real-time PCR was used to analyse isolated DNA.

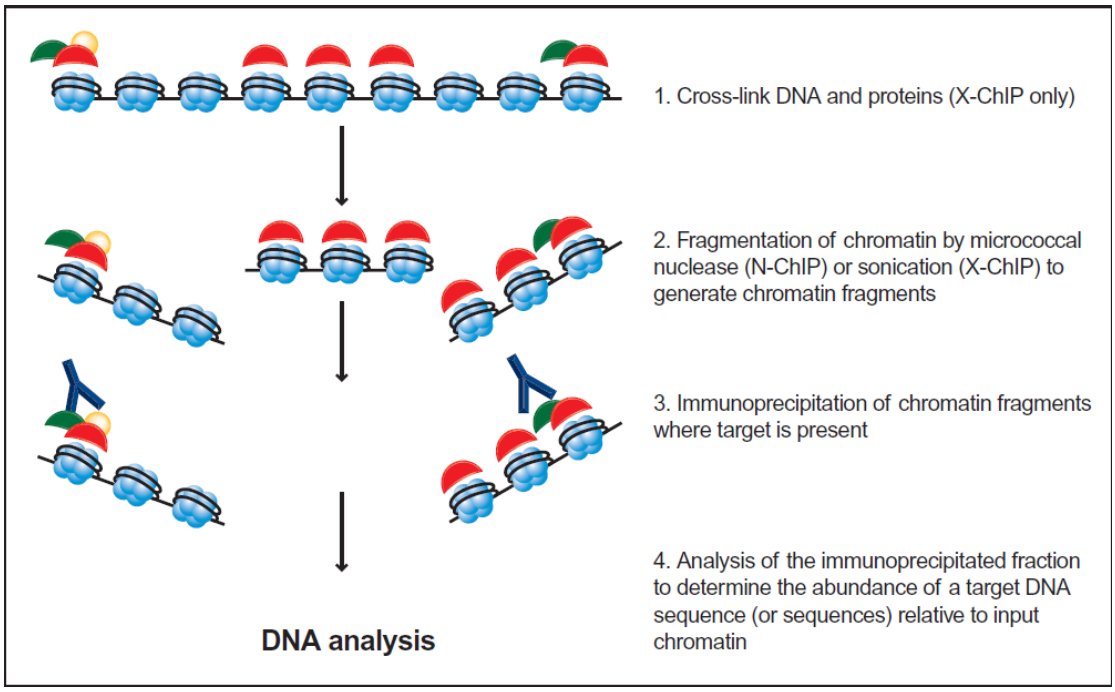

Figure 1.1 Schematic diagram of the X-ChIP and N-ChIP protocols. Figure adapted from "A Beginner's Guide to ChIP" (Abcam). Reproduced with permission from Abcam.

1.3 Aims of this study

This study is focused on understanding the effects of post-translational modifications of histones in epigenetics. In addition, the scope of this study was restricted to transcriptional regulation, where the other aspects of DNA biology were excluded.

In this study, three histone H4 mutants Y51A, E53A and Y98A were expressed in the simple model organism *S. cerevisiae* to study how histones affect the transcriptional regulation of gene expression via a genetic approach. The first aim of this study was to screen these three conditional histone mutants for multi-copy phenotypic suppressors, where the restrictive conditions tested were 3-AT sensitivity (AT), antimycin A sensitivity (AA) and temperature sensitivity (TS) phenotypes. The multi-copy phenotypic suppressors were isolated from a multi-copy library of genomic DNA fragments by their ability to confer growth under those restrictive conditions.

The second aim of this study was to elucidate the mechanism of suppression by the HATs Gcn5, Hpa1 and Hpa2, which were isolated as multi-copy phenotypic suppressors of the AT phenotype of the H4Y98A mutant strain. Strains expressing tagged forms of these HATs were used for quantitative real-time PCR, Western blot and chromatin immunoprecipitation studies. The effects of the H4Y98A mutation on known histone modifications in the histone H4 N-terminal tail were studied with the help of anti-modification specific antibodies, where these antibodies were further used to analyse the effect of the HATs Gcn5, Hpa1 and Hpa2 on the histone modifications.

2. Literature review

2.1 Nucleosomal structure

In the nucleus of eukaryotic cells, DNA is associated with histones and non-histone chromosomal proteins to form chromatin. The fundamental structural subunit of chromatin is the nucleosome, which is highly conserved evolutionarily and repeats at intervals of approximately 200 bp ± 40 bp throughout all eukaryotic genomes (Luger et al., 1997). The structure of chromatin imposes significant obstacles on all aspects of transcription, where the occupancy of nucleosomes was found to be lower at active promoters, as compared to inactive promoters (Bernstein et al., 2004; Pokholok et al., 2005; Belch et al., 2010). In fact, it has been found that nucleosomes are removed from gene promoters upon transcriptional activation, which is likely to help increase the accessibility of the transcriptional machinery to the exposed naked DNA (Reinke and Hörz, 2003; Boeger et al., 2004; Belch et al., 2010).

The nucleosome is a nucleoprotein complex consisting of 147 bp double stranded super helical DNA wound 1.65 turns around an octameric complex of core histone proteins, H2A, H2B, H3 and H4 (Luger et al., 1997; Millar and Grunstein, 2006; Peng et al., 2012). In a nucleosome, the H3-H4 heterodimers interact via a four helix bundle arrangement at the histone H3 C-termini to form a kernel of $(H3\text{-}H4)_2$ heterotetramer. Each H2A-H2B heterodimer interacts with the $(H3\text{-}H4)_2$ heterotetramer via a similar four helix bundle arrangement to form the compact octamer core (Figure 2.1; Luger et al., 1997; Wood et al., 2005; Peng et al., 2012). In some nucleosomes, the canonical histone H2A may be substituted by the histone variant H2A.Z in a wide but non-random genomic distribution (Kawano et al., 2011). Next, a DNA fibre is lined up with consecutive nucleosomes to form a beads-on-a-string structure with a diameter of 11 nm (Peterson and Laniel, 2004). The structure is further compacted into a 30 nm

fibre to form compact chromatin fibre (Margueron et al., 2005; Li and Reinberg, 2011).

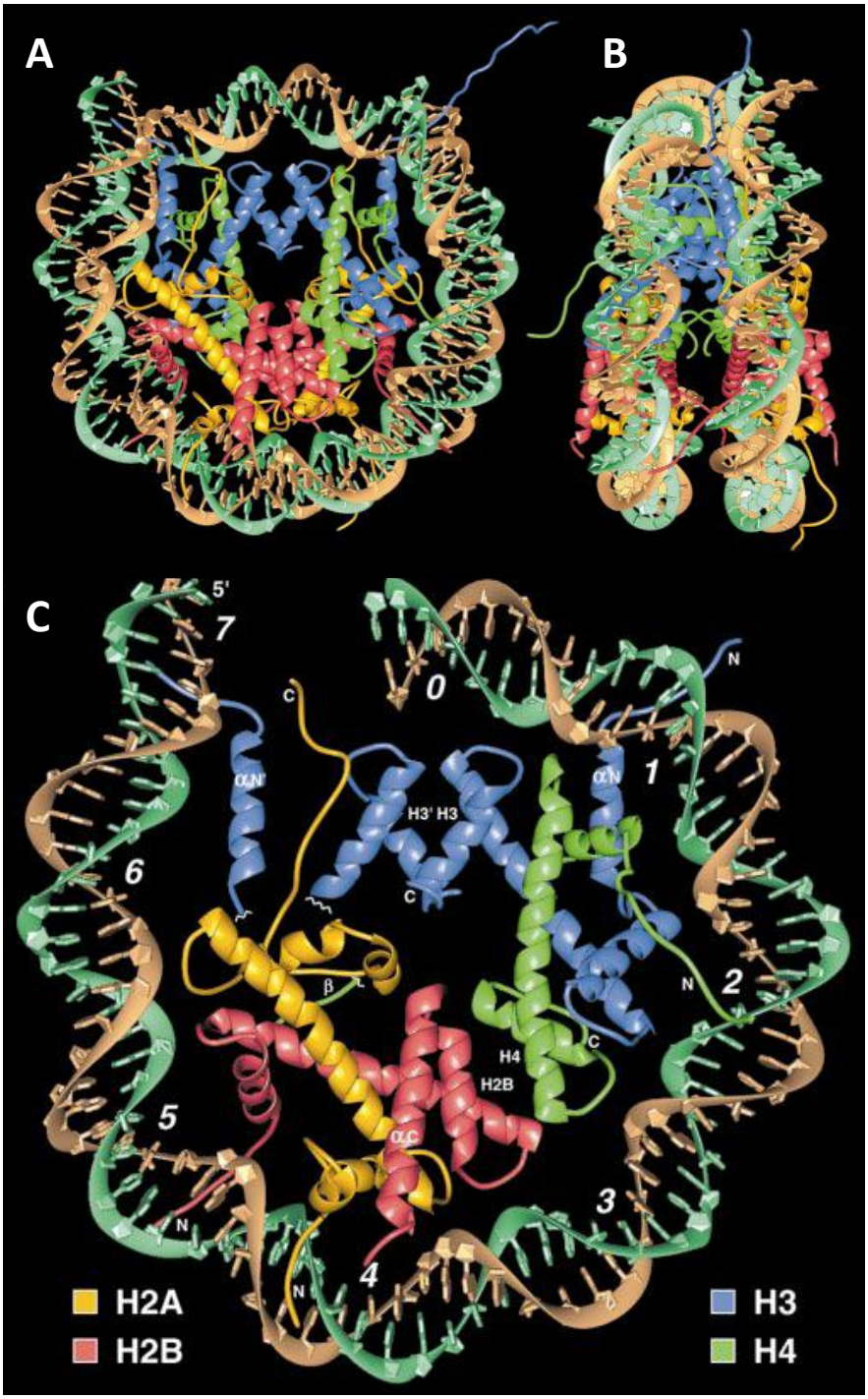

Figure 2.1 X-ray crystal structure of the nucleosome core particle. (A) The view of the nucleosome core particle down the DNA super helix axis. (B) The view of the nucleosome core particle perpendicular to the DNA super helix axis. (C) The view of half of the nucleosome core particle, showing the histone proteins primarily associated with 73 bp of double stranded super helical DNA. The histone tails resemble flexible strings that are unstructured and exposed on the nucleosomal surface. Figure adapted from Luger et al., 1997. Reproduced with permission from Nature Publishing Group.

In between successive nucleosomes, linker DNA of 10–60 bp in length is associated with histone H1 to allow for the formation of higher order structures (Kamieniarz et al., 2012). Unlike core histones, histone H1 shows appreciable variation between eukaryotic genomes and is not essential for viability (Mariño-Ramírez et al., 2005). In *S. cerevisiae*, the homologous Hho1 was found to have similar roles as histone H1 (Ushinsky et al., 1997; Baxevanis and Landsman, 1998; Yu et al., 2009) but Hho1 is restricted to specific chromosomal locations like ribosomal DNA sequences (Freidkin and Katcoff, 2001).

2.1.1 Core histones

Histones were once considered negative transcription factors that block the transcriptional machinery from associating with gene promoters, hindering the procession of transcriptional elongation. However, recent studies have now revealed that histones are important for both transcriptional repression and activation. Histones are rich in lysine and arginine, which are amino acid residues with basic side chains. This can effectively neutralise the negatively charged DNA backbone, where the histone-DNA interactions hold the DNA in place on the nucleosome (Füllgrabe et al., 2011).

Core histones H2A, H2B, H3 and H4 are highly conserved evolutionarily and are characterised by the presence of a tertiary structural motif known as the histone fold, where three α-helices are connected by two loops (“helix-loop-helix-loop-helix” motif). The histone fold is found in the globular core domain of histones and is critical for the maintenance of nucleosome structure through histone-histone and histone-DNA interactions. Besides the globular core domain, core histones also have flexible,

unstructured histone tails of about 15–30 amino acid residues at the N-termini, with the exception of histone H2A, which has histone tails at both the N-terminal and C-terminal (Luger et al., 1997; Biswas et al., 2011). The histone tails are exposed on the nucleosomal surface with sites available for post-translational modifications, which are crucial for the nucleosome's role in the regulation of gene expression and repression, silencing, DNA replication, DNA damage repair and apoptosis (Kornberg and Lorch, 1999; Peterson and Laniel, 2004; Peng et al., 2012).

2.1.2 Core histones in *S. cerevisiae*

In *S. cerevisiae*, each of the canonical core histones is encoded by two genes — histone H2A by *HTA1* and *HTA2*; histone H2B by *HTB1* and *HTB2*; histone H3 by *HHT1* and *HHT2*; and histone H4 by *HHF1* and *HHF2*. These eight genes are organised into four pairs of divergently transcribed loci — *HTA1-HTB1* and *HTA2-HTB2*, each encoding histones H2A and H2B; and *HHT1-HHF1* and *HHT2-HHF2*, each encoding histones H3 and H4 (Smith and Santisteban, 1998; Rando and Winston, 2012). Due to this redundancy, the deletion of any one histone locus does not lead to lethality. It is important to note that while *S. cerevisiae* does possess some histone variants, it has only one form of histone H3 that is similar to the vertebrate histone H3.3 variant (Nowak and Corces, 2004; Rando and Winston, 2012).

2.2 Histone code hypothesis

Histones were first regarded only as static, non-participating structural elements of the nucleosome for DNA packaging (Felsenfeld and McGhee, 1986). More recently, experimental evidence has shown histones to be dynamic and integral in regulating gene expression. As the genetic information contained within the genome is limited,

epigenetics imposed on histones may possibly exist to distinguish and direct nuclear processes, including transcriptional activation or repression. This adds several layers of complexity, effectively extending the wealth of information hidden within the genetic code and is known as the histone code hypothesis (Strahl and Allis, 2000; Jenuwein and Allis, 2001; Barth and Imhof, 2010). The histone code hypothesis predicts that residue specific post-translational modifications of histone tails would induce interaction affinities for chromatin associated proteins, where the modifications on the same or different histone tails may be interdependent and generate various combinations on any one nucleosome and it is likely that the local concentration and combination of differentially modified nucleosomes may have long range effects on the distinct qualities of higher order chromatin (Jenuwein and Allis, 2001; Barth and Imhof, 2010).

Two possibilities for the need of a histone code can be discussed, where firstly, different histone variants can provide various sequence modules that undergo different post-translational modifications for recognition by specific effectors to bring about distinct biological functions and secondly, different histone variants can alter nucleosomal structure to bring about changes in chromatin and underlying DNA (Bernstein and Hake, 2006; Kawano et al., 2011). Such alterations to generate different histone variants include at least three interrelated mechanisms — ATP-dependent chromatin remodelling involving ATP-driven complexes such as SWI/SNF, incorporation of specialised histone variants or non-histone chromosomal proteins into nucleosomes and post-translational modifications of histones.

2.2.1 ATP-dependent chromatin remodelling

Chromatin remodelling refers to the energy dependent modulation of interactions between histones and DNA in chromatin by dedicated nuclear enzymes that are often part of larger, multi-subunit complexes (Becker and Hörz, 2002; Hargreaves and Crabtree, 2011). Chromatin-remodelling ATPases have several catalytic functions, including catalysing mobilisation or repositioning of nucleosomes, transferring nucleosomes to a separate DNA, facilitating nuclease access to nucleosomal DNA and generating super helical torsion in DNA (Lusser and Kadonaga, 2003; Hargreaves and Crabtree, 2011). There are usually several different chromatin-remodelling complexes in each eukaryotic cell, where each complex has specific chromatin substrates and affects the transcription of a specific subset of genes by altering chromatin structure.

Based on the identity of the ATPase subunit, the chromatin-remodelling complexes can be divided into at least four classes (Narlikar et al., 2002; Martens and Winston, 2003; Hargreaves and Crabtree, 2011). The first class is the SWI2/SNF2 family, whose ATPase subunit contains an ATPase domain and a bromodomain. The members in this family include SWI/SNF and RSC complexes in *S. cerevisiae*, hSWI/SNF complex in humans and dSWI/SNF complex in *Drosophila melanogaster* (*D. melanogaster*). The second class is the ISWI family, whose ATPase subunit contains an ATPase domain and a SANT (SWI3/ADA2/N-CoR/TFIIIB) domain. The members in this family include ISW1 and ISW2 complexes in *S. cerevisiae*, RSF, hACF/WCRF and hCHRAC complexes in humans and NURF, CHRAC and ACF complexes in *D. melanogaster*. The third class is the Mi-2 family, whose ATPase subunit contains an ATPase domain, a plant homeodomain (PHD) finger and a double chromodomain. The representative member in this family is the NuRD complex in

humans (Narlikar et al., 2002; Rando and Winston, 2012). The fourth class is the INO80 family, whose ATPase subunit contains a split ATPase domain. The members in this family include INO80 complex, SWR1 complex and NuA4 complex in *S. cerevisiae*, Pho-dINO80 and Tip60 in *D. melanogaster*, as well as INO80 complex, SRCAP complex and TRAAP/Tip60 in humans (Hargreaves and Crabtree, 2011).

2.2.2 Nucleosomal incorporation

The incorporation of specialised histone variants or non-histone chromosomal proteins into nucleosomes allows for structural and functional modifications of chromatin (Kawano et al., 2011). Histone variants may differ from canonical histones by subtle differences or by significant alterations that could drastically change the nature of the histone and even the chromatin (Figure 2.2). These differences in combination with specific chaperone proteins mediate various localisation patterns in a cell (Bernstein and Hake, 2006). Unlike the other canonical histones, there is no known histone sequence variant for histone H4 (Kamakaka and Biggins, 2005).

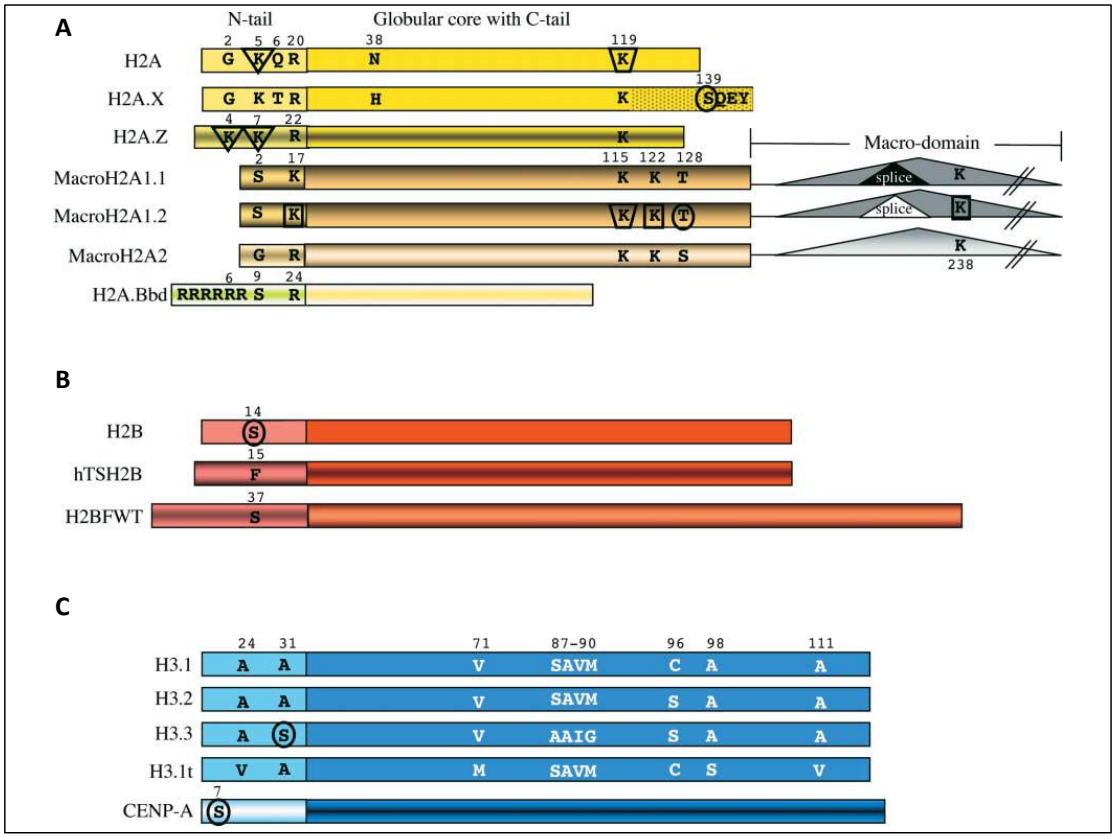

Figure 2.2 Schematic diagram of mammalian histone variants. (A) Histone H2A variants. (B) Histone H2B variants. (C) Histone H3 variants. Histone variants in different colour shades represent highly divergent protein sequences between the canonical histones and its histone variants. Figure adapted from Bernstein and Hake, 2006. Reproduced with permission from NRC Research Press.

According to the extent of amino acid sequence changes from the main isoforms, histone variants can be classified into the homomorphous family or heteromorphous family (Ausió, 2006). The homomorphous family contains histone variants that have only a few sequence changes, such as histone variants H2A.1, H2A.2, H3.1, H3.2 and H3.3. For example, there is only one amino acid sequence change between histone variants H3.1 and H3.2 (Bernstein and Hake, 2006). The heteromorphous family contains histone variants that have more extensive sequence changes, such as histone variants H2A.X, H2A.Z, macroH2A, H2A Barr body deficient and centromeric protein A. For example, there is a fusion of a histone H2A-like protein to a non-histone domain in histone variant macroH2A (Bernstein and Hake, 2006).

2.2.3 Post-translational modifications of histones

Post-translational modifications (PTMs) of histones are a component of the epigenome, where they may occur on a global scale to induce changes in chromatin structure and function as switches for the transcriptional regulation of gene expression (Mariño-Ramírez et al., 2005; Bannister and Kouzarides, 2011). However, only histone H3 has been shown to affect transcriptional regulation on a global scale, instead of a gene specific scale (He and Lehming, 2003).

Some PTMs of histones include interactions with adenosine diphosphate ribose polymers (Panzeter et al., 1993; Messner et al., 2010), noncovalent modifications like proline isomerisation of H3P30 and H3P38 (Nelson et al., 2006) and the enzymatic addition or removal of covalent modifications (Figure 2.3; Table 2.1). The molecules added covalently may be relatively large, such as sumoylation of lysine and ubiquitylation of lysine, or relatively small, such as acetylation of lysine, methylation of arginine, histidine and lysine, phosphorylation of histidine, serine, threonine and tyrosine, adenosine diphosphate ribosylation of arginine, glutamate, glutamine and lysine, biotinylation of lysine, butyrylation of lysine, propionylation of lysine, nitrosylation of cysteine and glycosylation of asparagine, serine and threonine (Berger, 2002; Fischle et al., 2003; Peterson and Laniel, 2004; Chen et al., 2007; Kouzarides, 2007; Portela and Esteller, 2010; Gardner et al., 2011; Singh and Gunjan, 2011; Waldmann et al., 2011; Besant and Attwood, 2012; Hanover et al., 2012). These PTMs may change the charge or conformation of histones, or in other cases, the attached molecule regulates protein-protein interaction by providing a better surface for binding partners like transcription factors, such as the histone acetyltransferase Gcn5 and the histone demethylase JMJD2A (Berger, 2002; Berger, 2007; Kouzarides,

2007).

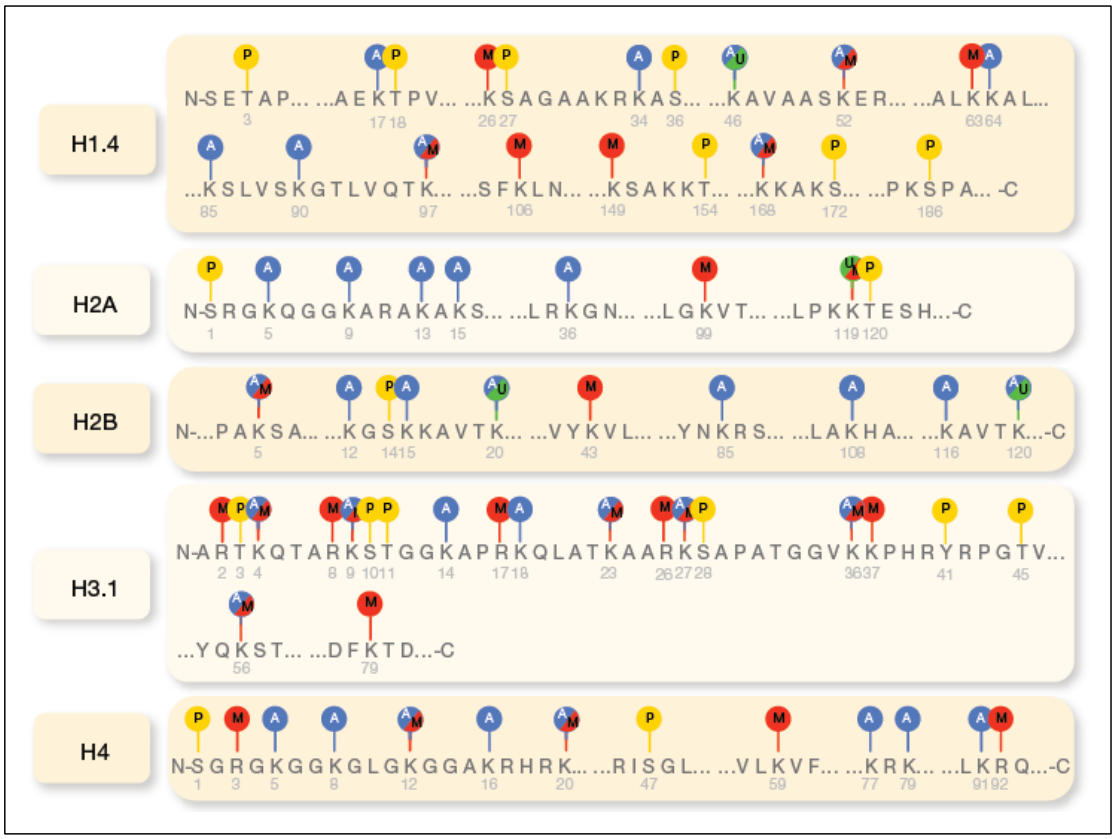

Figure 2.3 Schematic diagram of PTMs of histones. The main PTMs shown in this diagram are acetylation (blue), methylation (red), phosphorylation (yellow) and ubiquitination (green). Figure adapted from Portela and Esteller, 2010. Reproduced with permission from Nature Publishing Group.

Table 2.1 Some known sites of PTMs of histones (Table adapted from He and Lehming, 2003; Camporeale et al., 2004; Margueron et al., 2005; Millar and Grunstein, 2006; Portela and Esteller, 2010; Gardner et al., 2011; Singh and Gunjan, 2011; Waldmann et al., 2011; Besant and Attwood, 2012)

Histone	PTM	Residue modified
H1	Acetylation	K17, K26, K34, K46, K52, K64, K85, K90, K97, K168
	Methylation	K26, K52, K63, K97, K106, K149, K168
	Phosphorylation	T3, T18, S27, S36, T154, S172, S186
	Ubiquitination	K46
H2A	Acetylation	K5, K9, K13, K15, K36, K119
	Methylation	R3, R11, R29, K99, K119
	Phosphorylation	S1, T120
	Ubiquitination	K4, K119, K120, K123, K126
H2B	Acetylation	K5, K12, K15, K20, K85, K108, K116, K120
	Methylation	K5, K37, K49
	Phosphorylation	S10, S14
	Ubiquitination	K20, K120
H3	Acetylation	K4, K9, K14, K18, K23, K27, K36, K56
	Methylation	R2, K4, R8, K9, K14, R17, K23, R26, K27, K36, K37, K56, K79
	Phosphorylation	T3, S10, T11, S28, Y41, T45, Y99
H4	Acetylation	K5, K8, K12, K16, K20, K77, K79, K91
	Methylation	R3, K12, K20, K59, K92
	Phosphorylation	S1, H18, S47, H75
	Biotinylation	K8, K12

2.2.3.1 Fundamental PTMs of histones

Experimental findings have shown that PTMs of histones can either activate or repress transcription, where histone modifications on different amino acid residues may result in different effects on transcription and multiple levels of histone modifications on the same amino acid residue may result in different effects on transcription (Table 2.2). For example, histone H3K4, H3R17 or H3K79 methylation activates transcription but histone H3K9 methylation has the opposite effect of repressing transcription (He and Lehming, 2003; Lu et al., 2008; Murr, 2010). In addition, histone H3K4 has three states of methylation — mono-, di- and tri-

methylated states — where di-methylated H3K4 can be associated with both transcriptional activation and repression, while tri-methylated H3K4 is associated only with transcriptional activation of protein encoding genes (Santos-Rosa et al., 2002, He and Lehming, 2003; Murr, 2010).

Table 2.2 Some proposed functions of PTMs of core histones carried out by different histone modifying enzymes (Table adapted from Sterner and Berger, 2000; He and Lehming, 2003; Peterson and Laniel, 2004)

Histone	PTM	Histone modifying enzyme	Proposed function
H2A	K4ac	Esa1	Transcriptional activation
	K7ac	Hat1	Unknown
		Esa1	Transcriptional activation
	S1ph	Msk1	Transcriptional repression
	S129ph	Mec1, Tel1	DNA repair
H2B	K5ac	p300, Atf2	Transcriptional activation
	K11ac	Gcn5	Transcriptional activation
	K16ac	Gcn5, Esa1	Transcriptional activation
	K20ac	p300	Transcriptional activation
	S10ph	Ste20	Apoptosis
H3	K4ac	Esa1	Transcriptional activation
		Hpa2	Unknown
	K9ac	Gcn5, SRC-1	Transcriptional activation
	K14ac	Gcn5, PCAF	Transcriptional activation
		Esal, Tip60	Transcriptional activation, DNA repair
		Hpa1 (Elp3)	Transcriptional activation (elongation)
		Hpa2	Unknown
		Sas2	Euchromatin
	K18ac	Gcn5	Transcriptional activation, DNA repair
	K23ac	Gcn5	Transcriptional activation, DNA repair
	K27ac	Gcn5	Transcriptional activation
	K56ac	Spt10	Transcriptional activation, DNA repair
	K4me	Set1	Permissive euchromatin
	R8me	PRMT5	Transcriptional repression
	S10ph	Snf1	Transcriptional activation
H4	K5ac	Hat1	Histone deposition
		Esal, Tip60	Transcriptional activation, DNA repair
		Hpa2	Unknown
	K8ac	Gcn5, PCAF	Transcriptional activation
		Esal, Tip60	Transcriptional activation, DNA repair
		Hpa1 (Elp3)	Transcriptional activation (elongation)

Histone	PTM	Histone modifying enzyme	Proposed function
	K12ac	Hat1	Histone deposition, telomeric silencing
		Esal, Tip60	Transcriptional activation, DNA repair
		Hpa2	Unknown
	K16ac	Gcn5	Transcriptional activation
		Esal, Tip60	Transcriptional activation, DNA repair
		Sas2	Euchromatin
	K91ac	Hat1	Chromatin assembly
		Hat2	Chromatin assembly
	R3me	PMRT1	Transcriptional activation
		PMRT5	Transcriptional repression
	S1ph	CK2	DNA repair

PTMs of histones may also have effects on a global scale or on a gene specific scale. For example, high levels of lysine acetylation on core histones or high levels of trimethylation on histone H3K4, H3K36 and H3K79 allow for actively transcribed euchromatin, while low levels of lysine acetylation or high levels of methylation on H3K9, H3K27 and H4K20 allow for transcriptionally inactive heterochromatin (Berger, 2002; Edwards et al., 2011). The dynamic role of nucleosomes in the regulation of transcription may be influenced by the PTMs of histones (He and Lehming, 2003). When the histone tails of core histones are methylated and non-acetylated, they carry a high positive net charge that enhances interaction with the negatively charged DNA backbone, causing the DNA strands to become inaccessible to the transcriptional machinery (Figure 2.4A). When the histone tails of core histones are acetylated or phosphorylated, they carry a lower positive net charge that decreases the interaction with the negatively charged DNA backbone, causing the DNA strands to become accessible to the transcriptional machinery, especially at the promoter regions (Figure 2.4B). On the other hand, the promoter region of actively transcribed genes may have high levels of acetylation on histone H2BK5 and H3K27 and high levels of methylation on histone H3K4 and H4K20, while the open reading frame of actively transcribed genes may have high levels of methylation on H3K79 and H4K20

(Vakoc et al., 2005; Edwards et al., 2011).

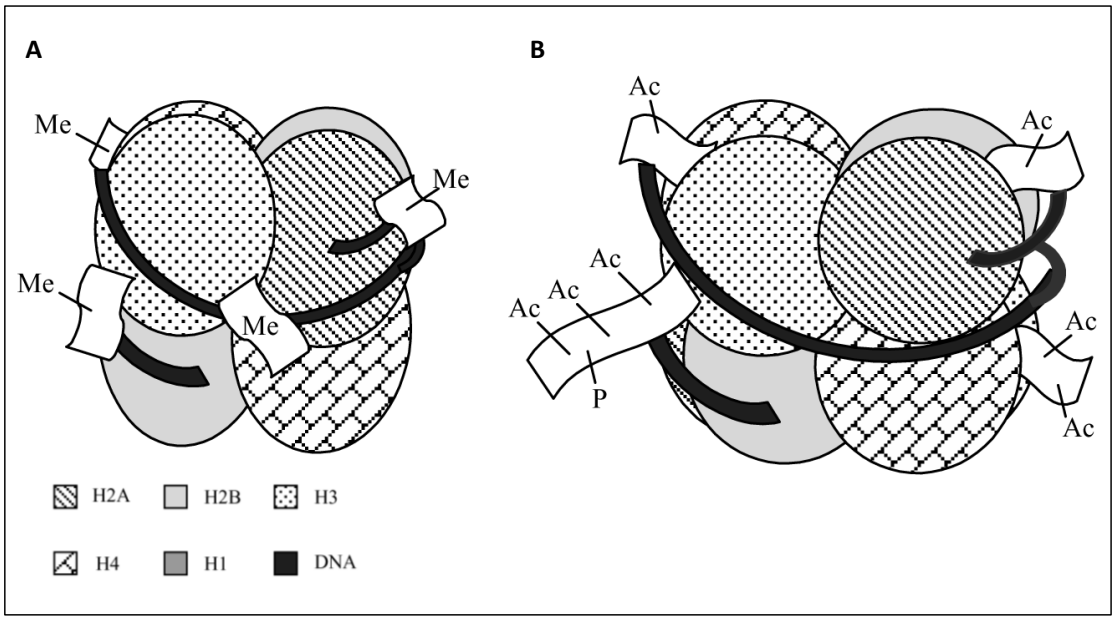

Figure 2.4 The dynamic role of nucleosomes in transcriptional regulation may be influenced by the PTMs of histones. (A) High levels of methylation on the histone tails of core histones allow for transcriptionally inactive heterochromatin. (B) High levels of acetylation or phosphorylation on the histone tails of core histones allow for actively transcribed euchromatin. Figure adapted from He and Lehming, 2003. Reproduced with permission from Oxford University Press.

PTMs of histones are catalysed by histone modifying enzymes (Table 2.2), such as histone acetyltransferases (HATs) for acetylation, histone deacetylases (HDACs) for deacetylation, histone methyltransferases (HMTs) for methylation, histone demethylases (HDMs) for demethylation, histone kinases for phosphorylation, histone phosphatases for dephosphorylation, E3 ubiquitin ligases for ubiquitination, deubiquitinases for deubiquitination, and small ubiquitin related modifier (SUMO) conjugating enzymes for sumoylation (Keppler and Archer, 2008a; Keppler and Archer, 2008b; Atanassov et al., 2011; Besant and Attwood, 2012). These histone modifying enzymes are recruited to histones through various signals. One signal is the direct interaction with sequence specific DNA-binding factors, such as the targeting of the SAGA complex by the activator Gal4 to lead to histone acetylation (Bhaumik and Green, 2001; Bhaumik, 2010). A second signal is the DNA-dependent protein

kinase-mediated phosphorylation of histone H2A or histone variant H2A.X after DNA damage, which leads to the recruitment of the histone acetylase complex Tip60 that turns off the DNA repair response after DNA has been repaired (Kusch et al., 2004; Li et al., 2010). A third signal is the recruitment of the HMT Clr4 and the chromodomain-binding protein Swi6 by siRNA to establish and maintain heterochromatin (Hall et al., 2002). The following sections detail some common PTMs of histones, where this study has increased emphasis on acetylation of histones.

2.2.3.1.1 Histone acetylation

Of the known PTMs of histones, acetylation is the best described histone modification. Histone acetylation was in fact, the first described modification of histones (Phillips, 1963). The acetylation state of core histone tails is important for chromatin structure and for the regulation of transcription. Moderate levels of histone acetylation by HATs destabilise chromatin higher order folding by weakening histone-DNA interactions and correlates with enhanced transcriptional elongation by RNA polymerase II, while reduced levels of histone acetylation by HDACs stabilise chromatin higher order folding by strengthening histone-DNA interactions and correlates with transcriptional repression (Horn and Peterson, 2002). The exact mechanism behind the effects of histone acetylation on transcriptional regulation is unknown. Two hypothetical models have been suggested to explain the link — the charge neutralisation model and the histone code model (Füllgrabe et al., 2011).

In the charge neutralisation model, histone acetylation may reduce the affinity between nucleosomes and DNA as acetylation neutralises the positive charge of the lysine side chain in the core histone tails (Figure 2.4B; Hong et al., 1993; Muller et al.,

2011). This change in the local chromatin structure may become more permissive for the access of transcriptional machinery to gene promoters (Grunstein, 1997). For example, the acetylation of histone H3K9 and H3K14 is strongly associated with euchromatin (Kurdistani and Grunstein, 2003; Guillemette et al., 2011).

In the histone code model, histone acetylation may produce a histone code, serving as a signal to recruit transcription factors and other effector proteins to the specific site of modification (Strahl and Allis, 2000; Kurdistani and Grunstein, 2003; Hahn and Young, 2011). The histone code model is supported by experimental findings where many transcriptional regulatory proteins and protein complexes contain binding domains that specifically recognise modified histone tails, such as the recognition of acetylated lysines by bromodomains found in transcription factors (Dhalluin et al., 1999; Jacobson et al., 2000; Khorasanizadeh, 2004; Hahn and Young, 2011; Muller et al., 2011). The charge neutralisation model and the histone code model are not mutually exclusive, where it is highly likely that the chromatin structure and the regulation of transcription are controlled by a combination of both models (refer to section 2.3).

2.2.3.1.2 Histone methylation

Methylation of arginine and lysine residues in histones serves as the major determinant for the formation of transcriptionally active or inactive chromatin and is important for proper genome programming during development, where the misregulation of the methylation machinery can lead to diseases like cancer (Jenuwein, 2001; Van Den Broeck et al., 2008). Unlike acetylation, methylation does not alter the charge of arginine and lysine residues in histones, thus it is unlikely to

directly modulate nucleosomal interactions for chromatin folding.

HMTs catalyse the methylation of histones, where in *S. cerevisiae*, specific lysine residues in histone H3 (K4, K9, K36 and K79), specific arginine residues in histone H3 (R2, R17 and R26) and specific arginine residue in histone H4 (R3) are covalently modified with methyl groups (Peterson and Laniel, 2004). Arginine methylation leads to the active state of transcription (Chen et al., 1999) and is mediated by protein arginine methyltransferases (PRMTs), including the coactivators PRMT1 and PRMT4 (CARM1) (Daujat et al., 2002; Huang et al., 2005; Feng et al., 2011). PRMTs do not contain a SET domain but they possess highly conserved non-contiguous amino acid residues that are essential for forming the catalytic core, which catalyses the transfer of the methyl group from S-adenosylmethionine to the guanidine group of arginine residues (Bauer et al., 2002).

Lysine methylation leads to the inactive state of transcription by blocking the binding of proteins that interact with unmethylated histones, by inhibiting the catalysis of regulatory modifications on neighbouring amino acid residues and by providing a binding surface for chromatin-remodelling complexes that regulate chromatin condensation and nucleosome mobility (Qian and Zhou, 2006; Hou and Yu, 2010). For example, histone H3K9 methylation serves as an epigenetic mark for silenced heterochromatin and provides a binding surface for the chromodomain protein heterochromatin associated protein (Jenuwein and Allis, 2001; Pokholok et al., 2005; Hou and Yu, 2010). Lysine methylation also leads to the active state of transcription, for example, tri-methylation of histone H3K4 is a mark for gene activation (Santos-Rosa et al., 2002). Lysine methylation is mediated by histone lysine

methyltransferases (HKMTs), whose catalytic core is the SET [Su(var)3-9, Enhancer of zeste and Trithorax] domain (Qian and Zhou, 2006; Rando and Winston, 2012).

2.2.3.1.3 Histone phosphorylation

Phosphorylation of serine and threonine residues in histones facilitates chromatin condensation and transcriptional activation, where phosphorylation of histone H3S10 is a well-known PTM that is important for mitosis, chromosome condensation and transcriptional activation (Berger, 2002; Nowak and Corces, 2004; Zippo et al., 2009). In mammals, phosphorylation of histone H3 is mediated by histone kinases that target serine and threonine residues surrounded by basic residues, which include Aurora-B/Ipl1, PKA, Rsk-2, and Msk1 (Khorasanizadeh, 2004). More interestingly, the interaction of the HAT domain of Gcn5 with the adjacent phosphoserine has been shown to increase lysine acetylation capacity (Khorasanizadeh, 2004).

2.2.3.2 Combinatorial PTMs of histones

As discussed earlier (refer to section 2.2.3), histones can undergo post-translational modifications and there exists several sites for modifications within each histone (Table 2.1). Although more than 60 modification sites on histones have been detected, a single histone PTM does not determine the resultant biological effect alone (Kouzarides, 2007). On the contrary, different histone PTMs in a nucleosome or chromatin region function in a combinatorial manner, where one histone PTM may induce or inhibit another histone PTM (He and Lehming, 2003; Kouzarides, 2007). For example, lysine residues on histones can be acetylated, methylated, sumoylated or ubiquitylated, where these various modifications obviously exclude one another on a particular lysine residue. In addition, there are several examples of interdependency

and crosstalk between different residues on the same histone or on different histones (Jenuwein and Allis, 2001; Rice and Allis, 2001; Fischle et al., 2003; Zippo et al., 2009).

There are several established mechanisms through which PTMs mediate crosstalk, where these mechanisms can be classified as positive or negative crosstalk (Hunter, 2007). Positive crosstalk refers to the situation where one histone PTM serves as a signal for either the addition or the removal of another PTM. Positive crosstalk can also refer to the situation where one histone PTM serves as the recognition site or docking site for a binding protein that leads to the addition or the removal of another PTM (Hunter, 2007). For example, mono-ubiquitination of histone H2BK123 by ubiquitin conjugating enzyme Rad6 is essential for methylation of histone H3K4 and H3K79 by HMTs Set1 and Dot1 respectively, while the loss of methylation appears to have no effect on ubiquitination in *S. cerevisiae* (Sun and Allis, 2002; Shahbazian et al., 2005). In a second example, phosphorylation of histone H3S10 was found to promote acetylation of histone H3K14 after stimulating mammalian cells with epidermal growth factor (Cheung et al., 2000). In a similar example, phosphorylation of histone H3S10 was found to promote acetylation of histone H4K16, leading to transcriptional activation (Zippo et al., 2009). In another example, acetylation of histone H3K18 and H3K23 by p300/CREB-binding protein acetyltransferase initiated the recruitment of PRMT4 (CARM1) to catalyse methylation of histone H3R17 (Daujat et al., 2002). In fact, non-covalent PTMs may even affect the occurrence of covalent PTMs, such as the necessity of proline isomerisation of histone H3P30 and H3P38 by proline isomerase Fpr4 for methylation of histone H3K36 by Set2 (Nelson et al., 2006).

On the other hand, negative crosstalk refers to the situation where there is direct competition for the modification of a particular residue in histones. Negative crosstalk can also refer to the situation where there is an indirect effect of one histone PTM on another PTM, possibly by masking the recognition site to prevent the other PTM from occurring (Hunter, 2007). For example, methylation of histone H3K4 prevents the binding of transcriptional repressor complex NuRD, thus NuRD is not able to catalyse the deacetylation of histone H3K9 (Zegerman et al., 2002). In a similar example, methylation of histone H3K9 by HMT SUV39H1 inhibits the subsequent methylation of histone H3K4 by HMT Set7 and vice versa (Wang et al., 2001). In another example, phosphorylation of histone H3S10 was found to inhibit the methylation of histone H3K9 (Rea et al., 2000).

2.2.3.3 Influences of histone H4 acetylation on transcription

As this study is focused on the understanding of the role of histone H4 and the effects of PTMs of histone H4 in epigenetics, especially acetylation, this section will discuss in detail the influences of histone H4 acetylation on transcription.

Matrix-assisted laser desorption ionisation time-of-flight (MALDI-TOF) mass spectrometry analysis of histone H4 purified from HeLa cells revealed that out of the 15 lysine acetylation sites possible, only four sites in the N-terminal histone tail were observed to be acetylated (Zhang et al., 2002) — H4K5 (tetra-acetylated), H4K8 (tri- and tetra-acetylated), H4K12 (di-, tri- and tetra-acetylated) and H4K16 (mono-, di-, tri- and tetra-acetylated). In addition, histone H4 was found to be acetylated in its globular core domain at H4K91 (Ye et al., 2005; Martinato et al., 2008; Yang et al., 2011). The PTMs of histones, especially acetylation of histone H4 N-terminal histone

tail, are conserved from unicellular eukaryotes, such as *S. cerevisiae* and *Tetrahymena thermophila* (*T. thermophila*), to multicellular eukaryotes, such as *Arabidopsis thaliana* (*A. thaliana*), mouse and human (Table 2.3; Smith et al., 2003; Garcia et al., 2007; Zhang et al., 2007).

Table 2.3 PTMs of histone H4 N-terminal histone tail in different organisms (Table adapted from Garcia et al., 2007; Zhang et al., 2007)

Modification site	***S. cerevisiae***	***T. thermophila***	***A. thaliana***	**Mouse**	**Human**
S1	Phosphorylation			Phosphorylation	Phosphorylation
K5	Acetylation	Acetylation	Acetylation	Acetylation	Acetylation
K8	Acetylation	Acetylation	Acetylation	Acetylation	Acetylation
K12	Acetylation	Acetylation	Acetylation	Acetylation	Acetylation
K16	Acetylation	Acetylation	Acetylation	Acetylation	Acetylation
K20			Acetylation	Methylation	Methylation

Histone H4 acetylation has been linked to both transcriptional activation and repression. For example, during transcriptional repression in *D. melanogaster*, three of the four lysine residues in the N-terminal histone tail of histone H4 (H4K5, H4K8 and H4K16) are hypoacetylated but H4K12 was found to be significantly acetylated (Braunstein et al., 1996). In a second example, histone H4K5 acetylation was found to decrease PRMT1 activity and increase PRMT5 activity (Feng et al., 2011). Although both HMTs mediate the methylation of histone H4R3, they have opposite biological impacts with PRMT1-mediated H4R3 methylation correlating to transcriptional activation and PRMT5-mediated H4R3 methylation correlating to transcriptional repression (Feng et al., 2011).

On the other hand, histone H4 acetylation has been found to promote transcriptional activation by recruiting bromodomain-containing chromatin-remodelling complexes to the promoters of target genes in order to alter chromatin structure and increase the

accessibility of the transcriptional machinery (Dhalluin et al., 1999; Jacobson et al., 2000). As different chromatin-remodelling complexes containing different HATs are recruited to different promoters, different lysine residues on histone H4 are acetylated (Millar and Grunstein, 2006). For example, the progesterone receptor interacts and recruits the coactivator SRC-1, which then recruits the HAT CBP that mediates histone H4K5 acetylation (Li et al., 2003). In a second example, the MSL complex in *D. melanogaster* contains the HAT MOF, a protein sharing amino acid sequence homology with the MYST family, which mediates histone H4K16 acetylation (Smith et al., 2000).

Histone H4 acetylation also prevents the spread of heterochromatin, where experimental findings have shown that acetylation of histone H4K16 leads to the destabilisation of nucleosomes, decondensation of chromatin and contributes to the establishment of euchromatin (Shogren-Knaak and Peterson, 2006; Shogren-Knaak et al., 2006; Zippo et al., 2009). In a second example, global acetylation of histone H4K16 mediated by Sas2 opposes the deacetylation of this residue by HDAC Sir2 to prevent the spread of telomeric heterochromatin (Suka et al., 2002; Kozak et al., 2010).

2.3 Histone acetyltransferases

As discussed earlier (refer to section 2.2.3.1.1), histones can undergo acetylation, where this process is catalysed by HATs. HATs carry out acetylation by transferring an acetyl group from acetyl coenzyme A onto the epsilon amino group of lysine residues in the N-terminal tail of core histones (Albaugh et al., 2011). Based on the cellular localisation, HATs can be classified into two groups — Type A HATs that

are localised in the nucleus, where they catalyse histone acetylation involved in transcription related events and Type B HATs that are localised in the cytoplasm, where they catalyse histone acetylation involved in the transport of newly synthesised histones from the cytoplasm to the nucleus for deposition onto newly replicated DNA during DNA replication (Grunstein, 1997; Kuo and Allis, 1998; Grant and Berger, 1999; Sterner and Berger, 2000; Roth et al., 2001; Bannister and Kouzarides, 2011; Ghizzoni et al., 2011).

Type B HATs are highly conserved, where they share amino acid sequence homology with the founding member, *S. cerevisiae* Hat1 (Grant and Berger, 1999; Bannister and Kouzarides, 2011; Zhang et al., 2012). Type B HATs usually target newly synthesised histone H4 at positions K5 and K12 for acetylation, where the acetylation marks are removed after the deposition of the histones (Parthun, 2007; Zhang et al., 2012).

Type A HATs are a more diverse family of enzymes as compared to Type B HATs, where Type A HATs can be further classified into at least three groups based on amino acid sequence homology and the motif organisation of the catalytic subunit — Gcn5-related acetyltransferase (GNAT) family, MOZ-Ybf2/Sas3-Sas2-Tip60 (MYST) family and p300/CREB-binding protein family (Bannister and Kouzarides, 2011; Sampley and Ozcan, 2012). The catalytic subunit of the GNAT family contains both a HAT domain and a bromodomain, the catalytic subunit of the MYST family contains both a HAT domain and a chromodomain and the catalytic subunit of the p300/CREB-binding protein family contains a HAT domain, a bromodomain and three C/H motifs (Grant and Berger, 1999; Marmorstein and Roth, 2001; Narlikar et al., 2002).

In vivo, HATs are large complexes with multiple subunits, i.e. HATs have varying protein compositions (Brown et al., 2000; Roth et al., 2001). The conserved core is the most important part of a HAT, where it is involved in the recognition of acetyl coenzyme A as the cofactor for acetylation. Many HATs also function as transcriptional coactivators, where they promote the association of the TATA-binding protein with the basal promoter (Brown et al., 2000; Berger, 2002).

There is a large number of HATs, where even within the relatively small *S. cerevisiae* genome, at least six different HATs can be characterised (Brown et al., 2000; Lee and Young, 2000; Sterner and Berger, 2000; Rando and Winston, 2012) — SAGA complex (containing Gcn5 as the catalytic subunit), ADA complex (containing Gcn5 as the catalytic subunit), TFIID complex (containing TFII130 as the catalytic subunit), NuA3 complex (containing Sas3 as the catalytic subunit), NuA4 complex (containing Esa1 as the catalytic subunit) and Elongator complex [containing Hpa1 (Elp3) as the catalytic subunit].

Different HATs target different histones, such as SAGA (Spt-Ada-Gcn5 acetyltransferase) complex and ADA (Ada-containing complex) complex acetylating nucleosomal histones H2B and H3, TFIID complex acetylating transcription factors and free histones H3 and H4, NuA3 complex acetylating nucleosomal histone H3, NuA4 complex acetylating nucleosomal histones H2A and H4, as well as Elongator complex acetylating nucleosomal histones H2A, H2B, H3 and H4 (Brown et al., 2000; Hahn and Young, 2011; Krebs et al., 2011). There are differences even for HATs when they are free and when they are part of a complex. For example, free Gcn5 and Hpa1 (Elp3) are able to acetylate histone H3K14, which is the only acetylation

activity they are known to share. When Gcn5 is a part of the SAGA complex, it acetylates nucleosomal histones H2B and H3. On the other hand, when Hpa1 (Elp3) is a part of the Elongator complex, it acetylates nucleosomal histones H3 and H4 (Grant et al., 1997; Li et al., 2005).

In addition, different HATs may be involved in distinct biological functions due to different catalytic specificities and recruitment to different chromatin domains (Turner, 2000). This is supported by experimental findings where deleting a crucial SAGA subunit affected only 10 % of *S. cerevisiae* genes, while deleting an essential TFIID subunit affected as much as 90 % of *S. cerevisiae* genes (Huisinga and Pugh, 2004). In addition, SAGA complex is recruited to GAL promoters by the activator Gal4 to stimulate activation of GAL genes, Elongator complex regulates transcriptional elongation together with RNA polymerase II, and Gcn5 is recruited by the activator Gcn4 to regulate genes targeted by Gcn4 (Kuo et al., 2000; Narlikar et al., 2002). The following sections detail some HATs that are of interest in this study, namely Gcn5, Hpa1 (Elp3) and Hpa2, all of which belong to the GNAT family of HATs (Neuwald and Landsman, 1997; Angus-Hill et al., 1999).

2.3.1 Gcn5

General control nonderepressible 5 (*GCN5*) encodes a HAT, whose activity affects the transcriptional activation of target genes in vivo (Brownell et al., 1996; Kuo et al., 1998; Lee and Young, 2000; Barth and Imhof, 2010). *T. thermophila* protein p55, a *S. cerevisiae* Gcn5 homologue, was the first HAT discovered, where this observation clearly established that *S. cerevisiae* Gcn5 possessed HAT activity (Brownell et al., 1996). Gcn5 was next identified as a transcriptional regulator, which collaborates with

specific DNA-binding activators for Gcn4-mediated transcriptional activation (Georgakopoulos and Thireos, 1992; Rando and Winston, 2012).

Gcn5 homologues have been identified in diverse eukaryotic organisms, including *Schizosaccharomyces pombe* (*S. pombe*), *T. thermophila*, *Toxoplasma gondii* (*T. gondii*), *D. melanogaster*, *A. thaliana*, mouse and human (Candau et al., 1996; Smith et al., 1998; Hettmann and Soldati, 1999). Humans possess two Gcn5 homologues, which are hGcn5 and p300/CREB-binding protein associated factor (PCAF) (Sterner and Berger, 2000). In particular, there are two forms of hGcn5 — hGcn5L (long) and hGcn5S (short) (Smith et al., 1998). Both human Gcn5 homologues have conserved functions similar to that found in *S. cerevisiae* Gcn5, where hGcn5 was found to have the same activity as *S. cerevisiae* Gcn5 (Candau et al., 1996) and PCAF was found to acetylate histone H3K14 and H4K8 in vitro (Schiltz et al., 1999).

Gcn5 homologues contain an N-terminal extension and three conserved functional domains — catalytic HAT domain, Ada2 interaction domain and C-terminal bromodomain that is required for SAGA complex-mediated histone acetylation (Figure 2.5; Candau et al., 1997; Sterner et al., 1999; Sterner et al., 2002b). The N-terminal extension lies upstream of the catalytic HAT domain and varies in size in different eukaryotic organisms (Figure 2.5; Smith et al., 1998; Xu et al., 1998). The N-terminal extension of Gcn5 homologues in plants is of moderate length between 150 amino acids (aa) to 250 aa (Bhat et al., 2003), while that of lower eukaryotes is usually of a shorter length approximately less than 100 aa (Brownell et al., 1996). The N-terminal extension of Gcn5 homologues in metazoans is usually of a longer length

approximately 500 aa (Xu et al., 1998; Bhat et al., 2003). The relatively longer N-terminal extensions present in plants and metazoans may be important for substrate recognition and nuclear localisation (Xu et al., 1998; Bhat et al., 2003). For example, the removal of the N-terminal extension from mouse and human Gcn5 homologues led to the inability of Gcn5 to recognise and acetylate nucleosomal histones in vitro (Xu et al., 1998). Experimental findings also suggest that the N-terminal extension of Gcn5 homologues in maize plants may be involved in nuclear targeting of the HAT (Bhat et al., 2003).

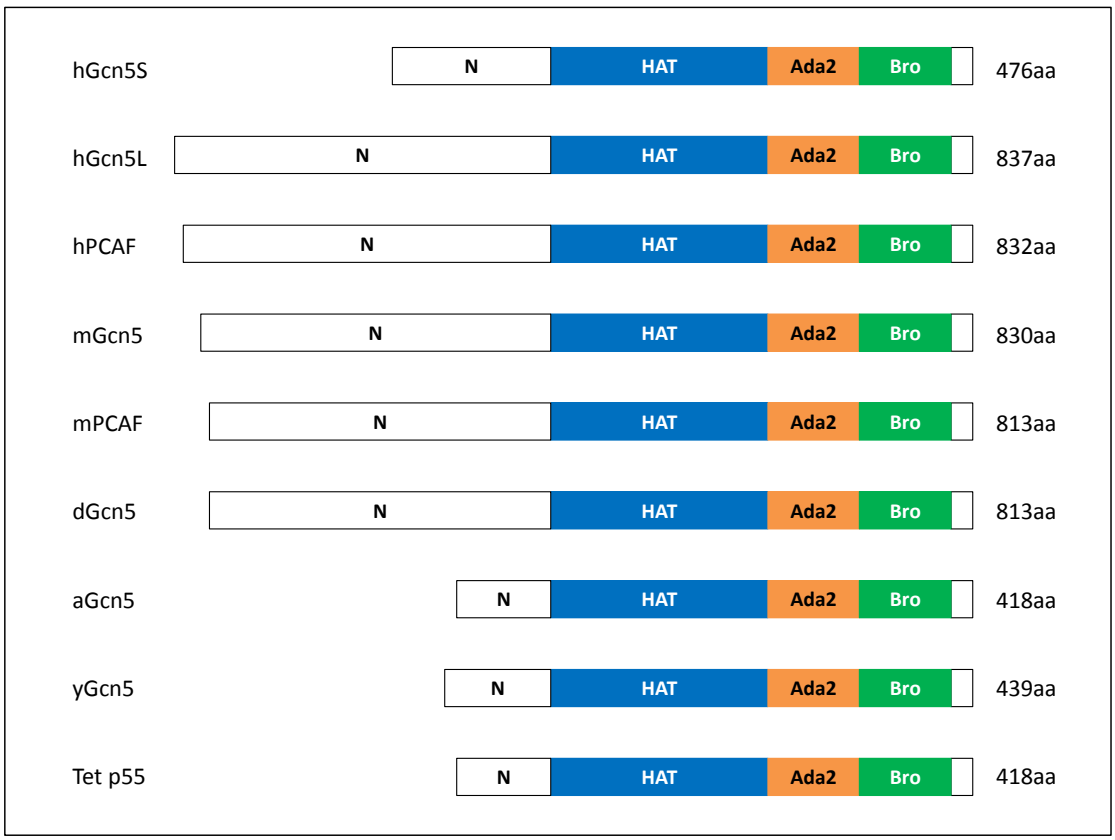

Figure 2.5 Schematic diagram of Gcn5 homologues and their sizes. All Gcn5 homologues contain three functional domains — catalytic HAT domain, Ada2 interaction domain and C-terminal bromodomain. The N-terminal extension lies upstream of the catalytic HAT domain and varies in size in different eukaryotic organisms. h: human, m: mouse, d: *D. melanogaster*, a: *A. thaliana*, y: *S. cerevisiae*, Tet: *T. thermophila*, N: N-terminal extension, HAT: catalytic HAT domain, Ada2: Ada2 interaction domain, Bro: C-terminal bromodomain.

Gcn5 functions as the catalytic subunit in three HAT complexes that are involved in transcriptional regulation — SAGA, ADA and SLIK/SALSA (Grant et al., 1997;

Pollard and Peterson, 1997; Sterner et al., 1999; Lee and Young, 2000; Lee et al., 2000; Pray-Grant et al., 2002; Sterner et al., 2002a; Krebs et al., 2011; Spedale et al., 2012). All three HAT complexes are recruited to specific gene promoters by the transcriptional activator Gcn4 (Kuo et al., 2000; Qiu et al., 2005). The transcriptional coactivator Ada2 found in all three HAT complexes functions by enhancing Gcn5 HAT activity (Candau et al., 1997; Syntichaki and Thireos, 1998).

The SAGA complex is a 1.8 MDa multi-subunit complex composed of the Ada proteins (Ada1, Ada2, Ada3, Gcn5 and Ada5), Spt proteins (Spt3, Spt7, Spt8 and Spt20), a subset of TATA-binding protein associated factors (TAF5, TAF6, TAF9, TAF10 and TAF12) and the essential Tra1 protein, where the complex functions as a cofactor to remodel chromatin for RNA polymerase II activity (Sterner et al., 1999; Sterner and Berger, 2000; Spedale et al., 2012). The ADA complex is a smaller 800 kDa multi-subunit complex composed of Gcn5, Ada2, Ada3 and Ahc1 (ADA HAT complex component 1), where the complex acetylates nucleosomes but its function remains unknown (Eberharter et al., 1999). The SLIK/SALSA complex is almost identical to the SAGA complex, except that it lacks Spt8 and contains a shortened form of Spt7 (Pray-Grant et al., 2002). It is associated with Chd1, which is a chromodomain-containing chromatin-remodelling complex, forming a link between acetylation and histone H3 methylation (Pray-Grant et al., 2005).

Experimental findings have shown that Gcn5 targets the N-terminal histone tails of histones H2B, H3 and H4 (Table 2.2; Kuo et al., 1996; Ruiz-García et al., 1997; Zhang et al., 1998; Suka et al., 2001; Kikuchi et al., 2005). When on its own, Gcn5 acetylates only free histones in vitro, primarily histone H3K14 and H4K8 (Kuo et al.,

1996; Grant et al., 1997), but Gcn5 alone is unable to acetylate nucleosomal histones (Grant et al., 1997). When in association with other subunits in HAT complexes, Gcn5 is able to acetylate nucleosomal histones in vivo (Grant et al., 1997; Grant et al., 1999; Brown et al., 2000; Roth et al., 2001). For example, Gcn5 in the SAGA complex acetylates histone H3K9, H3K14, H3K18, and H3K23, while Gcn5 in the ADA complex acetylates histone H3K14 and H3K18 (Kuo and Allis, 1998; Grant et al., 1999). In addition, Gcn5 in the ADA complex acetylates histone H2B as well (Grant et al., 1997).

Gcn5 is also involved in the combinatorial PTMs of histones. For example, phosphorylation of histone H3S10 promotes Gcn5-mediated acetylation of histone H3K14 in vitro (Lo et al., 2000). Similarly, the phosphorylation of histone H3S10 also promotes Gcn5-mediated acetylation of histone H3K14 in vivo after stimulating mammalian cells with epidermal growth factor (Cheung et al., 2000). In addition to acetylating lysine residues on N-terminal histone tails, Gcn5 also acetylates non-histone targets. For example, Gcn5 mediates *S. cerevisiae* Rsc4 K25 acetylation, where Rsc4 is a subunit of the chromatin-remodelling complex RSC (VanDemark et al., 2007; Rando and Winston, 2012). Gcn5 also mediates *D. melanogaster* chromatin-remodelling ATPase ISWI K753 acetylation (Ferreira et al., 2007) and human Cdc6 at three lysine residues flanking the cyclin docking motif (Paolinelli et al., 2009). Gcn5 itself can even be modified, where Gcn5 was found to undergo sumoylation that does not affect Gcn5 activity in vitro but may contribute to transcriptional regulation (Sterner et al., 2006).

Gcn5 is involved in transcriptional regulation, both on a global level and at specific

genes. For example, Gcn5 in the SAGA complex is recruited to the promoters of active genes on a global level, where Gcn5 localises to the promoter instead of spreading into the open reading frame (ORF) (Robert et al., 2004). Under certain conditions like amino acid starvation or phosphate starvation, Gcn5 is recruited on a gene specific basis. For example, Gcn5 was found to maintain substantial acetylation activity specifically at the *HIS3* promoter under histidine starvation conditions (Kuo et al., 2000). In a second example, cells lacking Gcn5 were found to have severely impaired basal level activation of the *PHO5* promoter, which suggests that Gcn5 may mediate chromatin remodelling under phosphate starvation conditions (Gregory et al., 1998; Rando and Winston, 2012).

Besides transcriptional defects at promoter regions, deletion of *GCN5* also leads to disruption of chromatin structure, chromosomal fusions, dysfunctional telomeres, increased G2 cells with unsegregated nuclei, delayed entrance to mitosis, meiotic arrest in diploid cells, cerebellar degeneration, retinal degeneration and embryonic lethality (Gregory et al., 1998; Pérez-Martín and Johnson, 1998; Burgess et al., 1999; Burgess and Zhang, 2010; Turner et al., 2010; Vernarecci et al., 2010; Chen et al., 2012). In addition, cells lacking Gcn5 also exhibit temperature sensitivity at 37°C, slow growth on minimal media, increased sensitivity to microtubule depolymerising agents and hypersensitivity to overexpression of Clb2, which is a B-type cyclin involved in normal cell cycle progression (Zhang et al., 1998; Turner et al., 2010).

2.3.1.1 *HIS3* as a model for the study of Gcn5

HIS3 is one of the known targets of Gcn5 regulation, where it codes for imidazoleglycerol phosphate dehydratase, which is an enzyme that catalyses the sixth

step in the histidine synthesis pathway (Sinha et al., 2004). The cross pathway regulatory system named general amino acid control regulates *HIS3* transcription (Harashima and Hinnebusch, 1986; Ljungdahl and Daignan-Fornier, 2012). The positive regulatory protein Gcn4 regulates most of the genes involved in this pathway (Joo et al., 2011). Under normal growth conditions, *HIS3* has a low basal level of transcription and does not require Gcn4 function (Oettinger and Struhl, 1985). Under histidine starvation conditions, Gcn4 production is stimulated, leading to transcriptional activation of the *HIS3* gene and other amino acid biosynthetic genes (Joo et al., 2011). This histidine starvation condition can be generated by the addition of the chemical 3-AT, which is an analogue that competitively inhibits imidazoleglycerol phosphate dehydratase (Joo et al., 2011).

Gcn5 HAT activity is important for both basal level and activated level of *HIS3* expression and acetylation (Mai et al., 2006). Under histidine starvation conditions, *HIS3* transcription and histone hyperacetylation is induced, where Gcn4 has been shown to recruit Gcn5 to the *HIS3* promoter, leading to activated levels of *HIS3* expression (Kuo and Allis, 1998; Kuo et al., 1998; Mai et al., 2000). *HIS3* regulation by the well-studied cis-acting elements (DNA and nucleosomes) and trans-acting elements (transcriptional coactivators) further aid the detailed study of the mechanisms for HAT targeting (Iyer and Struhl, 1995; Rando and Winston, 2012). Although *HIS3* and its neighbouring genes *PET56* and *DED1* are closely spaced, their expression has been shown to be independent of each other (Struhl, 1985; Struhl, 1986). This allows for a stringent test to determine whether histone acetylation is a global event or a targeted event (Kuo et al., 2000). The *HIS3* locus also allows for further analysis to map histone acetylation at single nucleosome level due to its

phased nucleosomal array organisation (Losa et al., 1990). Due to the reasons detailed above, the *HIS3* gene is an attractive model for studying the functions of Gcn5.

2.3.2 Hpa1 (Elp3)

Hpa1 (Histone and other protein acetyltransferase 1), also known as Elp3 (Elongator protein 3), is the HAT present in the Elongator complex, which is a six subunit complex that associates with the elongating form of RNA polymerase II (Otero et al., 1999; Wittschieben et al., 1999; Winkler et al., 2001). The association of the Elongator complex with RNA polymerase II requires the phosphorylation of RNA polymerase II at its C-terminal domain, before elongation can occur (Otero et al., 1999). As nucleosomes inhibit transcriptional elongation, Hpa1 HAT activity on nucleosomal histones may help increase the accessibility of the transcriptional machinery to DNA (Tse et al., 1998). When on its own, Hpa1 acetylates the N-terminal histone tails of all four core histones H2A, H2B, H3 and H4 in vitro (Wittschieben et al., 1999). When in association with other subunits in the Elongator complex, Hpa1 acetylates primarily histone H3K14 and H4K8 in vivo (Winkler et al., 2002). In addition, human Hpa1 was found to be functionally similar to *S. cerevisiae* Hpa1, where hHpa1 can rescue *S. cerevisiae HPA1* deletion strain (Li et al., 2005).

Although different HATs have their own specific targets, those of Gcn5 and Hpa1 sometimes overlap. For example, both Gcn5 in the SAGA complex and Hpa1 in the Elongator complex preferentially acetylate histone H3K14 (Grant et al., 1999; Wittschieben et al., 2000). However, Gcn5 is involved in SAGA-mediated transcriptional activation, while Hpa1 is involved in transcriptional elongation after activation (Georgakopoulos and Thireos, 1992; Wittschieben et al., 1999). More

importantly, the Δ*GCN5*Δ*HPA1* double deletion strain exhibited phenotypes similar to the *GCN5* deletion strain, which suggests that Gcn5 interacts with Hpa1 and this interaction is specific for their roles in transcriptional regulation (Wittschieben et al., 2000).

Deletion of *HPA1* led to a decreased activation of target genes, slow growth adaptation, salt sensitivity and temperature sensitivity (Otero et al., 1999; Wittschieben et al., 1999). More interestingly, the double deletion strain did not exhibit lethality, which suggests that there exists some redundancy of HAT activities (Wittschieben et al., 2000). However, the double deletion strain exhibited increased temperature sensitivity as compared to the single deletion strains (Turner et al., 2010; Wittschieben et al., 2000). In addition, unlike the single deletion strains, the double deletion strain was unable to grow on alternative carbon sources like galactose, raffinose and sucrose (Wittschieben et al., 2000).

2.3.3 Hpa2 and Hpa3

Hpa2 (Histone and other protein acetyltransferase 2) is a HAT that has similarity to Gcn5, Hpa1 (Elp3), Hpa3 and Hat1 (Angus-Hill et al., 1999). Hpa2 was found to form stable dimers in solution, which associate in the presence of the cofactor acetyl coenzyme A to form tetramers, where the crystal structure of the tetramer has been elucidated (Angus-Hill et al., 1999). Hpa2 is also able to autoacetylate itself in an intermolecular reaction, as well as acetylate histone H3K4, H3K14, H4K5 and H4K12 in vitro, although it has a preference for histone H3K14 (Angus-Hill et al., 1999, Sterner and Berger, 2000). The function of Hpa2 in vivo is still unknown, as deletion of *HPA2* conferred no apparent growth phenotype (Angus-Hill et al., 1999). However,

experimental findings have shown that Hpa2 may target a small proportion of genes for transcriptional activation (Rosaleny et al., 2007).

Hpa2 and Hpa3 were found to share a 49 % DNA sequence identity and 81 % amino acid sequence identity (Angus-Hill et al., 1999). However, although Hpa3 was also able to autoacetylate itself, it exhibited very weak HAT activity in vitro as compared to Hpa2 (Angus-Hill et al., 1999, Sterner and Berger, 2000). In addition, Gcn5 may also interact with Hpa2, where both HATs preferentially acetylate histone H3K14 (Angus-Hill et al., 1999; Grant et al., 1999). Experimental findings have also shown that the Δ*GCN5*Δ*HPA2* double deletion strain is viable (Howe et al., 2001).

2.4 Diseases

Histones are dynamic and integral in regulating chromatin condensation and DNA accessibility, where PTMs of histones are important in the regulation of all aspects of DNA biology, including transcriptional activation or repression, homologous recombination, DNA repair, DNA replication, cell cycle regulation and chromatin compaction in apoptosis. Thus, aberrant patterns of PTMs of histones predispose one towards diseases due to the dysregulation of gene expression (Portela and Esteller, 2010; Sawan and Herceg, 2010). In addition, other epigenetic modifications like DNA methylation and nucleosome positioning have also been implicated in diseases, which include cancers, neurological disorders and autoimmune diseases (Portela and Esteller, 2010; Sun et al., 2012).

Experimental findings are gradually elucidating the role of epigenetics in tumorigenesis, which often involve global changes in patterns of PTMs of histones,

DNA methylation and the expression profiles of chromatin-remodelling complexes in different types of cancers like myeloid and lymphoblastic leukaemia, breast, colon, liver, lung, skin and prostate cancers (Chi et al., 2010; Godley and Le Beau, 2012). Besides cancers, neurological disorders were also found to arise due to aberrant histone modifications like histone hypoacetylation and hypermethylation or hypomethylation of DNA. This includes neurodevelopmental disorders like Coffin-Lowry syndrome, Rett syndrome and Rubinstein-Taybi syndrome, neurodegenerative diseases like Alzheimer's disease, Huntington's disease and Parkinson's disease, as well as neurological disorders like amyotrophic lateral sclerosis, epilepsy and multiple sclerosis (Urdinguio et al., 2009; Ghizzoni et al., 2011). In addition, aberrant epigenetic mechanisms, especially hypermethylation or hypomethylation of DNA, have been shown to lead to autoimmune diseases like rheumatoid arthritis, systemic lupus erythromatus and Type 1 diabetes mellitus (Meda et al., 2011; Villeneuve et al., 2011).

In particular, dysregulation of histone acetylation events by HATs and histone deacetylation events by HDACs have been shown to lead to a diverse range of diseases (Timmermann et al., 2001). For example, the disease mechanism in Huntington's disease has been proposed to be due to defects in the HAT activity of transcription factors, which arose via the interaction with the mutant Huntingtin protein that led to a down regulation of the expression of specific genes (Bithell et al., 2009; Ross and Shoulson, 2009; Selvi et al., 2010). In a second example, acetylation of histone H4K8 and H4K12 was found to be significantly elevated in mice ulcerative colitis models (Tsaprouni et al., 2011). In a third example, the loss of acetylation at histone H4K16 together with trimethylation at histone H4K20 has been shown to be a

common hallmark of human cancer (Fraga et al., 2005; Cohen et al., 2011; Füllgrabe et al., 2011). In fact, acetylation at histone H4K16 was found to have profound effects on chromatin structure (Shogren-Knaak et al., 2006; Füllgrabe et al., 2011), where the loss of histone H4K16 acetylation was mediated by overexpressed or mutant HDACs in different cancer types (Shogren-Knaak and Peterson, 2006; Füllgrabe et al., 2011) that led to a global imbalance of histone acetylation and gene silencing. Even viral oncoprotein adenovirus-5 E1A has been shown to interact with HATs like p300/CREB-binding protein, which promotes oncogenic transformation of adenovirus infected human primary fibroblast (Frisch and Mymryk, 2002).

Thus, it is of no surprise that the inhibition of HDACs is an emerging novel therapeutic strategy against cancer and neurological disorders like Alzheimer's disease and stroke (Chuang et al., 2009; Lane and Chabner, 2009; Di Marcotullio et al., 2011; Xu et al., 2011). Although the chemotherapeutic potential of HAT targets requires more validation, the anti-cancer effects of HDAC inhibitors are well known, with vorinostat approved for treatment of cutaneous T-cell lymphoma and other HDAC inhibitors like depsipeptide and MGCD0103 in the advanced stages of clinical development (Lane and Chabner, 2009; Sarfstein et al., 2011; Fujita et al., 2012). This study aims to further elucidate the molecular pathways at the transcriptional level, particularly on the effects of HATs, which could form the basis for the design of novel approaches to treat human diseases.

3. Materials and methods

3.1 Project flowchart

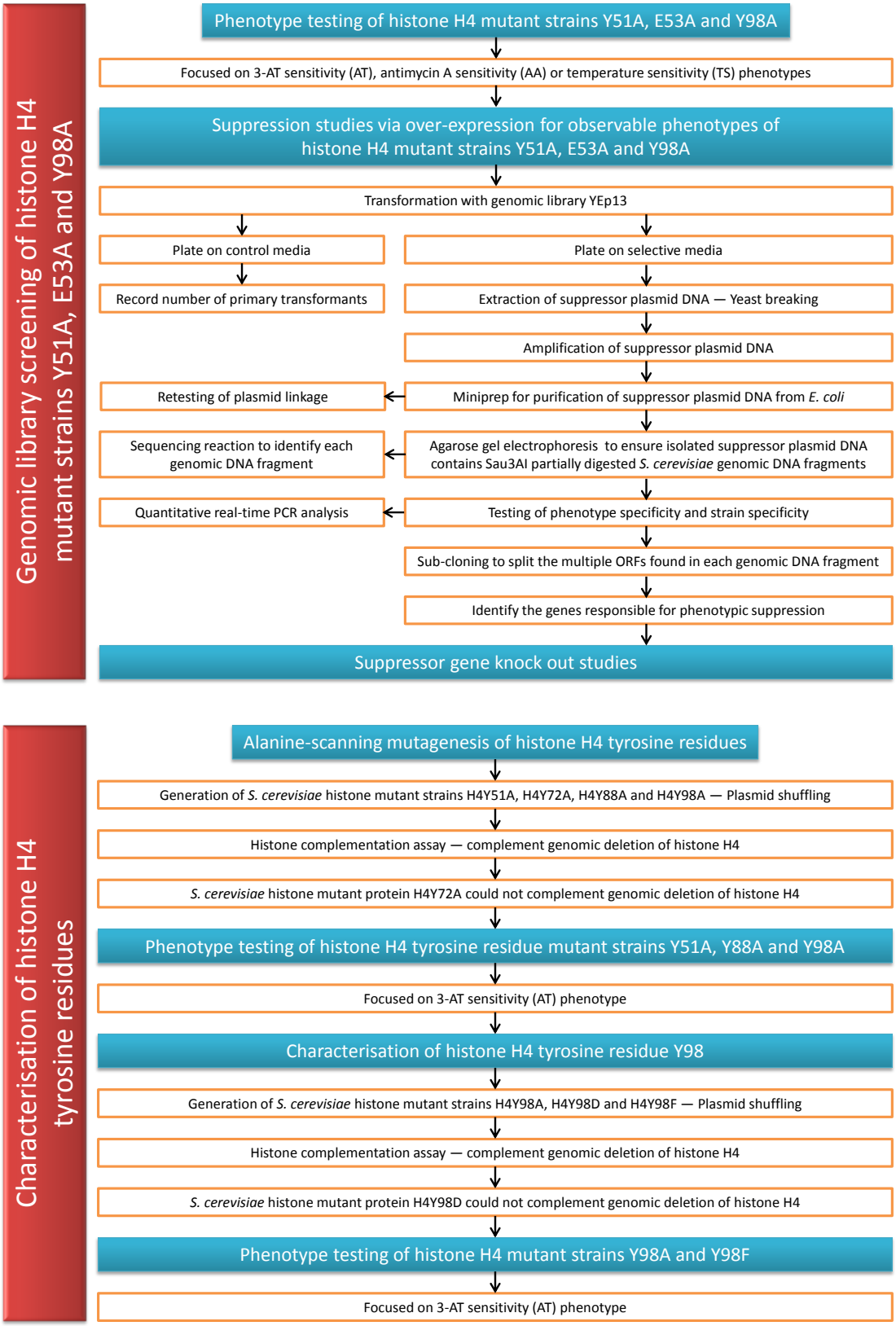

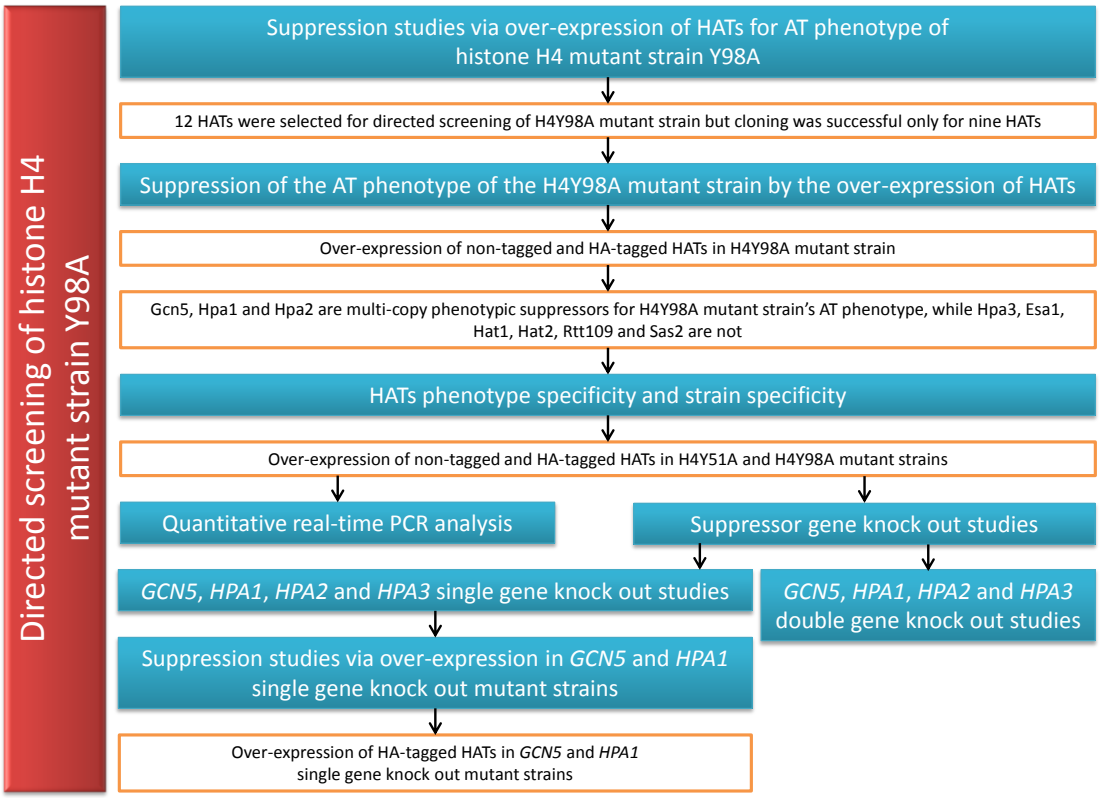
Directed screening of histone H4 mutant strain Y98A
Suppression studies via over-expression of HATs for AT phenotype of histone H4 mutant strain Y98A
12 HATs were selected for directed screening of H4Y98A mutant strain but cloning was successful only for nine HATs
Suppression of the AT phenotype of the H4Y98A mutant strain by the over-expression of HATs
Over-expression of non-tagged and HA-tagged HATs in H4Y98A mutant strain
Gcn5, Hpa1 and Hpa2 are multi-copy phenotypic suppressors for H4Y98A mutant strain's AT phenotype, while Hpa3, Esa1, Hat1, Hat2, Rtt109 and Sas2 are not
HATs phenotype specificity and strain specificity
Over-expression of non-tagged and HA-tagged HATs in H4Y51A and H4Y98A mutant strains
Quantitative real-time PCR analysis
Suppressor gene knock out studies
GCN5, HPA1, HPA2 and HPA3 single gene knock out studies
GCN5, HPA1, HPA2 and HPA3 double gene knock out studies
Suppression studies via over-expression in GCN5 and HPA1 single gene knock out mutant strains
Over-expression of HA-tagged HATs in GCN5 and HPA1 single gene knock out mutant strains

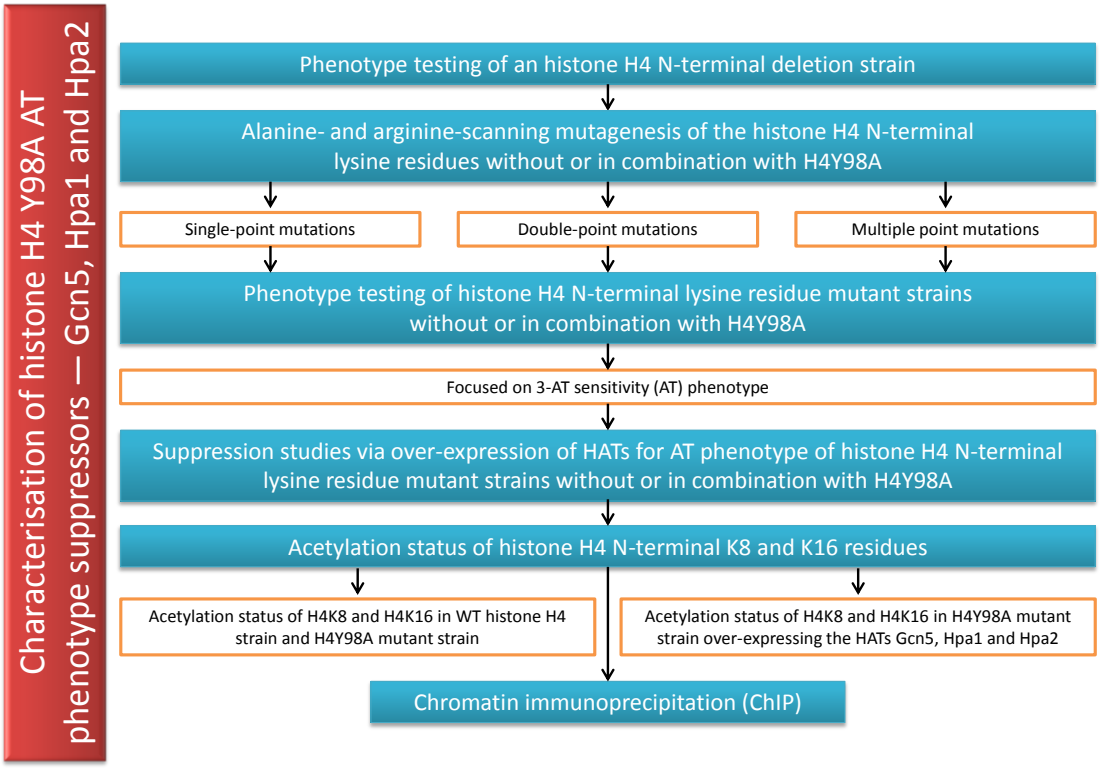
Characterisation of histone H4 Y98A AT phenotype suppressors — Gcn5, Hpa1 and Hpa2
Phenotype testing of an histone H4 N-terminal deletion strain
Alanine- and arginine-scanning mutagenesis of the histone H4 N-terminal lysine residues without or in combination with H4Y98A
Single-point mutations
Double-point mutations
Multiple point mutations
Phenotype testing of histone H4 N-terminal lysine residue mutant strains without or in combination with H4Y98A
Focused on 3-AT sensitivity (AT) phenotype
Suppression studies via over-expression of HATs for AT phenotype of histone H4 N-terminal lysine residue mutant strains without or in combination with H4Y98A
Acetylation status of histone H4 N-terminal K8 and K16 residues
Acetylation status of H4K8 and H4K16 in WT histone H4 strain and H4Y98A mutant strain
Acetylation status of H4K8 and H4K16 in H4Y98A mutant strain over-expressing the HATs Gcn5, Hpa1 and Hpa2
Chromatin immunoprecipitation (ChIP)

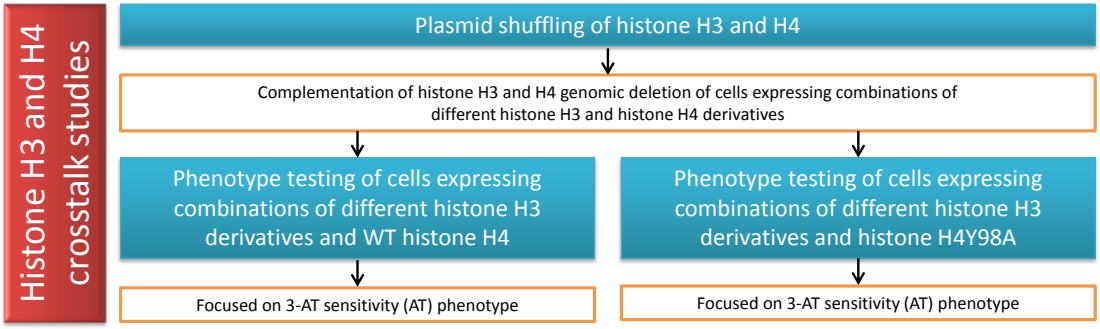
Histone H3 and H4 crosstalk studies
Plasmid shuffling of histone H3 and H4
Complementation of histone H3 and H4 genomic deletion of cells expressing combinations of different histone H3 and histone H4 derivatives
Phenotype testing of cells expressing combinations of different histone H3 derivatives and WT histone H4
Phenotype testing of cells expressing combinations of different histone H3 derivatives and histone H4Y98A
Focused on 3-AT sensitivity (AT) phenotype
Focused on 3-AT sensitivity (AT) phenotype

3.2 Materials

3.2.1 *E. coli* strains

Table 3.1 *E. coli* strains used

***E. coli* strain**	**Genotype**	**Usage**
DH5α	*F⁻ Φ80dlacZΔM15 Δ(lacZYA-argF)U169 deoR recA1 endA1 hsdR17($r_k^- m_k^+$) phoA supE44 λ⁻ thi-1 gyrA96 relA1*	Used for chemical transformation of plasmid DNA
DH10β	*F⁻ mcrA Δ(mrr⁻hsdRMS⁻mcrBC) Φ80dlacZΔM15 ΔlacX74 deoR recA1 endA1 araD139Δ(ara,leu)7697 galU galK λ⁻ rpsL nupG*	Used for electroporation of plasmid DNA as they are more electrocompetent

3.2.2 *S. cerevisiae* strains

Table 3.2 Parental *S. cerevisiae* strains used

Parental *S. cerevisiae* strain	**Genotype**	**Source**
BY4741	*MATa his3Δ1 leu2Δ0 met15Δ0 ura3Δ0*	EUROSCARF
BY4741ΔW	*MATa his3Δ1 leu2Δ0 met15Δ0 ura3Δ0 trp1::hisG*	Lab collection
BY4741ΔW::HIS3	*MATa leu2Δ0 met15Δ0 ura3Δ0 trp1::hisG*	Lab collection
BY4742	*MATα his3Δ1 leu2Δ0 lys2Δ0 ura3Δ0*	EUROSCARF
BY4742ΔW	*MATα his3Δ1 leu2Δ0 lys2Δ0 ura3Δ0 trp1::hisG*	Lab collection
BY4742ΔW::HIS3	*MATα leu2Δ0 lys2Δ0 ura3Δ0 trp1::hisG*	Lab collection

The parental *S. cerevisiae* strains BY4741 and BY4742 were derived from EUROSCARF (http://web.uni-frankfurt.de/fb15/mikro/euroscarf/). The *TRP1* gene was deleted with the help of NKY1009 (Alani et al., 1987) and the *HIS3* gene was repaired with the help of a genomic BamHI fragment containing the entire *HIS3* gene obtained from puc8+HIS3.

Table 3.3 *S. cerevisiae* knock out strains used

***S. cerevisiae* knock out strain**	**Source**	***S. cerevisiae* knock out strain**	**Source**
BY4741ΔHPA2	EUROSCARF	BY4742ΔGCN5	EUROSCARF
BY4741ΔKAR4	EUROSCARF	BY4742ΔHPA1	EUROSCARF
BY4741ΔMCK1	EUROSCARF	BY4742ΔHPA2	EUROSCARF
BY4741ΔMSC3	EUROSCARF	BY4742ΔHPA3	EUROSCARF
BY4741ΔSIP5	EUROSCARF	BY4742ΔWΔGAL4	Lab collection
BY4741ΔSKI8	EUROSCARF	BY4742ΔWΔGCN4	Lab collection
BY4741ΔSLH1	EUROSCARF	BY4742ΔWΔGCN5	This study
BY4741ΔYAP1	EUROSCARF	BY4742ΔWΔHPA1	This study
BY4741ΔYHR151C	EUROSCARF	BY4742ΔWΔHPA2	This study
BY4741ΔYHR177W	EUROSCARF	BY4742ΔWΔHPA3	This study
BY4741ΔWΔGCN4	Lab collection	BY4742ΔWΔHHF1/2 + PactT316-HA-HHF1	Lab collection

The endogenous *HHF1* and *HHF2* genes in the *S. cerevisiae* strain BY4742ΔWΔHHF1/2 + PactT316-HA-HHF1 were replaced by the *HIS3* gene through homologous recombination, in the presence of PactT316-HA containing WT *HHF1* gene flanked by 500 bp of promoter and terminator at their respective ends.

Table 3.4 *S. cerevisiae* double knock out strains used

***S. cerevisiae* double knock out strain**	**Source**
BY4742ΔWΔGCN5ΔHPA1	This study
BY4742ΔWΔGCN5ΔHPA2	This study
BY4742ΔWΔGCN5ΔHPA3	This study
BY4742ΔWΔHHTF1/2 + YCplac33-HHTF2	Lab collection

The endogenous *HPA1* and *HPA3* genes in the *S. cerevisiae* strain BY4742ΔWΔGCN5 were deleted with the help of puc8+LEU2. The endogenous *HPA2* gene in the *S. cerevisiae* strain BY4742ΔWΔGCN5 was deleted with the help of NKY51 (Alani et al., 1987). The endogenous *HHT2* and *HHF2* genes in the *S. cerevisiae* strain BY4742ΔWΔHHTF1/2 + YCplac33-HHTF2 were deleted with the help of NKY51 (Alani et al., 1987), after which the endogenous *HHT1* and *HHF1*

genes were deleted with the help of puc8+HIS3 through homologous recombination, in the presence of YCplac33 containing WT *HHTF2* gene flanked by 500 bp of promoter and terminator at their respective ends.

3.2.3 Plasmids

3.2.3.1 Plasmids used for gene targeting

NKY51 (*URA3* marked), NKY1009 (*URA3* marked), puc8+HIS3 (*HIS3* marked) and puc8+LEU2 (*LEU2* marked) targeting vectors from laboratory collection were used (refer to section 3.3.2.4).

3.2.3.2 Plasmids used for genetic interaction analysis

Table 3.5 Plasmids used for genetic interaction analysis

Plasmid	**Relevant characteristics**	**Markers**	**Source**
Bank 366 (p366)	Single-copy vector	Amp^R, *LEU2*	P. Heiter, ATCC 77162
Bank 13 (YEp13)	Multi-copy vector	Amp^R, *LEU2*	Nasmyth and Reed, 1980
Bank 13 (YEp13) — gene derivatives (Appendix 8.1, Table 8.1)	Multi-copy vector	Amp^R, *LEU2*	This study
PactT424	Multi-copy vector where proteins are under the control of the *ACT1* promoter and terminator	Amp^R, *TRP1*	Lab collection
PactT424 — genes inserted (Appendix 8.2, Table 8.2)	Multi-copy vector where proteins are under the control of the *ACT1* promoter and terminator	Amp^R, *TRP1*	This study
PactT424-HA	Multi-copy vector where haemagglutinin (HA) fusion proteins are under the control of the *ACT1* promoter and terminator	Amp^R, *TRP1*	Lab collection
PactT424-HA — genes inserted (Appendix 8.2, Table 8.2)	Multi-copy vector where haemagglutinin (HA) fusion proteins are under the control of the *ACT1* promoter and terminator	Amp^R, *TRP1*	This study

Plasmid	Relevant characteristics	Markers	Source
YCplac22	Single-copy vector	Amp^R, *TRP1*	Lab collection
YCplac22 — *HHF1* mutants (Appendix 8.3, Table 8.3)	Single-copy vector	Amp^R, *TRP1*	This study
YCplac111	Single-copy vector	Amp^R, *LEU2*	Lab collection
YCplac111-HHF1 ΔN(1-19)	Single-copy vector containing *HHF1* with N-terminus deletion of amino acids 1-19	Amp^R, *LEU2*	Lab collection
YCplac111 — *HHT1* and *HHF1* mutants (Appendix 8.4, Table 8.4; Appendix 8.5, Table 8.5)	Single-copy vector	Amp^R, *LEU2*	This study
YEplac181	Multi-copy vector	Amp^R, *LEU2*	Lab collection
YEplac181 — genes inserted (Appendix 8.6, Table 8.6)	Multi-copy vector	Amp^R, *LEU2*	This study

BamHI site had been used to clone Sau3AI partially digested *S. cerevisiae* genomic DNA fragments to generate library plasmids Bank 366 (P. Heiter, ATCC 77162) and Bank 13 (Nasmyth and Reed, 1980).

3.3 Methods

3.3.1 Generation of plasmids

3.3.1.1 Polymerase chain reaction (PCR)

PCR was carried out to amplify the desired gene, so that it could be inserted into a vector for genetic expression. For most genes, a one-step PCR was carried out using primers designed to anneal to the 5'atg and 3'stp ends of the desired gene (Table 3.6), where the ORF of the gene would be expressed under the control of different promoters and terminators. For some genes, a one-step PCR was carried out using primers designed to anneal to the 5'pro and 3'ter ends of the desired gene (Appendix 8.7, Table 8.7), where the ORF of the gene would be expressed under the control of endogenous promoters and terminators. For knock out targeting vectors, a one-step PCR was carried out using primers designed to anneal to the selected gene promoter and terminator sequences (Table 3.7). All primers were synthesised by 1st BASE.

Table 3.6 Primers used for amplification of selected histone acetyltransferases in one-step PCR

Gene	Primer name	Sequence
ESA1	5'ESA1atg-EcoRI	GCCGAATTCATGTCCCATGACGGAAAA
	3'ESA1stp-SalI	GCCGTCGACTTACCAGGCAAAGCGTAA
HAT1	5'HAT1atg-EcoRI	GCCGAATTCATGTCTGCCAATGATTTC
	3'HAT1stp-SalI	GCCGTCGACTTAACCTTGAGATTTATTTAT
HAT2	5'HAT2atg-EcoRI	GCCGAATTCATGGAAAACCAAGAGAAAC
	3'HAT2stp-SalI	GCCGTCGACTTAGCTTATTATATCCTTGT
HPA3	5'HPA3atg-EcoRI	GCCGAATTCATGAAAAAGACCCCAGAC
	3'HPA3stp-SalI	GCCGTCGACTCAGTATCCGTTTCTCTT
RTT109	5'RTT109atg-EcoRI	GCCGAATTCATGTCACTGAATGACTTC
	3'RTT109stp-SalI	GCCGTCGACTCAAGTTTTAGGCAAGGC
SAS2	5'SAS2atg-EcoRI	GCCGAATTCATGGCAAGATCTTTAAGTC
	3'SAS2stp-SalI	GCCGTCGACTAGTCATCTATCAGCAA

Table 3.7 Primers used for amplification of selected gene promoter and terminator sequences in one-step PCR

Gene	Primer name	Sequence
GCN5	5'Pgcn5-EcoRI	GCCGAATTCAAGTACTGAGTACGTTAAC
	3'Pgcn5-BglII	GCCAGATCTAATGTAGAATACGAACC
	5'Tgcn5-NsiIBamHI	GCCATGCATGGATCCTGCGTAGAAGAAGCTTTT
	3'Tgcn5-SalI	GCCGTCGACTGGTTATCAACTTTTCCAT
HPA1	5'Phpa1-EcoRI	GCCGAATTCTCAAGCAGGAGGGCTG
	3'Phpa1-BglII	GCCAGATCTTTGTCAGGGTGTTCTT
	5'Thpa1-NsiIBamHI	GCCATGCATGGATCCAGGTAAATAGAACTTTTATG
	3'Thpa1-SalI	GCCGTCGACTTATTTATATGGAGGTGG
HPA2	5'Phpa2-EcoRI	GCCGAATTCATAGTTTTGTAAACGTATAT
	3'Phpa2-BglII	GCCAGATCTGCTACACAGAAAGGGCTGTT
	5'Thpa2-BglII	GCCAGATCTAAACACTAATTACCTCAGTA
	3'Thpa2-SalI	GCCGTCGACGGCACCGCTATCCTATGTTT

For a one-step PCR carried out in a 200 µl PCR tube, 16.7 µl sterile water, 0.2 µl template DNA (either a known plasmid or the *S. cerevisiae* genomic library Bank 366), 0.25 µl 5' primer, 0.25 µl 3' primer, 2 µl 10X Expand High Fidelity PCR Buffer, 0.4 µl 10 mM dNTP, 0.2 µl Expand High Fidelity Polymerase were added in sequence and mixed. The Expand High Fidelity Polymerase (Roche) was used as it generates PCR products of high fidelity, due to its 3'-5' exonuclease proofreading activity.

For certain genes and *HHF1* mutants, site-directed mutagenesis was carried out using either one-step or two-step PCR. In the two-step PCR for certain histone acetyltransferases, an additional pair of primers was designed such that the internal EcoRI site was mutated to allow for subsequent cloning, without changing the identity of the original amino acid — silent mutation based on the degeneracy of the genetic code (Table 3.8). In the two-step PCR for *HHF1* mutants, an additional pair of primers was designed such that the original amino acid's codon was changed by replacing the bases in the codon (Tables 3.9, 3.10, 3.11, 3.12, 3.13 and 3.14). In order to ensure sufficient specificity and sufficient binding strength of the designed primers,

12 to 15 complementing bases flanking both upstream and downstream of the mutation were added. All primers were synthesised by 1st BASE.

Table 3.8 Primers used for amplification of selected histone acetyltransferases in two-step PCR

Gene	Primer name	Sequence
GCN5	5'GCN5atg-EcoRI	GCCGAATTCATGGTCACAAAACATCAG
	3'GCN5stp-SalI	GCCGTCGACTTAATCAATAAGGTGAGAAT
	GCN5+koEcoRI	CTTTCGATAAGAGAGAGTTCGCAGAAATTGTTT
	GCN5-koEcoRI	AAACAATTTCTGCGAACTCTCTCTTATCGAAAG
HPA1	5'HPA1atg-EcoRI	GCCGAATTCATGGCTCGTCATGGAAAA
	3'HPA1stp-SalI	GCCGTCGACTTAAATTCTTTTCGACATGT
	HPA1+koEcoRI	ATACATATAGAAAAGAGTTCACCTCCCAGAGGA
	HPA1-koEcoRI	TCCTCTGGGAGGTGAACTCTTTTCTATATGTAT
HPA2	5'HPA2atg-EcoRI	GCCGAATTCATGTCCAACACTAGCGAA
	3'HPA2stp-SalI	GCCGTCGACTTAATATCCCTTCCTCTTG
	HPA2+koEcoRI	TCTCTATGTTGATGAAAATTCTAGGGTCAAA
	HPA2-koEcoRI	TTTGACCCTAGAATTTTCATCAACATAGAGA

Table 3.9 Primers and PCR strategy used for amplification of HHF1 WT

HHF1	Primer name	Sequence	PCR strategy
WT (promoter to terminator)	5'HHF1pro-EcoRI	GCCGAATTCGTTATCTTCCACGCTAA	One-step PCR Template: *S. cerevisiae* genomic library Bank 366
	3'HHF1ter-SalI	GCCGCCGTCGACCACACACGAAAATCCTG	
WT (atg-BglII to stp)	5'HHF1atg-BglII	GCCAGATCTAAAATGTCCGGTAGAGGTAAAGG	
	3'HHF1stp-NotI	GCCGCGGCCGCTTAACCACCGAAACCGTA	
WT (atg-EcoRI to stp for insertion into PactT424-HA)	5'HHF1atg-EcoRI	GCCGAATTCAAAATGTCCGGTAGAGGTAAAGG	
	3'HHF1stp-NotI	GCCGCGGCCGCTTAACCACCGAAACCGTA	

Table 3.10 Primers and PCR strategy used for amplification of HHF1 mutants at positions Y51, Y72, Y88 and Y98

HHF1	Primer name	Sequence	PCR strategy
Y51A	Hhf-y51a+	TCTGGTTTGATCGCCGAAGAAGTCAG	Two-step PCR Template: YCplac111-HHF1 WT Forward primer: 5'HHF1pro-EcoRI Reverse primer: 3'HHF1ter-SalI
	Hhf-y51a-	CTGACTTCTTCGGCGATCAAACCAGA	
Y72A	Hhf-y72a+	GACTCTGTTACCGCCACCGAACACGC	
	Hhf-y72a-	GCGTGTTCGGTGGCGGTAACAGAGTC	
Y88A	Hhf-y88a+	TTGGATGTTGTTGCTGCTTTGAAGAG	
	Hhf-y88a-	CTCTTCAAAGCAGCAACAACATCCAA	
Y98A	3'HHF1-Y98Astp-NotI	GCCGCCGCGGCCGCTAACCACCGAAACCGGCTAAGGTTCTACCTTGTCTC	One-step PCR Template: YCplac111-HHF1 WT Forward primer: 5'HHF1atg-BglII or 5'HHF1atg-EcoRI (for insertion into PactT424-HA)
Y98D	3'HHF1-Y98Dstp-NotI	GCCGCGGCCGCTTAACCACCGAAACCGTCTAAGGTTCTACC	
Y98F	3'HHF1-Y98Fstp-NotI	GCCGCGGCCGCTTAACCACCGAAACCGAATAAGGTTCTACC	

Table 3.11 Primers and PCR strategy used for amplification of HHF1 single alanine mutants in combination with Y98A

HHF1	Primer name	Sequence	PCR strategy
K5A / K5A Y98A	Hhf-k5a+	TCCGGTAGAGGTGCAGGTGGTAAAGG	Two-step PCR Template: YCplac111-HHF1 WT or YCplac111-HHF1 Y98A Forward primer: 5'HHF1pro-EcoRI Reverse primer: 3'HHF1ter-SalI
	Hhf-k5a-	CCTTTACCACCTGCACCTCTACCGGA	
K8A / K8A Y98A	Hhf-k8a+	GGTAAAGGTGGTGCAGGTCTAGGTAA	
	Hhf-k8a-	TTACCTAGACCTGCACCACCTTTACC	
K12A / K12A Y98A	Hhf-k12a+	AAAGGTCTAGGTGCAGGTGGTGCCAA	
	Hhf-k12a-	TTGGCACCACCTGCACCTAGACCTTT	
K16A / K16A Y98A	Hhf-k16a+	AAAGGTGGTGCCGCGCGTCACAGAAA	
	Hhf-k16a-	TTTCTGTGACGCGCGGCACCACCTTT	
K20A / K20A Y98A	Hhf-k20a+	AAGCGTCACAGAGCGATTCTAAGAGA	
	Hhf-k20a-	TCTCTTAGAATCGCTCTGTGACGCTT	

Table 3.12 Primers and PCR strategy used for amplification of HHF1 single arginine mutants in combination with Y98A

HHF1	Primer name	Sequence	PCR strategy
K5R / K5R Y98A	Hhf-k5r+	ATGTCCGGTAGAGGTAGAGGTGGTAAAGGTCT	Two-step PCR Template: YCplac111-HHF1 WT or YCplac111-HHF1 Y98A Forward primer: 5'HHF1pro-EcoRI Reverse primer: 3'HHF1ter-SalI
	Hhf-k5r-	AGACCTTTACCACCTCTACCTCTACCGGACAT	
K8R / K8R Y98A	Hhf-k8r+	AGAGGTAAAGGTGGTAGAGGTCTAGGTAAAGG	
	Hhf-k8r-	CCTTTACCTAGACCTCTACCACCTTTACCTCT	
K12R / K12R Y98A	Hhf-k12r+	GGTAAAGGTCTAGGTAGAGGTGGTGCCAAGCG	
	Hhf-k12r-	CGCTTGGCACCACCTCTACCTAGACCTTTACC	
K16R / K16R Y98A	Hhf-k16r+	GGTAAAGGTGGTGCCAGACGTCACAGAAAGAT	
	Hhf-k16r-	ATCTTTCTGTGACGTCTGGCACCACCTTTACC	
K20R / K20R Y98A	Hhf-k20r+	GCCAAGCGTCACAGAAGAATTCTAAGAGATAA	
	Hhf-k20r-	TTATCTCTTAGAATTCTTCTGTGACGCTTGGC	

Table 3.13 Primers and PCR strategy used for amplification of HHF1 multiple alanine mutants in combination with Y98A

HHF1	Primer name	Sequence	PCR strategy
K5,8,12A / K5,8,12A Y98A	5'HHF1-K5,8,12A-atg-BglII	GCCAGATCTAAAATGTCCGGTAGAGGTGCAG GTGGTGCAGGTCTAGGTGCAGGTGGTGCC	One-step PCR Template: YCplac111-HHF1 WT or YCplac111-HHF1 Y98A
	3'HHF1ter-SalI	GCCGCCGTCGACCACACACGAAAATCCTG	
K5,8,12,16A / K5,8,12,16A Y98A	5'HHF1-K5,8,12A-atg-BglII	GCCAGATCTAAAATGTCCGGTAGAGGTGCAG GTGGTGCAGGTCTAGGTGCAGGTGGTGCC	One-step PCR Template: YCplac111-HHF1 K16A or YCplac111-HHF1 K16A Y98A
	3'HHF1ter-SalI	GCCGCCGTCGACCACACACGAAAATCCTG	
K5,8,12,20A / K5,8,12,20A Y98A	5'HHF1-K5,8,12A-atg-BglII	GCCAGATCTAAAATGTCCGGTAGAGGTGCAG GTGGTGCAGGTCTAGGTGCAGGTGGTGCC	One-step PCR Template: YCplac111-HHF1 K20A or YCplac111-HHF1 K20A Y98A
	3'HHF1ter-SalI	GCCGCCGTCGACCACACACGAAAATCCTG	

Table 3.14 Primers and PCR strategy used for amplification of HHF1 multiple arginine mutants in combination with Y98A

HHF1	Primer name	Sequence	PCR strategy
K8,16R / K8,16R Y98A	Hhf-k8r+	AGAGGTAAAGGTGGTAGAGGTCTAGGTAAAGG	Two-step PCR Template: YCplac111-HHF1 K16R or YCplac111-HHF1 K16R Y98A Forward primer: 5'HHF1pro-EcoRI Reverse primer: 3'HHF1ter-SalI
	Hhf-k8r-	CCTTTACCTAGACCTCTACCACCTTTACCTCT	
K5 K8,12,16,20R / K5 K8,12,16,20R Y98A	5'HHF1atg-BglII	GCCAGATCTAAAATGTCCGGTAGAGGTAAAGG	One-step PCR Template: HHF1 K5,8,12,16,20R or HHF1 K5,8,12,16,20R Y98A PCR amplification product Reverse primer: 3'HHF1ter-SalI
K8 K5,12,16,20R / K8 K5,12,16,20R Y98A	5'HHF1-K5R,K8-atg-BglII	GCCAGATCTAAAATGTCCGGTAGAGGTAGAGGTGGTAAAGGTCTAGGT	
K12 K5,8,16,20R / K12 K5,8,16,20R Y98A	5'HHF1-K5R,K8R,K12-atg-BglII	GCCAGATCTAAAATGTCCGGTAGAGGTAGAGGTGGTAGAGGTCTAGGTAAAGGTGGTGCC	

Table 3.14 Primers and PCR strategy used for amplification of HHF1 multiple arginine mutants in combination with Y98A (continued)

HHF1	Primer name	Sequence	PCR strategy
K16 K5,8,12,20R / K16 K5,8,12,20R Y98A	5'HHF1-K5,8,12R-atg-BglII	GCCAGATCTAAAATGTCCGGTAGAGGTAGAGGTGGTAGAGGTCTAGGTAGAGGTGGTGCC	One-step PCR Template: YCplac111-HHF1 K20R or YCplac111-HHF1 K20R Y98A Reverse primer: 3'HHF1ter-SalI
K20 K5,8,12,16R / K20 K5,8,12,16R Y98A	5'HHF1-K5,8,12,16R-atg-BglII	GCCAGATCTAAAATGTCCGGTAGAGGTAGAGGTGGTAGAGGTCTAGGTAGAGGTGGTGCCAGACGTCACAGA	One-step PCR Template: YCplac111-HHF1 WT or YCplac111-HHF1 Y98A Reverse primer: 3'HHF1ter-SalI
K5,8,12,16,20R / K5,8,12,16,20R Y98A	5'HHF1-K5,8,12,16R-atg-BglII	GCCAGATCTAAAATGTCCGGTAGAGGTAGAGGTGGTAGAGGTCTAGGTAGAGGTGGTGCCAGACGTCACAGA	One-step PCR Template: YCplac111-HHF1 K20R or YCplac111-HHF1 K20R Y98A Reverse primer: 3'HHF1ter-SalI

Site-directed mutagenesis was carried out using a two-step PCR and involved three separate PCR reactions. In the first step, two PCR reactions were carried out — one reaction containing the forward 5' primer and the mutant negative (-) primer to replicate the DNA sequence upstream of the mutation and the other reaction containing the reverse 3' primer and the mutant positive (+) primer to replicate the DNA sequence downstream of the mutation (Figure 3.1A). In the second step, the two PCR fragments generated from the first step were used as the template in a third PCR reaction containing the forward 5' primer and reverse 3' primer (Figure 3.1B).

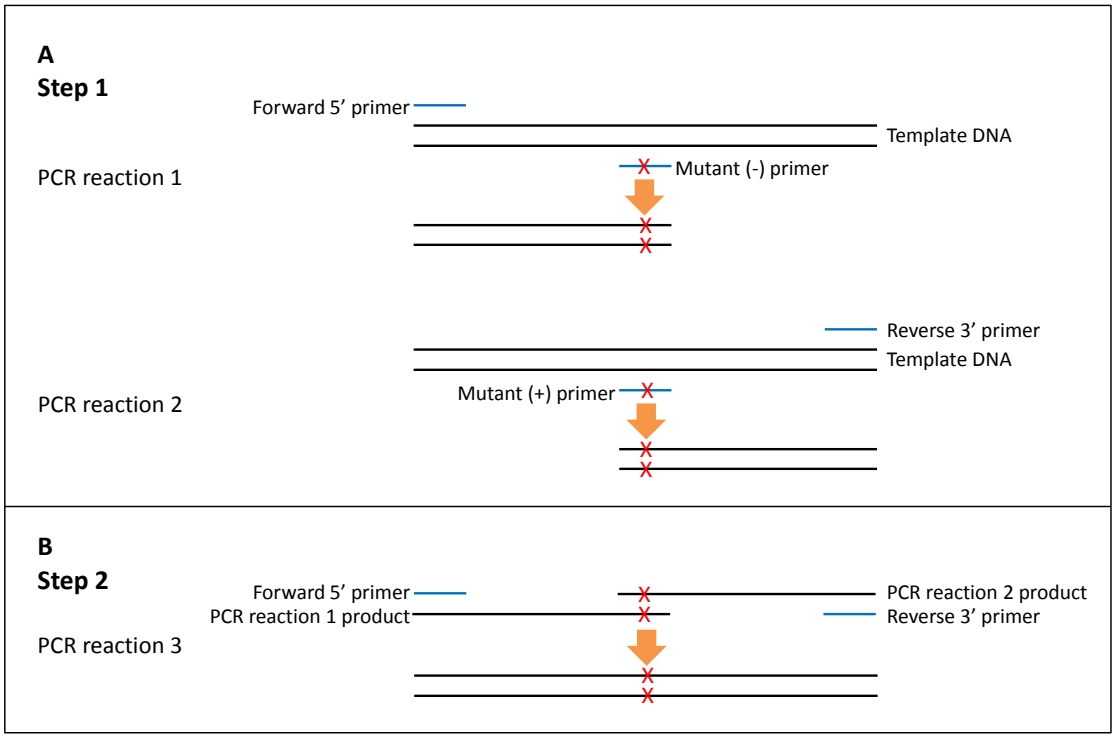

Figure 3.1 Schematic diagram of the two-step PCR. (A) Step 1 shows the generation of the DNA sequence upstream and downstream of the mutation. (B) Step 2 shows the generation of the complete DNA fragment containing the mutation.

In the first step of the two-step PCR, the PCR reactions were carried out with a similar reaction mixture as in the one-step PCR (Tables 3.9, 3.10, 3.11, 3.12, 3.13 and 3.14 for details on the template DNA used). In the second step, the PCR reaction was carried out in a 200 µl PCR tube, where 14.9 µl sterile water, 1 µl PCR reaction 1,

1 µl PCR reaction 2, 0.25 µl 5' primer, 0.25 µl 3' primer, 2 µl 10X Expand High Fidelity PCR Buffer, 0.4 µl 10 mM dNTP, 0.2 µl Expand High Fidelity Polymerase were added in sequence and mixed.

For all of the above PCR reactions, the following cycling parameters were repeated for 20 cycles — 95°C for 30 s, x°C for 1 min and 72°C for y min, where x°C is dependent on primer annealing temperature and y min is dependent on length of the DNA sequence amplified (100 s for every 1 kb). The extension products were analysed through 1 % agarose gel electrophoresis to ensure amplification of the correct DNA sequence occurred before insertion into a vector.

3.3.1.2 Purification of extension products

For each 20 µl PCR reaction, 5 µl was used for analysis through 1 % agarose gel electrophoresis. The extension products in the remaining 15 µl PCR reaction were purified using Roche High Pure PCR Product Purification Kit (Boehringer Mannheim) following the manufacturer's protocol.

3.3.1.3 Cloning and sub-cloning

In order to clone the desired genes into the plasmids, the PCR extension products and cloning vectors were cleaved with the same restriction enzymes or with restriction enzymes that generate compatible overhang DNA sequences. For sub-cloning of the candidate suppressor genes, two methods were carried out to generate the desired plasmids. In the first method, the candidate suppressor gene was isolated on YEp13 through the use of restriction enzymes to cleave the unwanted fragments, then the plasmid DNA was re-ligated. In the second method, the candidate suppressor gene

was cleaved from YEp13 and ligated to YEplac181.

Restriction digestion of PCR extension products was carried out in a 1.5 ml microtube, where 17.4 µl purified PCR extension products, 2 µl restriction digestion buffer, 0.2 µl bovine serum albumin (BSA), 0.2 µl of each restriction enzyme were added in sequence and mixed. Restriction digestion of plasmid DNA was carried out using a similar mix, with the exception that 16.4 µl sterile water and only 1 µl plasmid DNA were added. The restriction digestion mixture was incubated at 37°C overnight to ensure complete digestion of DNA has taken place.

3.3.1.4 Purification of restriction digested products

The restriction digested products in each 20 µl reaction were purified using Roche High Pure PCR Product Purification Kit (Boehringer Mannheim) following the manufacturer's protocol.

3.3.1.5 DNA ligation

In a 1.5 ml microtube, 4.8 µl sterile water, 1 µl 10X ligation buffer, 0.2 µl T4 DNA Ligase (Roche), 4 µl cut plasmid DNA or 2 µl cut plasmid DNA and 2 µl cut gene fragment were added and mixed. The ligation mixture was incubated at room temperature for 4 h or at 4°C overnight.

3.3.1.6 Amplification of plasmid DNA

Plasmid DNA can be transformed into competent *E. coli* for amplification through two methods — chemical transformation or electroporation. Chemical transformation of DH5α *E. coli* was used for amplification of ligated plasmid DNA or known

plasmid DNA. Electroporation of DH10β *E. coli* was used for amplification of plasmid DNA isolated from *S. cerevisiae*, where the more electrocompetent DH10β *E. coli* allows for a relatively higher transformation efficiency as *S. cerevisiae* genomic DNA present in the isolated plasmid DNA reduces transformation efficiency.

3.3.1.6.1 Chemical transformation into DH5α *E. coli*

DH5α *E. coli* was made competent by resuspending the cells in a calcium chloride ($CaCl_2$) solution (Appendix 8.8), where the divalent cation Ca^{2+} creates pores in the plasma membrane, helps plasmid DNA to bind the plasma membrane and masks the negative charge of the plasmid DNA. In a 1.5 ml microtube, 20 µl DH5α *E. coli* was added to the 10 µl ligation mixture or 0.5 µl known plasmid DNA and mixed. The mixture was placed on ice for 15 min, followed by heat shock in a 42°C water bath for 1 min to force the plasmid DNA through the hydrophobic plasma membrane and into the cells. 160 µl Luria-Bertani (LB; Appendix 8.9) media was added immediately to ensure maximal recovery of transformants and mixed using a pipette. The mixture was incubated with rotation at 37°C for 1 h to allow for expression of the antibiotic resistance gene, then plated on LB+ampicillin or LB+chloramphenicol plate (Appendix 8.9) and incubated at 37°C for more than 12 h or overnight.

Ampicillin inhibits synthesis of the bacterial cell wall, where ampicillin resistance relies on the production of beta-lactamase, which catalyses the degradation of the beta-lactam ring in the periplasmic space. Chloramphenicol binds the 50S subunit of ribosomes to prevent protein synthesis, where chloramphenicol resistance relies on the production of chloramphenicol acetyltransferase, which converts chloramphenicol into a form that cannot bind ribosomes.

3.3.1.6.2 Electroporation into DH10β *E. coli*

DH10β *E. coli* was made competent by extensive washing to remove all salts (Appendix 8.10) to ensure that the electric current applied is not conducted through the media. The electric current should be applied across DH10β *E. coli* to create pores in the plasma membrane so as to force the plasmid DNA through the plasma membrane and into the cells. Electroporation cuvettes were prepared by treating with denatured EtOH overnight, then the contents were poured away and the cuvettes were dried in a laminar hood. The cuvettes were placed under ultraviolet (UV) for 10 min and chilled on ice for 5 min before use. In a 1.5 ml microtube, 40 µl DH10β *E. coli* was added to 4 µl isolated plasmid DNA and mixed on ice before transferring the mixture carefully into a prepared cuvette to avoid bubble formation. After electroporation at 1.8 kV using an *E. coli* Pulser (Bio-Rad), 400 µl LB was added immediately to ensure maximal recovery of transformants and mixed vigorously using a pipette. The mixture was transferred back into the 1.5 ml microtube and incubated with rotation at 37°C for 1 h to allow for expression of the antibiotic resistance gene. The mixture was plated on LB+ampicillin (Appendix 8.9) and incubated at 37°C for more than 12 h or overnight.

3.3.1.7 Miniprep for purification of plasmid DNA from *E. coli*

Larger colonies formed on LB+ampicillin or LB+chloramphenicol plate were picked for inoculation in 2 ml LB+ampicillin or LB+chloramphenicol media at 37°C for more than 12 h or overnight. The culture was transferred into a 1.5 ml microtube, centrifuged at 13000 rpm for 30 s and the supernatant was removed. The plasmid DNA was isolated using the alkaline lysis method (Ausubel et al., 2006), involving Miniprep Solution I (Appendix 8.11, Table 8.10), Miniprep Solution II (Appendix

8.11, Table 8.11) and Miniprep Solution III (Appendix 8.11, Table 8.12). The plasmid DNA pellet was dried under vacuum for 15 min, then resuspended in 50 µl sterile water and stored at -20°C. Restriction digestion of plasmid DNA was carried out in a 1.5 ml microtube, where 12.7 µl sterile water, 5 µl plasmid DNA, 2 µl restriction digestion buffer, 0.1 µl BSA, 0.1 µl of each restriction enzyme were added in sequence and mixed. The restriction digestion mixture was incubated at 37°C for at least 2 h. This was followed by 1 % agarose gel electrophoresis and sequencing reaction to ensure that the plasmid generated was correct.

Restriction digestion of integration plasmid DNA was carried out in a 1.5 ml microtube, where 34 µl sterile water, 10 µl integration plasmid DNA, 5 µl restriction digestion buffer, 0.5 µl BSA, 0.25 µl of each restriction enzyme were added in sequence and mixed. The restriction digestion mixture was incubated at 37°C overnight to ensure complete digestion of integration plasmid DNA has taken place. This was followed by 1 % agarose gel electrophoresis to ensure that the integration plasmid DNA has been completely cleaved. The restriction digestion mixture does not have to be purified and was used to transform competent *S. cerevisiae* directly (refer to section 3.3.2.2).

3.3.1.8 Agarose gel electrophoresis

1 % agarose gel was cast with 1 g agarose and 100 ml 1X Tris Borate EDTA (TBE) buffer, which was then microwaved for 2 min to melt the agarose. Different percentages of agarose gel were obtained by varying the amount of agarose added. Before pouring the gel mixture into a gel tray to cool and solidify, 3 µl ethidium bromide (Bio-Rad) was added to enable visualisation of DNA upon intercalation

between nucleic acid base pairs and exhibition of fluorescence under UV. Before loading the samples, 1 µl 10X loading dye (Appendix 8.12, Table 8.13) was added and mixed. The gel was electrophoresed at a constant 100 volts for 40 min, then viewed under UV.

3.3.1.9 Sequencing reaction and purification of extension products

In a 200 µl PCR tube, 6 µl sterile water, 1.5 µl plasmid DNA, 0.5 µl forward or reverse primer (Table 3.15), 2 µl BigDye Terminator Cycle reaction mix (Applied Biosystems) were added in sequence and mixed. The following cycling parameters were repeated for 25 cycles — 96°C for 30 s, 50°C for 15 s, 60°C for 4 min.

Table 3.15 Primers used for sequencing reactions

Sequencing template	**Primer name**	**Sequence**
Bank 13 (YEp13)	YEp13+	GCCACTATCGACTACGCG
	YEp13-	GCGCCAGCAACCGCACCTGT
Histone mutants	5'HHF1pro-70	CCGTCGCATTATTGTACTCT
	3'HHF1ter-70	TACACTCATATTTGTAGAAG
Genes inserted into PactT424 and PactT424-HA	5'ACT1pro-60	ATCTTCTACTACATCAGCTT
	3'ACT1ter-60	TTATTTTATTGAGAGGGTGG

In order to purify the extension products, the contents of the PCR tube was transferred into a 1.5 ml microtube containing 80 µl of ethanol/sodium acetate (EtOH/NaAc) solution, which is a mixture of 14.5 µl sterile water, 62.5 µl 100 % EtOH, 3 µl 3 M NaAc (pH4.6). The mixture was vortexed briefly and allowed to stand at room temperature for 15 min to precipitate the extension products. After centrifuging at 13000 rpm for 10 min, the supernatant was carefully removed using a pipette. Upon addition of 500 µl 75 % EtOH to rinse the DNA pellet, the microtube was centrifuged at 13000 rpm for 5 min and the supernatant was removed. The DNA pellet was dried under vacuum for 15 min before sending the sample to a sequencing facility provided in Department of Microbiology, NUS.

3.3.2 Generation of *S. cerevisiae* strains

3.3.2.1 Production of competent *S. cerevisiae*

In order to generate competent cells for transformation, a preculture of the required *S. cerevisiae* strain was prepared by inoculating a single colony in 2 ml YPDA (Yeast extract Peptone Dextrose Adenine, Appendix 8.13) or other selective media (Appendix 8.14), then incubating at 28°C for more than 12 h or overnight. A suitable volume of the preculture was transferred into either 10 ml or 50 ml fresh media, depending on the amount of competent cells required for transformation, at a 50X dilution for fast growing strains or at a 25X dilution for slow growing strains. The culture was incubated at 28°C until OD_{600} = 1.0. The cells were made competent using the lithium acetate (LiAc, Appendix 8.15) method (Ausubel et al., 2006), followed by transformation or storage at 4°C for a maximum of one week.

3.3.2.2 Transformation of competent *S. cerevisiae*

Transformation of competent cells was carried out in a 1.5 ml microtube, where 2 µl fish sperm DNA (FS DNA, Roche), 1 µl plasmid DNA or cut integration plasmid DNA (refer to section 3.3.1.7), 5 µl competent cells and 50 µl 40 % polyethylene glycol (PEG, Appendix 8.16) were added in sequence and mixed. The transformation mixture was incubated at 28°C for 1 h, followed by heat shock in a 42°C water bath for 15 min to trigger DNA uptake. After centrifuging at 7000 rpm for 1 min, the supernatant was removed and the cells were resuspended in 10-15 µl sterile water. The cell resuspension was plated on the relevant selection plate to select for transformants that have taken up the plasmid DNA and incubated at 28°C for three days.

3.3.2.3 Generation of *S. cerevisiae* histone mutant strains — Plasmid shuffling

The histone knock out strains bear chromosomal null mutations for the indicated histone genes, BY4742ΔWΔHHF1/2 + PactT316-HA-HHF1 and BY4742ΔWΔHHTF1/2 + YCplac33-HHTF2. Thus, they were maintained by the presence of *URA3* marked PactT316-HA-HHF1 and YCplac33-HHTF2 respectively. *URA3* is a widely used marker as it allows both positive and negative selections. *URA3* encodes for the enzyme orotidine-5'-phosphate (OMP) decarboxylase, which is required for the *de novo* biosynthesis of uracil where it converts OMP into uridine monophosphate (UMP). Thus, cells containing *URA3* marked plasmids can grow on media lacking uracil, i.e. positive selection (Figure 3.2A). However, the same enzyme encoded by *URA3* converts 5-fluoro-orotic acid (5-FOA) into the toxic metabolite 5-fluorouracil (5-FU), which inhibits thymidylate synthase (an enzyme involved in the synthesis of deoxy-thymidine monophosphate for DNA replication). Thus, cells containing *URA3* marked plasmids cannot grow on media containing 5-FOA, i.e. negative selection (Figure 3.2B).

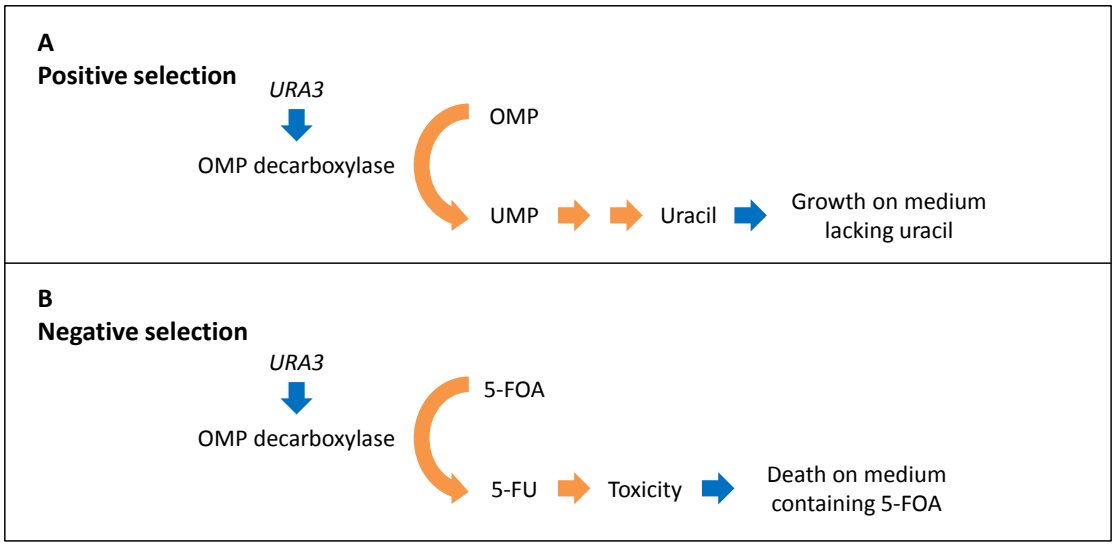

Figure 3.2 Schematic diagram of the *URA3* marker's positive and negative selections. (A) The positive selection of the *URA3* marker leads to cell growth. (B) The negative selection of the *URA3* marker leads to cell death.

In order to elucidate the effects of various *HHT1* and *HHF1* mutants, plasmid shuffling was carried out to replace the *URA3* marked plasmids carrying WT genes with the *TRP1* or *LEU2* marked plasmids carrying mutant genes (Figure 3.3A). Transformation was first carried out to introduce the plasmid carrying the mutant gene into the strain. For the single knock out *HHF1/2* strain, single transformation was carried out as described in section 3.3.2.2. For the double knock out *HHTF1/2* strain, double transformation was carried out by adding 1 µl of each desired plasmid into the transformation mixture. The transformants were titrated (refer to section 3.3.2.3.1) onto histidine-depleted selection plates containing 5-FOA (H- + FOA). Histidine-depleted selection plates were used to select for the strains that have the chromosomal histone genes replaced by the *HIS3* gene through homologous recombination. If the mutant histone gene encodes for a functional protein, the cells would lose the *URA3* marked plasmids carrying WT gene and colonies will be observed on the H- + FOA plates due to counter selection (Figure 3.3B). The histone mutant strains that grew were restreaked on H- + FOA plates for another generation, before testing for 3-amino-1,2,4-triazole (3-AT) sensitivity (AT), antimycin A sensitivity (AA) or temperature sensitivity (TS) phenotypes.

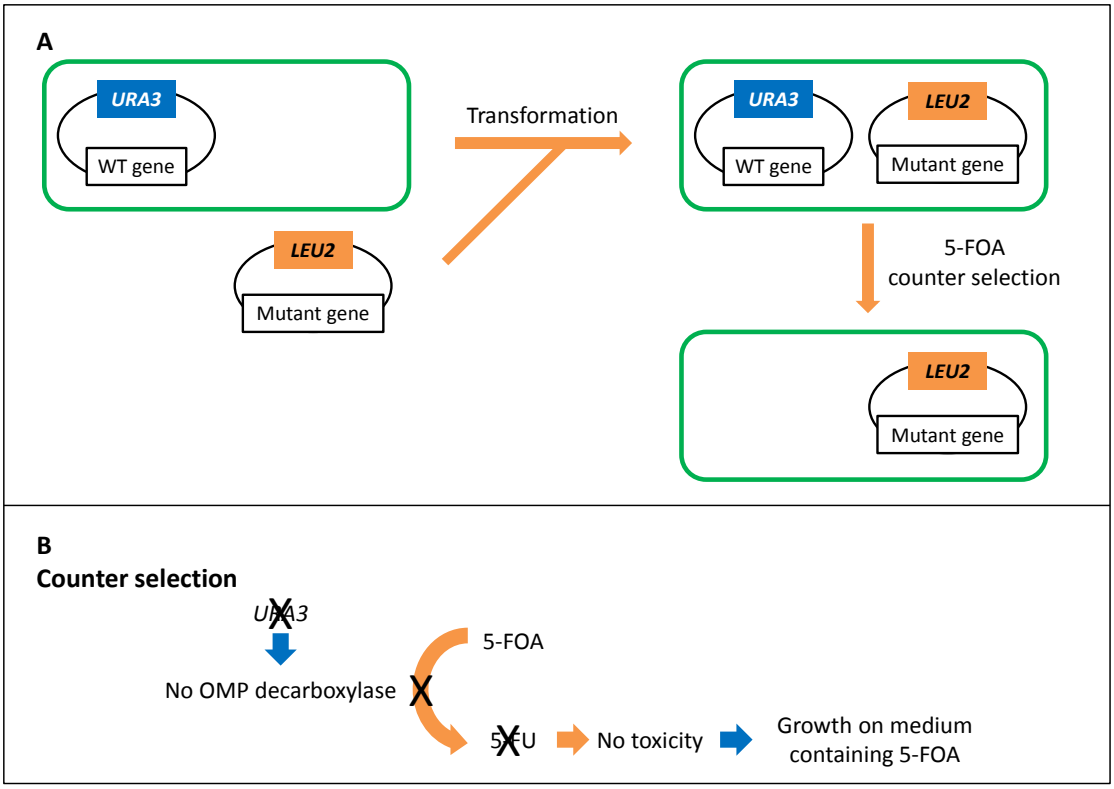

Figure 3.3 Schematic diagram of plasmid shuffling and *URA3* marker's counter selection involved. (A) The process of plasmid shuffling starts with a *URA3* marked plasmid in the cell, followed by two plasmids after transformation. This eventually results in the presence of only the second plasmid after shuffling the *URA3* marked plasmid out of the cell. (B) The schematic of counter selection of the *URA3* marker, where the absence of the *URA3* marked plasmid in the cell allows growth on media containing 5-FOA.

3.3.2.3.1 Titration — Droplet growth assay

Titration or droplet growth assay was carried out in a 96-well plate. A pipette tip was used to inoculate a scoop of cells into 90 µl sterile water, followed by tenfold serial dilutions of up to 10^{-6}. A multi-channel pipette was used to load 5 µl from each well onto relevant control and selection plates, then the droplets were allowed to dry. The plates were incubated at 28°C or at 38°C (to test for TS phenotype) for three to six days and were scanned into a computer at regular intervals.

3.3.2.4 Generation of *S. cerevisiae* mutant strains — Gene targeting

In order to generate *S. cerevisiae* mutant strains, two methods of gene targeting were used. The first method involved the hisG-*URA3*-hisG cassette present in NKY51 and

NKY1009 targeting vectors (Alani et al., 1987). The hisG-*URA3*-hisG cassette can be flanked by approximately 500 bp of the targeted gene's promoter and terminator (NKY51) or by approximately half of the targeted gene on either ends (NKY1009, Figure 3.4). Before the targeting vectors were transformed into the desired *S. cerevisiae* strain, they were linearised by restriction digestion (refer to section 3.3.1.7).

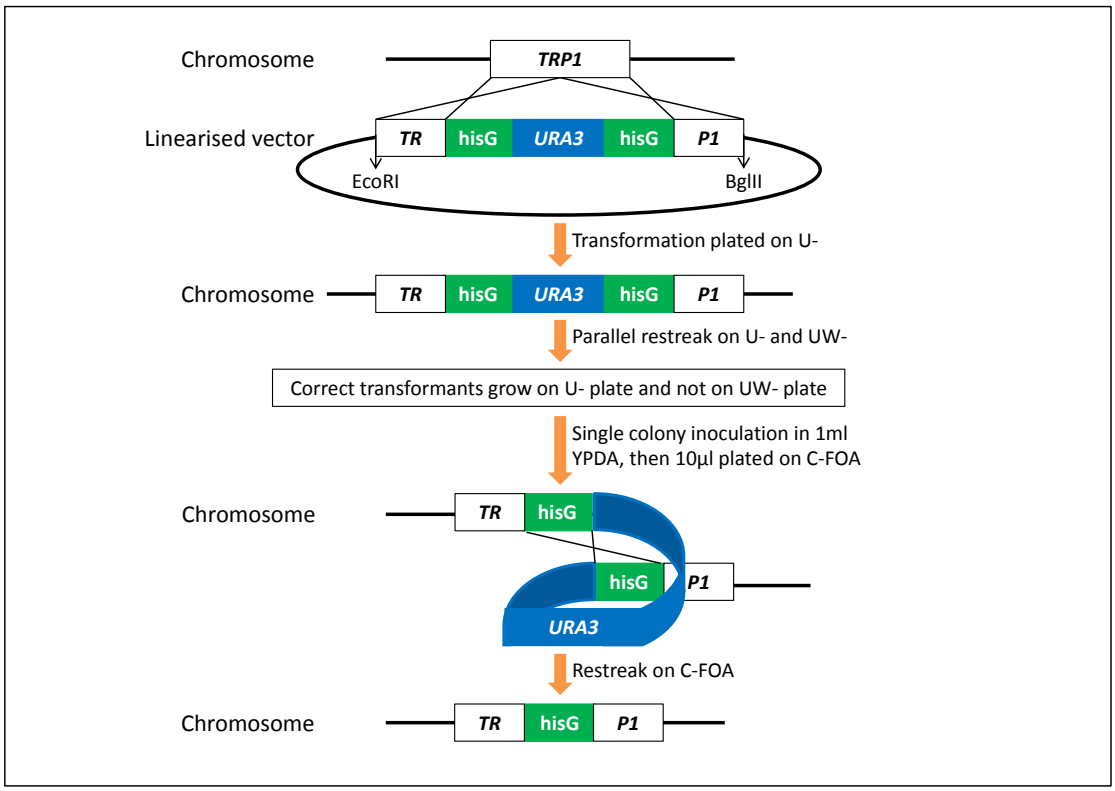

Figure 3.4 Schematic diagram of gene targeting involving the hisG-*URA3*-hisG cassette present in NKY1009 targeting vector. The *TRP1* gene was disrupted due to the presence of a hisG sequence in the middle of the gene after counter selection of the *URA3* marker. *TR*: first half of *TRP1* gene, *P1*: second half of *TRP1* gene, U-: media lacking uracil, UW-: media lacking uracil and tryptophan, C-FOA: media containing complete amino acid mixture and 5-FOA.

The second method involved the use of relevant selection markers with the help of differently marked targeting vectors — puc8+HIS3 and puc8+LEU2 (Figure 3.5). Before the targeting vectors were transformed into the desired *S. cerevisiae* strain, they were linearised by restriction digestion (refer to section 3.3.1.7). In order to confirm whether the targeted gene had been knocked out, yeast breaking to extract genomic DNA was carried out (refer to section 3.3.3.2), followed by PCR using

primers designed to anneal to the 5'pro and 3'ter of the targeted gene (refer to section 3.3.1.1). If the length of the targeted gene and the selected marker are different, analysis of the extension products through agarose gel electrophoresis was sufficient. If the length of the targeted gene and the selected marker are similar, a sequencing reaction was carried out using the extension products as template.

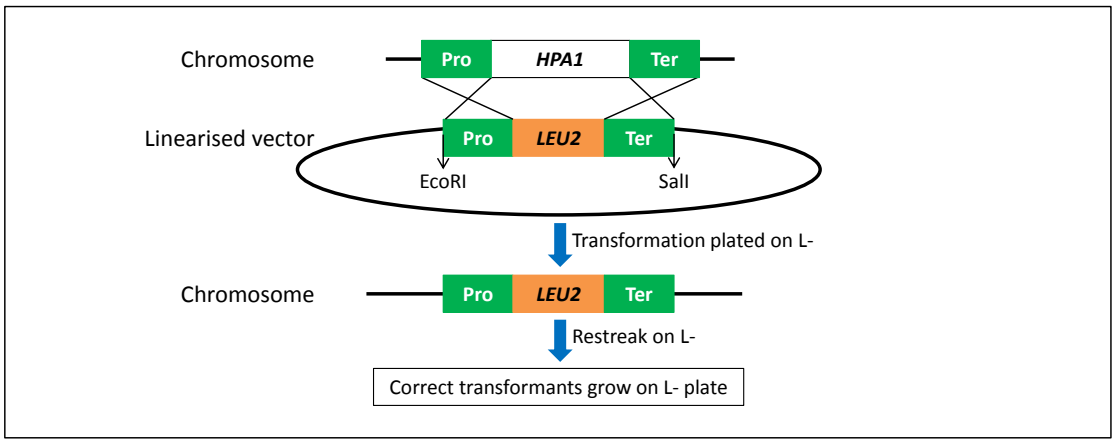

Figure 3.5 Schematic diagram of gene targeting involving the *LEU2* marker present in puc8+LEU2 targeting vector. The *HPA1* gene was replaced by the *LEU2* marker after homologous recombination of the promoter and terminator sequences of *HPA1* gene on the chromosome and the linearised vector. Pro: promoter sequence of *HPA1* gene, Ter: terminator sequence of *HPA1* gene, L-: media lacking leucine.

3.3.2.5 Generation of *S. cerevisiae* glycerol stock

Once the *S. cerevisiae* mutant strains have been confirmed, glycerol stocks were generated. A preculture of each *S. cerevisiae* mutant strain was prepared by inoculating a single colony in 1 ml YPDA or other selective media, then incubating at 28°C for more than 12 h or overnight. 400 µl of the preculture was mixed with 400 µl 50 % glycerol to obtain a 25 % glycerol-cells mixture. The mixture was stored immediately at -80°C to avoid settling of the cells.

3.3.3 Genomic library screening

The *S. cerevisiae* histone H4 mutant strains Y51A, E53A and Y98A generated were

conferred with phenotypic deficiencies that arose most probably due to defective genetic interactions. A genomic library screen was carried out in order to identify the specific gene involved in the defective genetic interactions.

3.3.3.1 Transformation of competent *S. cerevisiae* with YEp13 library plasmids

Transformation of competent cells (refer to section 3.3.2.1) was carried out in a 1.5 ml microtube, where 25 µl FS DNA, 25 µl YEp13 library plasmids (concentration of 0.5 µg/µl), 25 µl competent cells and 375 µl 40 % PEG were added in sequence and mixed. The transformation mixture was incubated at 28°C for 1 h, followed by heat shock in a 42°C water bath for 15 min to trigger DNA uptake. After centrifuging at 7000 rpm for 1 min, the supernatant was removed and the cells were resuspended in 250 µl sterile water. In a first protocol, the cell resuspension was plated directly on the selection plate and incubated at 28°C or at 38°C (to test for TS phenotype) for three days. In a second protocol, the cell resuspension was plated directly on L- plate and incubated at 28°C for three days. The colonies formed were washed off twice with 5 ml sterile water each time, of which only 1 % was plated on the selection plate and incubated at 28°C or at 38°C for three days. The second protocol helped to increase the number of cells plated on the selection plate to improve the colony numbers obtained. The volumes of each transformation component and sterile water for resuspension were multiplied according to the number of selection plates used.

The size of the *S. cerevisiae* genome is approximately 12000 kb with more than 6000 genes, while the average fragment size of the genomic library is approximately 6 kb. Theoretically, there should be at least 2000 transformants on each transformation plate to cover the *S. cerevisiae* genome. However, in order to ensure a complete

coverage of the *S. cerevisiae* genome, a more practical number to aim for would be at least 10000 transformants on each transformation plate. This means that the *S. cerevisiae* genome would be covered about five times. Thus, to determine the number of primary transformants screened, two dilutions of the transformed cells were carried out, plated on L- plate and incubated at 28°C for six days. For the 1000X dilution, 6 µl cell resuspension and 54 µl sterile water were mixed, where only 50 µl was plated. For the 10000X dilution, 5 µl 1000X diluted cell resuspension and 45 µl sterile water were mixed, where only 50 µl was plated. The number of primary transformants was recorded twice, after three days and after six days of incubation.

3.3.3.2 Extraction of genomic or plasmid DNA — Yeast breaking

Yeast breaking was carried out to extract genomic DNA from *S. cerevisiae* mutant strains or to extract YEp13 library plasmids from transformants. A single colony was inoculated in 5 ml YPDA or other selective media and incubated at 28°C (*S. cerevisiae* mutant strains or AT and AA phenotype suppressors) or 38°C (TS phenotype suppressors) until OD_{600} = 1.0. The DNA was isolated using the phenol-chloroform extraction method (Ausubel et al., 2006), which involves the use of yeast breaking buffer (Appendix 8.17, Table 8.18). The DNA pellet was dried under vacuum for 30 min, then resuspended in 50 µl sterile water and stored at -20°C.

After the YEp13 library plasmids were extracted from the transformants, they were amplified in DH10β *E. coli* and restriction digestion was carried out to ensure that the plasmids contained an insert. The isolated plasmids were transformed into their respective *S. cerevisiae* histone mutant strains and also cross transformed into other *S. cerevisiae* histone mutant strains conferred with the phenotype suppressed by the

isolated plasmids. The same isolated plasmids were also transformed into BY4742ΔWΔHHF1/2 + PactT316-HA-HHF1 strain. Titration was carried out on selection plates to retest suppression efficiency of the isolated plasmids and on H-FOA plates to ensure that the isolated plasmids did not encode WT HHF1. The isolated plasmids that suppressed the phenotypes conferred by the HHF1 mutations and failed to complement HHF1 deletion were sequenced.

3.3.4 Quantitative real-time PCR analysis

Real-time PCR involves the monitoring of the progress of a PCR reaction as it occurs. Data is collected throughout the PCR reaction, rather than at the end of the reaction. A PCR reaction is characterised by the point in time during cycling when the amplification of a target is first detected.

3.3.4.1 Purification of total ribonucleic acid (RNA)

Cells were grown for total RNA purification using two methods — broth method and plate method. In the broth method, the required *S. cerevisiae* strain was inoculated in 40 ml glucose complete media or other selective media. The culture was incubated at 28°C until OD_{600} = 1.0, before splitting it into two 20 ml cultures. For one culture, after centrifuging at 4000 rpm for 5 min, the supernatant was removed and the cells were washed in 20 ml sterile water. After centrifuging at 4000 rpm for 5 min, the supernatant was removed and a 2 h induction in 20 ml media containing 3-AT was carried out. After centrifuging at 4000 rpm for 5 min, the supernatant was removed and the cells from both cultures were washed in 1 ml sterile water. The resuspension was transferred into a 1.5 ml microtube. After centrifuging at 7000 rpm for 1 min, the supernatant was completely removed in order to prevent lysis inhibition or lysate

dilution, both of which could reduce RNA yield.

In the plate method, the required *S. cerevisiae* strain was inoculated in 5 ml glucose complete media or other selective media and incubated at 28°C until OD_{600} = 1.0. After centrifuging at 4000 rpm for 5 min, the supernatant was removed and the cells were washed in 1 ml sterile water. The resuspension was transferred into a 1.5 ml microtube. After centrifuging at 7000 rpm for 1 min, the supernatant was removed and the cells were resuspended in 100 µl sterile water. Serial dilutions of up to 10^{-6} were carried out and plated on control plates and plates containing 3-AT, then incubated at 28°C for four days. The colonies formed from the most diluted diluent that survived on the 3-AT plate and the corresponding control plate were harvested by washing off with 10 ml sterile water (5 ml sterile water twice). After centrifuging at 4000 rpm for 5 min, the supernatant was removed and the cells were washed in 1 ml sterile water. The resuspension was transferred into a 1.5 ml microtube. After centrifuging at 7000 rpm for 1 min, the supernatant was completely removed.

Mechanical disruption was used to homogenise the harvested cells and total RNA was purified using the RNeasy® Mini Kit (Qiagen) following the manufacturer's protocol in the RNeasy® Mini Kit Handbook. RNA was eluted from the RNeasy® spin column with 60 µl RNase-free water and stored at -80°C.

3.3.4.2 Quantitation of total RNA

Quantitation of total RNA was carried out using a nanodrop machine, where 2 µl of the purified total RNA was pipetted onto the end of a fibre optic cable. The following values were recorded to determine the integrity of the total RNA purified:

- ng/µl: sample concentration based on absorbance at 260 nm, which was used to calculate the amount of RNA added in a reverse transcription reaction
- 260/280: ratio of sample absorbance at 260 nm and 280 nm, which indicates the purity of RNA (a ratio of ~2.0 indicates a pure RNA sample)
- 260/230: ratio of sample absorbance at 260 nm and 230 nm, which is a secondary indication of the purity of nucleic acids (a ratio of 2.0–2.2 indicates a pure nucleic acid sample)

3.3.4.3 Formaldehyde agarose (FA) gel electrophoresis of total RNA

In order to determine the integrity and size distribution of total RNA purified, FA (denaturing) gel electrophoresis was carried out. Intact total RNA run on a denaturing gel will display sharp 28S (4718 bp) and 18S rRNA (1874 bp) bands, where the 28S rRNA band should be approximately twice as intense as the 18S rRNA band. This indicates that the rRNA and mRNA purified were not degraded during the extraction procedure.

1.2 % FA gel was cast with 1.2 g agarose, 10 ml 10X FA gel buffer (Appendix 8.18, Table 8.19) and 90 ml RNase-free water, which was then microwaved for 2 min to melt the agarose. Before pouring the gel mixture into a gel tray to cool and solidify, the gel mixture was cooled to 65°C, after which 1 µl ethidium bromide and 1.8 ml 37 % formaldehyde was added. The FA gel was equilibrated in 1X FA gel running buffer (Appendix 8.18, Table 8.20) for at least 30 min. The total RNA sample was prepared for FA gel electrophoresis by mixing 3 µl total RNA sample with 3 µl 2X RNA loading buffer. The mixture was incubated at 65°C for 5 min and chilled on ice before loading onto the equilibrated FA gel. After loading 4 µl RiboRuler RNA Ladder High

Range (Fermentas), the FA gel was electrophoresed at a constant 80 volts for 1 h, then viewed under UV. Preparation and electrophoresis of the FA gel was carried out in a fume hood due to the usage of formaldehyde.

3.3.4.4 DNaseI treatment of DNA contaminants

The purified total RNA samples were treated with DNaseI to degrade genomic DNA that could otherwise result in false positive signals during real-time PCR. A dilution using RNase-free water was carried out to obtain 4 µg purified total RNA in a reaction volume of 35 µl. 3.5 µl 10X DNaseI buffer (Ambion) and 1 µl Turbo DNaseI (Ambion) were added in sequence and mixed, then the mixture was incubated at 37°C for 2 h. Upon addition of 1.2 µl Turbo DNaseI, the mixture was again incubated at 37°C for 2 h. Upon addition of 4 µl DNaseI inactivation reagent (Ambion), the mixture was incubated at room temperature for 5 min with occasional mixing to ensure the effective sequestering of DNaseI and divalent cations. After centrifuging at 13000 rpm for 2 min, the supernatant was transferred into a new 1.5 ml microtube and stored at -80°C.

In order to ensure that there was no detectable DNA contamination, a PCR reaction was carried out in a 200 µl PCR tube, where 10.9 µl RNase-free water, 5 µl DNaseI treated purified total RNA, 1 µl 5' primer (Table 3.16), 1 µl 3' primer (Table 3.16), 5 µl 5X PCR buffer (Promega), 1.5 µl 25 mM $MgCl_2$, 0.5 µl 10 mM dNTP, 0.1 µl Taq polymerase (Promega) were added in sequence and mixed. The following cycling parameters were repeated for 40 cycles — 95°C for 30 s, 50°C for 30 s and 72°C for 30 s. The extension products were analysed through 2.5 % agarose gel electrophoresis to ensure that there was no detectable DNA band.

3.3.4.5 Reverse transcription (RT) PCR

In order to generate complementary DNA (cDNA) from the DNaseI treated purified total RNA samples, a RT-PCR reaction was carried out using the TaqMan® MicroRNA reverse transcription kit (Roche). In a 200 µl PCR tube, 5.55 µl RNase-free water, 6 µl DNaseI treated purified total RNA, 1.5 µl 50 µM random hexamer, 3 µl 10X RT buffer, 6.6 µl 25 mM $MgCl_2$, 6 µl 10 mM dNTP, 0.6 µl RNase inhibitor, 0.75 µl reverse transcriptase were added in sequence and mixed. The following cycling parameters were carried out — 25°C for 5 min, 42°C for 60 min and 70°C for 5 min. In order to analyse the quality of cDNA generated, a PCR reaction and 2.5 % agarose gel electrophoresis were carried out to ensure that there was a defined DNA band (refer to section 3.3.4.4).

3.3.4.6 Quantitative real-time PCR

For quantitative real-time PCR, two sets of triplicates that contained different primers (Table 3.16) were prepared for each DNaseI treated purified total RNA sample. One set contained *HIS3* ORF 5' and 3' primers, while the second set contained primers for the reference gene (*ACT1* ORF 5' and 3' primers for samples grown in broth and 18S rRNA 5' and 3' primers for samples grown on plates). For *HIS3* and *ACT1* ORF primers, 6.5 µl RNase-free water, 5 µl 1:10 diluted cDNA obtained from RT-PCR, 0.5 µl 10 µM 5' primer, 0.5 µl 10 µM 3' primer, 12.5 µl 2X Maxima® SYBR Green/ROX qPCR Master Mix (Fermentas) were added in sequence and mixed. For 18S rRNA primers, 11 µl RNase-free water and 0.5 µl 1:10 diluted cDNA obtained from RT-PCR were used instead. A non-template control to verify amplification quality was included for each pair of primers used. The ABI PRISM® 7000 sequence detection system (Applied Biosystems) was used to carry out real-time PCR using

standard thermal cycling parameters.

Table 3.16 Primers used for quantitative real-time PCR

Gene	Primer name	Sequence
Target gene	*HIS3* ORF 5'	CTTACACATAGACGACCATCAC
	HIS3 ORF 3'	GCAAATCCTGATCCAAACCT
Reference gene	*ACT1* ORF 5'	GACCAAACTACTTACAACTCCA
	ACT1 ORF 3'	CATTCTTTCGGCAATACCTG
	18S rRNA 5'	ATTCCTAGTAAGCGCAAGTCATCAG
	18S rRNA 3'	GACGGGCGGTGTGTACAAA

The amount of *HIS3* mRNA relative to *ACT1* mRNA was determined by quantitative real-time PCR. The relative expression level of *HIS3* mRNA was calculated using the comparative delta Ct (threshold cycle number) method. ΔCt values were first obtained by taking the difference between the average *HIS3* Ct values and the average *ACT1* Ct values. $2^{-\Delta Ct}$ values were calculated, where the values obtained were then calculated relative to the uninduced WT histone H4 strain containing the PactT424-HA empty vector that was set as 1. The results are means ± S.D. for three replicate experiments.

3.3.5 Protein analysis

3.3.5.1 Sodium dodecyl sulphate polyacrylamide gel electrophoresis (SDS-PAGE)

Proteins in the samples were separated using SDS-PAGE, where each SDS polyacrylamide denaturing gel was cast with a 4 % stacking gel (Appendix 8.19, Table 8.21) overlaying a 10–18 % resolving gel (Appendix 8.19, Table 8.22) for separating proteins of different sizes. Before loading the samples, they were mixed with equal volume 2X loading dye (Bio-Rad Laemmli sample buffer with 5 % β-mercaptoethanol) and the proteins in the samples were denatured by heating at 95°C for 5 min. A protein ladder (Bio-Rad or Genedirex) was loaded together with the samples, where the proteins in the samples were allowed to stack at a constant

100 volts in 1X Tris-glycine SDS running buffer. When the dye front had reached the resolving gel, the voltage was increased to a constant 120 volts for separation of the proteins in the samples.

3.3.5.2 Western blot

Separated proteins on the gel were transferred onto a nitrocellulose membrane (Bio-Rad) using the Semi-Dry Electrophoretic Transfer Cell system (Bio-Rad). The transfer for two gels was carried out at 0.23 A for 75 min in freshly prepared 1X transfer buffer, which is a mixture of 30 ml sterile water, 10 ml methanol and 10 ml 5X transfer buffer (Appendix 8.20, Table 8.23). The membrane was blocked with either 5 % skim milk (for detection of most proteins) or 3 % BSA (for detection of histones) in Tris-buffered Saline Tween-20 (TBST, Appendix 8.21, Table 8.24) for 2 h. After blocking the membrane, the blocking solution was removed and primary antibodies (Table 3.17) were added using TBST as diluent, then incubated at 4°C overnight. After incubation, the solution was removed and the membrane was washed three times with TBST for 15 min each. Secondary antibodies (Table 3.17) were added using TBST as diluent, then incubated at 4°C for 2 h. After incubation, the solution was removed and the membrane was washed three times with TBST for 15 min each.

Table 3.17 Primary and secondary antibodies used in Western blotting

Primary antibody	**Dilution used**	**Corresponding secondary antibody**	**Dilution used**
Mouse α-HA (Roche)	1:10000	Rabbit α-mouse horseradish peroxidase-conjugated (Abcam)	1:10000
Rabbit α-H4 (Millipore)	1:10000	Goat α-rabbit horseradish peroxidase-conjugated (Abcam)	1:10000
Rabbit α-H4K8ac (Millipore)	1:10000		
Rabbit α-H4K16ac (Active Motif)	1:5000		

Chemiluminescence detection was carried out using Amersham ECL Plus WB Detection Reagents (GE Healthcare) and Amersham ECL Advanced WB Detection Kit (GE Healthcare) on films for the various indicated exposure time. In order to determine the loading control, Coomassie Blue staining of the membrane was carried out after stripping the membrane with 0.2 M NaOH for 5 min. The membrane was washed with distilled water for 5 min, both before and after stripping the membrane with 0.2 M NaOH. The membrane was incubated in Coomassie Blue (Sigma-Aldrich) staining solution (Appendix 8.22, Table 8.25) until it turned dark blue, then incubated in destaining solution until the protein bands were clearly discernible (Appendix 8.22, Table 8.26).

3.3.6 Chromatin immunoprecipitation (ChIP)

As discussed earlier (refer to section 1.2.5), ChIP is an immunoprecipitation experimental technique that allows the study of interactions between proteins and DNA in a cell. 37 % formaldehyde is used to crosslink the proteins to the DNA, while 2.5 M glycine is used to quench the 37 % formaldehyde and stop the crosslinking reaction. Chromatin is isolated and antibodies against the protein or histone modification-of-interest are used to determine whether the target binds to a specific region of the genome.

3.3.6.1 Culturing and crosslinking of sample

Cells were grown for ChIP using the broth method, where the required *S. cerevisiae* strain was inoculated in 100 ml glucose complete media or other selective media. The culture was incubated at 28°C until OD_{600} = 1.0, before splitting it into two 50 ml cultures. For one culture, after centrifuging at 4000 rpm for 5 min, the supernatant

was removed and the cells were washed in 50 ml sterile water. After centrifuging at 4000 rpm for 5 min, the supernatant was removed and a 2 h induction in 50 ml media containing 3-AT was carried out. 1.5 ml 37 % formaldehyde was added to each culture and crosslinking was carried out for 20 min with gentle agitation at 28°C. 3 ml 2.5 M glycine was added to each culture and termination of the crosslinking reaction was carried out for 5 min with gentle agitation at 28°C. After centrifuging at 4000 rpm for 5 min, the supernatant was discarded into a formaldehyde waste bottle and the cells were washed in 50 ml ice cold sterile water. After centrifuging at 4000 rpm for 5 min, the supernatant was removed and the cells were washed again in 50 ml ice cold sterile water. After centrifuging at 4000 rpm for 5 min, the supernatant was removed and the cells were washed in 1 ml ice cold sterile water. The resuspension was transferred into a 1.5 ml microtube. After centrifuging at 7000 rpm for 1 min, the supernatant was completely removed and the cell pellet was stored at -80°C.

3.3.6.2 Cell lysis and sonication

The cell pellet was resuspended in 1 ml ice cold yeast lysis buffer (Appendix 8.23, Table 8.27) containing 10 µl 200 mM phenylmethanesulphonylfluoride (PMSF), before transferring to a 2 ml screw cap tube containing 500 µl glass beads. In a bead beater (BioSpec Products), the cells were homogenised at top speed for 1 min four times, with 1 min rest on ice in between. The top and bottom of the 2 ml screw cap tube were punctured using a 25 g needle. The tube was assembled on top of the flared portion of an adaptor, which was prepared from a 5 ml syringe, then the set-up was rested on top of a 15 ml falcon tube. After centrifuging at 1000 rpm for 1 min, the flow through was transferred into a 1.5 ml microtube. After centrifuging at 13000 rpm

for 30 min at 4°C, the supernatant was removed and the cell lysate was carefully resuspended completely in 500 µl ice cold yeast lysis buffer containing 5 µl 200 mM PMSF. The cell lysate was sonicated using a microtip sonicator (Sanyo Soniprep 150). The ultrasonic probe was first cleaned with 70 % ethanol, then inserted into the lysate suspension, close to the bottom of the 1.5 ml microtube. The lysate suspension was sonicated at a continuous power output of 50 % for 15 s six times, with 1 min rest on ice in between. It is important to take note that the cell lysate should be sonicated over a time course to identify the optimum sonication conditions to be used for the remaining samples. After centrifuging at 13000 rpm for 15 min at 4°C, the supernatant (chromatin solution) was transferred into a new 1.5 ml microtube and stored at -80°C.

3.3.6.3 Analysis of chromatin fragment size

In order to ensure that the sonicated cell lysate contained DNA sheared to the desired fragment sizes of 100–500 bp, 50 µl of the chromatin solution was used for reversal of crosslinks. In a 500 µl PCR tube, 50 µl chromatin solution, 140 µl pronase working buffer (Appendix 8.24, Table 8.28) and 10 µl pronase (20 µg/µl) were added in sequence and mixed. Pronase contains various proteolytic components and is used to degrade proteins both extensively and completely in order to aid DNA purification. For the reversal of crosslinks, the mixture was incubated at 42°C for 2 h, then 65°C for 6 h, before being transferred into a 1.5 ml microtube. Upon addition of 200 µl phenol:chloroform 5:1 (pH4.7, Sigma-Aldrich), the mixture was vortexed at high speed for 5 min. After centrifuging at 13000 rpm for 10 min, the mixture was separated into two phases — aqueous DNA at the top and phenol at the bottom. Without disturbing the other phase, the top aqueous DNA phase was carefully

extracted and transferred into a new 1.5 ml microtube. Upon addition of 200 µl 0.3 M NaAc and 1 µl glycogen, the microtube was vortexed briefly to mix the contents. Upon addition of 1 ml 100 % EtOH, the microtube was vortexed briefly to mix the contents. The mixture was incubated at -80°C for 2 h to precipitate the DNA. After centrifuging at 13000 rpm for 10 min, the supernatant was removed. Upon addition of 700 µl 70 % EtOH, the mixture was centrifuged at 13000 rpm for 5 min and the supernatant was removed. The DNA pellet was dried under vacuum for 15 min, then resuspended in 50 µl sterile water and stored at -20°C. 10 µl of the input DNA resuspension was analysed through 1.5 % agarose gel electrophoresis to check the DNA fragment sizes, while 2 µl of the input DNA resuspension was used for the quantitation of DNA carried out using a nanodrop machine (refer to section 3.3.4.2).

3.3.6.4 Immunoprecipitation

For each immunoprecipitation reaction, an equal mix of rProtein A Sepharose™ Fast Flow beads (GE Healthcare) and Protein G Sepharose™ 4 Fast Flow beads (GE Healthcare) were used. 10 µl protein A/G beads mixture was washed with 250 µl yeast lysis buffer. After centrifuging at 5000 rpm for 1 min, the supernatant was removed. Upon addition of 250 µl yeast lysis buffer, the protein A/G beads mixture was incubated at 4°C for 1 h for equilibration. After centrifuging at 5000 rpm for 1 min, the supernatant was removed. Upon addition of 400 µl yeast lysis buffer, 5 µl 200 mM PMSF, 100 µl chromatin solution and the desired antibody (Table 3.18), the mixture was incubated with rotation at 4°C for 2 h. A no-antibody control was included for each chromatin solution sample.

Table 3.18 Antibodies used in immunoprecipitation

Antibody	Volume used
Rabbit α-H4 (Millipore)	4 µl
Rabbit α-H4K16ac (Active Motif)	8 µl
Rabbit α-GCN5 (Santa Cruz)	8 µl

After incubation, the mixture was centrifuged at 5000 rpm for 1 min, where the supernatant was kept for subsequent protein analysis to check protein stability and protein level. Upon addition of 700 µl yeast lysis buffer, the mixture was transferred to Corning® Costar® Spin-X® polypropylene centrifuge tube filters (Sigma-Aldrich). The protein A/G beads mixture was washed three times for 10 min each with yeast lysis buffer, two times for 10 min each with yeast lysis buffer with 0.5 M NaCl (Appendix 8.25, Table 8.29), once for 15 min with ChIP wash buffer (Appendix 8.25, Table 8.30), then once for 15 min with 1X TE buffer (Appendix 8.25, Table 8.31). Each wash was incubated with rotation at 4°C, before centrifuging at 5000 rpm for 1 min. After centrifuging at 5000 rpm for 1 min again to ensure dryness of the filter, the filter portion of the centrifuge tube filter was transferred to a 1.5 ml microtube. Upon addition of 120 µl ChIP elution buffer (Appendix 8.25, Table 8.32), the proteins bound to the beads were eluted by heating at 65°C for 10 min. After centrifuging at 6000 rpm for 1 min, 80 µl of the flow through was used for reversal of crosslinks. In a 500 µl PCR tube, 80 µl flow through, 110 µl 1X TE buffer and 10 µl pronase (20 µg/µl) were added in sequence and mixed. The subsequent steps were the same as that described before (refer to section 3.3.6.3). The DNA pellet was dried under vacuum for 15 min, then resuspended in 20 µl sterile water and stored at -20°C.

3.3.6.5 PCR and quantitative real-time PCR analysis

In order to check both input DNA resuspension and immunoprecipitated DNA

resuspension for presence of DNA before real-time PCR, a PCR reaction was carried out in a 200 µl PCR tube, where 11.8 µl sterile water, 1 µl 1:10 diluted input DNA resuspension or 1 µl neat immunoprecipitated DNA resuspension, 0.5 µl 5' primer (Table 3.19), 0.5 µl 3' primer (Table 3.19), 4 µl 5X PCR buffer (Promega), 1.5 µl 25 mM $MgCl_2$, 0.5 µl 10 mM dNTP, 0.2 µl Taq polymerase (Promega) were added in sequence and mixed. The following cycling parameters were repeated for 40 cycles — 95°C for 30 s, 50°C for 30 s and 72°C for 30 s. The extension products were analysed through 2.5 % agarose gel electrophoresis. Quantitative real-time PCR was carried out as previously described (refer to section 3.3.4.6) using various pairs of primers that amplify the indicated DNA fragments (Table 3.19).

Table 3.19 Primers used for PCR and quantitative real-time PCR

Gene	**Primer name**	**Sequence**	**Fragment amplified**
Target gene	*HIS3* Pro 5'	CACCTAGCGGATGACTCTTT	*S. cerevisiae* chromosome XV: 721813–721943 131 bp
	HIS3 Pro 3'	TTGCCTTCGTTTATCTTGCC	
	HIS3 ORF 5'	CTTACACATAGACGACCATCAC	*S. cerevisiae* chromosome XV: 722197–722310 114 bp
	HIS3 ORF 3'	GCAAATCCTGATCCAAACCT	

In order to calculate the relative percent IP, ΔCt values were first obtained by taking the difference between the average IP Ct values and the average input Ct values. $2^{-\Delta Ct}$ values were calculated, followed by the ratio of Input:IP. The values were normalised to the input DNA sample and the no-antibody control for each strain after factoring the 50-fold dilution into the calculations. The values obtained were then calculated relative to the uninduced WT histone H4 strain that was set as 1. The results are means ± S.D. for three replicate experiments.

4. Results

Chapter I	Genomic library screening of histone H4 mutant strains Y51A, E53A and Y98A
Chapter II	Characterisation of histone H4 tyrosine residues
Chapter III	Directed screening of histone H4 mutant strain Y98A
Chapter IV	Characterisation of histone H4 Y98A AT phenotype suppressors — Gcn5, Hpa1 and Hpa2
Chapter V	Histone H3 and H4 crosstalk studies

I

Genomic library screening of histone H4 mutant strains Y51A, E53A and Y98A

4I.1 Phenotype testing of histone H4 mutant strains Y51A, E53A and Y98A

Previous studies had shown that alanine-scanning mutagenesis of histone H4 amino acid residues Y51, E53 and Y98 conferred observable phenotypes, where phenotype testing was focused on 3-AT sensitivity that arose due to defects in transcriptional activation of the *HIS3* gene by Gcn4 (AT), antimycin A sensitivity that arose due to defects in transcriptional activation of the GAL genes by Gal4 (AA) or temperature sensitivity that arose due to general transcriptional defects (TS) phenotypes (refer to section 1.2.3; Lee, 2007).

On histidine-depleted media containing 3-AT, the H4Y51A and H4Y98A mutant strains exhibited reduced growth as compared to the positive control WT histone H4 strain (Figure 4.1, second panel, compare lanes 2 and 4 to lane 1). In fact, the H4Y98A mutant strain exhibited a more severe AT phenotype as compared to the H4Y51A mutant strain (Figure 4.1, second panel, compare lane 2 to lane 4). However, unlike the negative control Δ*GCN4* deletion strain, there was some background growth of the H4Y51A and H4Y98A mutant strains (Figure 4.1, second panel, compare lanes 2 and 4 to lane 6). This was most likely due to the use of different batches of plates, so both a positive control and a negative control were included on each plate as far as possible.

At the non-permissive temperature of 38°C, the growth of the H4Y51A, H4E53A and H4Y98A mutant strains was completely inhibited as compared to the WT histone H4 strain (Figure 4.1, third panel, compare lanes 2, 3 and 4 to lane 1).

On galactose media containing antimycin A, the H4Y98A mutant strain exhibited

reduced growth as compared to the WT histone H4 strain (Figure 4.1, fourth panel, compare lane 4 to lane 1). However, unlike the negative control Δ*GAL4* deletion strain, there was some background growth of the H4Y98A mutant strain (Figure 4.1, fourth panel, compare lane 4 to lane 5).

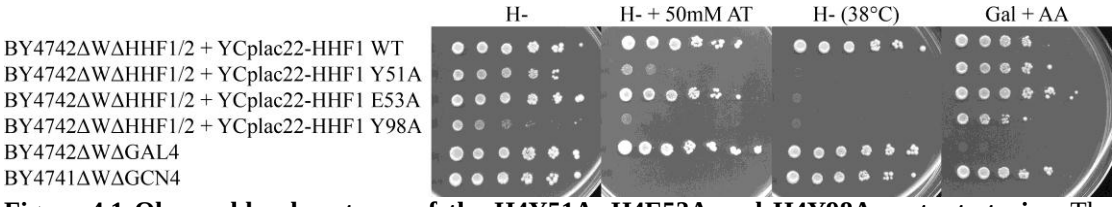

Figure 4.1 Observable phenotypes of the H4Y51A, H4E53A and H4Y98A mutant strains. The histone H4 deletion strain BY4742ΔWΔHHF1/2 expressing WT histone H4 served as the positive control, while the Δ*GCN4* and Δ*GAL4* deletion strains served as the negative controls for AT and AA phenotypes, respectively. The H- plate served as the loading control. Tenfold serial dilutions were titrated onto the indicated plates and incubated at 28°C for six days, unless otherwise indicated. H-: media lacking histidine, AT: 3-amino-1,2,4-triazole, Gal: galactose, AA: Antimycin A.

Thus, the H4Y51A mutant strain exhibited the AT and TS phenotypes, the H4E53A mutant strain exhibited the TS phenotype, and the H4Y98A mutant strain exhibited the AT, TS and AA phenotypes (Table 4.1).

Table 4.1 Tabulation of observable phenotypes of the H4Y51A, H4E53A and H4Y98A mutant strains

Histone H4 mutant strain	AT phenotype	TS phenotype	AA phenotype
H4Y51A	√	√	×
H4E53A	×	√	×
H4Y98A	√	√	√

4I.2 Suppression studies via over-expression for observable phenotypes of histone H4 mutant strains Y51A, E53A and Y98A

As the average fragment size of the genomic library YEp13 is approximately 6 kb, at least 10,000 transformants on each transformation plate had to be obtained in order to ensure coverage of the approximately 12,000 kb *S. cerevisiae* genome for about five

times. For the H4Y51A, H4E53A and H4Y98A mutant strains, the number of primary transformants obtained was 63,000 primary transformants, 45,000 primary transformants and 56,000 primary transformants, respectively (Lee, 2007).

Different numbers of YEp13 suppressor plasmids were isolated for each of the observable phenotypes of the histone H4 mutant strains Y51A, E53A and Y98A (Table 4.2). However, no YEp13 suppressor plasmids were isolated for the TS phenotype of the H4Y51A mutant strain and for the TS and AA phenotypes of the H4Y98A mutant strain despite repeated attempts (Lee, 2007).

The isolated YEp13 suppressor plasmids were transformed into the Δ*HHF1/2* deletion strain and a histone complementation assay was carried out to ensure that the isolated YEp13 suppressor plasmids did not encode WT histone H4 (Lee, 2007). The plasmids were also transformed back into the original histone mutant strain for which they were determined to be multi-copy phenotypic suppressors, in order to establish plasmid linkage of phenotypic suppression. It was found that phenotypic suppression by the isolated YEp13 suppressor plasmids was 100 % plasmid linked (Lee, 2007).

In addition, the isolated YEp13 suppressor plasmids were tested for phenotype specificity and strain specificity (Table 4.2). For phenotype specificity, the isolated YEp13 suppressor plasmids were transformed into the original histone mutant strain for which they were determined to be multi-copy phenotypic suppressors and tested for their ability to suppress the other phenotypes of the original histone mutant strain (Lee, 2007). For example, the five YEp13 suppressor plasmids isolated as suppressors for the AT phenotype of the H4Y98A mutant strain were tested for their ability to

suppress the TS and AA phenotypes of the H4Y98A mutant strain (Table 4.2). For strain specificity, the isolated YEp13 suppressor plasmids were cross transformed into the other histone mutant strains that exhibited the same phenotype as the original histone mutant strain (Lee, 2007). For example, the 11 YEp13 suppressor plasmids isolated as suppressors for the TS phenotype of the H4E53A mutant strain were tested for their ability to suppress the TS phenotype of the H4Y51A and H4Y98A mutant strains (Table 4.2).

Table 4.2 Details of YEp13 suppressor plasmids isolated for each of the observable phenotypes of histone H4 mutant strains Y51A, E53A and Y98A

Histone H4 mutant strain	**Number of suppressor plasmids isolated**		
	AT phenotype	**TS phenotype**	**AA phenotype**
H4Y51A	9 ➢ AT phenotype specific ➢ 3 suppressor plasmids not strain specific, could partially supress H4Y98A AT phenotype	0	NA
H4E53A	NA	11 ➢ TS phenotype specific ➢ 11 suppressor plasmids not strain specific, could partially suppress H4Y51A and H4Y98A TS phenotype	NA
H4Y98A	5 ➢ AT phenotype specific ➢ Strain specific	0	0

In order to identify the genomic DNA fragments contained in the isolated YEp13 suppressor plasmids, sequencing results were analysed using the Basic Local Alignment Search Tool (BLAST). Coupled with sub-cloning to split the multiple ORFs found in each genomic DNA fragment (Appendix 8.1, Table 8.1; Appendix 8.6,

Table 8.6), the identities of the genes responsible for suppression of the AT phenotype of the H4Y51A mutant strain (Table 4.3), the TS phenotype of the H4E53A mutant strain (Table 4.4) and the AT phenotype of the H4Y98A mutant strain (Table 4.5) were elucidated (Lee, 2007).

Table 4.3 Suppressors identified from H4Y51A AT phenotype suppression studies (Table adapted from Saccharomyces Genome Database)

Gene	Protein function	Protein size (Da)	Viability of null mutant
CCT6 / YDR188W	Subunit of the cytosolic chaperonin Cct ring complex, related to Tcp1p, essential protein that is required for the assembly of actin and tubulins in vivo; contains an ATP-binding motif	59,923	Inviable
KAR4 / YCL055W	Transcription factor required for gene regulation in response to pheromones; also required during meiosis; exists in two forms, a slower-migrating form more abundant during vegetative growth and a faster-migrating form induced by pheromone	38,672	Viable
MCK1 / YNL307C	Protein serine/threonine/tyrosine (dual-specificity) kinase involved in control of chromosome segregation and in regulating entry into meiosis; related to mammalian glycogen synthase kinases of the GSK-3 family	43,136	Viable
MSC3 / YLR219W	Protein of unknown function, green fluorescent protein (GFP)-fusion protein localizes to the cell periphery; msc3 mutants are defective in directing meiotic recombination events to homologous chromatids; potential Cdc28p substrate	80,530	Viable
MTC6 / YHR151C	Protein of unknown function; mtc6 is synthetically sick with cdc13-1	59,818	Viable
SUF2 / tP(AGG)C	Proline tRNA (tRNA-Pro), predicted by tRNAscan-SE analysis; can mutate to suppress +1 frame shift mutations in proline codons	-	-
YAP1 / YML007W	Basic leucine zipper (bZIP) transcription factor required for oxidative stress tolerance; activated by H2O2 through the multistep formation of disulfide bonds and transit from the cytoplasm to the nucleus; mediates resistance to cadmium	72,532	Viable
YDR187C	Dubious open reading frame unlikely to encode a protein, based on available experimental and comparative sequence data; partially overlaps the verified, essential ORF CCT6/YDR188W	18,444	Inviable
YHR177W	Putative protein of unknown function; overexpression causes a cell cycle delay or arrest	52,047	Viable

Table 4.4 Suppressors identified from H4E53A TS phenotype suppression studies (Table adapted from Saccharomyces Genome Database)

Gene	Protein function	Protein size (Da)	Viability of null mutant
CSE4 / YKL049C	Centromere protein that resembles histone H3, required for proper kinetochore function; homolog of human CENP-A; levels are regulated by E3 ubiquitin ligase Psh1p	26,841	Inviable

Table 4.5 Suppressors identified from H4Y98A AT phenotype suppression studies (Table adapted from Saccharomyces Genome Database)

Gene	Protein function	Protein size (Da)	Viability of null mutant
HPA2 / YPR193C	Tetrameric histone acetyltransferase with similarity to Gcn5p, Hat1p, Elp3p, and Hpa3p; acetylates histones H3 and H4 in vitro and exhibits autoacetylation activity	18,334	Viable
SIP5 / YMR140W	Protein of unknown function; interacts with both the Reg1p/Glc7p phosphatase and the Snf1p kinase	55,859	Viable
SKI8 / YGL213C	Ski complex component and WD-repeat protein, mediates 3'-5' RNA degradation by the cytoplasmic exosome; also required for meiotic double-strand break recombination; null mutants have superkiller phenotype	44,231	Viable
SLH1 / YGR271W	Putative RNA helicase related to Ski2p, involved in translation inhibition of non-poly(A) mRNAs; required for repressing propagation of dsRNA viruses	224,849	Viable
YMR141C	Dubious open reading frame unlikely to encode a functional protein, based on available experimental and comparative sequence data	12,108	Viable
YOR314W	Dubious open reading frame unlikely to encode a protein, based on available experimental and comparative sequence data	12,523	Viable

4I.3 Suppressor gene knock out studies

The screening of the three conditional histone H4 mutant strains Y51A, E53A and Y98A for multi-copy phenotypic suppressors was a tool to understand how histones

regulate gene expression in WT cells. Thus, it was important to determine whether gene knock out strains of the genes identified as multi-copy phenotypic suppressors could phenocopy the conditional histone H4 mutant alleles. However, gene knock out strains could not be obtained for those genes identified where the null mutant was inviable (Tables 4.3 and 4.4), such as *CCT6* and YDR187C that suppressed the AT phenotype of the H4Y51A mutant strain and *CSE4* that suppressed the TS phenotype of the H4E53A mutant strain. In addition, gene knock out strains were obtained only for those genes identified that encoded for functional proteins and not for those genes identified that were unlikely to encode for functional proteins (Table 4.5), such as YMR141C and YOR314W that suppressed the AT phenotype of the H4Y98A mutant strain.

On histidine-depleted media containing 3-AT, the Δ*SKI8*, Δ*YAP1* and Δ*MCK1* deletion strains exhibited a slight AT phenotype (Figure 4.2, second panel, compare lanes 4, 10 and 13 to lanes 1 and 8). This indicated that these genes encode for proteins that could play a minor role in the Gcn4-mediated transcriptional activation of the *HIS3* gene.

On the other hand, the Δ*HPA2*, Δ*SLH1*, Δ*SIP5*, ΔYHR151C, Δ*MSC3*, Δ*KAR4* and ΔYHR177W deletion strains did not exhibit the AT phenotype (Figure 4.2, second panel, compare lanes 3, 5, 6, 7, 11, 12 and 14 to lanes 1 and 8). This indicated that these genes do not encode for proteins involved in the Gcn4-mediated transcriptional activation of the *HIS3* gene. A second reason to explain the absence of an AT phenotype is functional redundancy, where a different protein possessing similar functions could be present in the cell.

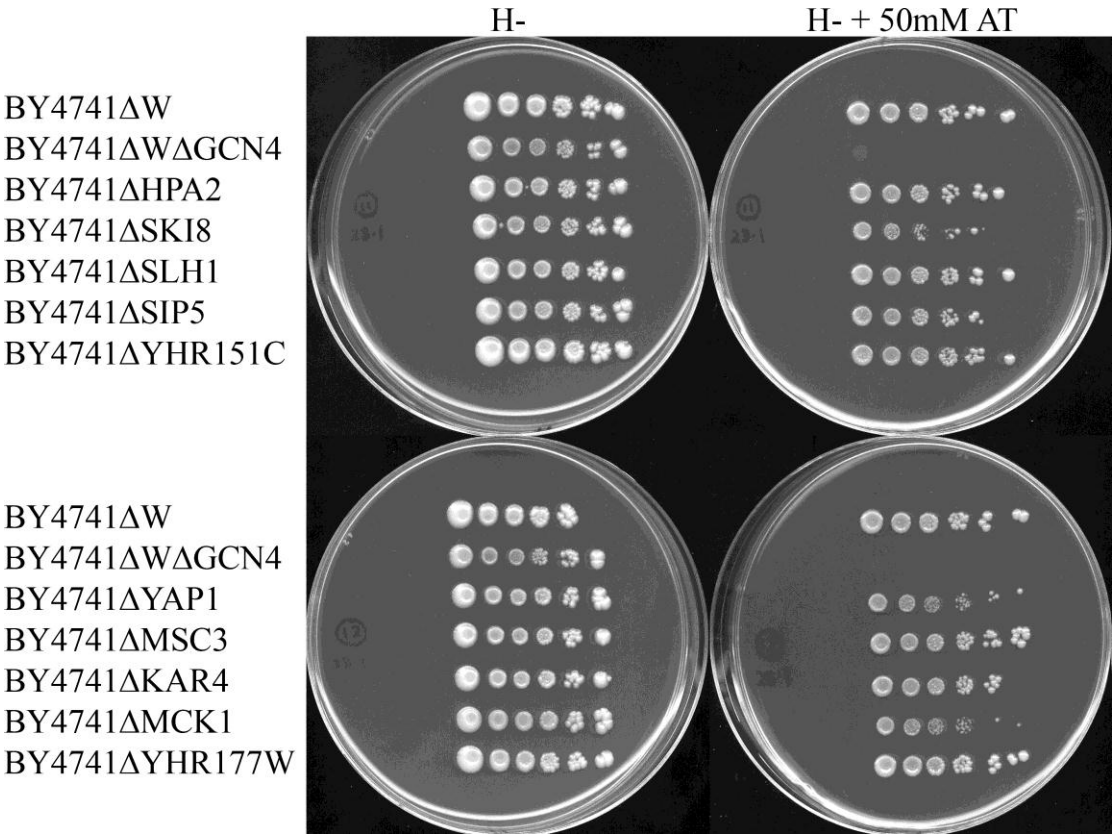

Figure 4.2 Observable phenotypes of gene knock out strains of the genes identified as multi-copy phenotypic suppressors. The WT BY4741ΔW strain served as the positive control, while the Δ*GCN4* deletion strain served as the negative control for AT phenotype. The H- plate served as the loading control. Tenfold serial dilutions were titrated onto the indicated plates and incubated at 28°C for six days. H-: media lacking histidine, AT: 3-amino-1,2,4-triazole.

II

Characterisation of

histone H4 tyrosine residues

4II.1 Alanine-scanning mutagenesis of histone H4 tyrosine residues

As alanine-scanning mutagenesis of histone H4 tyrosine residues Y51 and Y98 conferred observable phenotypes (refer to section 4I.1), it was of interest to determine whether site-directed alanine mutagenesis of the other two histone H4 tyrosine residues Y72 and Y88 would confer similar observable phenotypes.

The histone H4 tyrosine-alanine single-point mutant proteins each expressed from a *LEU2*-marked YCplac111 vector were transformed into the histone H4 deletion strain BY4742ΔWΔHHF1/2, which was dependent on a stable and essential episomal source of WT histone H4 expressed from a *URA3*-marked PactT316 vector. As cells containing *URA3*-marked plasmids cannot grow on media containing 5-FOA, negative selection was used to shuffle out the *URA3*-marked PactT316 vector, such that the histone H4 deletion strain BY4742ΔWΔHHF1/2 contained only the *LEU2*-marked YCplac111 vector expressing non-lethal histone H4 tyrosine-alanine single-point mutant proteins (refer to section 3.3.2.3).

On media containing 5-FOA, the H4Y51A and H4Y98A mutant strains exhibited reduced growth as compared to the positive control WT histone H4 strain (Figure 4.3, second panel, compare lanes 3 and 4 to lane 1). In fact, the H4Y98A mutant strain exhibited less growth as compared to the H4Y51A mutant strain (Figure 4.3, second panel, compare lane 3 to lane 4). The H4Y88A mutant strain exhibited growth comparable to the positive control WT histone H4 strain (Figure 4.3, second panel, compare lane 6 to lane 1). This indicated that these three histone H4 mutant proteins could complement the genomic deletion of histone H4, although to different degrees, where the H4Y88A mutant protein complemented fully, while the H4Y98A mutant

protein complemented only partially. On the other hand, the growth of the H4Y72A mutant strain was completely inhibited as compared to the WT histone H4 strain (Figure 4.3, second panel, compare lane 5 to lane 1). This indicated that the H4Y72A mutant protein was unable to complement the genomic deletion of histone H4, indicating that this residue may be essential for cell viability.

The growth of the negative control YCplac111 empty vector was completely inhibited as compared to the WT histone H4 strain (Figure 4.3, second panel, compare lane 2 to lane 1). This indicated that the plasmid shuffling procedure was efficient in shuffling out the *URA3*-marked PactT316 vector expressing WT histone H4 and that the growth of a histone H4 mutant strain on media containing 5-FOA was due solely to a complementation event.

Figure 4.3 Plasmid shuffling and complementation of histone H4 genomic deletion of cells expressing histone H4 tyrosine-alanine single-point mutant proteins. The WT histone H4 expressed from YCplac111 served as the positive control, while the YCplac111 empty vector served as the negative control. The L- plate served as the loading control. Tenfold serial dilutions were titrated onto the indicated plates and incubated at 28°C for three days. L-: media lacking leucine, H-: media lacking histidine, FOA: 5-FOA.

4II.1.1 Phenotype testing of histone H4 tyrosine residue mutant strains Y51A, Y88A and Y98A

As discussed earlier (refer to section 4I.1), on histidine-depleted media containing 3-AT, the H4Y51A and H4Y98A mutant strains exhibited the AT phenotype (Figure 4.4, second panel, compare lanes 2 and 3 to lane 1). However, the H4Y88A mutant

strain did not exhibit the AT phenotype as it exhibited growth comparable to the positive control WT histone H4 strain (Figure 4.4, second panel, compare lane 4 to lane 1). This indicated that the histone H4 tyrosine residues Y51 and Y98 were likely to be involved in the Gcn4-mediated transcriptional activation of the *HIS3* gene, while the histone H4 tyrosine residue Y88 was not.

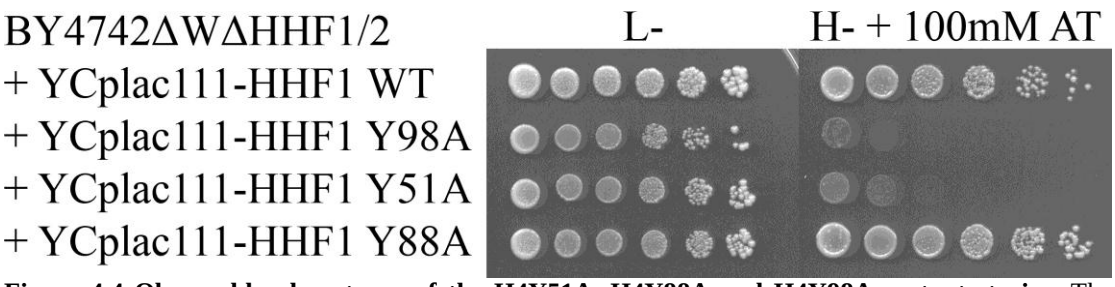

Figure 4.4 Observable phenotypes of the H4Y51A, H4Y88A and H4Y98A mutant strains. The histone H4 deletion strain BY4742ΔWΔHHF1/2 expressing WT histone H4 served as the positive control. The L- plate served as the loading control. Tenfold serial dilutions were titrated onto the indicated plates and incubated at 28°C for six days, unless otherwise indicated. L-: media lacking leucine, H-: media lacking histidine, AT: 3-amino-1,2,4-triazole.

4II.2 Characterisation of histone H4 tyrosine residue Y98

As tyrosine residues can be phosphorylated upon PTM of histones (Singh and Gunjan, 2011), it was of interest to determine whether histone H4 is phosphorylated at tyrosine residue Y98 or whether other factors come into play during the Gcn4-mediated transcriptional activation of the *HIS3* gene.

In addition to the original site-directed alanine mutagenesis of histone H4 Y98, histone H4 Y98 tyrosine-phenylalanine and tyrosine-aspartic acid single-point mutants were generated. Phenylalanine (F) resembles tyrosine (Y) structurally, except that the hydroxyl group of the aromatic ring is absent, which prevents phosphorylation from taking place. Unlike the hydrophobic tyrosine, aspartic acid (D) is a negatively charged residue, where this single-point mutation allows the study of whether hydrophobicity at histone H4 position 98 is required for the Gcn4-mediated

transcriptional activation of the *HIS3* gene.

On media containing 5-FOA, the H4Y98F mutant strain exhibited growth comparable to the positive control WT histone H4 strain (Figure 4.5, second panel, compare lane 5 to lane 1). In fact, the H4Y98A mutant strain exhibited less growth as compared to the H4Y98F mutant strain (Figure 4.5, second panel, compare lane 3 to lane 5). This indicated that these two histone H4 mutant proteins could complement the genomic deletion of histone H4, although to different degrees, where the H4Y98F mutant protein complemented fully, while the H4Y98A mutant protein complemented only partially. On the other hand, the growth of the H4Y98D mutant strain was completely inhibited as compared to the WT histone H4 strain (Figure 4.5, second panel, compare lane 4 to lane 1). This indicated that the H4Y98D mutant protein was unable to complement the genomic deletion of histone H4.

Figure 4.5 Plasmid shuffling and complementation of histone H4 genomic deletion of cells expressing histone H4 tyrosine-phenylalanine and tyrosine-aspartic acid single-point mutant proteins. The WT histone H4 expressed from YCplac111 served as the positive control, while the YCplac111 empty vector served as the negative control. The L- plate served as the loading control. Tenfold serial dilutions were titrated onto the indicated plates and incubated at 28°C for three days. L-: media lacking leucine, H-: media lacking histidine, FOA: 5-FOA.

Similar results were also obtained when the histone H4 tyrosine-phenylalanine and tyrosine-aspartic acid single-point mutant proteins were each expressed from the *TRP1*-marked PactT424-HA vector (Figure 4.6, second panel, compare lanes 4, 5, and 6 to lane 3).

Figure 4.6 Plasmid shuffling and complementation of histone H4 genomic deletion of cells expressing histone H4 tyrosine-phenylalanine and tyrosine-aspartic acid single-point mutant proteins. The WT histone H4 expressed from PactT424-HA served as the positive control, while the PactT424-HA empty vector served as the negative control. The W- plate served as the loading control. Tenfold serial dilutions were titrated onto the indicated plates and incubated at 28°C for three days. W-: media lacking tryptophan, H-: media lacking histidine, FOA: 5-FOA.

4II.2.1 Phenotype testing of histone H4 mutant strains Y98A and Y98F

As discussed earlier (refer to section 4I.1), on histidine-depleted media containing 3-AT, the H4Y98A mutant strain exhibited the AT phenotype (Figure 4.7, second panel, compare lane 2 to lane 1). However, the H4Y98F mutant strain did not exhibit the AT phenotype as it showed growth comparable to the positive control WT histone H4 strain (Figure 4.7, second panel, compare lane 3 to lane 1). This indicated that histone H4Y98 phosphorylation plays no role in the Gcn4-mediated transcriptional activation of the *HIS3* gene. Rather, either hydrophobicity or the steric effect of the aromatic ring at histone H4 position 98 is required for the Gcn4-mediated transcriptional activation of the *HIS3* gene.

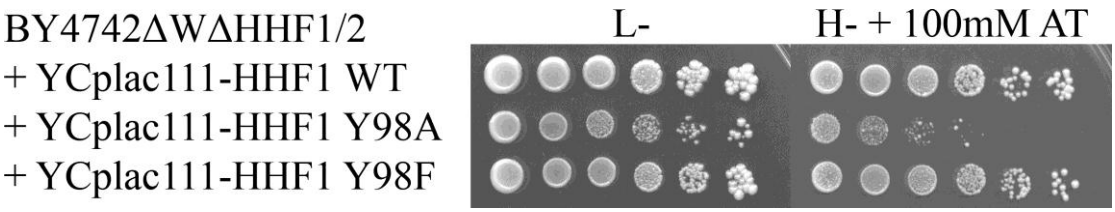

Figure 4.7 Observable phenotypes of the H4Y98A and H4Y98F mutant strains. The histone H4 deletion strain BY4742ΔWΔHHF1/2 expressing WT histone H4 served as the positive control. The L- plate served as the loading control. Tenfold serial dilutions were titrated onto the indicated plates and incubated at 28°C for six days, unless otherwise indicated. L-: media lacking leucine, H-: media lacking histidine, AT: 3-amino-1,2,4-triazole.

III

Directed screening of

histone H4 mutant strain Y98A

4III.1 Suppression studies via over-expression of HATs for AT phenotype of histone H4 mutant strain Y98A

As discussed earlier (refer to section 4I.2), on histidine-depleted media containing 3-AT, the H4Y98A mutant strain exhibited the AT phenotype that was suppressed by the over-expression of the HAT Hpa2. However, the Δ*HPA2* deletion strain could not phenocopy the conditional histone H4Y98A mutant allele (refer to section 4I.3). This indicated the possibility of functional redundancy, where a different protein possessing similar functions could be present in the cell. Thus, a second, directed screening of the H4Y98A mutant strain was carried out with the focus on HATs.

Although 12 HATs were selected for the directed screening of the H4Y98A mutant strain, cloning was successful only for nine HATs (Table 4.6). In addition, the over-expression of the HATs was analysed in the H4Y98A mutant strain to ensure that the proteins are expressed (Figure 4.8).

Table 4.6 HATs selected for H4Y98A AT phenotype suppression studies (Table adapted from Saccharomyces Genome Database)

Gene	Protein function	Protein size (Da)	Viability of null mutant	Cloning
EAF7 / YNL136W	Subunit of the NuA4 histone acetyltransferase complex, which acetylates the N-terminal tails of histones H4 and H2A	49,391	Viable	Not successful
ESA1 / YOR244W	Catalytic subunit of the histone acetyltransferase complex (NuA4) that acetylates four conserved internal lysines of the histone H4 N-terminal tail; required for cell cycle progression and transcriptional silencing at the rDNA locus	52,612	Inviable	Successful
GCN5 / YGR252W	Acetyltransferase, modifies N-terminal lysines on histones H2B and H3; acetylates Rsc4p, a subunit of the RSC chromatin-remodeling complex, altering replication stress tolerance; catalytic subunit of the ADA and SAGA histone acetyltransferase complexes; founding member of the Gcn5p-related N-acetyltransferase superfamily; mutant displays reduced transcription elongation in the G-less-based run-on (GLRO) assay	51,069	Viable	Successful
HAT1 / YPL001W	Catalytic subunit of the Hat1p-Hat2p histone acetyltransferase complex that uses the cofactor acetyl coenzyme A, to acetylate free nuclear and cytoplasmic histone H4; involved in telomeric silencing and DNA double-strand break repair	43,872	Viable	Successful
HAT2 / YEL056W	Subunit of the Hat1p-Hat2p histone acetyltransferase complex; required for high affinity binding of the complex to free histone H4, thereby enhancing Hat1p activity; similar to human RbAp46 and 48; has a role in telomeric silencing	45,060	Viable	Successful
HPA1 (*ELP3*) / YPL086C	Subunit of Elongator complex, which is required for modification of wobble nucleosides in tRNA; exhibits histone acetyltransferase activity that is directed to histones H3 and H4; disruption confers resistance to K. lactis zymotoxin	63,657	Viable	Successful
HPA2 / YPR193C	Tetrameric histone acetyltransferase with similarity to Gcn5p, Hat1p, Elp3p, and Hpa3p; acetylates histones H3 and H4 in vitro and exhibits autoacetylation activity	18,334	Viable	Successful

Table 4.6 HATs selected for H4Y98A AT phenotype suppression studies (continued) (Table adapted from Saccharomyces Genome Database)

Gene	Protein function	Protein size (Da)	Viability of null mutant	Cloning
HPA3 / YEL066W	D-Amino acid N-acetyltransferase, catalyzes N-acetylation of D-amino acids through ordered bi-bi mechanism in which acetyl-CoA is first substrate bound and CoA is last product liberated; similar to Hpa2p, acetylates histones weakly in vitro	20,698	Viable	Successful
RTT109 / YLL002W	Histone acetyltransferase critical for cell survival in the presence of DNA damage during S phase; acetylates H3-K56 and H3-K9; involved in non-homologous end joining and in regulation of Ty1 transposition; interacts physically with Vps75p	50,095	Viable	Successful
SAS2 / YMR127C	Histone acetyltransferase (HAT) catalytic subunit of the SAS complex (Sas2p-Sas4p-Sas5p), which acetylates free histones and nucleosomes and regulates transcriptional silencing; member of the MYSTacetyltransferase family	39,206	Viable	Successful
SAS3 / YBL052C	Histone acetyltransferase catalytic subunit of NuA3 complex that acetylates histone H3, involved in transcriptional silencing; homolog of the mammalian MOZ proto-oncogene; mutant has aneuploidy tolerance; sas3gcn5 double mutation is lethal	97,582	Viable	Not successful
TAF1 / YGR274C	TFIID subunit (145 kDa), involved in RNA polymerase II transcription initiation; possesses in vitro histone acetyltransferase activity but its role in vivo appears to be minor; involved in promoter binding and G1/S progression	120,695	Inviable	Not successful

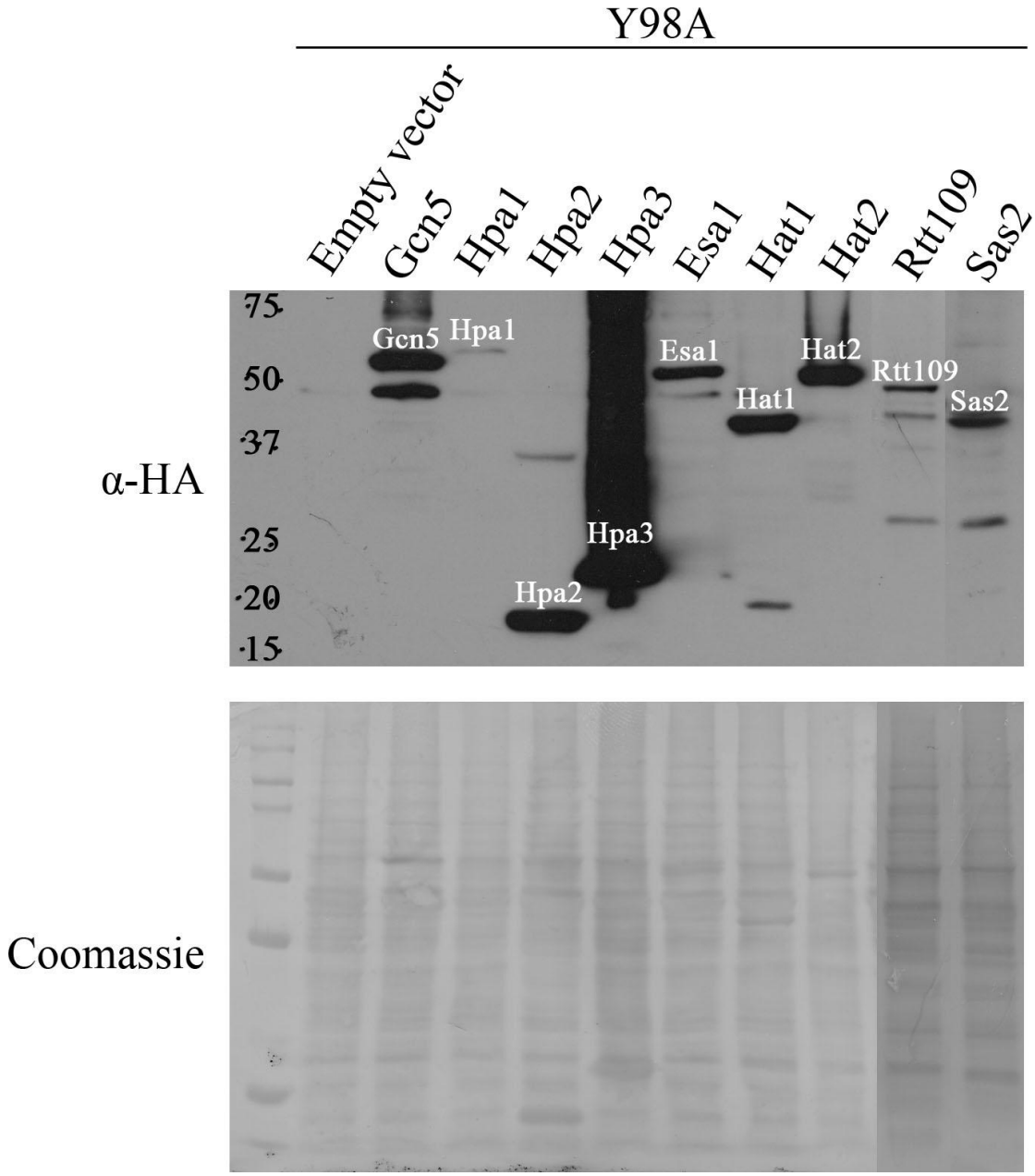

Figure 4.8 Over-expression of the HATs in the H4Y98A mutant strain. The H4Y98A mutant strain over-expressing the HATs Gcn5, Hpa1, Hpa2, Hpa3, Esa1, Hat1, Hat2, Rtt109 and Sas2 were grown in tryptophan-depleted liquid media to an OD_{600} value of 1. All the HATs were expressed from PactT424-HA. The H4Y98A mutant strain containing the PactT424-HA empty vector served as the negative control. Y98A: BY4742ΔWΔHHF1/2 + YCplac111-HHF1 Y98A.

4III.1.1 Suppression of the AT phenotype of the H4Y98A mutant strain by the over-expression of HATs

On histidine-depleted media containing different concentrations of 3-AT, the H4Y98A mutant strain over-expressing non-tagged and HA-tagged Gcn5 exhibited increased growth as compared to the negative controls PactT424 and PactT424-HA

empty vectors (Figure 4.9, second and third panels, compare lanes 5, 6, 7 and 8 to lanes 3 and 4). At the lower concentration of 3-AT (50 mM), both non-tagged and HA-tagged Gcn5 suppressed the AT phenotype of the H4Y98A mutant strain such that it exhibited growth comparable to the positive control WT histone H4 strain (Figure 4.9, second panel, compare lanes 5, 6, 7 and 8 to lanes 1 and 2). At the higher concentration of 3-AT (100 mM), both non-tagged and HA-tagged Gcn5 could suppress the AT phenotype of the H4Y98A mutant strain, but not as efficiently as compared to the lower concentration of 3-AT (Figure 4.9, third panel, compare lanes 5, 6, 7 and 8 to lanes 1 and 2).

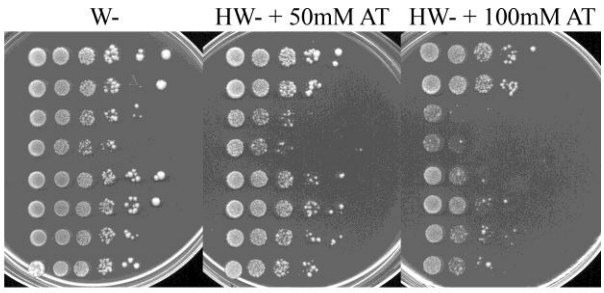

BY4742ΔWΔHHF1/2 + YCplac111-HHF1 WT
+ PactT424
+ PactT424-HA
BY4742ΔWΔHHF1/2 + YCplac111-HHF1 Y98A
+ PactT424
+ PactT424-HA
+ PactT424-GCN5
+ PactT424-GCN5
+ PactT424-HA-GCN5
+ PactT424-HA-GCN5

Figure 4.9 Gcn5 suppression of the AT phenotype of the H4Y98A mutant strain. The WT histone H4 strain containing PactT424 and PactT424-HA empty vectors served as the positive controls, while the H4Y98A mutant strain containing PactT424 and PactT424-HA empty vectors served as the negative controls. The W- plate served as the loading control. Tenfold serial dilutions were titrated onto the indicated plates and incubated at 28°C for six days. W-: media lacking tryptophan, HW-: media lacking histidine and tryptophan, AT: 3-amino-1,2,4-triazole.

On histidine-depleted media containing different concentrations of 3-AT, the H4Y98A mutant strain over-expressing non-tagged and HA-tagged Hpa1 and Hpa2 exhibited increased growth as compared to the negative controls PactT424 and PactT424-HA empty vectors (Figure 4.10, second and third panels, compare lanes 5, 6, 7 and 8 to lanes 3 and 4). At the lower concentration of 3-AT, both non-tagged and HA-tagged Hpa1 and Hpa2 suppressed the AT phenotype of the H4Y98A mutant strain such that it exhibited growth comparable to the positive control WT histone H4 strain (Figure 4.10, second panel, compare lanes 5, 6, 7 and 8 to lanes 1 and 2). At the

higher concentration of 3-AT, both non-tagged and HA-tagged Hpa1 and Hpa2 could suppress the AT phenotype of the H4Y98A mutant strain, but not as efficiently as compared to the lower concentration of 3-AT (Figure 4.10, third panel, compare lanes 5, 6, 7 and 8 to lanes 1 and 2).

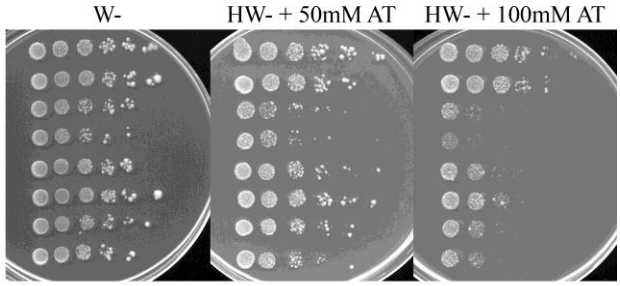

Figure 4.10 Hpa1 and Hpa2 suppression of the AT phenotype of the H4Y98A mutant strain. The WT histone H4 strain containing PactT424 and PactT424-HA empty vectors served as the positive controls, while the H4Y98A mutant strain containing PactT424 and PactT424-HA empty vectors served as the negative controls. The W- plate served as the loading control. Tenfold serial dilutions were titrated onto the indicated plates and incubated at 28°C for six days. W-: media lacking tryptophan, HW-: media lacking histidine and tryptophan, AT: 3-amino-1,2,4-triazole.

Hpa2 and Hpa3 are close homologues, as they were found to share a 49 % DNA sequence identity and 81 % amino acid sequence identity (Angus-Hill et al., 1999). However, on histidine-depleted media containing different concentrations of 3-AT, the H4Y98A mutant strain over-expressing non-tagged and HA-tagged Hpa3 exhibited growth comparable to the negative controls PactT424 and PactT424-HA empty vectors (Figure 4.11, second and third panels, compare lanes 5, 6, 7 and 8 to lanes 3 and 4).

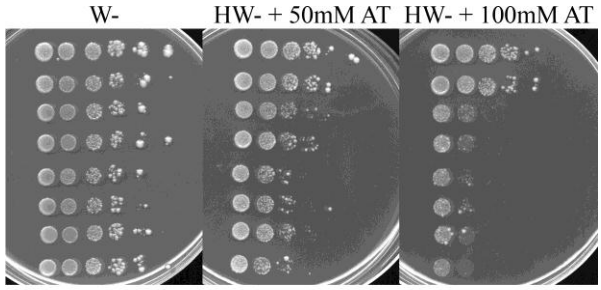

Figure 4.11 Hpa3 non-suppression of the AT phenotype of the H4Y98A mutant strain. The WT histone H4 strain containing PactT424 and PactT424-HA empty vectors served as the positive controls, while the H4Y98A mutant strain containing PactT424 and PactT424-HA empty vectors served as the negative controls. The W- plate served as the loading control. Tenfold serial dilutions were titrated onto the indicated plates and incubated at 28°C for six days. W-: media lacking tryptophan, HW-: media lacking histidine and tryptophan, AT: 3-amino-1,2,4-triazole.

Similarly, on histidine-depleted media containing different concentrations of 3-AT, the H4Y98A mutant strain over-expressing non-tagged and HA-tagged Esa1, Hat1, Hat2, Rtt109 and Sas2 exhibited growth comparable to the negative controls PactT424 and PactT424-HA empty vectors (Figure 4.12, second and third panels, compare lanes 5–14 to lanes 3 and 4). This indicated that the HATs Gcn5, Hpa1 and Hpa2 are multi-copy phenotypic suppressors of the AT phenotype of the H4Y98A mutant strain, while the HATs Hpa3, Esa1, Hat1, Hat2, Rtt109 and Sas2 are not.

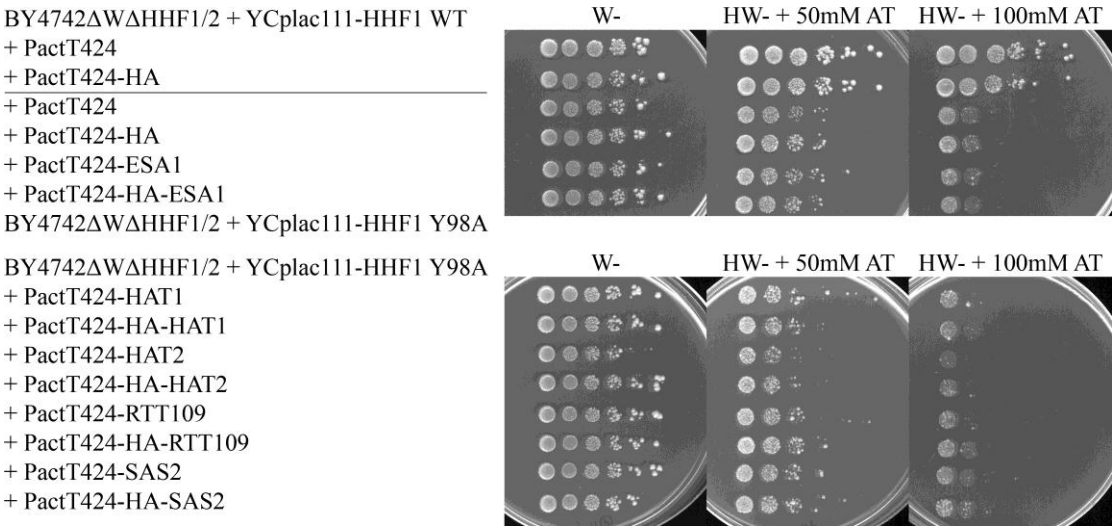

Figure 4.12 Esa1, Hat1, Hat2, Rtt109 and Sas2 non-suppression of the AT phenotype of the H4Y98A mutant strain. The WT histone H4 strain containing PactT424 and PactT424-HA empty vectors served as the positive controls, while the H4Y98A mutant strain containing PactT424 and PactT424-HA empty vectors served as the negative controls. The W- plate served as the loading control. Tenfold serial dilutions were titrated onto the indicated plates and incubated at 28°C for six days. W-: media lacking tryptophan, HW-: media lacking histidine and tryptophan, AT: 3-amino-1,2,4-triazole.

4III.1.2 HATs phenotype specificity and strain specificity

In addition, the HATs were tested for phenotype specificity and strain specificity. For phenotype specificity, the nine HATs were transformed into the H4Y98A mutant strain and tested for their ability to suppress the TS and AA phenotypes of the H4Y98A mutant strain. At the non-permissive temperature of 38°C, the growth of the H4Y98A mutant strain over-expressing HA-tagged HATs was completely inhibited as

compared to the WT histone H4 strain (Figure 4.13, second panel, compare lanes 3–5 and 8–13 to lanes 1 and 6). On galactose media containing antimycin A, the H4Y98A mutant strain over-expressing HA-tagged HATs exhibited reduced growth as compared to the WT histone H4 strain (Figure 4.13, third panel, compare lanes 3–5 and 8–13 to lanes 1 and 6). This indicated that the nine HATs, in particular the HATs Gcn5, Hpa1 and Hpa2, were phenotype-specific suppressors for the AT phenotype of the H4Y98A mutant strain.

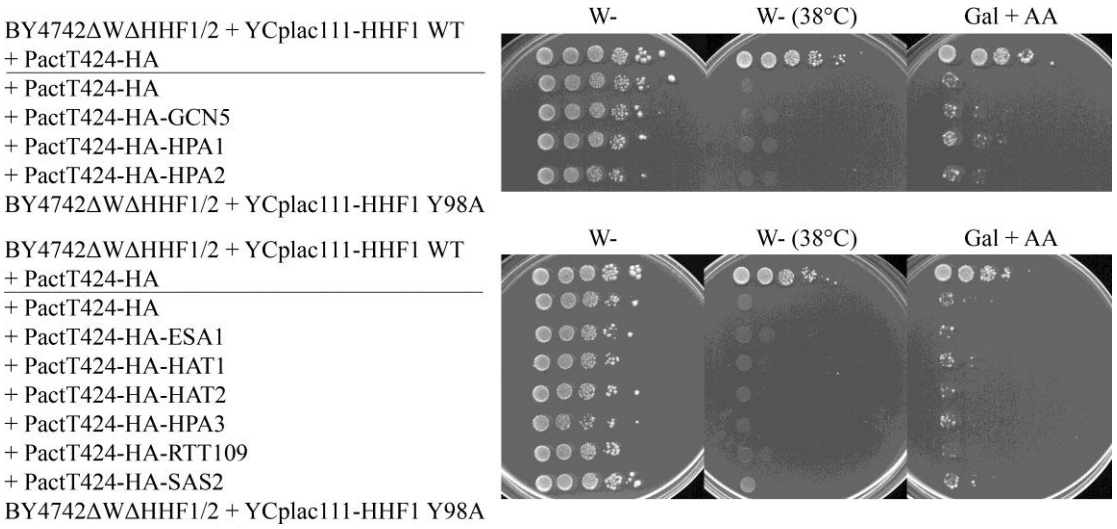

Figure 4.13 HATs phenotype specificity to the AT phenotype of the H4Y98A mutant strain. The WT histone H4 strain containing PactT424-HA empty vector served as the positive control, while the H4Y98A mutant strain containing PactT424-HA empty vector served as the negative control. The W- plate served as the loading control. Tenfold serial dilutions were titrated onto the indicated plates and incubated at 28°C for six days, unless otherwise indicated. W-: media lacking tryptophan, Gal: galactose, AA: Antimycin A.

For strain specificity, the HATs Gcn5, Hpa1 and Hpa2 were transformed into the H4Y51A mutant strain and tested for their ability to suppress the AT and TS phenotypes of the H4Y51A mutant strain. On histidine-depleted media containing different concentrations of 3-AT, the H4Y51A mutant strain over-expressing HA-tagged Gcn5, Hpa1 and Hpa2 exhibited growth comparable to the negative control PactT424-HA empty vector (Figure 4.14, second and third panels, compare lanes 4, 5 and 6 to lane 3). At the non-permissive temperature of 38°C, the growth of the

H4Y51A mutant strain over-expressing HA-tagged Gcn5, Hpa1 and Hpa2 was completely inhibited as compared to the WT histone H4 strain (Figure 4.14, second and third panels, compare lanes 4, 5 and 6 to lane 1). This indicated that the HATs Gcn5, Hpa1 and Hpa2 were both strain-specific and phenotype-specific suppressors for the AT phenotype of the H4Y98A mutant strain.

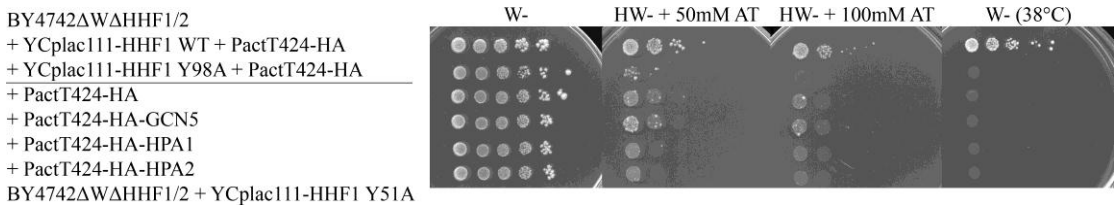

Figure 4.14 Gcn5, Hpa1 and Hpa2 strain specificity and phenotype specificity. The WT histone H4 strain containing PactT424-HA empty vector served as the positive control, while the H4Y51A mutant strain containing PactT424-HA empty vector served as the negative control. The W- plate served as the loading control. Tenfold serial dilutions were titrated onto the indicated plates and incubated at 28°C for six days, unless otherwise indicated. W-: media lacking tryptophan, HW-: media lacking histidine and tryptophan, AT: 3-amino-1,2,4-triazole.

4III.2 Suppressor gene knock out studies

4III.2.1 *GCN5*, *HPA1*, *HPA2* and *HPA3* single gene knock out studies

On histidine-depleted media containing lower concentration of 3-AT, the Δ*GCN5* and Δ*HPA1* deletion strains exhibited the AT phenotype (Figure 4.15, second panel, compare lanes 3 and 4 to lane 1), while the Δ*HPA2* and Δ*HPA3* deletion strains did not (Figure 4.15, second panel, compare lanes 5 and 6 to lane 1). On histidine-depleted media containing higher concentration of 3-AT, the Δ*GCN5*, Δ*HPA1* and Δ*HPA3* deletion strains exhibited the AT phenotype (Figure 4.15, third panel, compare lanes 3, 4 and 6 to lane 1), while the Δ*HPA2* deletion strain did not (Figure 4.15, third panel, compare lane 5 to lane 1). Interestingly, at the higher concentration of 3-AT, the Δ*GCN5* and Δ*HPA3* deletion strains exhibited an AT phenotype as severe as that of the negative control Δ*GCN4* deletion strain (Figure 4.15, third panel, compare lanes 3 and 6 to lane 2). On the other hand, the Δ*HPA1* deletion strain

exhibited a similar AT phenotype at both concentrations of 3-AT (Figure 4.15, second and third panels, compare lane 5 to lane 2).

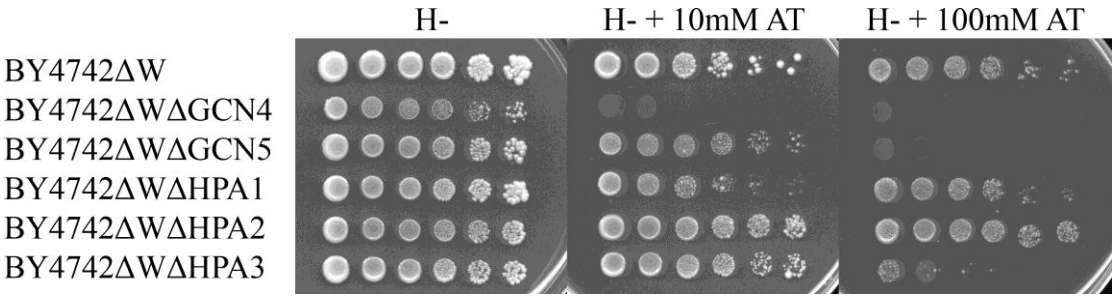

Figure 4.15 Observable AT phenotype of the Δ*GCN5*, Δ*HPA1*, Δ*HPA2* and Δ*HPA3* deletion strains. The WT BY4742ΔW strain served as the positive control, while the Δ*GCN4* deletion strain served as the negative control for AT phenotype. The H- plate served as the loading control. Tenfold serial dilutions were titrated onto the indicated plates and incubated at 28°C for six days. H-: media lacking histidine, AT: 3-amino-1,2,4-triazole.

4III.2.1.1 Suppression studies via over-expression in *GCN5* and *HPA1* single gene knock out mutant strains

As discussed earlier (refer to section 4III.1.3), on histidine-depleted media containing 3-AT, the Δ*GCN5* and Δ*HPA1* deletion strains exhibited the AT phenotype. In respect to the issue of redundancy, it was of interest to determine whether over-expression of any HAT could restore the growth of the deletion strains.

On histidine-depleted media containing 3-AT, the Δ*GCN5* deletion strain over-expressing HA-tagged Gcn5 exhibited increased growth as compared to the negative control PactT424-HA empty vector (Figure 4.16, second panel, compare lane 2 to lane 1), while the Δ*GCN5* deletion strain over-expressing HA-tagged Hpa1, Hpa2 and Hpa3 exhibited growth comparable to the negative control PactT424-HA empty vector (Figure 4.16, second panel, compare lanes 3, 4 and 5 to lane 1). This indicated that the function of Gcn5 in the Gcn4-mediated transcriptional activation of the *HIS3* gene cannot be replaced by the over-expression of the HATs Hpa1, Hpa2 or Hpa3.

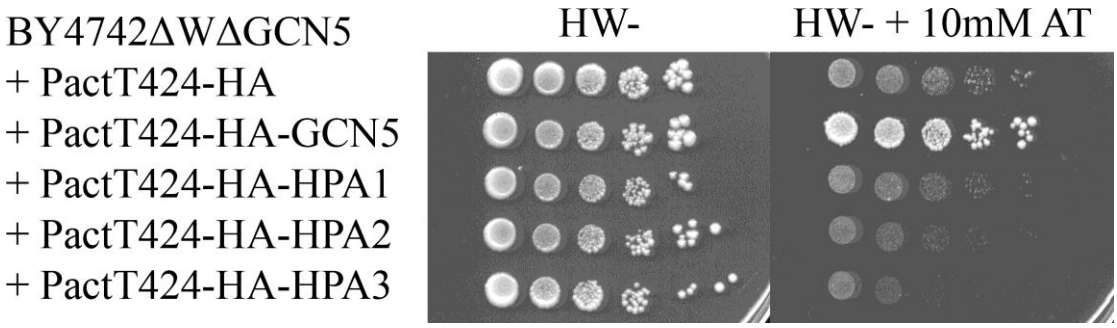

Figure 4.16 HATs over-expression in the Δ*GCN5* deletion strain. The PactT424-HA empty vector served as the negative control. The HW- plate served as the loading control. Tenfold serial dilutions were titrated onto the indicated plates and incubated at 28°C for six days. HW-: media lacking histidine and tryptophan, AT: 3-amino-1,2,4-triazole.

On histidine-depleted media containing 3-AT, the Δ*HPA1* deletion strain over-expressing HA-tagged Hpa1 exhibited increased growth as compared to the negative control PactT424-HA empty vector (Figure 4.17, second panel, compare lane 3 to lane 1), while the Δ*HPA1* deletion strain over-expressing HA-tagged Gcn5 and Hpa2 exhibited growth comparable to the negative control PactT424-HA empty vector (Figure 4.17, second panel, compare lanes 2 and 4 to lane 1). Interestingly, the Δ*HPA1* deletion strain over-expressing HA-tagged Hpa3 exhibited decreased growth as compared to the negative control PactT424-HA empty vector (Figure 4.17, second panel, compare lane 5 to lane 1). This indicated that the HATs Gcn5, Hpa1, Hpa2 and Hpa3 likely do not function redundantly as HATs.

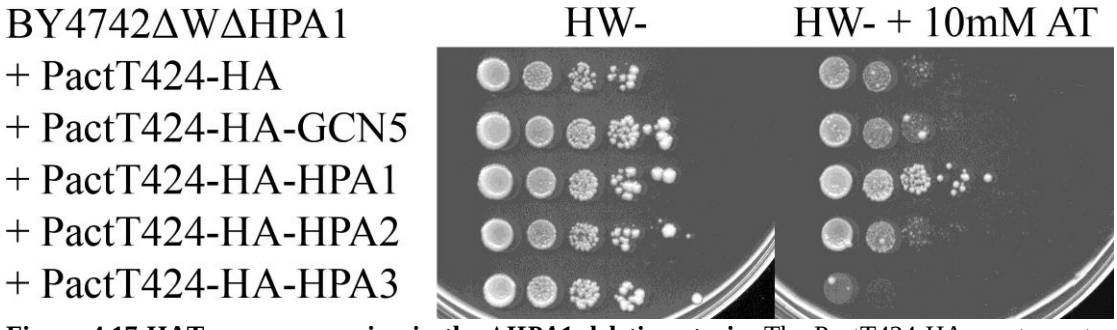

Figure 4.17 HATs over-expression in the Δ*HPA1* deletion strain. The PactT424-HA empty vector served as the negative control. The HW- plate served as the loading control. Tenfold serial dilutions were titrated onto the indicated plates and incubated at 28°C for six days. HW-: media lacking histidine and tryptophan, AT: 3-amino-1,2,4-triazole.

4III.2.2 *GCN5*, *HPA1*, *HPA2* and *HPA3* double gene knock out studies

On histidine-depleted media containing lower concentration of 3-AT, the Δ*GCN5*, Δ*GCN5*Δ*HPA1* and Δ*GCN5*Δ*HPA3* deletion strains exhibited the AT phenotype (Figure 4.18, second panel, compare lanes 3, 4 and 6 to lane 1), while the Δ*GCN5*Δ*HPA2* double deletion strain did not (Figure 4.18, second panel, compare lane 5 to lane 1). In fact, the Δ*GCN5*Δ*HPA1* and Δ*GCN5*Δ*HPA3* double deletion strains exhibited a more severe AT phenotype as compared to the Δ*GCN5* single deletion strain (Figure 4.18, second panel, compare lanes 4 and 6 to lane 3). Interestingly, at the higher concentration of 3-AT, the Δ*GCN5*, Δ*GCN5*Δ*HPA1*, Δ*GCN5*Δ*HPA2* and Δ*GCN5*Δ*HPA3* deletion strains exhibited an AT phenotype as severe as that of the negative control Δ*GCN4* deletion strain (Figure 4.18, second panel, compare lanes 3, 4, 5 and 6 to lane 2).

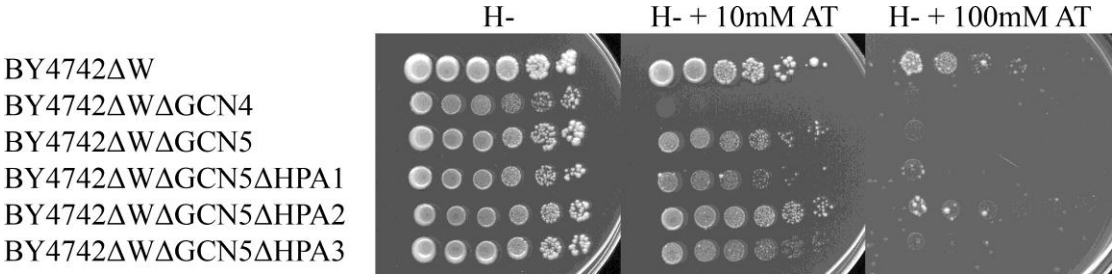

Figure 4.18 Observable AT phenotype of the Δ*GCN5*, Δ*GCN5*Δ*HPA1*, Δ*GCN5*Δ*HPA2* and Δ*GCN5*Δ*HPA3* deletion strains. The WT BY4742ΔW strain served as the positive control, while the Δ*GCN4* deletion strain served as the negative control for AT phenotype. The H- plate served as the loading control. Tenfold serial dilutions were titrated onto the indicated plates and incubated at 28°C for six days. H-: media lacking histidine, AT: 3-amino-1,2,4-triazole.

4III.3 Quantitative real-time PCR analysis

In order to quantitate the activation level of the *HIS3* gene by Gcn4 in the presence of each multi-copy phenotypic suppressor, quantitative real-time PCR analysis was carried out. Before carrying out quantitative real-time PCR analysis, the integrity and size distribution of total RNA purified had to be determined through formaldehyde (denaturing) agarose gel electrophoresis. Intact total RNA run on a denaturing gel was

shown to display sharp 28S (4718 bp) and 18S rRNA (1874 bp) bands (Figure 4.19, lanes 1 and 2; results were representative of all the samples), where the 28S rRNA band was more intense as compared to the 18S rRNA band (Figure 4.19, lanes 1 and 2, compare the upper 28S rRNA band to the lower 18S rRNA band). This indicated that the purified RNA was intact after the extraction procedure. In addition, the optimum 3-AT induction period for the strains used in this study was determined to be 2 h (Lee, 2007), after which accumulated transcripts were likely to be subsequently processed or degraded by the cellular machinery.

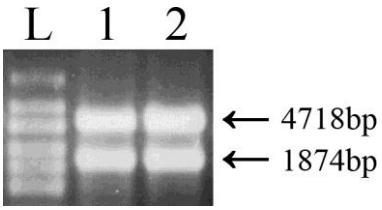

Figure 4.19 Integrity and size distribution of total RNA purified after the extraction procedure. Samples were separated on a 1.2 % FA gel, where the sharp 28S (4718 bp) and 18S rRNA (1874 bp) bands indicated that the rRNA and mRNA purified were not degraded during the extraction procedure.

When the WT histone H4 strain containing the PactT424-HA empty vector was induced in histidine-depleted media containing 3-AT for 2 h, *HIS3* mRNA expression levels increased by approximately 4-fold as compared to the uninduced WT histone H4 strain containing the PactT424-HA empty vector (Figure 4.20, compare lane 2 to lane 1). On the other hand, there were no significant differences in *HIS3* mRNA expression levels when the H4Y98A mutant strain containing the PactT424-HA empty vector was induced in histidine-depleted media containing 3-AT for 2 h as compared to the uninduced H4Y98A mutant strain containing the PactT424-HA empty vector (Figure 4.20, compare lane 4 to lane 3). This indicated that the histone H4 tyrosine residue Y98 is likely to be involved in the Gcn4-mediated transcriptional activation of the *HIS3* gene. These results also correlated with the growth of the positive control WT histone H4 strain and the reduced growth of the H4Y98A mutant

strain on histidine-depleted media containing 3-AT (Figure 4.1).

Upon over-expression of Gcn5, *HIS3* mRNA expression levels increased by approximately 2.7-fold for the induced strain as compared to the uninduced strain (Figure 4.20, compare lane 6 to lane 5). Upon over-expression of Hpa1, there were no significant differences in *HIS3* mRNA expression levels for the induced strain as compared to the uninduced strain (Figure 4.20, compare lane 8 to lane 7). Upon over-expression of Hpa2, *HIS3* mRNA expression levels increased by approximately 1.8-fold for the induced strain as compared to the uninduced strain (Figure 4.20, compare lane 10 to lane 9). This indicated that over-expression of Gcn5 led to the highest activation level of the *HIS3* gene, while over-expression of Hpa1 led to the lowest activation level of the *HIS3* gene (Figure 4.20, compare lanes 6, 8 and 10). These results also correlated with the suppression of the AT phenotype of the H4Y98A mutant strain by the over-expression of Gcn5, Hpa1 and Hpa2 on histidine-depleted media containing 3-AT (Figures 4.9 and 4.10).

However, it is important to take note that over-expression of Gcn5, Hpa1 and Hpa2 did not increase the activation level of the *HIS3* gene to that of the WT histone H4 strain containing the PactT424-HA empty vector (Figure 4.20, compare lanes 6, 8 and 10 to lane 2), although over-expression of Hpa1 increased the activation level of the *HIS3* gene even for the uninduced strain as compared to the uninduced WT histone H4 strain containing the PactT424-HA empty vector (Figure 4.20, compare lane 7 to lane 1).

Interestingly, upon over-expression of Hpa3, *HIS3* mRNA expression levels increased

by approximately 1.1-fold for the induced strain as compared to the uninduced strain (Figure 4.20, compare lane 12 to lane 11), although the overall activation level of the *HIS3* gene was comparable to that of the H4Y98A mutant strain containing the PactT424-HA empty vector (Figure 4.20, compare lane 12 to lane 4). In fact, upon over-expression of Hpa3, *HIS3* mRNA expression levels decreased by approximately 1.7-fold for the uninduced strain as compared to the uninduced H4Y98A mutant strain containing the PactT424-HA empty vector (Figure 4.20, compare lane 11 to lane 3). These results also correlated with the non-suppression of the AT phenotype of the H4Y98A mutant strain by the over-expression of Hpa3 on histidine-depleted media containing 3-AT (Figure 4.11).

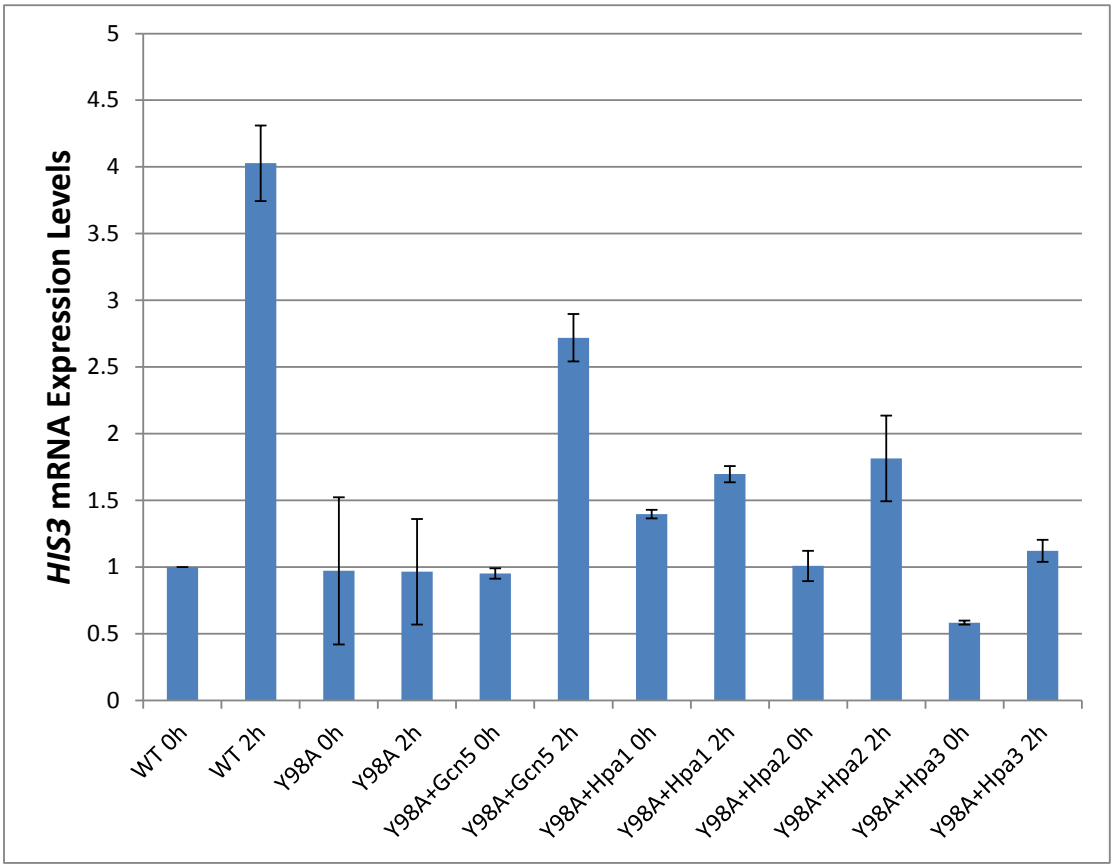

Figure 4.20 Over-expression of multi-copy phenotypic suppressors and the correlation to the activation level of the *HIS3* gene. Samples were grown in tryptophan-depleted liquid media to an OD_{600} value of 1 and induced in histidine-depleted liquid media containing 3-AT for the indicated number of hours. Total RNA was isolated and the amount of *HIS3* mRNA relative to *ACT1* mRNA was determined by quantitative real-time PCR. The results are means ± S.D. for three replicate experiments, where the values are relative to the uninduced WT histone H4 strain containing the PactT424-HA empty vector that was set as 1 (Appendix 8.26, Table 8.33). WT: BY4742ΔWΔHHF1/2 + YCplac111-HHF1 WT + PactT424-HA, Y98A: BY4742ΔWΔHHF1/2 + YCplac111-HHF1 Y98A + PactT424-HA.

IV

Characterisation of histone H4 Y98A AT phenotype suppressors — Gcn5, Hpa1 and Hpa2

4IV.1 Phenotype testing of an histone H4 N-terminal deletion strain

As discussed earlier (refer to section 4III.1.1), on histidine-depleted media containing 3-AT, the H4Y98A mutant strain exhibited the AT phenotype that was suppressed by the over-expression of the HATs Gcn5, Hpa1 and Hpa2. Previous reports have shown that the HATs Gcn5, Hpa1 and Hpa2 target core histones for acetylation, particularly at the N-terminal histone tails (Table 4.7). Thus, it was of interest to determine whether an histone H4 N-terminal deletion strain could phenocopy the histone H4Y98A mutant strain.

Table 4.7 Acetylation of core histones carried out by the HATs Gcn5, Hpa1 and Hpa2 (Table adapted from Sterner and Berger, 2000; He and Lehming, 2003; Peterson and Laniel, 2004)

Histone	**PTM**	**Histone modifying enzyme**
H2B	K11ac	Gcn5
	K16ac	Gcn5
H3	K4ac	Hpa2
	K9ac	Gcn5
	K14ac	Gcn5, Hpa1, Hpa2
	K18ac	Gcn5
	K23ac	Gcn5
	K27ac	Gcn5
H4	K5ac	Hpa2
	K8ac	Gcn5, Hpa1
	K12ac	Hpa2
	K16ac	Gcn5

As discussed earlier (refer to section 4I.1), on histidine-depleted media containing 3-AT, the H4Y98A mutant strain exhibited the AT phenotype (Figure 4.21, second panel, compare lane 2 to lane 1). Similarly, a mutant strain expressing a histone H4 deletion derivative lacking the first 19 amino acid residues also exhibited the AT phenotype (Figure 4.21, second panel, compare lane 3 to lane 1). In fact, the mutant strain expressing a histone H4 deletion derivative lacking the first 19 amino acid

residues exhibited a more severe AT phenotype as compared to the H4Y98A mutant strain (Figure 4.21, second panel, compare lane 3 to lane 2). This indicated that both the histone H4 tyrosine residue Y98 and the N-terminal 19 amino acid residues were likely to be involved in the Gcn4-mediated transcriptional activation of the *HIS3* gene.

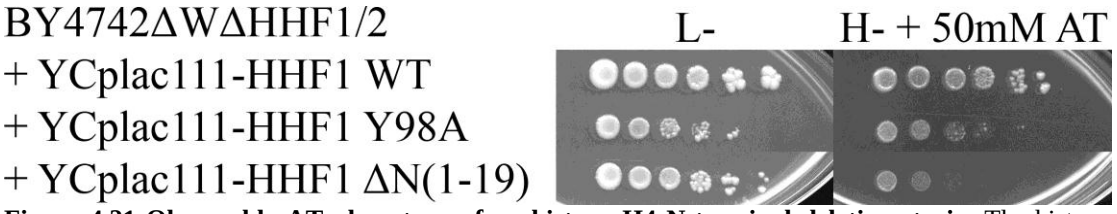

Figure 4.21 Observable AT phenotype of an histone H4 N-terminal deletion strain. The histone H4 deletion strain BY4742ΔWΔHHF1/2 expressing WT histone H4 served as the positive control. The L- plate served as the loading control. Tenfold serial dilutions were titrated onto the indicated plates and incubated at 28°C for six days, unless otherwise indicated. L-: media lacking leucine, H-: media lacking histidine, AT: 3-amino-1,2,4-triazole.

4IV.2 Alanine- and arginine-scanning mutagenesis of the histone H4 N-terminal lysine residues

As deletion of histone H4 N-terminal 19 amino acid residues conferred an observable AT phenotype (refer to section 4IV.1), it was of interest to determine whether site-directed alanine and arginine mutagenesis of the histone H4 N-terminal lysine residues would confer a similar AT phenotype. Lysine to alanine single-point mutations do not impose electrostatic or steric effects on a protein, as alanine does not undergo covalent modifications, will not alter the main chain conformation and eliminates side chains beyond the β carbon (Lefèvre et al., 1997). Lysine to arginine single-point mutations mimic unacetylated lysine residues and allow the study of whether positive charges at histone H4 position 5, 8, 12, 16 and 20 are required for the Gcn4-mediated transcriptional activation of the *HIS3* gene.

On media containing 5-FOA, the H4K5A, H4K8A, H4K12A, H4K16A and H4K20A mutant strains exhibited growth comparable to the positive control WT histone H4

strain (Figure 4.22, second panel, compare lanes 2, 3, 4, 5 and 6 to lane 1).This indicated that these five histone H4 mutant proteins complemented the genomic deletion of histone H4 as well as the positive control WT histone H4 protein.

Figure 4.22 Plasmid shuffling and complementation of histone H4 genomic deletion of cells expressing histone H4 N-terminal lysine to alanine single-point mutant proteins. The WT histone H4 expressed from YCplac111 served as the positive control. The L- plate served as the loading control. Tenfold serial dilutions were titrated onto the indicated plates and incubated at 28°C for three days. L-: media lacking leucine, H-: media lacking histidine, FOA: 5-FOA.

Similarly, on media containing 5-FOA, the H4K5R, H4K8R, H4K12R, H4K16R and H4K20R mutant strains exhibited growth comparable to the positive control WT histone H4 strain (Figure 4.23, second panel, compare lanes 2, 3, 4, 5 and 6 to lane 1).This indicated that these five histone H4 mutant proteins complemented the genomic deletion of histone H4 as well as the positive control WT histone H4 protein.

Figure 4.23 Plasmid shuffling and complementation of histone H4 genomic deletion of cells expressing histone H4 N-terminal lysine to arginine single-point mutant proteins. The WT histone H4 expressed from YCplac111 served as the positive control. The L- plate served as the loading control. Tenfold serial dilutions were titrated onto the indicated plates and incubated at 28°C for three days. L-: media lacking leucine, H-: media lacking histidine, FOA: 5-FOA.

4IV.2.1 Phenotype testing of the histone H4 N-terminal lysine residue mutant strains

As discussed earlier (refer to section 4I.1), on histidine-depleted media containing

3-AT, the H4Y98A mutant strain exhibited the AT phenotype (Figure 4.24, second panel, compare lane 2 to lane 1). Similarly, the H4K16A and H4K20A mutant strains also exhibited the AT phenotype (Figure 4.24, second panel, compare lanes 6 and 7 to lane 1). However, the H4K5A, H4K8A and H4K12A mutant strains did not display the AT phenotype as they exhibited growth comparable to the positive control WT histone H4 strain (Figure 4.24, second panel, compare lanes 3, 4 and 5 to lane 1).

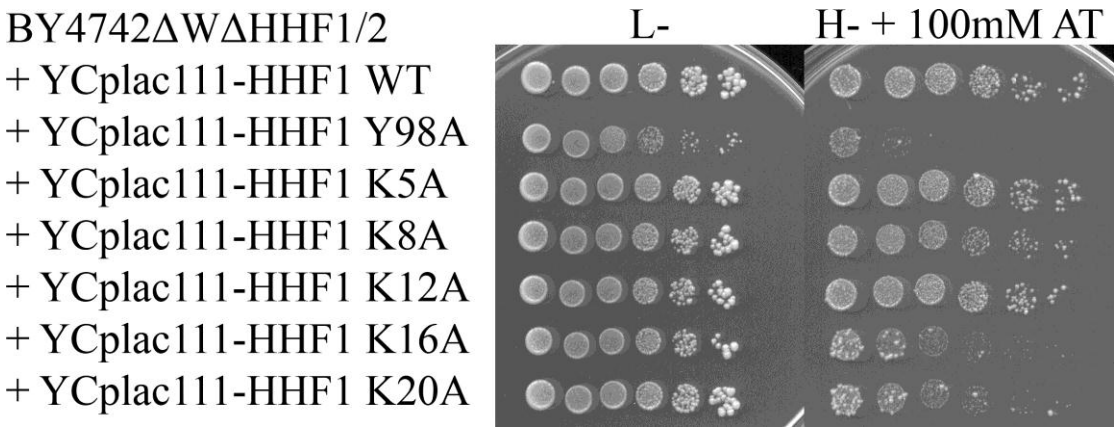

Figure 4.24 Observable AT phenotype of the histone H4 N-terminal lysine to alanine single-point mutant strains. The histone H4 deletion strain BY4742ΔWΔHHF1/2 expressing WT histone H4 served as the positive control. The L- plate served as the loading control. Tenfold serial dilutions were titrated onto the indicated plates and incubated at 28°C for six days, unless otherwise indicated. L-: media lacking leucine, H-: media lacking histidine, AT: 3-amino-1,2,4-triazole.

As discussed earlier (refer to section 4I.1), on histidine-depleted media containing 3-AT, the H4Y98A mutant strain exhibited the AT phenotype (Figure 4.25, second panel, compare lane 2 to lane 1). Similarly, the H4K16R mutant strain also exhibited the AT phenotype (Figure 4.25, second panel, compare lane 6 to lane 1). However, the H4K5R, H4K8R, H4K12R and H4K20R mutant strains did not display the AT phenotype as they exhibited growth comparable to the positive control WT histone H4 strain (Figure 4.25, second panel, compare lanes 3, 4, 5 and 7 to lane 1).

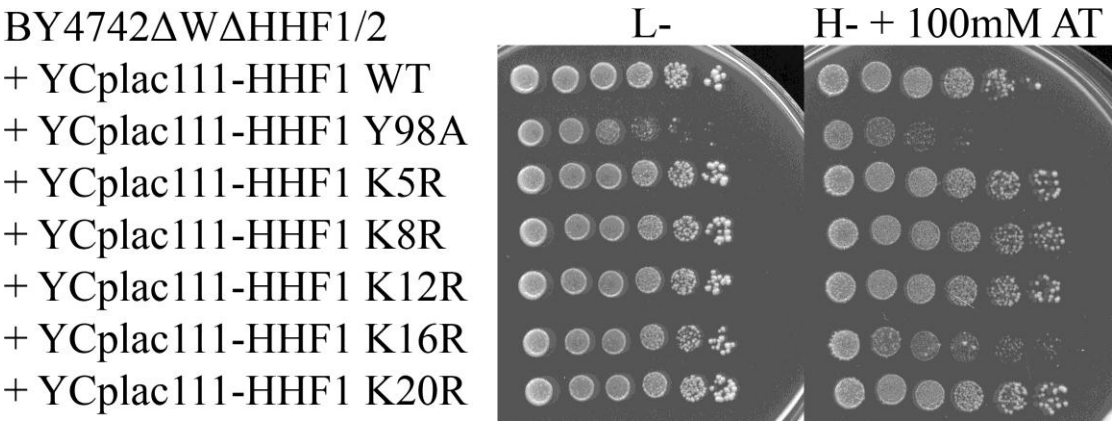

Figure 4.25 Observable AT phenotype of the histone H4 N-terminal lysine to arginine single-point mutant strains. The histone H4 deletion strain BY4742ΔWΔHHF1/2 expressing WT histone H4 served as the positive control. The L- plate served as the loading control. Tenfold serial dilutions were titrated onto the indicated plates and incubated at 28°C for six days, unless otherwise indicated. L-: media lacking leucine, H-: media lacking histidine, AT: 3-amino-1,2,4-triazole.

The above results indicate that the histone H4 N-terminal K5, K8 and K12 residues are likely not to be required for the Gcn4-mediated transcriptional activation of the *HIS3* gene, or at the very least, are less important for the Gcn4-mediated transcriptional activation of the *HIS3* gene. This is because site-directed alanine and arginine mutagenesis of these lysine residues did not phenocopy the conditional histone H4Y98A mutant strain (Table 4.8).

On the other hand, the histone H4 N-terminal K16 and K20 residues are likely to be required for the Gcn4-mediated transcriptional activation of the *HIS3* gene, where K16 may have a more important role for the Gcn4-mediated transcriptional activation of the *HIS3* gene. This is because site-directed alanine and arginine mutagenesis of K16 phenocopied the conditional histone H4Y98A mutant strain (Table 4.8), while only site-directed alanine mutagenesis of K20 phenocopied the conditional histone H4Y98A mutant strain (Table 4.8).

Table 4.8 Tabulation of observable AT phenotype of site-directed alanine and arginine mutagenesis of the histone H4 N-terminal lysine residues

Histone H4 N-terminal lysine residue	AT phenotype	
	Alanine mutagenesis	Arginine mutagenesis
K5	×	×
K8	×	×
K12	×	×
K16	√	√
K20	√	×

4IV.3 Alanine- and arginine-scanning mutagenesis of the histone H4 N-terminal lysine residues in combination with H4Y98A

As site-directed alanine and arginine mutagenesis of certain histone H4 N-terminal lysine residues conferred an observable AT phenotype (refer to section 4IV.2.1), it was of interest to determine whether site-directed alanine and arginine mutagenesis of the histone H4 N-terminal lysine residues in combination with H4Y98A would confer a similar observable AT phenotype.

On media containing 5-FOA, the H4K5A Y98A, H4K8A Y98A, H4K12A Y98A, H4K16A Y98A and H4K20A Y98A double mutant strains exhibited reduced growth as compared to the positive control WT histone H4 strain (Figure 4.26, second panel, compare lanes 4, 5, 6, 7 and 8 to lane 1). This indicated that these five histone H4 double mutant proteins complemented the genomic deletion of histone H4, although to different degrees.

In fact, the H4K5A Y98A, H4K8A Y98A and H4K12A Y98A double mutant strains exhibited less growth as compared to the H4Y98A mutant strain (Figure 4.26, second panel, compare lanes 4, 5 and 6 to lane 3), where this additive phenotypic effect indicated that these N-terminal and C-terminal mutations are independent of each

other. On the other hand, the H4K16A Y98A and H4K20A Y98A double mutant strains exhibited growth comparable to the H4Y98A mutant strain (Figure 4.26, second panel, compare lanes 7 and 8 to lane 3), where the lack of an additive phenotypic effect indicated that these N-terminal and C-terminal mutations are not independent of each other.

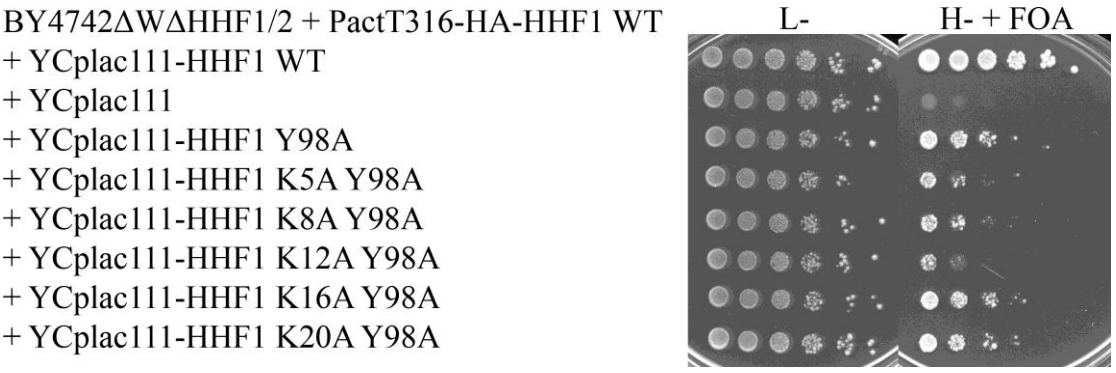

Figure 4.26 Plasmid shuffling and complementation of histone H4 genomic deletion of cells expressing histone H4 N-terminal lysine to alanine single-point mutant proteins in combination with H4Y98A. The WT histone H4 expressed from YCplac111 served as the positive control, while the YCplac111 empty vector served as the negative control. The L- plate served as the loading control. Tenfold serial dilutions were titrated onto the indicated plates and incubated at 28°C for three days. L-: media lacking leucine, H-: media lacking histidine, FOA: 5-FOA.

On media containing 5-FOA, the H4K5R Y98A, H4K8R Y98A, H4K12R Y98A, H4K16R Y98A and H4K20R Y98A double mutant strains exhibited reduced growth as compared to the positive control WT histone H4 strain (Figure 4.27, second panel, compare lanes 2, 3, 4, 5 and 6 to lane 1). This indicated that these five histone H4 double mutant proteins complemented the genomic deletion of histone H4, although to different degrees.

In fact, the H4K5R Y98A and H4K8R Y98A double mutant strains exhibited less growth as compared to the H4Y98A mutant strain (Figure 4.27, second panel, compare lanes 2 and 3 to lane 3 in Figure 4.26), where this additive phenotypic effect indicated that these N-terminal and C-terminal mutations are independent of each

other. On the other hand, the H4K12R Y98A, H4K16R Y98A and H4K20R Y98A double mutant strains exhibited growth comparable to the H4Y98A mutant strain (Figure 4.27, second panel, compare lanes 4, 5 and 6 to lane 3 in Figure 4.26), where the lack of an additive phenotypic effect indicated that these N-terminal and C-terminal mutations are not independent of each other.

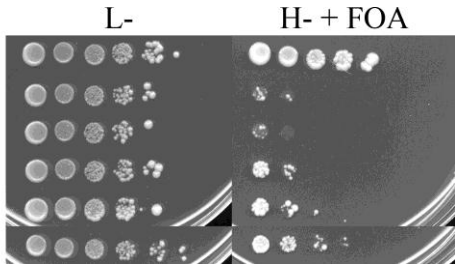

Figure 4.27 Plasmid shuffling and complementation of histone H4 genomic deletion of cells expressing histone H4 N-terminal lysine to arginine single-point mutant proteins in combination with H4Y98A. The WT histone H4 expressed from YCplac111 served as the positive control. The L- plate served as the loading control. Tenfold serial dilutions were titrated onto the indicated plates and incubated at 28°C for three days. L-: media lacking leucine, H-: media lacking histidine, FOA: 5-FOA.

4IV.3.1 Phenotype testing of the histone H4 N-terminal lysine residue mutant strains in combination with H4Y98A

As discussed earlier (refer to section 4I.1), on histidine-depleted media containing 3-AT, the H4Y98A mutant strain exhibited the AT phenotype (Figure 4.28, second panel, compare lane 2 to lane 1). Similarly, the H4K5A Y98A, H4K8A Y98A, H4K12A Y98A, H4K16A Y98A and H4K20A Y98A double mutant strains also exhibited the AT phenotype (Figure 4.28, second panel, compare lanes 3, 4, 5, 6 and 7 to lane 1). Interestingly, the H4K8A Y98A double mutant strain exhibited the AT phenotype that was less severe than the one of the H4Y98A mutant strain (Figure 4.28, second panel, compare lane 4 to lane 2).

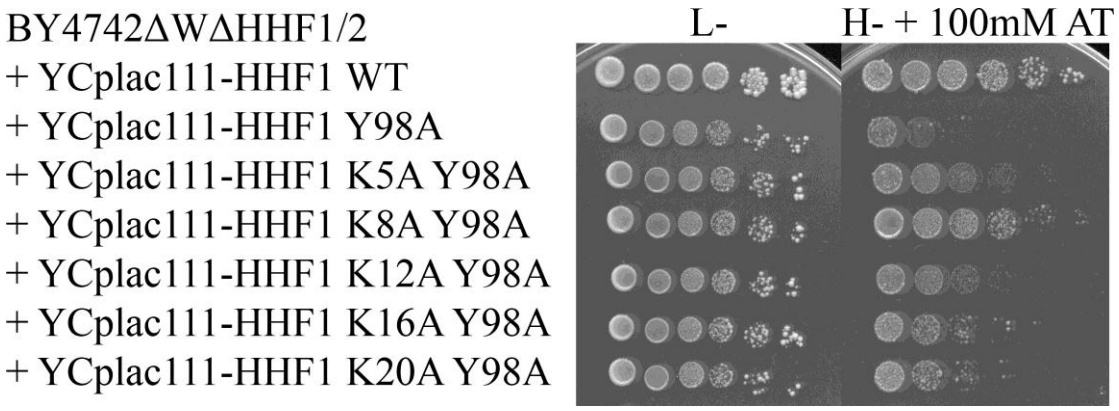

Figure 4.28 Observable AT phenotype of the histone H4 N-terminal lysine to alanine single-point mutant strains in combination with H4Y98A. The histone H4 deletion strain BY4742ΔWΔHHF1/2 expressing WT histone H4 served as the positive control. The L- plate served as the loading control. Tenfold serial dilutions were titrated onto the indicated plates and incubated at 28°C for six days, unless otherwise indicated. L-: media lacking leucine, H-: media lacking histidine, AT: 3-amino-1,2,4-triazole.

As discussed earlier (refer to section 4I.1), on histidine-depleted media containing 3-AT, the H4Y98A mutant strain exhibited the AT phenotype (Figure 4.29, second panel, compare lane 2 to lane 1). Similarly, the H4K5R Y98A, H4K8R Y98A, H4K12R Y98A, H4K16R Y98A and H4K20R Y98A double mutant strains also exhibited the AT phenotype (Figure 4.29, second panel, compare lanes 3, 4, 5, 6 and 7 to lane 1). Interestingly, the H4K5R Y98A, H4K8R Y98A, H4K16R Y98A and H4K20R Y98A double mutant strains exhibited the AT phenotype that was less severe than the one of the H4Y98A mutant strain (Figure 4.29, second panel, compare lanes 3, 4, 6 and 7 to lane 2).

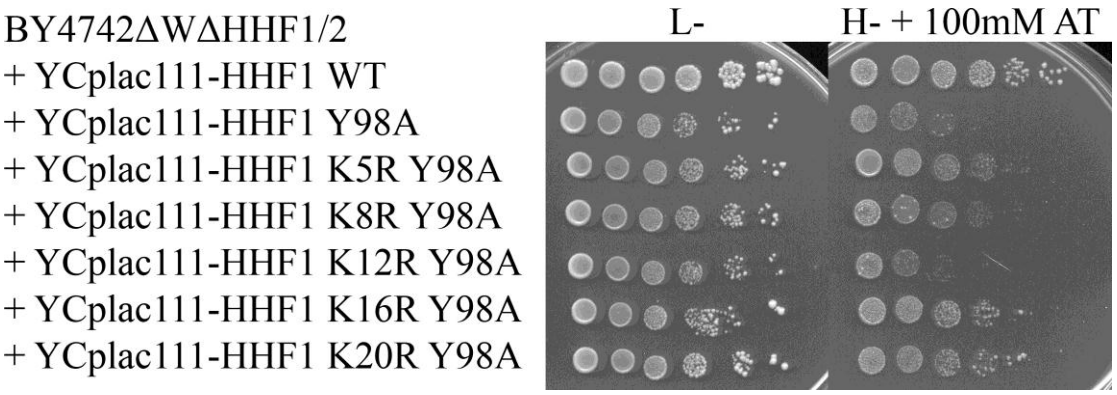

Figure 4.29 Observable AT phenotype of the histone H4 N-terminal lysine to arginine single-point mutant strains in combination with H4Y98A. The histone H4 deletion strain BY4742ΔWΔHHF1/2 expressing WT histone H4 served as the positive control. The L- plate served as the loading control. Tenfold serial dilutions were titrated onto the indicated plates and incubated at 28°C for six days, unless otherwise indicated. L-: media lacking leucine, H-: media lacking histidine, AT: 3-amino-1,2,4-triazole.

4IV.3.2 Suppression studies via over-expression of HATs for AT phenotype of the histone H4 N-terminal lysine residue mutant strains in combination with H4Y98A

As discussed earlier (refer to section 4IV.3.1), on histidine-depleted media containing 3-AT, the histone H4 N-terminal lysine to alanine and lysine to arginine single-point mutant strains in combination with H4Y98A exhibited the AT phenotype. Thus, it was of interest to determine whether the HATs Gcn5, Hpa1 and Hpa2 (which are multi-copy phenotypic suppressors for the AT phenotype of the H4Y98A mutant strain) could also suppress the AT phenotype of these mutant strains, in order to elucidate the histone H4 N-terminal lysine targets of the HATs. However, results were generally inconclusive and further experimentation via mass spectrometry would be necessary to determine the histone H4 N-terminal lysine targets of the HATs Gcn5, Hpa1 and Hpa2 (Figures 4.30 and 4.31).

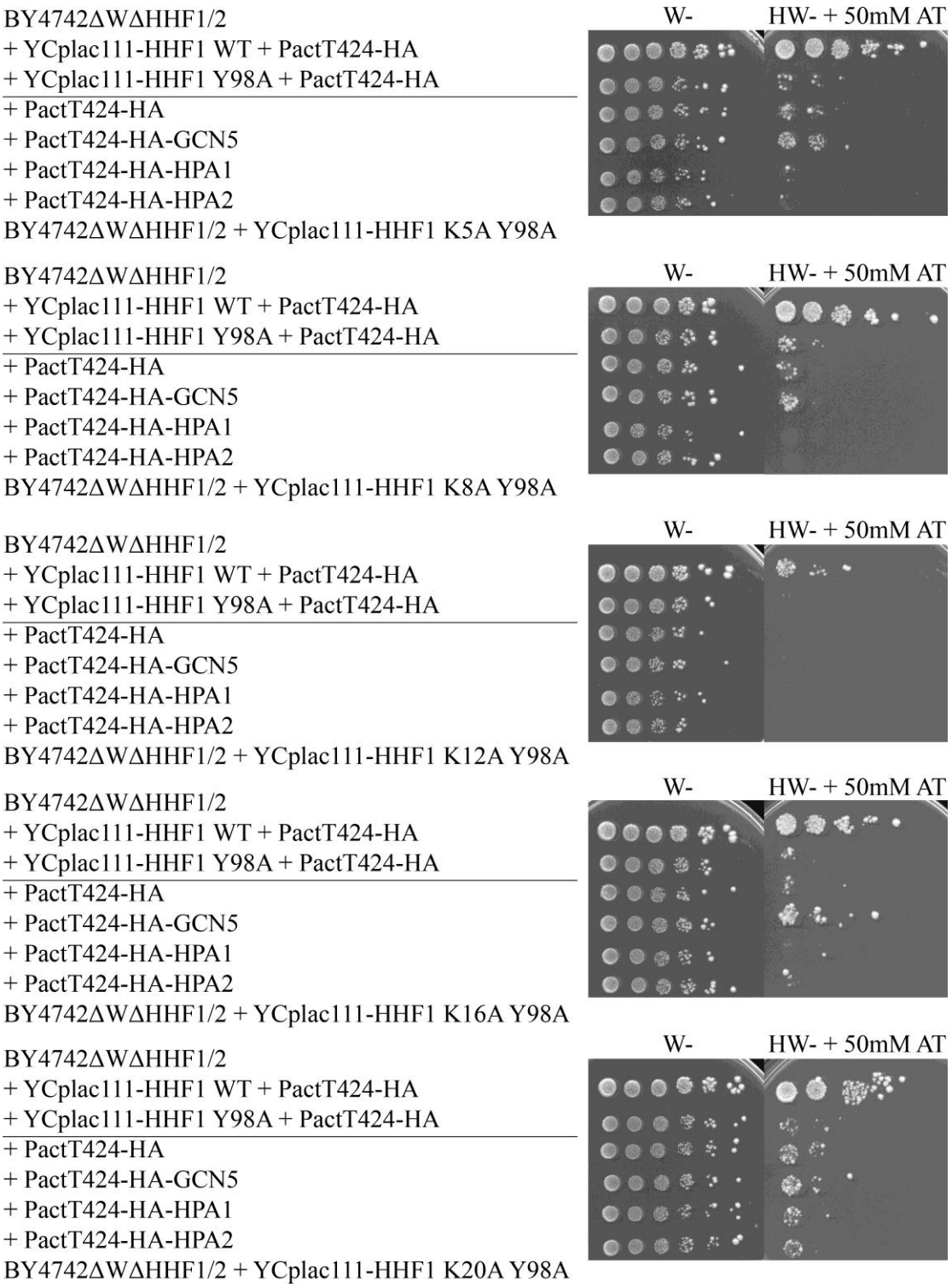

Figure 4.30 Suppression by Gcn5, Hpa1 and Hpa2 of observable AT phenotype of the histone H4 N-terminal lysine to alanine single-point mutant strains in combination with H4Y98A. The histone H4 deletion strain BY4742ΔWΔHHF1/2 expressing WT histone H4 and PactT424-HA empty vector served as the positive control. The W- plate served as the loading control. Tenfold serial dilutions were titrated onto the indicated plates and incubated at 28°C for six days, unless otherwise indicated. W-: media lacking tryptophan, HW-: media lacking histidine and tryptophan, AT: 3-amino-1,2,4-triazole.

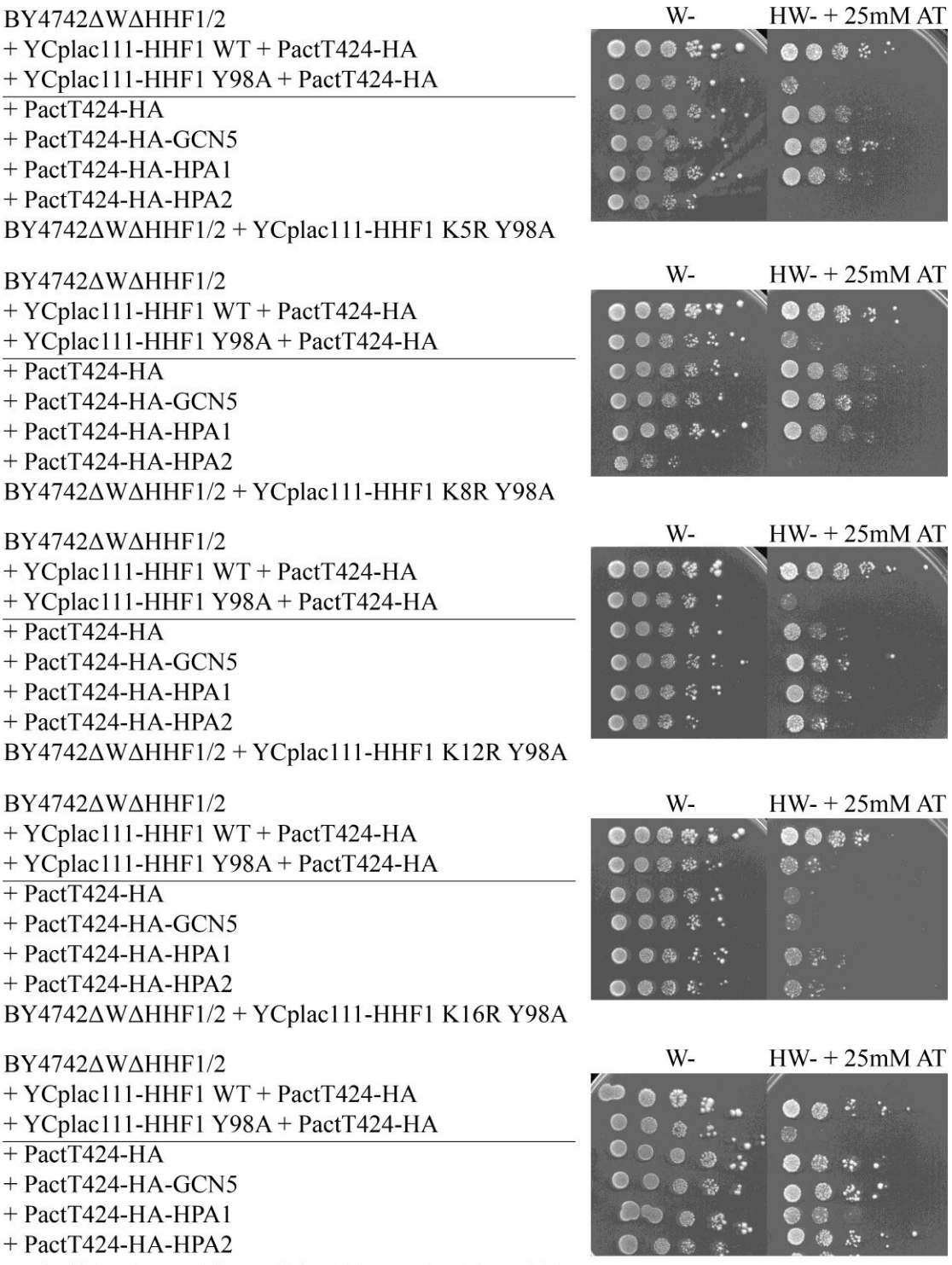

Figure 4.31 Suppression by Gcn5, Hpa1 and Hpa2 of observable AT phenotype of the histone H4 N-terminal lysine to arginine single-point mutant strains in combination with H4Y98A. The histone H4 deletion strain BY4742ΔWΔHHF1/2 expressing WT histone H4 and PactT424-HA empty vector served as the positive control. The W- plate served as the loading control. Tenfold serial dilutions were titrated onto the indicated plates and incubated at 28°C for six days, unless otherwise indicated. W-: media lacking tryptophan, HW-: media lacking histidine and tryptophan, AT: 3-amino-1,2,4-triazole.

4IV.4 Arginine-scanning mutagenesis of histone H4 N-terminal K8 and K16 residues

As discussed earlier (refer to section 4IV.2.1), histone H4 N-terminal K16 and K20 residues are likely to be required for the Gcn4-mediated transcriptional activation of the *HIS3* gene, where K16 may have a more important role for the Gcn4-mediated transcriptional activation of the *HIS3* gene. Previous reports have shown that Gcn5 targets H4K8 and H4K16 for acetylation (Table 4.7). Thus, it was of interest to determine whether the histone H4 N-terminal K8,16R double mutant strain without and in combination with H4Y98A could phenocopy the conditional histone H4Y98A mutant strain.

On media containing 5-FOA, the H4K8,16R double mutant strain exhibited growth comparable to the positive control WT histone H4 strain (Figure 4.32, second panel, compare lane 2 to lane 1). This indicated that the H4K8,16R double mutant protein complemented the genomic deletion of histone H4 as well as the positive control WT histone H4 protein. On the other hand, the growth of the H4K8,16R Y98A triple mutant strain was completely inhibited as compared to the WT histone H4 strain (Figure 4.32, second panel, compare lane 3 to lane 1). This indicated that the H4K8,16R Y98A triple mutant protein was unable to complement the genomic deletion of histone H4.

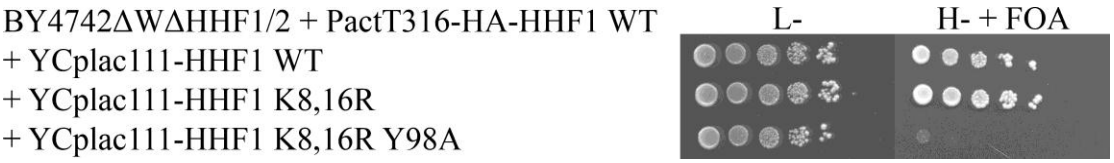

Figure 4.32 Plasmid shuffling and complementation of histone H4 genomic deletion of cells expressing histone H4 N-terminal K8 and K16 residues lysine to arginine double mutant proteins without and in combination with H4Y98A. The WT histone H4 expressed from YCplac111 served as the positive control. The L- plate served as the loading control. Tenfold serial dilutions were titrated onto the indicated plates and incubated at 28°C for three days. L-: media lacking leucine, H-: media lacking histidine, FOA: 5-FOA.

4IV.4.1 Phenotype testing of the histone H4K8,16R double mutant strain

As discussed earlier (refer to section 4I.1), on histidine-depleted media containing 3-AT, the H4Y98A mutant strain exhibited the AT phenotype (Figure 4.33, second panel, compare lane 2 to lane 1). Similarly, the H4K8,16R double mutant strain also exhibited the AT phenotype (Figure 4.33, second panel, compare lane 3 to lane 1).

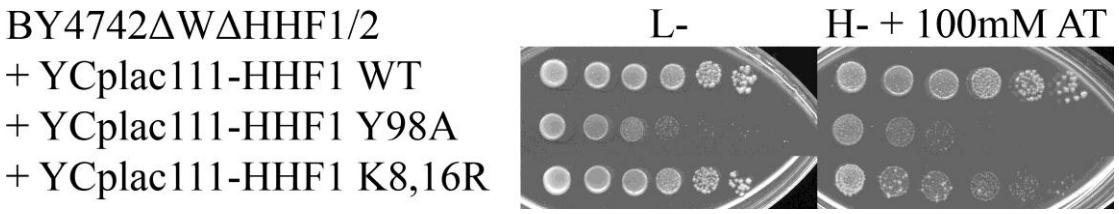

Figure 4.33 Observable AT phenotype of the histone H4K8,16R double mutant strain. The histone H4 deletion strain BY4742ΔWΔHHF1/2 expressing WT histone H4 served as the positive control. The L- plate served as the loading control. Tenfold serial dilutions were titrated onto the indicated plates and incubated at 28°C for six days, unless otherwise indicated. L-: media lacking leucine, H-: media lacking histidine, AT: 3-amino-1,2,4-triazole.

4IV.4.2 Suppression of the AT phenotype of the histone H4K8,16R double mutant strain by the over-expression of HATs

As discussed earlier (refer to section 4IV.4.1), on histidine-depleted media containing 3-AT, the histone H4K8,16R double mutant strain exhibited the AT phenotype. Thus, it was of interest to determine whether the HATs Gcn5, Hpa1 and Hpa2 (which are multi-copy phenotypic suppressors for the AT phenotype of the H4Y98A mutant strain) could also suppress the AT phenotype of the histone H4K8,16R double mutant strain in order to elucidate the histone H4 N-terminal lysine targets of the HATs.

On histidine-depleted media containing 3-AT, the H4K8,16R double mutant strain over-expressing HA-tagged Gcn5, Hpa1 and Hpa2 exhibited growth comparable to the negative control PactT424-HA empty vector (Figure 4.34, second panel, compare lanes 4, 5 and 6 to lane 3). This indicated that over-expression of the HATs Gcn5,

Hpa1 and Hpa2 was unable to suppress the AT phenotype of the H4K8,16R double mutant strain. Thus, it is likely that the HATs Gcn5, Hpa1 and Hpa2 either target H4K8 and/or H4K16 directly for acetylation or that the histone H4K8R and H4K16R mutations mask their recognition motif required for acetylation to take place.

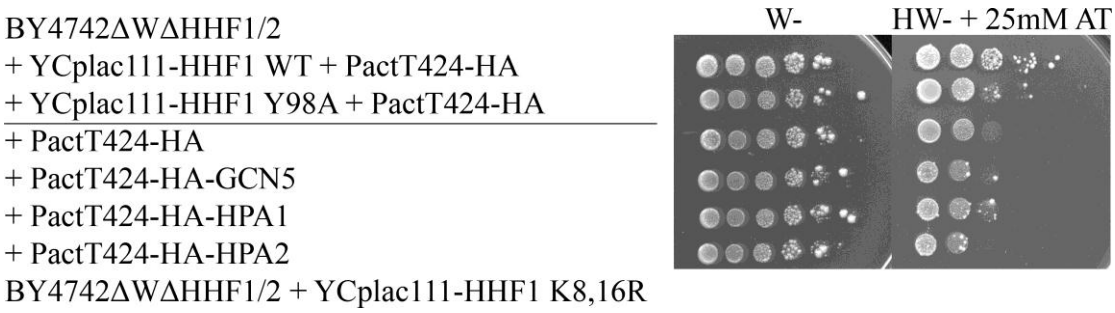

Figure 4.34 The over-expression of the HATs Gcn5, Hpa1 and Hpa2 did not suppress the AT phenotype of the H4K8,16R double mutant strain. The histone H4 deletion strain BY4742ΔWΔHHF1/2 expressing WT histone H4 and PactT424-HA empty vector served as the positive control. The W- plate served as the loading control. Tenfold serial dilutions were titrated onto the indicated plates and incubated at 28°C for six days, unless otherwise indicated. W-: media lacking tryptophan, HW-: media lacking histidine and tryptophan, AT: 3-amino-1,2,4-triazole.

4IV.5 Alanine- and arginine-scanning mutagenesis of multiple histone H4 N-terminal lysine residues without and in combination with H4Y98A

As alanine- and arginine-scanning mutagenesis of certain histone H4 N-terminal lysine residues without and in combination with H4Y98A conferred an observable AT phenotype (refer to sections 4IV.2, 4IV.3 and 4IV.4), it was of interest to determine whether alanine- and arginine-scanning mutagenesis of multiple histone H4 N-terminal lysine residues without and in combination with H4Y98A would confer a similar observable AT phenotype.

On media containing 5-FOA, the H4K5,8,12,16A and H4K5,8,12,16A Y98A mutant strains exhibited reduced growth as compared to the positive control WT histone H4 strain (Figure 4.35, second panel, compare lanes 4 and 7 to lane 1). In fact, the H4K5,8,12,16A Y98A mutant strain exhibited less growth as compared to the

H4K5,8,12,16A mutant strain (Figure 4.35, second panel, compare lane 7 to lane 4). The H4K5,8,12A and H4K5,8,12,20A mutant strains exhibited growth comparable to the positive control WT histone H4 strain (Figure 4.35, second panel, compare lanes 3 and 5 to lane 1). This indicated that these four histone H4 mutant proteins complemented the genomic deletion of histone H4, although to different degrees. On the other hand, the growth of the H4K5,8,12A Y98A and the H4K5,8,12,20A Y98A mutant strains was completely inhibited as compared to the WT histone H4 strain (Figure 4.35, second panel, compare lanes 6 and 8 to lane 1). This indicated that the H4K5,8,12A Y98A and the H4K5,8,12,20A Y98A mutant proteins were unable to complement the genomic deletion of histone H4.

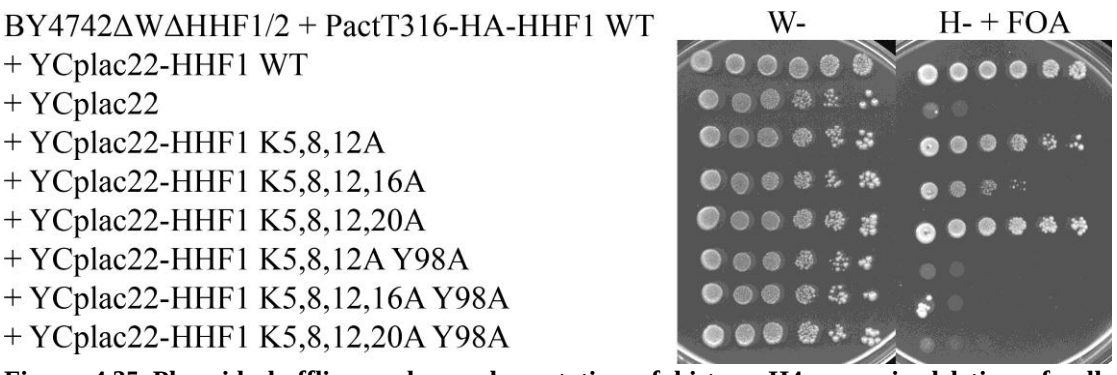

Figure 4.35 Plasmid shuffling and complementation of histone H4 genomic deletion of cells expressing histone H4 N-terminal lysine to alanine multiple point mutant proteins without and in combination with H4Y98A. The WT histone H4 expressed from YCplac22 served as the positive control, while the YCplac22 empty vector served as the negative control. The W- plate served as the loading control. Tenfold serial dilutions were titrated onto the indicated plates and incubated at 28°C for three days. W-: media lacking tryptophan, H-: media lacking histidine, FOA: 5-FOA.

On media containing 5-FOA, all histone H4 N-terminal lysine to arginine multiple point mutants exhibited reduced growth as compared to the positive control WT histone H4 strain (Figure 4.36, second panel, compare lanes 2–7 to lane 1). In fact, the H4K5,8,12,16R mutant strain and the H4K5,8,12,16,20R mutant strain exhibited less growth as compared to the H4K8,12,16,20R mutant strain, the H4K5,12,16,20R mutant strain, the H4K5,8,16,20R mutant strain and the H4K5,8,12,20R mutant strain

(Figure 4.36, second panel, compare lanes 2 and 6 to lanes 3, 4, 5 and 7). This indicated that these six histone H4 mutant proteins complemented the genomic deletion of histone H4, although to different degrees.

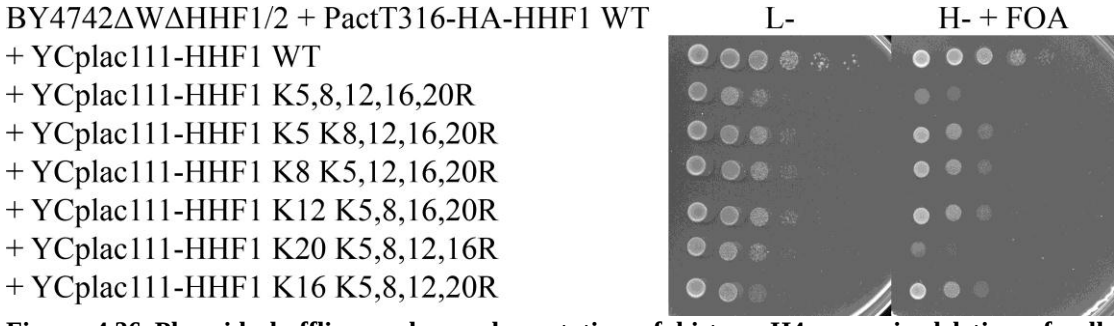

Figure 4.36 Plasmid shuffling and complementation of histone H4 genomic deletion of cells expressing histone H4 N-terminal lysine to arginine multiple point mutant proteins. The WT histone H4 expressed from YCplac111 served as the positive control. The L- plate served as the loading control. Tenfold serial dilutions were titrated onto the indicated plates and incubated at 28°C for three days. L-: media lacking leucine, H-: media lacking histidine, FOA: 5-FOA.

On the other hand, on media containing 5-FOA, the growth of all histone H4 N-terminal lysine to arginine multiple point mutants in combination with H4Y98A was completely inhibited as compared to the WT histone H4 strain (Figure 4.37, second panel, compare lanes 3–8 to lane 1). This indicated that these six histone H4 mutant proteins were unable to complement the genomic deletion of histone H4.

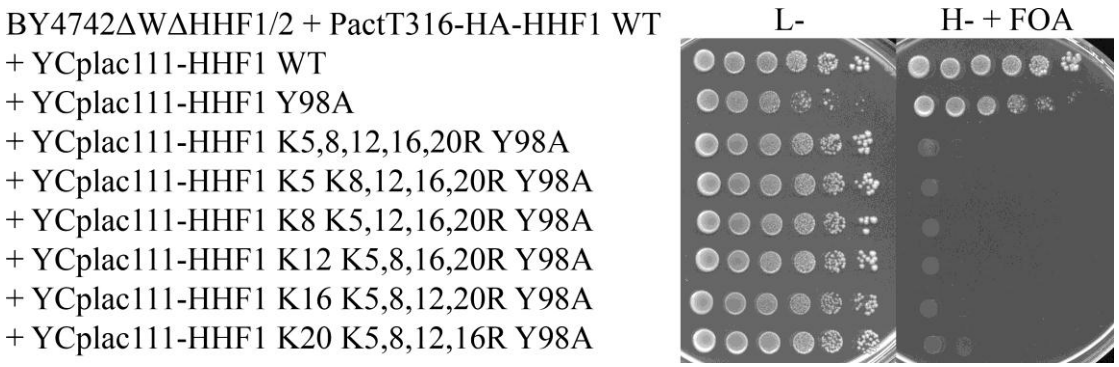

Figure 4.37 Plasmid shuffling and complementation of histone H4 genomic deletion of cells expressing histone H4 N-terminal lysine to arginine multiple point mutant proteins in combination with H4Y98A. The WT histone H4 expressed from YCplac111 served as the positive control. The L- plate served as the loading control. Tenfold serial dilutions were titrated onto the indicated plates and incubated at 28°C for three days. L-: media lacking leucine, H-: media lacking histidine, FOA: 5-FOA.

4IV.5.1 Phenotype testing of the histone H4 N-terminal multiple lysine residues mutant strains without and in combination with H4Y98A

As discussed earlier (refer to section 4I.1), on histidine-depleted media containing 3-AT, the H4Y98A mutant strain exhibited the AT phenotype (Figure 4.38, second panel, compare lane 6 to lane 1). Similarly, the H4K5,8,12A mutant strain, the H4K5,8,12,16A mutant strain, the H4K5,8,12,20A mutant strain and the H4K5,8,12,16A Y98A mutant strain also exhibited the AT phenotype (Figure 4.38, second panel, compare lanes 2, 3, 4 and 5 to lane 1).

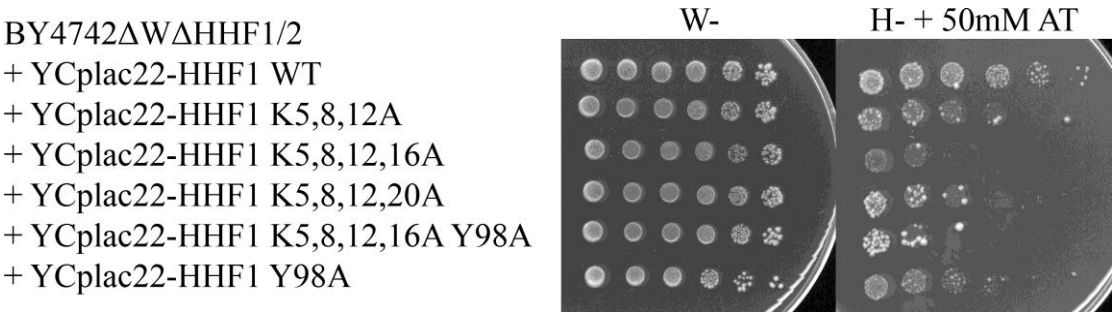

Figure 4.38 Observable AT phenotype of the histone H4 N-terminal lysine to alanine multiple point mutant strains without and in combination with H4Y98A. The histone H4 deletion strain BY4742ΔWΔHHF1/2 expressing WT histone H4 served as the positive control. The W- plate served as the loading control. Tenfold serial dilutions were titrated onto the indicated plates and incubated at 28°C for six days, unless otherwise indicated. W-: media lacking tryptophan, H-: media lacking histidine, AT: 3-amino-1,2,4-triazole.

As discussed earlier (refer to section 4I.1), on histidine-depleted media containing 3-AT, the H4Y98A mutant strain exhibited the AT phenotype (Figure 4.39, second panel, compare lane 2 to lane 1). Similarly, all histone H4 N-terminal lysine to arginine multiple point mutants also exhibited the AT phenotype (Figure 4.39, second panel, compare lanes 3–8 to lane 1). In fact, the H4K5,8,12,16R mutant strain and the H4K5,8,12,16,20R mutant strain exhibited a more severe AT phenotype as compared to the H4K8,12,16,20R mutant strain, the H4K5,12,16,20R mutant strain, the H4K5,8,16,20R mutant strain and the H4K5,8,12,20R mutant strain (Figure 4.39, second panel, compare lanes 7 and 8 to lanes 3, 4, 5 and 6).

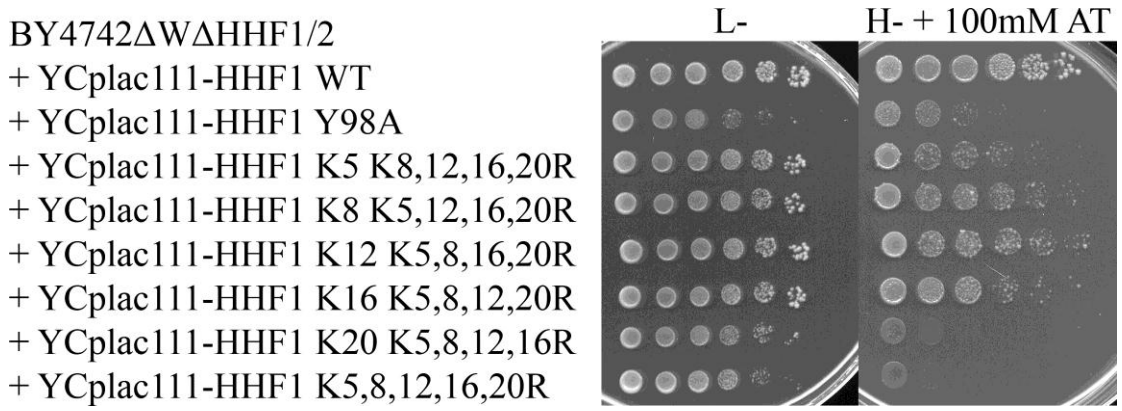

Figure 4.39 Observable AT phenotype of the histone H4 N-terminal lysine to arginine multiple point mutant strains. The histone H4 deletion strain BY4742ΔWΔHHF1/2 expressing WT histone H4 served as the positive control. The L- plate served as the loading control. Tenfold serial dilutions were titrated onto the indicated plates and incubated at 28°C for six days, unless otherwise indicated. L-: media lacking leucine, H-: media lacking histidine, AT: 3-amino-1,2,4-triazole.

4IV.6 Acetylation status of histone H4 N-terminal K8 and K16 residues

As discussed earlier (refer to section 4IV.4.2), the HATs Gcn5, Hpa1 and Hpa2 may target histone H4 N-terminal K8 and K16 residues for acetylation. Thus, it was of interest to determine whether there are differences in the acetylation status of H4K8 and H4K16 in the WT histone H4 strain as compared to the H4Y98A mutant strain. In addition, it would be interesting to determine whether the over-expression of the HATs Gcn5, Hpa1 and Hpa2 in the H4Y98A mutant strain affects the acetylation status of H4K8 and H4K16.

Upon induction in histidine-depleted media containing 3-AT, there were no significant differences in the acetylation status of H4K8 in the WT histone H4 strain (Figures 4.40 and 4.41, compare lane 2 to lane 1). Similarly, upon induction in histidine-depleted media containing 3-AT, there were no significant differences in the acetylation status of H4K8 in the H4Y98A mutant strain (Figures 4.40 and 4.41, compare lane 4 to lane 3). In addition, the over-expression of the HATs Gcn5, Hpa1 and Hpa2 in the H4Y98A mutant strain did not affect the acetylation status of H4K8 significantly (Figures 4.40 and 4.41, compare lanes 5–10 to lanes 3 and 4). This

indicated that the HATs Gcn5, Hpa1 and Hpa2 are not likely to target histone H4K8 for acetylation upon histidine starvation.

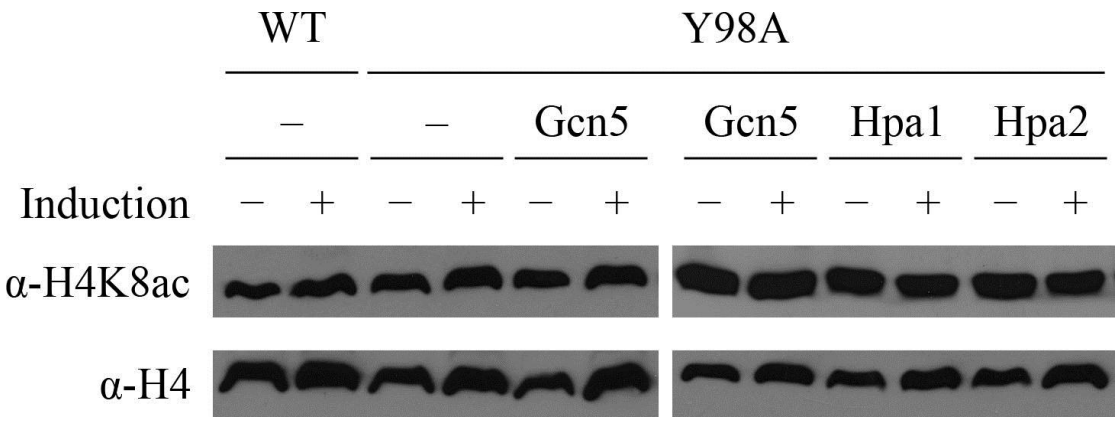

Figure 4.40 Acetylation status of H4K8. The WT histone H4 strain and the H4Y98A mutant strain were grown in glucose complete liquid media to an OD_{600} value of 1 and induced in histidine-depleted media containing 3-AT for 2 h. The H4Y98A mutant strain over-expressing the HATs Gcn5, Hpa1 or Hpa2 was grown in tryptophan-depleted liquid media to an OD_{600} value of 1 and induced in histidine-depleted media containing 3-AT for 2 h. The expression of total histone H4 detected by α-H4 antibody served as the control. WT: BY4742ΔWΔHHF1/2 + YCplac111-HHF1 WT, Y98A: BY4742ΔWΔHHF1/2 + YCplac111-HHF1 Y98A.

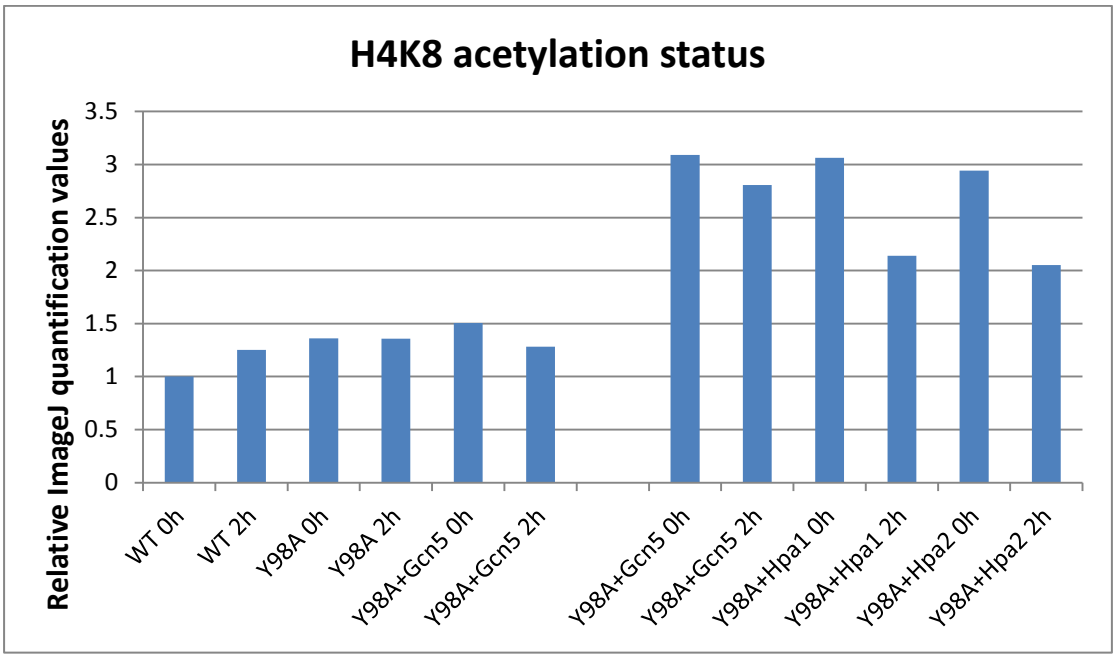

Figure 4.41 ImageJ quantification of the acetylation status of H4K8. The WT histone H4 strain and the H4Y98A mutant strain were grown in glucose complete liquid media to an OD_{600} value of 1 and induced in histidine-depleted media containing 3-AT for 2 h. The H4Y98A mutant strain over-expressing the HATs Gcn5, Hpa1 or Hpa2 was grown in tryptophan-depleted liquid media to an OD_{600} value of 1 and induced in histidine-depleted media containing 3-AT for 2 h. The expression of total histone H4 detected by α-H4 antibody served as the control. The ImageJ quantification values obtained for acetylated histone H4K8 were normalised to the ImageJ quantification values obtained for total histone H4, which was carried out only once. The values obtained were then calculated relative to the uninduced WT histone H4 strain that was set as 1 (Appendix 8.27, Table 8.34). WT: BY4742ΔWΔHHF1/2 + YCplac111-HHF1 WT, Y98A: BY4742ΔWΔHHF1/2 + YCplac111-HHF1 Y98A.

Upon induction in histidine-depleted media containing 3-AT, there were no significant differences in the acetylation status of H4K16 in the WT histone H4 strain (Figures 4.42 and 4.43, compare lane 2 to lane 1). However, upon induction in histidine-depleted media containing 3-AT, the acetylation status of H4K16 in the H4Y98A mutant strain decreased significantly (Figures 4.42 and 4.43, compare lane 4 to lane 3). In addition, the over-expression of the HATs Gcn5, Hpa1 and Hpa2 in the H4Y98A mutant strain increased the acetylation status of H4K16 significantly (Figures 4.42 and 4.43, compare lanes 5–10 to lanes 3 and 4). This indicated that the HATs Gcn5, Hpa1 and Hpa2 are likely to target histone H4K16 for acetylation upon histidine starvation.

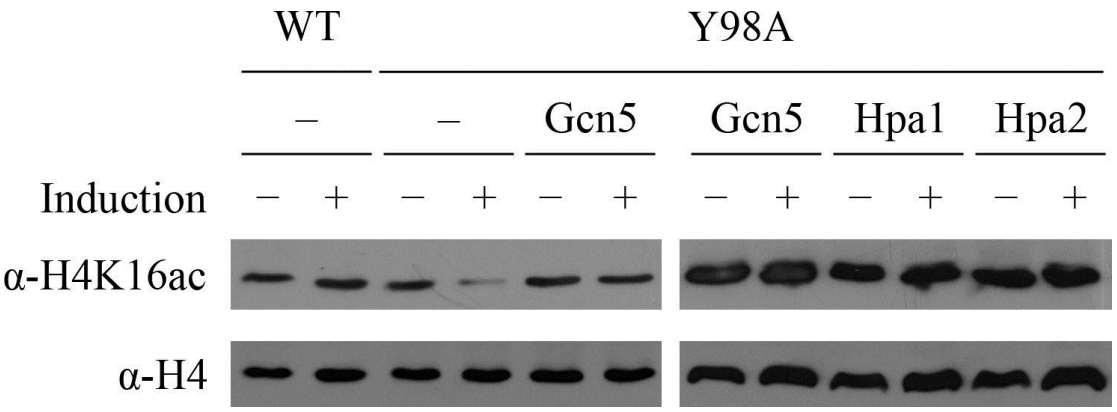

Figure 4.42 Acetylation status of H4K16. The WT histone H4 strain and the H4Y98A mutant strain were grown in glucose complete liquid media to an OD_{600} value of 1 and induced in histidine-depleted media containing 3-AT for 2 h. The H4Y98A mutant strain over-expressing the HATs Gcn5, Hpa1 or Hpa2 was grown in tryptophan-depleted liquid media to an OD_{600} value of 1 and induced in histidine-depleted media containing 3-AT for 2 h. The expression of total histone H4 detected by α-H4 antibody served as the control. WT: BY4742ΔWΔHHF1/2 + YCplac111-HHF1 WT, Y98A: BY4742ΔWΔHHF1/2 + YCplac111-HHF1 Y98A.

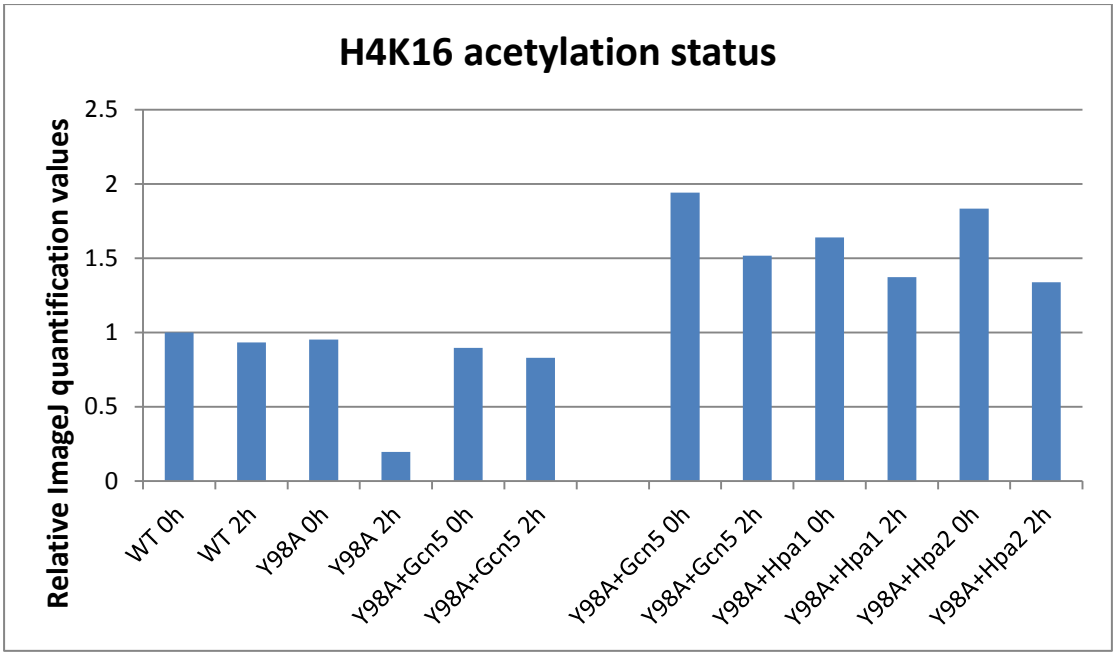

Figure 4.43 ImageJ quantification of the acetylation status of H4K16. The WT histone H4 strain and the H4Y98A mutant strain were grown in glucose complete liquid media to an OD_{600} value of 1 and induced in histidine-depleted media containing 3-AT for 2 h. The H4Y98A mutant strain over-expressing the HATs Gcn5, Hpa1 or Hpa2 was grown in tryptophan-depleted liquid media to an OD_{600} value of 1 and induced in histidine-depleted media containing 3-AT for 2 h. The expression of total histone H4 detected by α-H4 antibody served as the control. The ImageJ quantification values obtained for acetylated histone H4K16 were normalised to the ImageJ quantification values obtained for total histone H4, which was carried out only once. The values obtained were then calculated relative to the uninduced WT histone H4 strain that was set as 1 (Appendix 8.28, Table 8.35). WT: BY4742ΔWΔHHF1/2 + YCplac111-HHF1 WT, Y98A: BY4742ΔWΔHHF1/2 + YCplac111-HHF1 Y98A.

The results obtained above for the acetylation status of histone H4 N-terminal K8 and K16 residues reflect the global histone levels in the cells. However, as this study was focused on 3-AT sensitivity that arose due to defects in transcriptional activation of the *HIS3* gene by Gcn4, it would be of more interest to analyse the local histone levels in the cells specifically at the *HIS3* locus through chromatin immunoprecipitation. This is because the global histone levels in the cells may not be representative of the local histone levels in the cells at the *HIS3* locus, which was the locus of interest.

4IV.7 Chromatin immunoprecipitation (ChIP)

As discussed earlier (refer to section 1.2.5), ChIP is an immunoprecipitation experimental technique that allows the study of interactions between histone H4 and

DNA in a cell. After cell lysis, cell lysates for the uninduced and induced WT histone H4 strain was sonicated over a time course to identify the optimum sonication conditions to be used for the remaining samples (refer to section 3.3.6). It was determined that the cell lysate should be sonicated at a continuous power output of 50 % for 15 s six times as this sonication condition yielded the highest amount of chromatin DNA with the desired fragment sizes of 100–500 bp (Figure 4.44, compare lanes 3 and 6 to lanes 1, 2, 4 and 5).

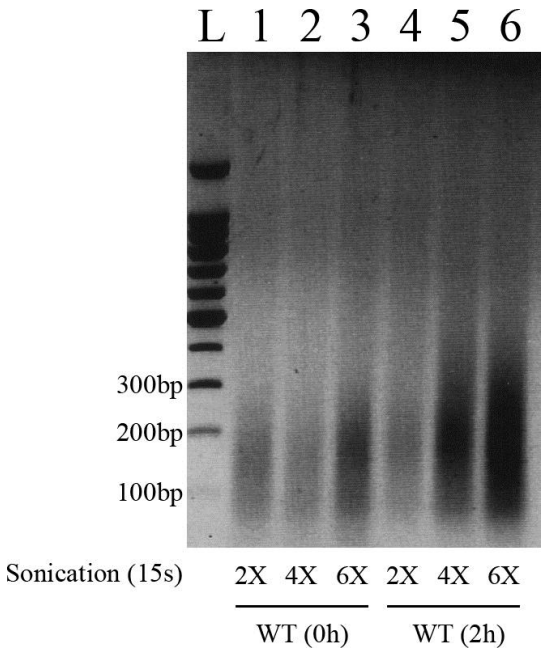

Figure 4.44 Sonication over a time course to identify the optimum sonication conditions. The cell lysate for uninduced and induced WT histone H4 strain was sonicated at a continuous power output of 50 % for 15 s two, four and six times. The amount of chromatin DNA with the desired fragment sizes of 100–500 bp was separated on a 1.5 % agarose gel.

In order to check both input DNA resuspension and immunoprecipitated DNA resuspension for presence of DNA before quantitative real-time PCR, a PCR reaction was carried out using primers against the target *HIS3* gene promoter and ORF. The *HIS3* promoter primers amplify a 131 bp DNA fragment from position 721813 to 721943 on chromosome XV. The *HIS3* ORF primers amplify a 114 bp DNA fragment from position 722197 to 722310 on chromosome XV.

It was determined that DNA was present in both uninduced and induced WT histone H4 strain and H4Y98A mutant strain (Figures 4.45 and 4.46, lanes 3 and 4). It was also determined that the no antibody control used in ChIP for both uninduced and induced WT histone H4 strain and H4Y98A mutant strain had a very low background (Figures 4.45 and 4.46, lanes 5 and 7).

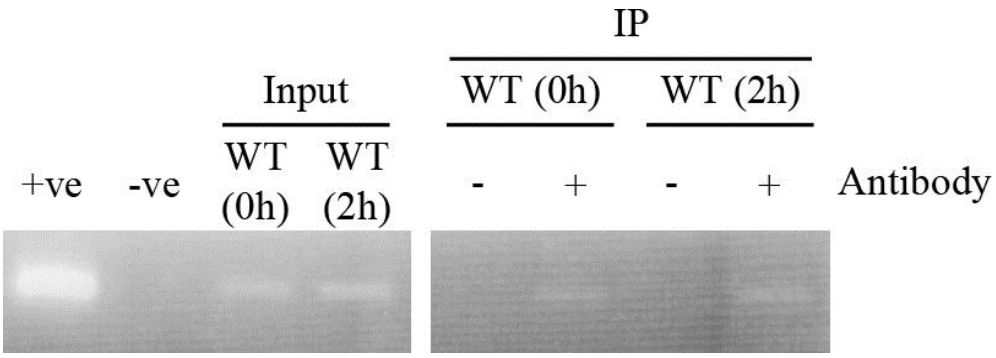

Figure 4.45 PCR to check for presence of DNA in samples obtained for WT histone H4 strain. The antibody used was rabbit α-H4, where the PCR results obtained are representative for the other antibodies used in immunoprecipitation. +ve: positive control, -ve: negative control.

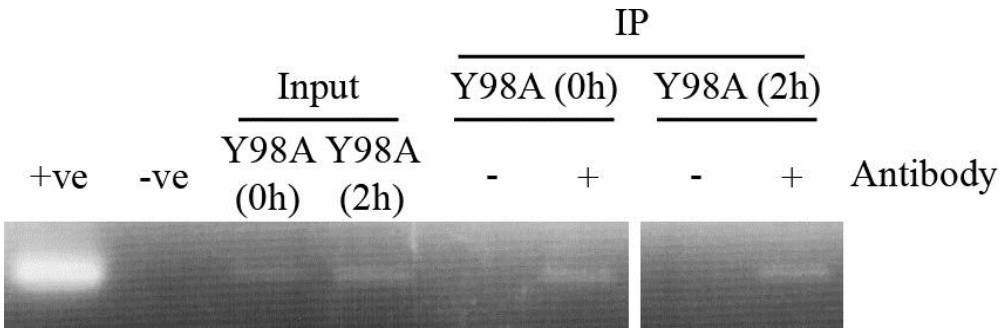

Figure 4.46 PCR to check for presence of DNA in samples obtained for the H4Y98A mutant strain. The antibody used was rabbit α-H4, where the PCR results obtained are representative for the other antibodies used in immunoprecipitation. +ve: positive control, -ve: negative control.

4IV.7.1 Histone H4 occupancy at the *HIS3* promoter and ORF

Occupancy of histone H4 at the *HIS3* promoter and ORF decreased in the WT histone H4 strain upon histidine starvation (Figures 4.47 and 4.48, compare lane 2 to lane 1), and the decrease was more significant at the *HIS3* promoter. However, occupancy of histone H4 at the *HIS3* promoter was even lower in the H4Y98A mutant strain than in the WT histone H4 strain under both inducing and non-inducing conditions (Figure 4.47, compare lanes 3 and 4 to lanes 1 and 2), indicating that occupancy of histone H4 at the *HIS3* promoter might not be relevant for the AT sensitivity of the H4Y98A mutant strain. Interestingly, occupancy of histone H4 at the *HIS3* ORF was higher in the H4Y98A mutant strain than in the WT histone H4 strain under both inducing and non-inducing conditions (Figure 4.48, compare lanes 3 and 4 to lanes 1 and 2), indicating that excess histone H4Y98A at the *HIS3* ORF under inducing conditions could be the cause for the AT sensitivity of the H4Y98A mutant strain.

Consistently, over-expression of Gcn5 reduced occupancy of histone H4 at the *HIS3* ORF in the H4Y98A mutant strain down to levels even lower than in the WT histone H4 strain (Figure 4.48, compare lanes 5 and 6 to lanes 1 and 2). Therefore, the over-expression of Gcn5 restored both the histidine starvation-induced histone eviction from the *HIS3* ORF and the transcriptional activation of the *HIS3* gene in the H4Y98A mutant strain, confirming the hypothesis that the inability to remove H4Y98A from the *HIS3* ORF had caused this transcriptional defect of the H4Y98A mutant strain.

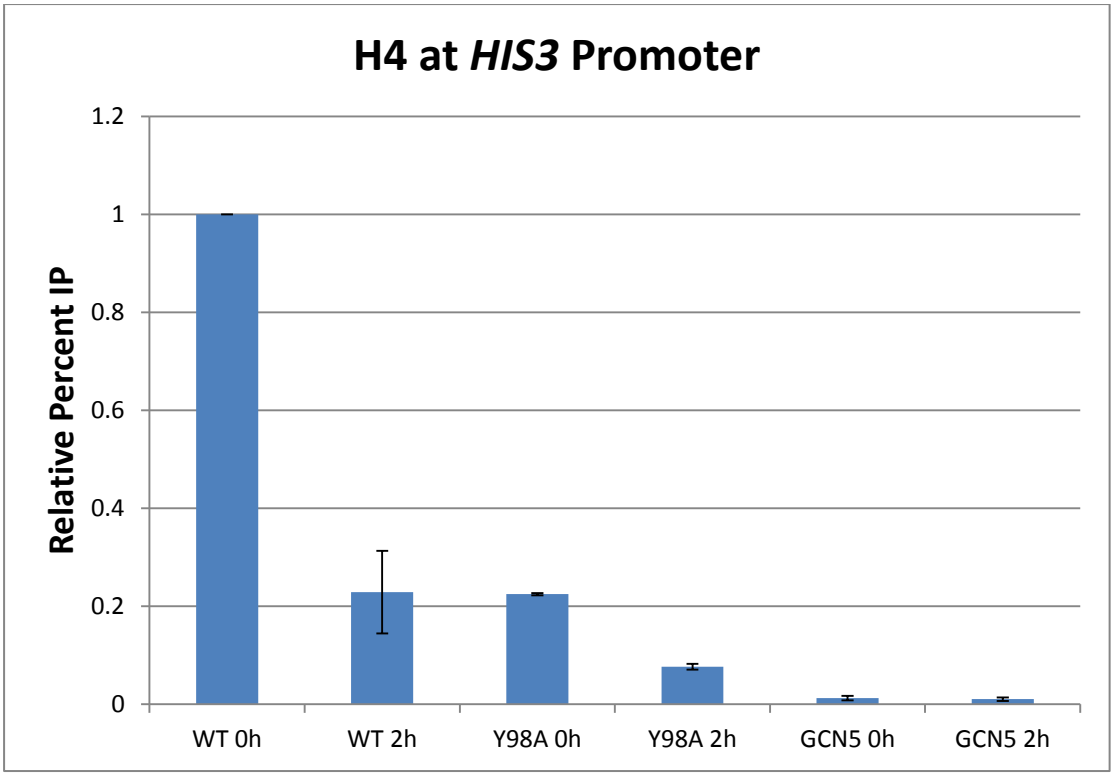

Figure 4.47 Histone H4 occupancy at the *HIS3* promoter. Samples were grown in liquid media containing histidine to an OD_{600} value of 1 and induced in histidine-depleted liquid media containing 3-AT for the indicated number of hours before carrying out the crosslinking reaction. The chromatin solution for each sample was prepared and immunoprecipitation using α-H4 antibody was carried out. Immunoprecipitation without using an antibody served as the negative control. The results are means ± S.D. for three replicate experiments, where the values were normalised to the input DNA sample with no-antibody control for each strain after factoring a dilution factor of 50 into the calculations. The values obtained were then calculated relative to the uninduced WT histone H4 strain that was set as 1 (Appendix 8.29, Table 8.36). WT: WT histone H4 strain, Y98A: H4Y98A mutant strain, GCN5: H4Y98A mutant strain over-expressing the HAT Gcn5.

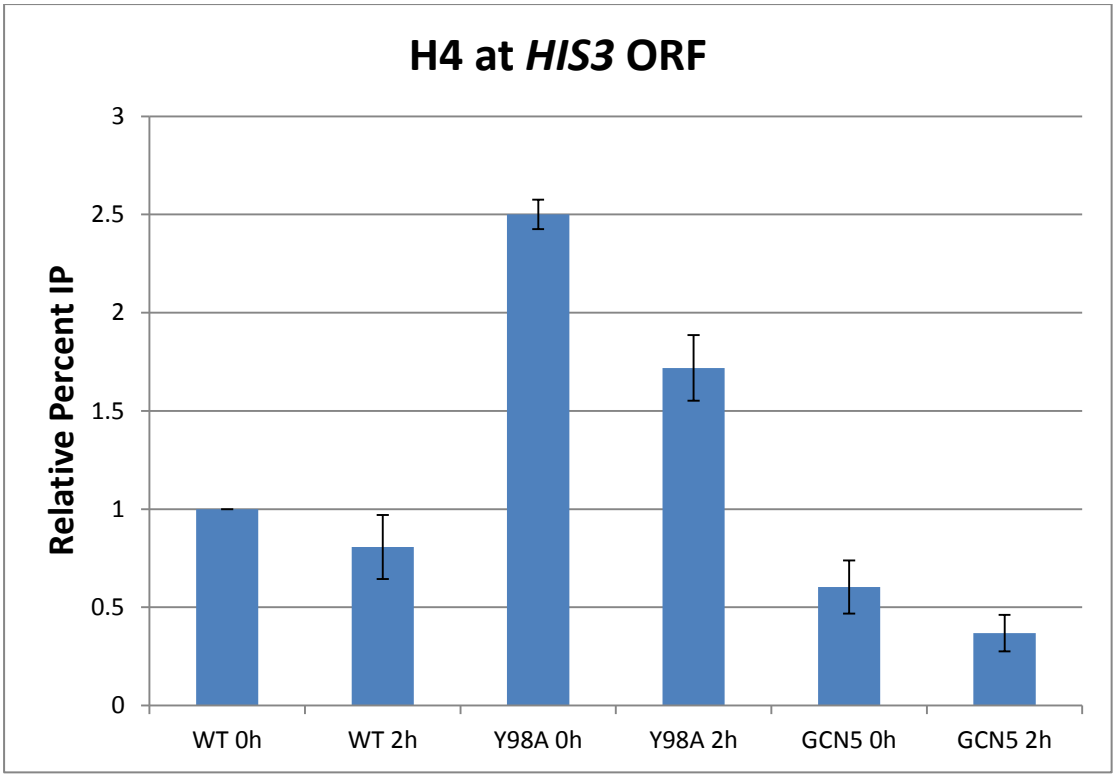

Figure 4.48 Histone H4 occupancy at the *HIS3* ORF. Samples were grown in liquid media containing histidine to an OD_{600} value of 1 and induced in histidine-depleted liquid media containing 3-AT for the indicated number of hours before carrying out the crosslinking reaction. The chromatin solution for each sample was prepared and immunoprecipitation using α-H4 antibody was carried out. Immunoprecipitation without using an antibody served as the negative control. The results are means ± S.D. for three replicate experiments, where the values were normalised to the input DNA sample with no-antibody control for each strain after factoring a dilution factor of 50 into the calculations. The values obtained were then calculated relative to the uninduced WT histone H4 strain that was set as 1 (Appendix 8.29, Table 8.36). WT: WT histone H4 strain, Y98A: H4Y98A mutant strain, GCN5: H4Y98A mutant strain over-expressing the HAT Gcn5.

4IV.7.2 Histone H4K16ac occupancy at the *HIS3* promoter and ORF

Occupancy of histone H4K16ac at the *HIS3* promoter and ORF decreased in the WT histone H4 strain upon histidine starvation (Figures 4.49 and 4.50, compare lane 2 to lane 1) and the decrease was more significant at the *HIS3* promoter. Occupancy of histone H4K16ac at the *HIS3* ORF was higher in the H4Y98A mutant strain than in the WT histone H4 strain under both inducing and non-inducing conditions (Figure 4.50, compare lanes 3 and 4 to lanes 1 and 2), reflecting the higher nucleosome occupancy in the H4Y98A mutant strain (Figure 4.48, lanes 3 and 4).

Consistently, over-expression of Gcn5 reduced occupancy of histone H4K16ac at the

HIS3 ORF in the H4Y98A mutant strain down to levels even lower than in the WT histone H4 strain under inducing conditions (Figure 4.50, compare lane 6 to lanes 1 and 2), reflecting the lower nucleosome occupancy in the H4Y98A mutant strain over-expressing Gcn5 (Figure 4.48, lanes 5 and 6).

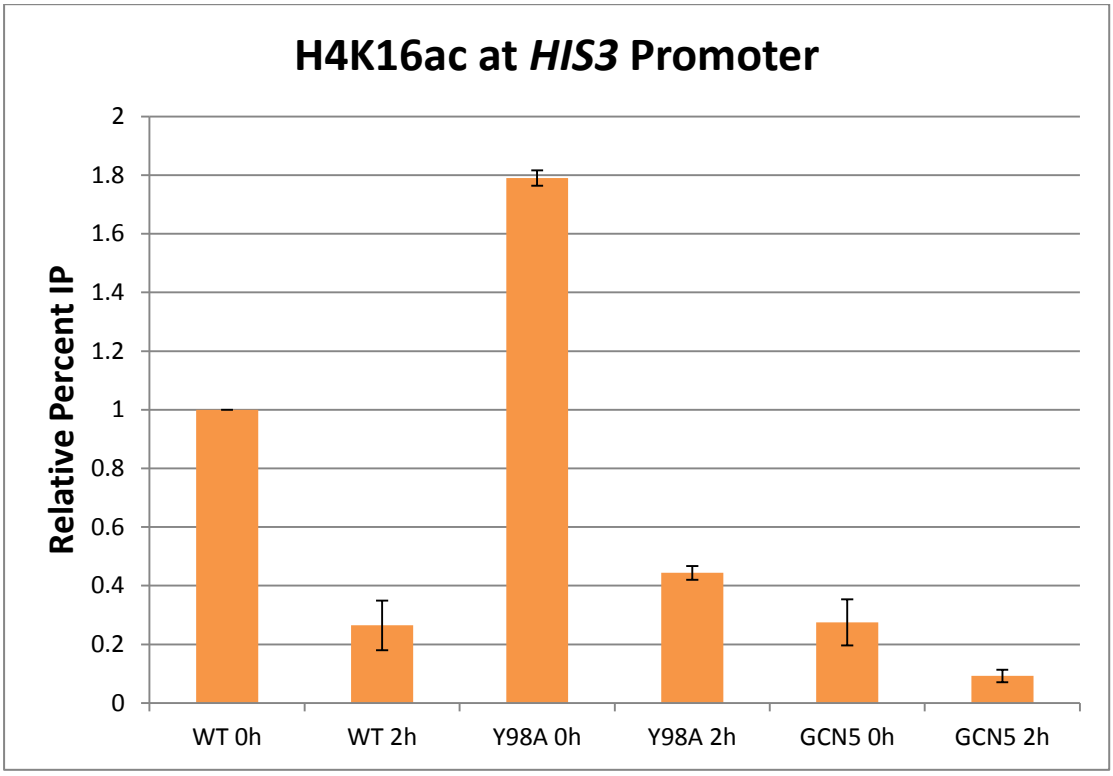

Figure 4.49 Histone H4K16ac occupancy at the *HIS3* promoter. Samples were grown in liquid media containing histidine to an OD_{600} value of 1 and induced in histidine-depleted liquid media containing 3-AT for the indicated number of hours before carrying out the crosslinking reaction. The chromatin solution for each sample was prepared and immunoprecipitation using α-H4K16ac antibody was carried out. Immunoprecipitation without using an antibody served as the negative control. The results are means ± S.D. for three replicate experiments, where the values were normalised to the input DNA sample with no-antibody control for each strain after factoring a dilution factor of 50 into the calculations. The values obtained were then calculated relative to the uninduced WT histone H4 strain that was set as 1 (Appendix 8.29, Table 8.36). WT: WT histone H4 strain, Y98A: H4Y98A mutant strain, GCN5: H4Y98A mutant strain over-expressing the HAT Gcn5.

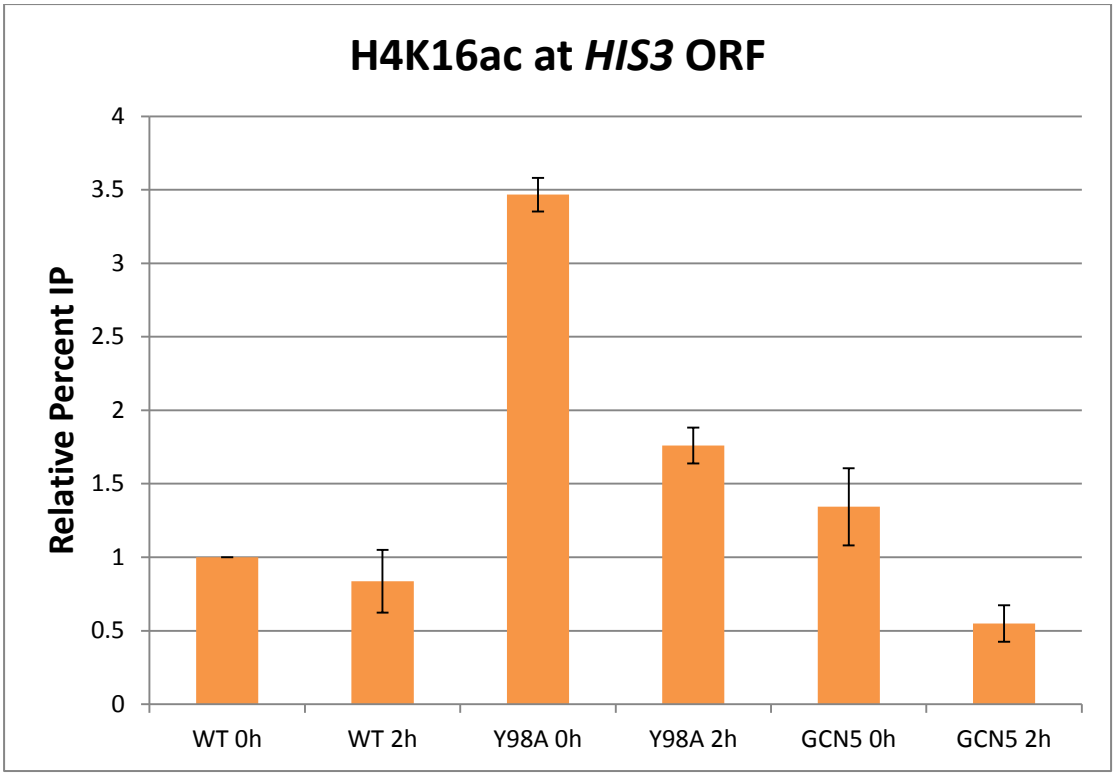

Figure 4.50 Histone H4K16ac occupancy at the *HIS3* ORF. Samples were grown in liquid media containing histidine to an OD_{600} value of 1 and induced in histidine-depleted liquid media containing 3-AT for the indicated number of hours before carrying out the crosslinking reaction. The chromatin solution for each sample was prepared and immunoprecipitation using α-H4K16ac antibody was carried out. Immunoprecipitation without using an antibody served as the negative control. The results are means ± S.D. for three replicate experiments, where the values were normalised to the input DNA sample with no-antibody control for each strain after factoring a dilution factor of 50 into the calculations. The values obtained were then calculated relative to the uninduced WT histone H4 strain that was set as 1 (Appendix 8.29, Table 8.36). WT: WT histone H4 strain, Y98A: H4Y98A mutant strain, GCN5: H4Y98A mutant strain over-expressing the HAT Gcn5.

4IV.7.3 Gcn5 occupancy at the *HIS3* promoter and ORF

As the over-expression of the HAT Gcn5 had restored the histidine starvation-induced histone eviction from the *HIS3* ORF and the transcriptional activation of the HIS3 gene in the H4Y98A mutant strain, it was of interest to determine Gcn5 occupancy at the *HIS3* promoter and ORF.

Occupancy of Gcn5 at the *HIS3* promoter and ORF increased in the WT histone H4 strain upon histidine starvation (Figures 4.51 and 4.52, compare lane 2 to lane 1). Interestingly, occupancy of Gcn5 at the *HIS3* ORF was lower in the H4Y98A mutant strain than in the WT histone H4 strain under inducing conditions (Figure 4.52,

compare lane 4 to lane 2), indicating that the recruitment of Gcn5 to the *HIS3* ORF is influenced by the histone H4 tyrosine residue Y98.

Consistently, over-expression of Gcn5 increased occupancy of Gcn5 at the *HIS3* ORF in the H4Y98A mutant strain up to levels even higher than in the WT histone H4 strain (Figure 4.52, compare lanes 5 and 6 to lanes 1 and 2), indicating that the recruitment of Gcn5 to the *HIS3* ORF had suppressed the AT sensitivity of the H4Y98A mutant strain.

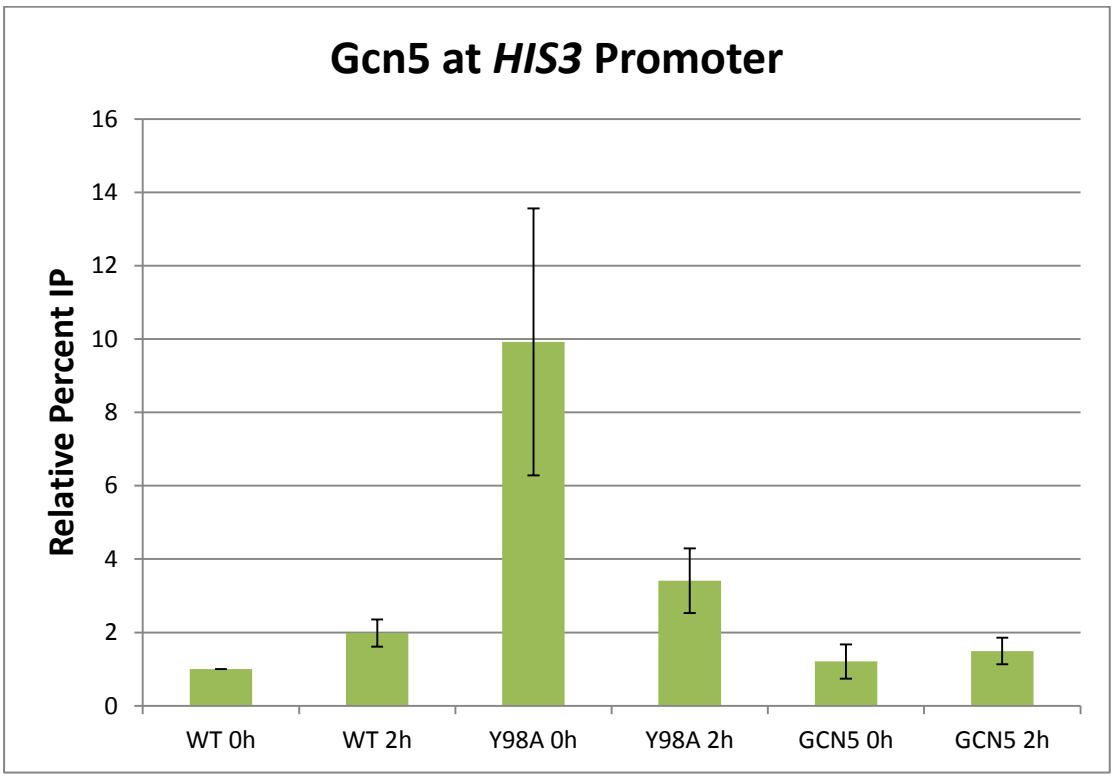

Figure 4.51 Gcn5 occupancy at the *HIS3* promoter. Samples were grown in liquid media containing histidine to an OD_{600} value of 1 and induced in histidine-depleted liquid media containing 3-AT for the indicated number of hours before carrying out the crosslinking reaction. The chromatin solution for each sample was prepared and immunoprecipitation using α-Gcn5 antibody was carried out. Immunoprecipitation without using an antibody served as the negative control. The results are means ± S.D. for three replicate experiments, where the values were normalised to the input DNA sample with no-antibody control for each strain after factoring a dilution factor of 50 into the calculations. The values obtained were then calculated relative to the uninduced WT histone H4 strain that was set as 1 (Appendix 8.29, Table 8.36). WT: WT histone H4 strain, Y98A: H4Y98A mutant strain, GCN5: H4Y98A mutant strain over-expressing the HAT Gcn5.

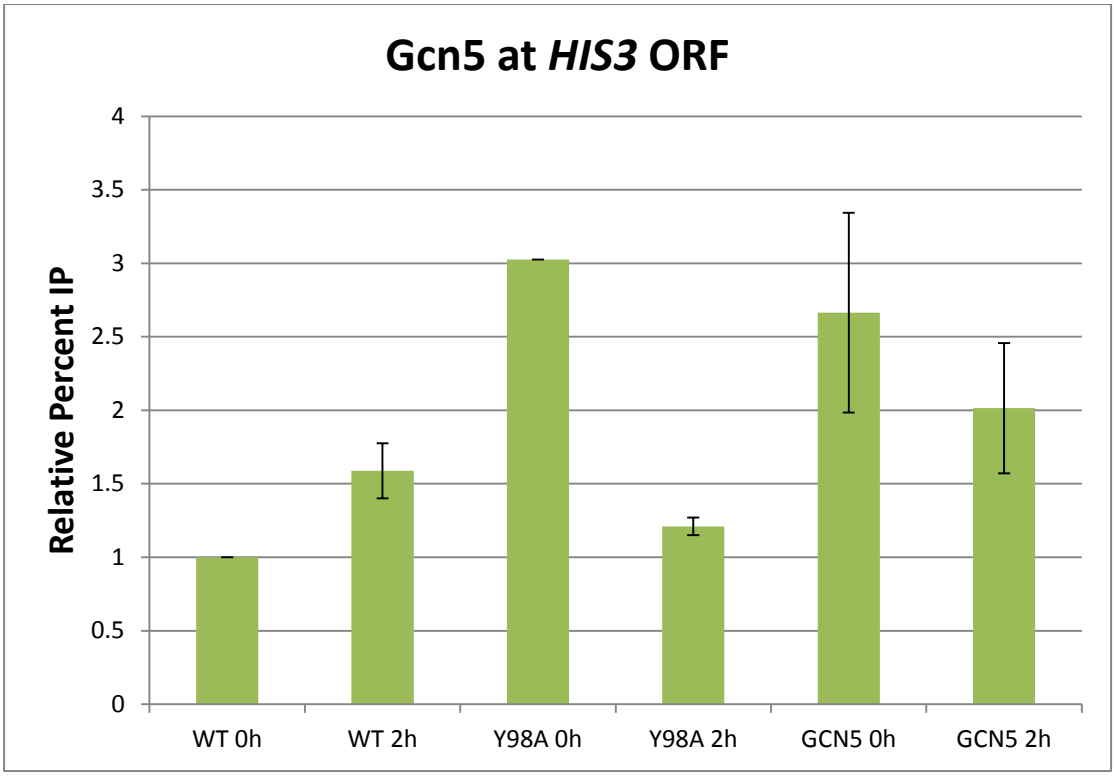

Figure 4.52 Gcn5 occupancy at the *HIS3* ORF. Samples were grown in liquid media containing histidine to an OD_{600} value of 1 and induced in histidine-depleted liquid media containing 3-AT for the indicated number of hours before carrying out the crosslinking reaction. The chromatin solution for each sample was prepared and immunoprecipitation using α-Gcn5 antibody was carried out. Immunoprecipitation without using an antibody served as the negative control. The results are means ± S.D. for three replicate experiments, where the values were normalised to the input DNA sample with no-antibody control for each strain after factoring a dilution factor of 50 into the calculations. The values obtained were then calculated relative to the uninduced WT histone H4 strain that was set as 1 (Appendix 8.29, Table 8.36). WT: WT histone H4 strain, Y98A: H4Y98A mutant strain, GCN5: H4Y98A mutant strain over-expressing the HAT Gcn5.

V

Histone H3 and H4

crosstalk studies

4V.1 Plasmid shuffling of histone H3 and H4

As discussed earlier (refer to section 2.2.3.2), there are several examples of interdependency and crosstalk between different residues on the same histone or on different histones. Thus, it was of interest to elucidate further nuances in histone H3 and H4 crosstalk.

On media containing 5-FOA, combinations of different histone H3 mutants with WT histone H4 exhibited growth comparable to the positive control WT histone H3/H4 strain (Figure 4.53, second panel, compare lanes 4, 6 and 8 to lane 2), except the combination of histone H3T118A with WT histone H4 that exhibited reduced growth as compared to the positive control WT histone H3/H4 strain (Figure 4.53, second panel, compare lane 10 to lane 2). This indicated that histone H3T118 may be essential for cell viability.

On media containing 5-FOA, combinations of different histone H3 mutants with histone H4Y98A exhibited growth comparable to the combination of WT histone H3 with histone H4Y98A (Figure 4.53, second panel, compare lanes 5, 7 and 9 to lane 3), except the combination of histone H3T118A with histone H4Y98A that exhibited reduced growth as compared to the combination of WT histone H3 with histone H4Y98A (Figure 4.53, second panel, compare lane 11 to lane 3). This also indicated that histone H3T118 may be essential for cell viability.

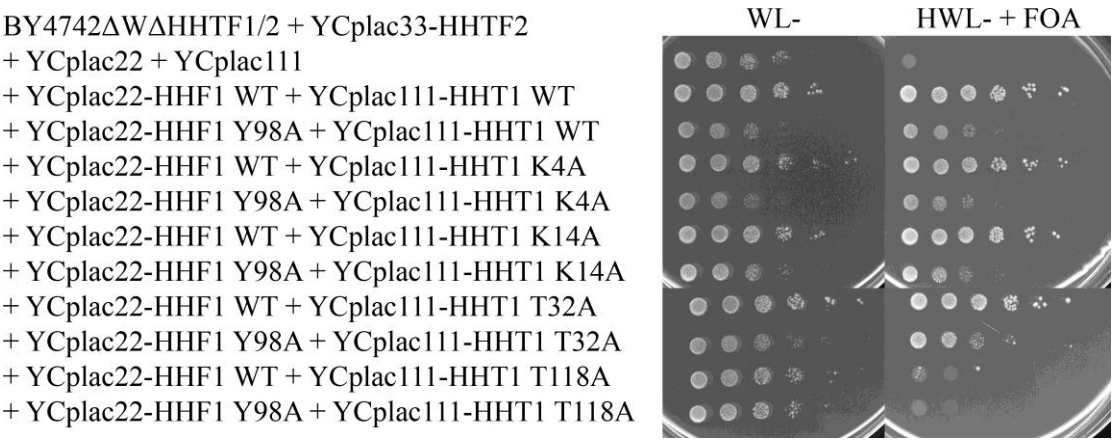

Figure 4.53 Plasmid shuffling and complementation of histone H3 and H4 genomic deletion of cells expressing combinations of different histone H3 and histone H4 derivatives. The WT histone H4 expressed from YCplac22 in combination with WT histone H3 expressed from YCplac111 served as the positive control, while the YCplac22 empty vector in combination with YCplac111 empty vector served as the negative control. The WL- plate served as the loading control. Tenfold serial dilutions were titrated onto the indicated plates and incubated at 28°C for three days. WL-: media lacking tryptophan and leucine, HWL-: media lacking histidine, tryptophan and leucine, FOA: 5-FOA.

4V.1.1 Phenotype testing of cells expressing combinations of different histone H3 derivatives and WT histone H4

On histidine-depleted media containing 3-AT, the combinations of histone H3K4A with WT histone H4 and histone H3T118A with WT histone H4 did not exhibit the AT phenotype as they showed more growth than the positive control WT histone H3/H4 strain (Figure 4.54, second panel, compare lanes 2 and 5 to lane 1). On the other hand, the combinations of histone H3K14A with WT histone H4 and histone H3T32A with WT histone H4 exhibited the AT phenotype as they showed less growth than the positive control WT histone H3/H4 strain (Figure 4.54, second panel, compare lanes 3 and 4 to lane 1). This indicated that histone H4K14 and histone H4T32 were likely to be involved in the Gcn4-mediated transcriptional activation of the *HIS3* gene.

Figure 4.54 Observable AT phenotype of cells expressing combinations of different histone H3 derivatives and WT histone H4. The WT histone H4 expressed from YCplac22 in combination with WT histone H3 expressed from YCplac111 served as the positive control. The WL- plate served as the loading control. Tenfold serial dilutions were titrated onto the indicated plates and incubated at 28°C for six days. WL-: media lacking tryptophan and leucine, H-: media lacking histidine, AT: 3-amino-1,2,4-triazole.

4V.1.2 Phenotype testing of cells expressing combinations of different histone H3 derivatives and histone H4Y98A

On histidine-depleted media containing 3-AT, the combination of histone H3T118A with histone H4Y98A did not exhibit the AT phenotype as it showed growth comparable to the positive control WT histone H3/H4 strain (Figure 4.55, second panel, compare lane 5 to lane 1 in Figure 4.54). On the other hand, the combinations of histone H3K4A with histone H4Y98A, histone H3K14A with histone H4Y98A and histone H3T32A with histone H4Y98A exhibited the AT phenotype as they showed less growth than the positive control WT histone H3/H4 strain (Figure 4.55, second panel, compare lanes 2, 3 and 4 to lane 1 in Figure 4.54).

In fact, the combinations of histone H3K4A with histone H4Y98A and histone H3T32A with histone H4Y98A exhibited growth comparable to the combination of WT histone H3 with histone H4Y98A (Figure 4.55, second panel, compare lanes 2 and 4 to lane 1), while the combination of histone H3K14A with histone H4Y98A exhibited a more severe AT phenotype as it showed less growth than the combination of WT histone H3 with histone H4Y98A (Figure 4.55, second panel, compare lane 3 to lane 1).

Figure 4.55 Observable AT phenotype of cells expressing combinations of different histone H3 derivatives and histone H4Y98A. The WL- plate served as the loading control. Tenfold serial dilutions were titrated onto the indicated plates and incubated at 28°C for six days. WL-: media lacking tryptophan and leucine, H-: media lacking histidine, AT: 3-amino-1,2,4-triazole.

5. Discussion

5.1 Preface

Epigenetics, by definition, is the study of all mitotically and meiotically heritable changes in phenotype that do not result from changes in the genomic deoxyribonucleic acid (DNA) nucleotide sequence (Petronis, 2010; Zhu and Reinberg, 2011). The epigenome refers to a complete description of potentially heritable changes across the entire genome (Bernstein et al., 2007). Several epigenome studies and recent advances in technology to allow for comprehensive epigenetic mapping have emerged, where they are only beginning to describe the global distributions and dynamics of the diverse and immensely complex epigenetic regulatory network that controls genomic function in normal physiology, development and cellular differentiation (Bernstein et al., 2007; Goldberg et al., 2007; Turner, 2007; Martens et al., 2011). As the perturbation of proper epigenetic regulation may predispose one towards diseases, including cancers, neurological disorders, autoimmune diseases and respiratory diseases (Waggoner, 2007; Urdinguio et al., 2009; Chi et al., 2010; Portela and Esteller, 2010; Sawan and Herceg, 2010; Ghizzoni et al., 2011; Meda et al., 2011; Villeneuve et al., 2011; Godley and Le Beau, 2012; Sun et al., 2012), the emerging technology of epigenetic analysis is likely to encompass the diagnosis, prognostic assessment and therapeutic treatment of such malignant diseases (Stebbing et al., 2006; Chuang et al., 2009; Lane and Chabner, 2009; Di Marcotullio et al., 2011; Sarfstein et al., 2011; Xu et al., 2011; Fujita et al., 2012).

One basis for epigenetics is histone modifications (refer to section 1.1.3), where experimental evidence has shown histones to be dynamic and integral in regulating chromatin condensation and DNA accessibility (Egger et al., 2004). Post-translational modification (PTMs) of histones are important in the regulation of all aspects of DNA

biology, including transcriptional activation or repression, homologous recombination, DNA repair or replication, cell cycle regulation and chromatin compaction in apoptosis. This study was focused on histone H4, which is the most highly conserved in evolution, with a difference of only eight amino acids out of 102 between *S. cerevisiae* and humans (Table 5.1; Wolffe, 1995), i.e. the amino acid sequence identity between *S. cerevisiae* and humans is 92 % for histone H4 (Huang et al., 2009).

Table 5.1 Histone H4 amino acid sequence identity between *S. cerevisiae* (S) and humans (H)

	1	**2**	**3**	**4**	**5**	**6**	**7**	**8**	**9**	**10**	**11**	**12**	**13**	**14**	**15**
H	S	G	R	G	K	G	G	K	G	L	G	K	G	G	A
S	S	G	R	G	K	G	G	K	G	L	G	K	G	G	A

	16	**17**	**18**	**19**	**20**	**21**	**22**	**23**	**24**	**25**	**26**	**27**	**28**	**29**	**30**
H	K	R	H	R	K	V	L	R	D	N	I	Q	G	I	T
S	K	R	H	R	K	I	L	R	D	N	I	Q	G	I	T

	31	**32**	**33**	**34**	**35**	**36**	**37**	**38**	**39**	**40**	**41**	**42**	**43**	**44**	**45**
H	K	P	A	I	R	R	L	A	R	R	G	G	V	K	R
S	K	P	A	I	R	R	L	A	R	R	G	G	V	K	R

	46	**47**	**48**	**49**	**50**	**51**	**52**	**53**	**54**	**55**	**56**	**57**	**58**	**59**	**60**
H	I	S	G	L	I	Y	E	E	T	R	G	V	L	K	V
S	I	S	G	L	I	Y	E	E	V	R	A	V	L	K	S

	61	**62**	**63**	**64**	**65**	**66**	**67**	**68**	**69**	**70**	**71**	**72**	**73**	**74**	**75**
H	F	L	E	N	V	I	R	D	A	V	T	Y	T	E	H
S	F	L	E	S	V	I	R	D	S	V	T	Y	T	E	H

	76	**77**	**78**	**79**	**80**	**81**	**82**	**83**	**84**	**85**	**86**	**87**	**88**	**89**	**90**
H	A	K	R	K	T	V	T	A	M	D	V	V	Y	A	L
S	A	K	R	K	T	V	T	S	L	D	V	V	Y	A	L

	91	**92**	**93**	**94**	**95**	**96**	**97**	**98**	**99**	**100**	**101**	**102**
H	K	R	Q	G	R	T	L	Y	G	F	G	G
S	K	R	Q	G	R	T	L	Y	G	F	G	G

5.2 Histone H4 amino acid residues Y51, E53 and Y98

In this study, single alanine exchange mutations to generate three histone H4 mutants Y51A, E53A and Y98A had been carried out in order to study the role of histone H4 in the transcriptional regulation of gene expression, upon the loss of potential sites of PTMs. It was found that the H4Y51A mutant strain exhibited AT and TS phenotypes, the H4E53A mutant strain exhibited TS phenotype, and the H4Y98A mutant strain exhibited AT, TS and AA phenotypes (Figure 4.1 and Table 4.1). In addition, the H4Y51A mutant strain was reported to exhibit suppressor of Ty (Spt) and sensitivity to methyl-methanesulfonate (MMS) phenotypes (Matsubara et al., 2007), the H4E53A mutant strain was reported to exhibit sensitivity to 6-azauracil and nicotinamide (6AU-NAM) phenotype (Sato et al., 2010) and the H4Y98A mutant strain was reported to exhibit MMS and sensitivity to hydroxyurea (HU) phenotypes (Matsubara et al., 2007).

The histone H4 amino acid residues Y51 and E53 are situated near the nucleosome entry site (Figure 5.1; Matsubara et al., 2007; Sato et al., 2010), where H4Y51 had been found to interact with H4I34, H4I46 and H4I50, while H4E53 had been found to interact with H3I124 (Sakamoto et al., 2009). Thus, it is likely that the phenotypes conferred by the H4Y51A and H4E53A mutations involved a perturbation of the interactions necessary for proper nucleosome entry (Figure 4.1 and Table 4.1). Interestingly, H4Y51 was reported to be unreactive in the $(H3\text{-}H4)_2$ heterotetramer but could be modified when individual histones were isolated (Figure 5.1B; Zweidler, 1992). In addition, H4E53 was reported to be closely associated with amino acid residue M217 of Cse4 (Glowczewski et al., 2000), which agreed with the results obtained in this study, where over-expression of Cse4 was found to suppress the TS

phenotype of the H4E53A mutant strain (Table 4.4).

The histone H4 amino acid residue Y98 was reported to form one of two independent binding surfaces between each histone H4 in the $(H3\text{-}H4)_2$ heterotetramer and the flanking H2A-H2B heterodimers (Figure 5.1A; Arents et al., 1991; Luger et al., 1997; Santisteban et al., 1997). In addition, H4Y98 had been found to interact with histone H2A residues L98, V101 and I103, histone H2B residues I64, S67, F68 and D71, as well as histone H4 residues T96 and L97 (Sakamoto et al., 2009). Thus, it is likely that the phenotypes conferred by the H4Y98A mutation involved a perturbation of the interactions necessary for proper histone octamer formation (Figure 4.1 and Table 4.1). In addition, the H4Y98A mutant strain exhibited a more severe AT phenotype as compared to the H4Y51A mutant strain (Figure 4.1), which indicates that H4Y98 may be a more crucial residue for the Gcn4-mediated transcriptional activation of the *HIS3* gene as compared to H4Y51.

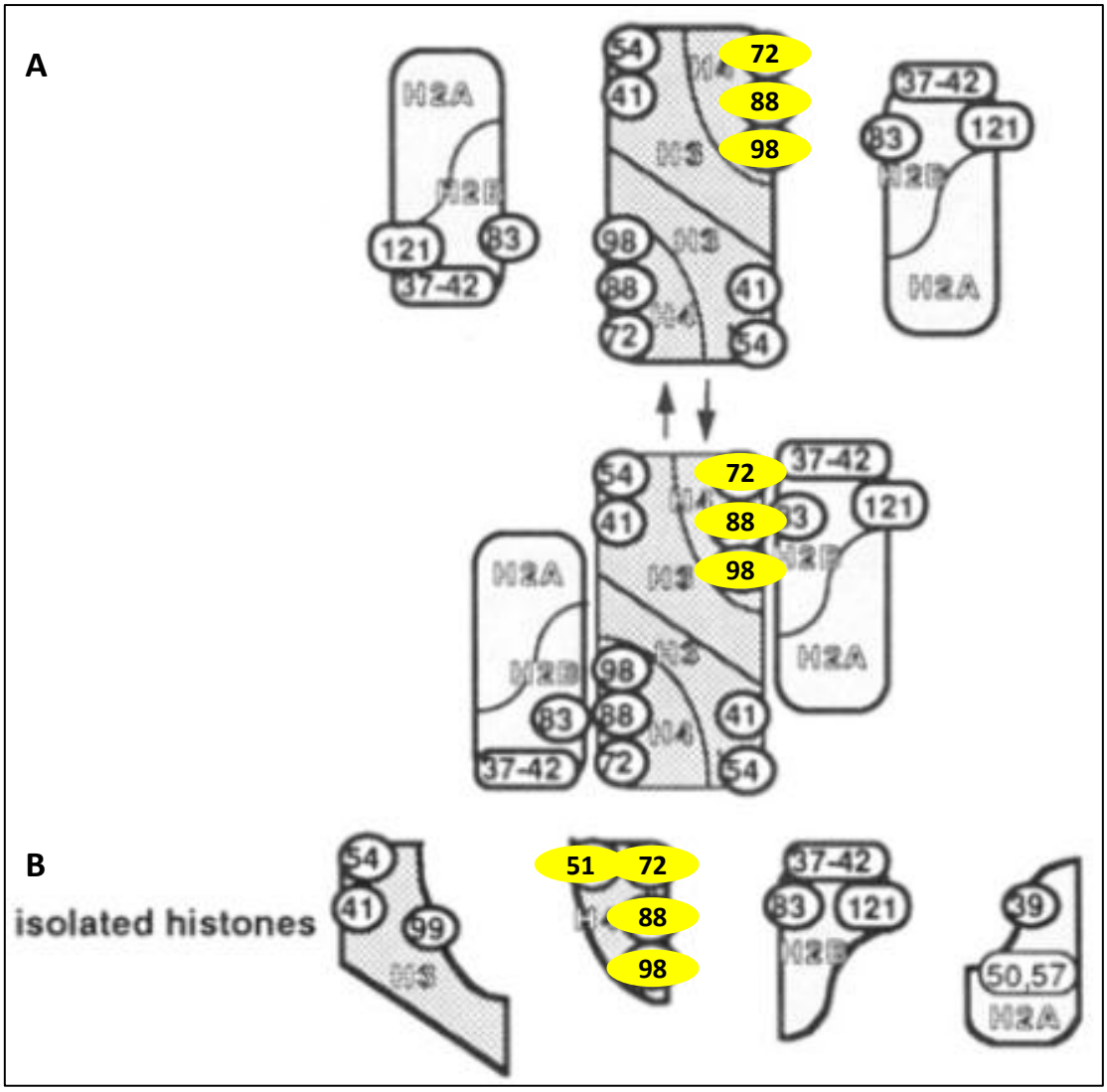

Figure 5.1 Locations of tyrosine residues in histone binding sites within the nucleosome core particle. (A) The view of the nucleosome core particle, with histone H4 tyrosine residues Y51, Y72, Y88 and Y98 in yellow. (B) The view of the isolated histones of the nucleosome core particle, with histone H4 tyrosine residues Y51, Y72, Y88 and Y98 in yellow. Figure adapted from Zweidler, 1992. Reproduced with permission from American Chemical Society.

5.3 Histone H4 tyrosine residues Y51, Y72, Y88 and Y98

In this study, single alanine exchange mutations to generate the four histone H4 mutants Y51A, Y72A, Y88A and Y98A had been carried out in order to study the roles of the tyrosine residues in the biological functions of histone H4 and their impact on transcriptional regulation of gene expression. The H4Y72A mutant protein was found to be unable to complement the genomic deletion of histone H4, while the H4Y88A mutant protein was able to complement the genomic deletion of histone H4

as well as WT histone H4 protein (Figure 4.3). The H4Y51A and H4Y98A mutant proteins were found to complement the genomic deletion of histone H4 to varying degrees, where the H4Y98A mutant protein complemented to a lesser degree as compared to the H4Y51A mutant protein (Figure 4.3).

In a nucleosome, each H2A-H2B heterodimer interacts with the $(H3\text{-}H4)_2$ heterotetramer via a four helix bundle arrangement to form the compact octamer core (Luger et al., 1997; Wood et al., 2005; Peng et al., 2012). The interfaces between the $(H3\text{-}H4)_2$ heterotetramer and the flanking H2A-H2B heterodimers are formed from fold and non-fold elements, which include four tyrosine residues in two distinct groups (Figure 5.1; Zweidler, 1992; Santisteban et al., 1997; Santisteban et al., 2000; Xu et al., 2005). In the first group, H4Y72 and H4Y88 interact directly with H2BY83 to form a large hydrophobic cluster (Figure 5.2C), which creates a molecular interaction that contributes to the integrity of the nucleosome core particle (Recht and Osley, 1999). In the second group, H4Y98 inserts its large tyrosyl ring into a hydrophobic cleft on the surface of the H2A-H2B heterodimer (Figure 5.2).

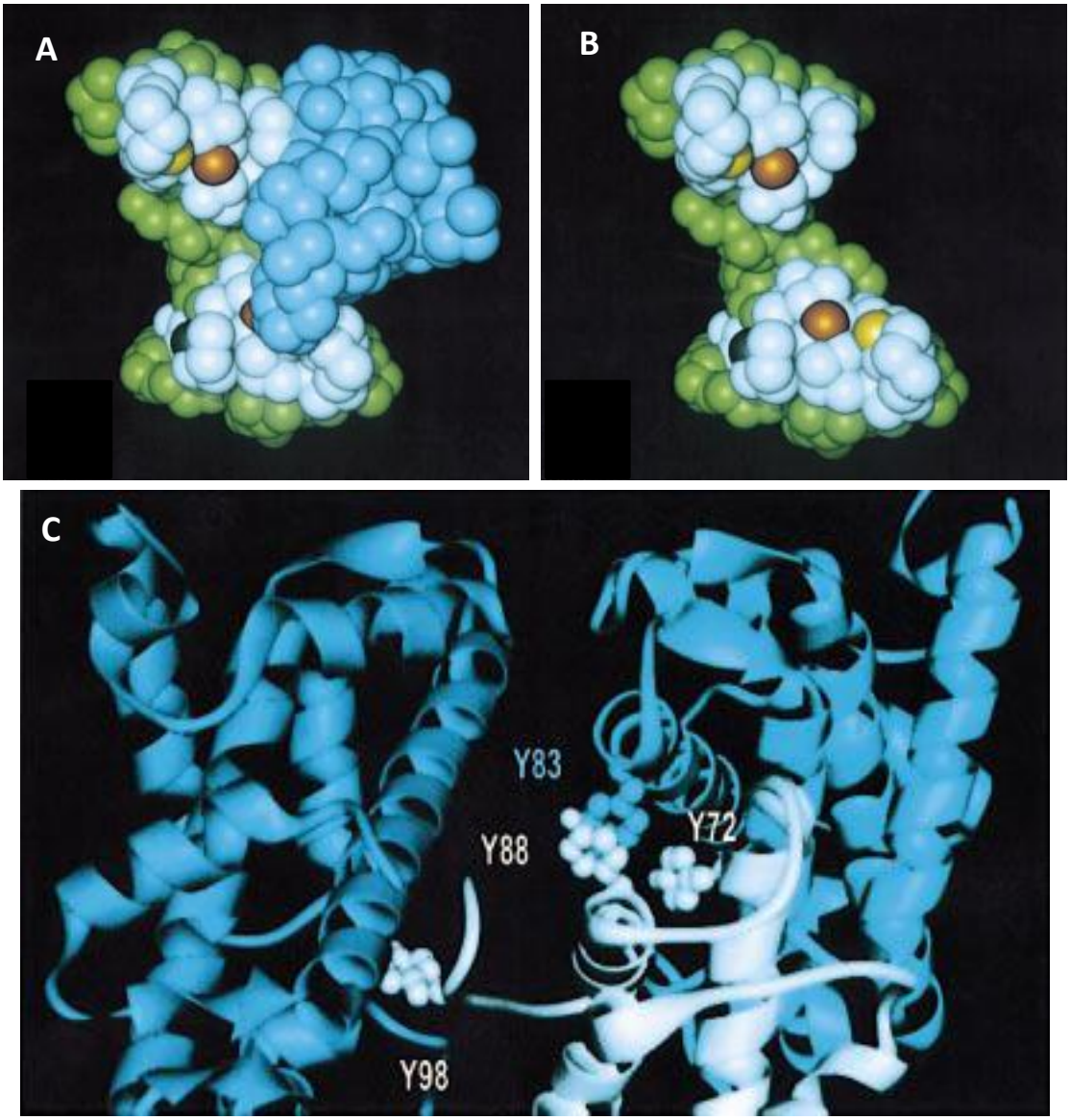

Figure 5.2 Tyrosine residues in the interfaces between the $(H3\text{-}H4)_2$ heterotetramer and the flanking H2A-H2B heterodimers. (A) The view of the nucleosome core particle with one H2A-H2B heterodimer removed, showing the histone H4 tyrosine residues Y72 (yellow), Y88 (red) and Y98 (black). (B) The view of the nucleosome core particle with both H2A-H2B heterodimers removed, showing the histone H4 tyrosine residues Y72 (yellow), Y88 (red) and Y98 (black). (C) A ribbon representation of the interfaces between the $(H3\text{-}H4)_2$ heterotetramer and the flanking H2A-H2B heterodimers, showing the histone H4 tyrosine residues Y72, Y88 and Y98 and the histone H2B tyrosine residue Y83. Figure adapted from Santisteban et al., 1997. Reproduced with permission from Nature Publishing Group.

The H4Y72G mutant strain was reported to exhibit TS phenotype and arrest at G_1 phase due to the failure to transcribe G_1 cyclin genes, possibly resulting from an altered interaction with the flanking H2A-H2B heterodimer (Santisteban et al., 1997; Glowczewski et al., 2000; Santisteban et al., 2000). In addition, H4Y72 had been found to interact with histone H2B residues E79, Y83 and L103, as well as histone H4

residues D68, D85, Y88, A89 and R92 (Sakamoto et al., 2009). Thus, the H4Y72A mutant protein was found to be unable to complement the genomic deletion of histone H4 (Figure 4.3), possibly due to destabilising interactions between the $(H3\text{-}H4)_2$ heterotetramer and the flanking H2A-H2B heterodimer during nucleosome assembly and disassembly (Sakamoto et al., 2009).

The H4Y88G mutant strain was reported to exhibit TS (Santisteban et al., 1997; Santisteban et al., 2000) and MMS (Yu et al., 2009) phenotypes, which indicates that hydrophobic interactions between the $(H3\text{-}H4)_2$ heterotetramer and the flanking H2A-H2B heterodimer are important for cellular functions. Thus, it is likely that the H4Y88A mutant protein was able to complement the genomic deletion of histone H4 as well as WT histone H4 protein due to the maintenance of the necessary hydrophobic interactions (Figure 4.3). In addition, the H4Y88F mutant strain was reported to support cell viability but not the H4Y88E mutant strain (Dai et al., 2008). This suggests that H4Y88 may serve as a molecular spring to maintain tensile strength in the nucleosome core particle, where H4Y88 stacks on top of H2BY86 to form the molecular spring-like structure (Dai et al., 2008). However, unlike the H4Y51A and H4Y98A mutant strains, the H4Y88A mutant strain did not exhibit the AT phenotype (Figure 4.4), which indicates that H4Y88 may not be involved in the Gcn4-mediated transcriptional activation of the *HIS3* gene.

5.3.1 Histone H4 tyrosine residue Y98

The H4Y98A mutant strain was reported to exhibit a growth defect on media containing 5-FOA (Yu et al., 2011a), which agreed with the results obtained in this study, where the H4Y98A mutant protein was found to complement the genomic

deletion of histone H4 to a low degree (Figure 4.3). In addition, the H4Y98A mutant strain was reported to have poor cell viability unless it obtained compensatory mutations (Yu et al., 2011a) and was in fact, reported to be lethal in one strain background but slow growing in another strain background (Dai et al., 2008). This is likely due to the improper assembly of kinetochores, which caused the H4Y98A mutant strain to grow slowly, become polyploid or aneuploid rapidly and lose chromosomes rapidly (Yu et al., 2011a).

Site-directed mutagenesis of H4Y98 yielded a plethora of observable phenotypes, which indicates that the functions of histone H4 are highly sensitive to different amino acid substitutions at H4Y98. In this study, the H4Y98A mutant strain was found to exhibit AT, TS and AA phenotypes (Figure 4.1 and Table 4.1). The H4Y98A mutant strain was also reported to exhibit MMS and HU phenotypes (Matsubara et al., 2007). The H4Y98H mutant strain was reported to function only partially and exhibited MMS (Yu et al., 2009) and TS phenotypes, with poor growth at 25°C (Santisteban et al., 1997; Santisteban et al., 2000). The TS phenotype of the H4Y98H mutant strain was reported to be suppressed by over-expression of histone variant H2A.Z (Santisteban et al., 2000), which suggests that the buried residue H4Y98 is important for incorporation of histone variant H2A.Z via interaction between H4Y98 and H2BD71 (Kawashima et al., 2011). The H4Y98G mutant strain was reported to be inviable (Santisteban et al., 1997), possibly due to the disruption of histones H2A-H4 β sheet docking interactions and histones H2A-H3-H4 molecular cluster interactions (Santisteban et al., 1997; Wood et al., 2005). In this study, the H4Y98D mutant protein was found to be unable to complement the genomic deletion of histone H4 (Figures 4.5 and 4.6).

On the other hand, the H4Y98F and H4Y98W mutant strains were reported to function and grow as well as the WT histone H4 strain (Santisteban et al., 1997; Yu et al., 2009; Yu et al., 2011a), which agreed with the results obtained in this study, where the H4Y98F mutant protein was able to fully complement the genomic deletion of histone H4 (Figures 4.5 and 4.6). In addition, the H4Y98F and H4Y98W mutant strains were reported not to exhibit any observable phenotypes (Santisteban et al., 1997; Yu et al., 2009; Yu et al., 2011a), which also agreed with the results obtained in this study for the H4Y98F mutant strain (Figure 4.7).

The comparison of the lethality conferred by the smaller glycine (G) residue and the partial or complete functional restoration conferred by the larger alanine (A), histidine (H), tryptophan (W) or phenylalanine (F) residues indicates that the larger the side chain structure of the substituted amino acid residue, the more likely the restoration of the functions of histone H4. In addition, the comparison of the lethality conferred by the negatively charged aspartic acid (D) residue and the lack of observable phenotypes conferred by the hydrophobic tryptophan (W) or phenylalanine (F) residues indicate that the hydrophobicity of the side chain structure of the substituted amino acid residue allows the restoration of the functions of histone H4. These support the notion that H4Y98 inserts its large tyrosyl ring into a hydrophobic cleft on the surface of the H2A-H2B heterodimer (Zweidler, 1992; Santisteban et al., 1997; Santisteban et al., 2000; Xu et al., 2005), where experimental calculations also revealed that position 98 of histone H4 is suitable only for aromatic residues (Ramachandran et al., 2011).

Tryptophan (W) resembles tyrosine (Y) structurally, where it conserves the side chain

aromatic ring and can be phosphorylated (Santisteban et al., 1997; Yu et al., 2009). Phenylalanine (F) resembles tyrosine (Y) structurally, except that the hydroxyl group on the aromatic ring is absent, which prevents phosphorylation from taking place. As the H4Y98F and H4Y98W mutant strains were reported to function and grow as well as the WT histone H4 strain (Santisteban et al., 1997; Yu et al., 2009; Yu et al., 2011a), it is unlikely that phosphorylation of H4Y98 is important for the functions of histone H4 (Yu et al., 2011a). In fact, it is most likely that hydrophobic interactions between the $(H3\text{-}H4)_2$ heterotetramer and the flanking H2A-H2B heterodimer mediated by H4Y98 are important for cellular functions (Yu et al., 2009), including the Gcn4-mediated transcriptional activation of the *HIS3* gene.

In addition, it was reported that H4Y98 is sometimes modified by nitration, where this tyrosine modification serves as a biomarker to detect nitric oxide dependent oxidative stress (Haqqani et al., 2002). In other words, the genomic instability associated with cancer cells may arise due to nitration of H4Y98 (Yu et al., 2011a), thus forming an interesting link between H4Y98 and the advent of cancer.

5.3.2 Histone H4 tyrosine residue Y98 in relation to the HATs Gcn5, Hpa1 and Hpa2

In this study, it was found that the H4Y98A mutant strain exhibited the AT phenotype (Figure 4.1 and Table 4.1), which was suppressed by over-expression of the HATs Gcn5, Hpa1 and Hpa2 (Figures 4.9 and 4.10). It was also found that the multi-copy phenotypic suppressors Gcn5, Hpa1 and Hpa2 were specific for both the AT phenotype (Figure 4.13) and for the H4Y98A allele (Figure 4.14).

The above observations were further corroborated by quantitative real-time PCR

analysis of the activation level of the *HIS3* gene by Gcn4. As upregulation of *HIS3* transcription in *S. cerevisiae* involves a delay upon sensing histidine starvation or disruptions in the cross pathway regulatory system named general amino acid control, differences in mRNA expression levels serve as a useful indicator of transcriptional activity in order to understand the kinetics behind the response to 3-AT competitive inhibition (Joo et al., 2011). It was found that transcriptional activation of the *HIS3* mRNA by histidine starvation was abolished in the H4Y98A mutant strain (Figure 4.20). When the HATs Gcn5, Hpa1 and Hpa2 were over-expressed, the *HIS3* mRNA expression levels in the H4Y98A mutant strain increased upon histidine starvation (Figure 4.20). This indicates that H4Y98 may be involved in the Gcn4-mediated transcriptional activation of the *HIS3* gene, which is also likely to be mediated by the HATs Gcn5, Hpa1 and Hpa2.

As discussed earlier (refer to section 2.3.1.1), the HAT activity of Gcn5 is important for both basal level and activated level of *HIS3* expression and acetylation (Mai et al., 2006). Under histidine starvation conditions, histone hyperacetylation and *HIS3* transcription are induced, where Gcn4 has been shown to recruit Gcn5 to the *HIS3* promoter to lead to activated levels of *HIS3* expression (Kuo and Allis, 1998; Kuo et al., 1998; Mai et al., 2000). Thus, it is likely that the HAT activity of Gcn5, Hpa1 and Hpa2 is responsible for the suppression of the AT phenotype of the H4Y98A mutant strain (Figures 4.9 and 4.10). In this study, it was found that the *GCN5* deletion strain exhibited the AT phenotype (Figure 4.15), which became more severe when the *GCN5* deletion was combined with the *HPA1* or the *HPA2* deletion (Figure 4.18), i.e. an additive effect on the AT phenotype. In addition, the AT phenotype of the *GCN5* deletion strain was complemented by the over-expression of Gcn5, while the

over-expression of Hpa1 and Hpa2 had no effect (Figure 4.16). This indicates that the HATs Gcn5, Hpa1 and Hpa2 are likely to function independently of each other.

Although different HATs have their own specific targets, those of Gcn5, Hpa1 and Hpa2 sometimes overlap, especially at the N-terminal histone tails of core histones. The HATs Gcn5, Hpa1 and Hpa2 are known to target H3K14 for acetylation, while Gcn5 and Hpa1 are known to target H4K8 for acetylation (Tables 2.2 and 4.7). In addition, acetylation by Gcn5 and Hpa1 is known to activate transcription, while acetylation by Hpa2 has unknown functions yet to be elucidated (Table 2.2). More importantly, a strain expressing a histone H4 deletion derivative lacking the first 19 amino acid residues was found to exhibit the AT phenotype, which phenocopied the conditional histone H4Y98A mutant strain (Figure 4.21). This indicates that the N-terminal 19 amino acid residues of histone H4 and H4Y98 may be involved in the Gcn4-mediated transcriptional activation of the *HIS3* gene. It is also possible that the deletion of the N-terminal 19 amino acid residues of histone H4 may affect either the recognition of H4K20 for PTM or the recognition of modified H4K20 for subsequent functionalities (Sarg et al., 2004). In fact, it was reported that acetylation of H4K16 suppresses methylation of H4K20 and vice versa (Nishioka et al., 2002).

5.3.3 Histone H4 tyrosine residue Y98 and N-terminal lysine residues

In this study, the lysine to alanine and lysine to arginine single-point mutations of histone H4 N-terminal lysine residues K5, K8, K12, K16 and K20 were analysed to determine whether they could phenocopy the conditional histone H4Y98A allele. It was found that the H4K5A, H4K8A, H4K12A, H4K16A and H4K20A mutant proteins fully complemented the genomic deletion of histone H4 (Figure 4.22).

Similarly, the H4K5R, H4K8R, H4K12R, H4K16R and H4K20R mutant proteins fully complemented the genomic deletion of histone H4 (Figure 4.23).

The H4K16A, H4K20A and H4K16R mutant strains but not the other mutant strains were found to display the AT phenotype, which phenocopied the conditional histone H4Y98A mutant strain (Figures 4.24 and 4.25). This indicates that the histone H4 N-terminal lysine residues K5, K8 and K12 are not as important for the Gcn4-mediated transcriptional activation of the *HIS3* gene as compared to H4K16 and H4K20. In addition, H4K16 may be a more crucial residue for the Gcn4-mediated transcriptional activation of the *HIS3* gene as compared to H4K20, where a positive charge and the lack of a charge at position 16 of histone H4 are detrimental for the Gcn4-mediated transcriptional activation of the *HIS3* gene. In fact, it was reported that H4K16 is the predominant site of acetylation in mono-acetylated histone H4, followed by H4K12 and H4K8, then finally H4K5 (Smith et al., 2003). Interestingly, it was reported that H4K16A and H4K16R reduced the negative supercoiling of HML DNA, with H4K16R having a significantly smaller effect on the disruption of heterochromatin structure as compared to H4K16A (Yu et al., 2011b).

As discussed earlier (refer to section 2.2.3.1.1), in the charge neutralisation model, histone acetylation may reduce the affinity between nucleosomes and DNA as acetylation neutralises the positive charge of the lysine side chain in the core histone tails (Hong et al., 1993). This change in the local chromatin structure may become more permissive for the access of the transcription machinery to gene promoters (Grunstein, 1997). Although it is not wrong to think that acetylation at different positions in the histone H4 N-terminal tail are functionally interchangeable, it is clear

from this study that histone H4K16 acetylation has distinct functional roles. In addition, histone H4K16 acetylation has been reported to have profound effects on chromatin structure, where it inhibits the formation of the 30 nm fibre and the generation of higher order structures via cross-fibre interactions to form compact chromatin fibre in vitro (Shogren-Knaak et al., 2006). It was also reported that histone H4K16 acetylation reduces the propensity for histone H4 N-terminal tail to form an α-helix that can dock into an acidic patch groove of the nucleosome, which leads to the partial unfolding of chromatin (Yang and Arya, 2011). Interestingly, the class III HDAC Sir2 in *S. cerevisiae* and SirT2 in humans were found to induce chromatin condensation in vivo by having some HDAC activity on acetylated histone H4K16 (Kouzarides, 2007; Vaquero et al., 2007).

In this study, H4Y98A mutant proteins carrying additionally the lysine to alanine and lysine to arginine single-point mutations of histone H4 N-terminal lysine residues K5, K8, K12, K16 and K20 were also analysed to determine the effects on the histone H4Y98A mutant allele. It was found that these mutant proteins complemented the genomic deletion of histone H4 to varying degrees, where histone H4 N-terminal lysine residues K5, K8 and K12 lysine to alanine and lysine to arginine single-point mutant proteins in combination with H4Y98A complemented to a lesser degree as compared to histone H4 N-terminal lysine residues K16 and K20 lysine to alanine and lysine to arginine single-point mutant proteins in combination with H4Y98A (Figures 4.26 and 4.27). The additive effect on growth of strains expressing H4Y98A mutant proteins carrying additionally the lysine to alanine and lysine to arginine single-point mutations of histone H4 N-terminal lysine residues K5, K8 and K12 indicates that these three histone H4 N-terminal lysine residues and H4Y98 are likely to function

independently of each other. Similarly, the lack of an additive effect on growth of strains expressing H4Y98A mutant proteins carrying additionally the lysine to alanine and lysine to arginine single-point mutations of histone H4 N-terminal lysine residues K16 and K20 indicates that these two histone H4 N-terminal lysine residues and H4Y98 are likely not to function independently of each other.

Interestingly, it was found that the H4K12R Y98A double mutant protein was able to complement the genomic deletion of histone H4 as well as the H4K16R Y98A and H4K20R Y98A double mutant proteins (Figure 4.27). This indicates that H4K12 may have some contribution to the recognition of H4K16 or vice versa, where it was reported that the acetylation status of both residues may play critical roles in transcriptional elongation (Sato et al., 2010). It was also reported that acetylation of H4K16 recruits class I HDACs to facilitate the deacetylation of H4K12 (Zhou and Grummt, 2005), which indicates a direct association between H4K12ac and H4K16ac in *S. cerevisiae*.

5.3.4 Histone H4 tyrosine residue Y98 and N-terminal lysine residues K8 and K16 in relation to the HATs Gcn5, Hpa1 and Hpa2

Recombinant *S. cerevisiae* Gcn5 was reported to acetylate H3K14 preferentially and H4K8 and K4K16 to a lesser degree in vitro (Kuo et al., 1996). Thus, H4K8 and H4K16 lysine to arginine double-point mutant proteins without and with the H4Y98A mutation were analysed in this study to determine whether the mutant strains could exhibit any observable phenotypes. The H4K8,16R Y98A triple mutant protein was unable to complement the genomic deletion of histone H4, while the H4K8,16R double mutant protein was able to fully complement the genomic deletion of histone

H4 (Figure 4.32). This indicates that H4Y98 is a crucial residue to support cell viability, especially when H4K8 and K4K16 undergo mutation such that they cannot be acetylated. This also indicates that under normal conditions, H4K8 and K4K16 are not acetylated globally in order to maintain cell viability (refer to section 5.3.3).

In this study, it was found that the H4K8,16R double mutant strain exhibited a less severe AT phenotype as compared to the H4Y98A mutant strain (Figure 4.33), which could not be suppressed by over-expression of the HATs Gcn5, Hpa1 and Hpa2 (Figure 4.34). This indicates that the HAT activity of Gcn5, Hpa1 and Hpa2 either acetylates H4K8 and/or K4K16 or that the H4K8,16R double mutation masked the recognition motif required for acetylation to occur at another lysine residue.

In order to determine whether H4K8 and K4K16 are involved in the Gcn4-mediated transcriptional activation of the *HIS3* gene, the acetylation status of H4K8 and H4K16 in the WT histone H4 strain and in the H4Y98A mutant strain were analysed in this study. It was found that there were no significant differences in the acetylation status of H4K8 in the WT histone H4 strain, in the H4Y98A mutant strain and in the H4Y98A mutant strain over-expressing the HATs Gcn5, Hpa1 and Hpa2 upon histidine starvation (Figures 4.40 and 4.41). It was also found that there were no significant differences in the acetylation status of H4K16 in the WT histone H4 strain upon histidine starvation (Figures 4.42 and 4.43). Interestingly, the acetylation status of H4K16 in the H4Y98A mutant strain decreased significantly upon histidine starvation, which was restored by the over-expression of the HATs Gcn5, Hpa1 and Hpa2 (Figures 4.42 and 4.43). This indicates that the HATs Gcn5, Hpa1 and Hpa2 target H4K16 for acetylation and not H4K8 in the H4Y98A mutant strain. In fact, it

was reported that H4K8ac and H4K16ac have distinct roles and mark separate regions of chromatin as shown in the selective staining of H4K16ac in transcriptionally hyperactive X chromosome in male *D. melanogaster* polytene chromosomes (Turner et al., 1992).

5.3.4.1 Recruitment of Gcn5 to the *HIS3* locus is dependent on H4Y98

It was reported that ChIP carried out to compare the occupancy of histone H4 at three *S. cerevisiae* loci — *CENIII*, *GAL10* and *PMA1* — showed that there was less H4Y98A as compared to WT histone H4 (Yu et al., 2011a). This observation partially agreed with the results obtained in this study, where ChIP carried out to compare the occupancy of histone H4 at the *HIS3* promoter showed that there was less H4Y98A as compared to WT histone H4 (Figure 4.47). However, this was not observed at the *HIS3* ORF, where ChIP demonstrated that there was instead more H4Y98A as compared to WT histone H4 (Figure 4.48).

While the observations made at the *HIS3* promoter are insufficient to explain the in vivo effects of the H4Y98A mutant strain (Figure 4.1) and how these effects are rescued upon the over-expression of the HATs Gcn5, Hpa1 and Hpa2 (Figures 4.9 and 4.10), the observations made at the *HIS3* ORF indicate an exciting possibility. In the WT histone H4 strain at the *HIS3* ORF, the occupancy of Gcn5 increased upon histidine starvation (Figure 4.52), while the occupancy of acetylated histone H4K16 decreased upon histidine starvation (Figure 4.50). As Gcn5 was shown to target histone H4K16 for acetylation (Kuo et al., 1996; Figures 4.42 and 4.43), the observations made from the ChIP experiment indicated the possibility of histone eviction after the acetylation of histone H4K16, where this correlated with the

decrease in the occupancy of histone H4 upon histidine starvation (Figure 4.48). Thus, it is likely that the higher amount of Gcn5 present at the *HIS3* ORF mediated increased acetylation of histone H4K16, leading to histone eviction and an overall decrease in the amount of histone H4 that reflects an overall decrease in nucleosome occupancy. This decrease in nucleosome occupancy upon histidine starvation allows for an increase in the expression of the *HIS3* gene in the WT histone H4 strain.

It is important to note that histone acetylation leads to eviction, making it difficult to correlate the levels of histone H4K16ac occupancy with transcription. In addition, phosphorylation of Gcn5 by Snf1 could regulate its enzymatic activity (Liu et al., 2005), also making it difficult to correlate Gcn5 occupancy with H4 acetylation levels.

Under inducing conditions, there was less Gcn5 at the *HIS3* ORF in the H4Y98A mutant strain as compared to the WT histone H4 strain (Figure 4.52), which was correlated with higher nucleosome occupancy at the *HIS3* ORF in the H4Y98A mutant strain (Figure 4.48). Thus, it is likely that the lower amount of Gcn5 present at the *HIS3* ORF resulted in decreased acetylation of histone H4K16, leading to reduced histone eviction and an overall increase in the amount of histone H4 that reflects an overall increase in nucleosome occupancy. According to this model, the inability of the H4Y98A mutant strain to evict histones from the *HIS3* ORF upon histidine starvation had caused the transcriptional defect of the H4Y98A mutant strain.

The over-expression of Gcn5 led to an increase in the occupancy of Gcn5 at the *HIS3* ORF under inducing conditions (Figure 4.52). This correlated with the decrease in the occupancy of histone H4 upon histidine starvation to levels comparable to that of the

WT histone H4 strain (Figure 4.48). Thus, it is likely that the higher amount of Gcn5 present at the *HIS3* ORF mediated increased acetylation of histone H4K16, leading to histone eviction and an overall decrease in the amount of histone H4 that reflects an overall decrease in nucleosome occupancy. Due to this decrease in nucleosome occupancy upon histidine starvation, there is an increase in the transcriptional activation of the *HIS3* gene in the H4Y98A mutant strain over-expressing the HAT Gcn5 as compared to the H4Y98A mutant strain. This also indicates that the recruitment of Gcn5 to the *HIS3* locus is dependent on H4Y98, where H4Y98A affects the recruitment of Gcn5 negatively and this effect is restored to WT levels upon the over-expression of the HAT Gcn5.

In fact, it was reported that Gcn5, functioning in the SAGA complex, carries out histone PTMs and stimulates optimal histone eviction from highly transcribed ORF coding sequences, which promotes Pol II elongation (Govind et al., 2007). It was also reported that Gcn5 stimulates the eviction of histones that are positioned downstream of promoters to allow for efficient Pol II progression (Sansó et al., 2011), where this corresponds to the observations made in this study that the effect of Gcn5 over-expression was more significant at the *HIS3* ORF as compared to the *HIS3* promoter. In addition, it was reported that histone eviction kinetics were delayed in the absence of Gcn5 (Wippo et al., 2009), where Gcn5 may function together with the SWI/SNF complex to mediate either the sliding of the acetylated nucleosomes or the eviction of the histones (Kim et al., 2010).

5.4 Histone H3 and H4 crosstalk

In this study, combinations of different histone H3 mutants with WT histone H4 or

H4Y98A were analysed to elucidate further nuances in histone H3 and H4 crosstalk. It was found that all combinations of different histone H3 mutant proteins with WT histone H4 protein were able to fully complement the genomic deletion of histone H3 and H4, except histone H3T118A + histone H4 WT proteins (Figure 4.53). It was also found that all combinations of different histone H3 mutant proteins with H4Y98A complemented the genomic deletion of histone H3 and H4 to varying degrees, with histone H3T118A + histone H4Y98A proteins being the least able to complement (Figure 4.53). This indicated that H3T118 is a crucial residue to support cell viability and agreed with the previous report that H3T118 may be important for histone H3 and H4 crosstalk (Teo, 2008). In fact, H3T118 is a site of phosphorylation and is involved in transcriptional regulation and DNA repair (North et al., 2011). H3T118ph was found to reduce DNA-histone binding, increase nucleosome mobility and increase DNA accessibility near the nucleosome dyad region (North et al., 2011).

Strains expressing combinations of histone H3K4A, H3K14A and H3T32A mutant proteins with H4Y98A were found to display the AT phenotype, where the histone H3K14A + histone H4Y98A strain exhibited the most severe AT phenotype (Figure 4.55). This indicates that H3K4, H3K14 and H3T32 may be crucial residues for histone H3 and H4 crosstalk to lead to the Gcn4-mediated transcriptional activation of the *HIS3* gene. An example of histone H3 and H4 crosstalk was previously reported, where it was found that the acetylation levels of H3K14 was lower in the H4Y98A mutant strain (Teo, 2008). Thus, it is likely that histone H3 and H4 crosstalk may play a role in the Gcn4-mediated transcriptional activation of the *HIS3* gene, although this remains to be further elucidated.

6. Conclusion and future studies

6.1 Conclusion and future studies

The HATs Gcn5, Hpa1 and Hpa2 were found to be multi-copy phenotypic suppressors of the AT phenotype of the H4Y98A mutant strain. It was found that at the *HIS3* ORF, there was reduced histidine starvation-induced histone eviction in the H4Y98A mutant strain as compared to that of the WT histone H4 strain, which was restored to the WT levels upon the over-expression of Gcn5 in the H4Y98A mutant strain.

In order to further validate the targeting specificity of the HATs Gcn5, Hpa1 and Hpa2 identified in this study, Western blot using antibodies specific to acetylated histone H4 N-terminal lysine residues K5, K12 and K20 could be carried out. These Western blot results could also be further evaluated through MALDI-TOF mass spectrometry analysis or synthetic genetic array analysis. In addition, in vitro expression of full length Gcn5 and truncated Gcn5 containing the three functional domains — catalytic HAT domain, Ada2 interaction domain and C-terminal bromodomain — in separate truncations may elucidate the domain of Gcn5 that is affected by the H4Y98A mutation through co-immunoprecipitation studies or crystal structure studies. It would also be interesting to determine the induction kinetics at the *HIS3* locus in the WT histone H4 strain, the H4Y98A mutant strain and the H4Y98A mutant strain over-expressing Gcn5.

It was reported that two small molecules 2-methyl-3-carbethoxyquinoline 9 and its 2-desmethyl analogue 18 have been discovered as inhibitors of Gcn5 (Mai et al., 2006). This is very exciting news as it shows that there is potential for drug development with further in depth studies on the functions of Gcn5.

7. Bibliography

Alani E, Cao L, Kleckner N. A method for gene disruption that allows repeated use of URA3 selection in the construction of multiply disrupted yeast strains. *Genetics.* **1987**;116(4):541-5.

Albaugh BN, Arnold KM, Denu JM. KAT(ching) metabolism by the tail: insight into the links between lysine acetyltransferases and metabolism. *Chembiochem.* **2011**;12(2):290-8.

Angus-Hill ML, Dutnall RN, Tafrov ST, Sternglanz R, Ramakrishnan V. Crystal structure of the histone acetyltransferase Hpa2: A tetrameric member of the Gcn5-related N-acetyltransferase superfamily. *J Mol Biol*. **1999**;294(5):1311-25.

Arents G, Burlingame RW, Wang BC, Love WE, Moudrianakis EN. The nucleosomal core histone octamer at 3.1 A resolution: a tripartite protein assembly and a left-handed superhelix. *Proc Natl Acad Sci U S A*. **1991**;88(22):10148-52.

Atanassov BS, Koutelou E, Dent SY. The role of deubiquitinating enzymes in chromatin regulation. *FEBS Lett*. **2011**;585(13):2016-23.

Ausió J. Histone variants--the structure behind the function. *Brief Funct Genomic Proteomic*. **2006**;5(3):228-43.

Ausubel F, Brent R, Kingston RE, Moore DD, Seifman JG, Smith JA, Struhl K. **2006**. Current Protocols in Molecular Biology. John Wiley & Sons Inc., New York, NY.

Bannister AJ, Kouzarides T. Regulation of chromatin by histone modifications. *Cell Res*. **2011**;21(3):381-95.

Barth TK, Imhof A. Fast signals and slow marks: the dynamics of histone modifications. *Trends Biochem Sci*. **2010**;35(11):618-26.

Bauer UM, Daujat S, Nielsen SJ, Nightingale K, Kouzarides T. Methylation at arginine 17 of histone H3 is linked to gene activation. *EMBO Rep*. **2002**;3(1):39-44.

Baxevanis AD, Landsman D. Homology model building of Hho1p supports its role as a yeast histone H1 protein. *In Silico Biol*. **1998**;1(1):5-11.

Becker PB, Hörz W. ATP-dependent nucleosome remodeling. *Annu Rev Biochem*. **2002**;71:247-73.

Belch Y, Yang J, Liu Y, Malkaram SA, Liu R, Riethoven JJ, Ladunga I. Weakly positioned nucleosomes enhance the transcriptional competency of chromatin. *PLoS One*. **2010**;5(9):e12984.

Berger SL. Histone modifications in transcriptional regulation. *Curr Opin Genet Dev*. **2002**;12(2):142-8.

Berger SL. The complex language of chromatin regulation during transcription. *Nature*. **2007**;447(7143):407-12.

Bernstein BE, Liu CL, Humphrey EL, Perlstein EO, Schreiber SL. Global nucleosome occupancy in yeast. *Genome Biol.* **2004**;5(9):R62.

Bernstein BE, Meissner A, Lander ES. The mammalian epigenome. *Cell*. **2007**;128(4):669-81.

Bernstein E, Hake SB. The nucleosome: a little variation goes a long way. *Biochem Cell Biol*. **2006**;84(4):505-17.

Besant PG, Attwood PV. Histone H4 histidine phosphorylation: kinases, phosphatases, liver regeneration and cancer. *Biochem Soc Trans*. **2012**;40(1):290-3.

Bhat RA, Riehl M, Santandrea G, Velasco R, Slocombe S, Donn G, Steinbiss HH, Thompson RD, Becker HA. Alteration of GCN5 levels in maize reveals dynamic responses to manipulating histone acetylation. *Plant J*. **2003**;33(3):455-69.

Bhaumik SR, Green MR. SAGA is an essential in vivo target of the yeast acidic activator Gal4p. *Genes Dev*. **2001**;15(15):1935-45.

Bhaumik SR. Distinct regulatory mechanisms of eukaryotic transcriptional activation by SAGA and TFIID. *Biochim Biophys Acta*. **2011**;1809(2):97-108.

Biswas M, Voltz K, Smith JC, Langowski J. Role of histone tails in structural stability of the nucleosome. *PLoS Comput Biol*. **2011**;7(12):e1002279.

Bithell A, Johnson R, Buckley NJ. Transcriptional dysregulation of coding and non-coding genes in cellular models of Huntington's disease. *Biochem Soc Trans*. **2009**;37(Pt 6):1270-5.

Boeger H, Griesenbeck J, Strattan JS, Kornberg RD. Removal of promoter nucleosomes by disassembly rather than sliding in vivo. *Mol Cell*. **2004**;14(5):667-73.

Botstein D, Chervitz SA, Cherry JM. Yeast as a model organism. *Science*. **1997**;277(5330):1259-60.

Botstein D, Fink GR. Yeast: an experimental organism for 21st Century biology. *Genetics*. **2011**;189(3):695-704.

Braunstein M, Sobel RE, Allis CD, Turner BM, Broach JR. Efficient transcriptional silencing in *Saccharomyces cerevisiae* requires a heterochromatin histone acetylation pattern. *Mol Cell Biol*. **1996**;16(8):4349-56.

Brown CE, Lechner T, Howe L, Workman JL. The many HATs of transcription coactivators. *Trends Biochem Sci*. **2000**;25(1):15-9.

Brownell JE, Zhou J, Ranalli T, Kobayashi R, Edmondson DG, Roth SY, Allis CD. Tetrahymena histone acetyltransferase A: a homolog to yeast Gcn5p linking histone acetylation to gene activation. *Cell*. **1996**;84(6):843-51.

Burgess RJ, Zhang Z. Roles for Gcn5 in promoting nucleosome assembly and maintaining genome integrity. *Cell Cycle*. **2010**;9(15):2979-85.

Burgess SM, Ajimura M, Kleckner N. GCN5-dependent histone H3 acetylation and RPD3-dependent histone H4 deacetylation have distinct, opposing effects on IME2

transcription, during meiosis and during vegetative growth, in budding yeast. *Proc Natl Acad Sci U S A*. **1999**;96(12):6835-40.

Camporeale G, Shubert EE, Sarath G, Cerny R, Zempleni J. K8 and K12 are biotinylated in human histone H4. *Eur J Biochem*. **2004**;271(11):2257-63.

Candau R, Moore PA, Wang L, Barlev N, Ying CY, Rosen CA, Berger SL. Identification of human proteins functionally conserved with the yeast putative adaptors ADA2 and GCN5. *Mol Cell Biol*. **1996**;16(2):593-602.

Candau R, Zhou JX, Allis CD, Berger SL. Histone acetyltransferase activity and interaction with ADA2 are critical for GCN5 function in vivo. *EMBO J*. **1997**;16(3):555-65.

Chen D, Ma H, Hong H, Koh SS, Huang SM, Schurter BT, Aswad DW, Stallcup MR. Regulation of transcription by a protein methyltransferase. *Science*. **1999**;284(5423):2174-7.

Chen Y, Sprung R, Tang Y, Ball H, Sangras B, Kim SC, Falck JR, Peng J, Gu W, Zhao Y. Lysine propionylation and butyrylation are novel post-translational modifications in histones. *Mol Cell Proteomics*. **2007**;6(5):812-9.

Chen YC, Gatchel JR, Lewis RW, Mao CA, Grant PA, Zoghbi HY, Dent SY. Gcn5 loss-of-function accelerates cerebellar and retinal degeneration in a SCA7 mouse model. *Hum Mol Genet*. **2012**;21(2):394-405.

Cheung P, Tanner KG, Cheung WL, Sassone-Corsi P, Denu JM, Allis CD. Synergistic coupling of histone H3 phosphorylation and acetylation in response to epidermal growth factor stimulation. *Mol Cell*. **2000**;5(6):905-15.

Chi P, Allis CD, Wang GG. Covalent histone modifications--miswritten, misinterpreted and mis-erased in human cancers. *Nat Rev Cancer*. **2010**;10(7):457-69.

Chuang DM, Leng Y, Marinova Z, Kim HJ, Chiu CT. Multiple roles of HDAC inhibition in neurodegenerative conditions. *Trends Neurosci*. **2009**;32(11):591-601.

Cohen I, Poręba E, Kamieniarz K, Schneider R. Histone modifiers in cancer: friends or foes? *Genes Cancer*. **2011**;2(6):631-47.

Cunningham BC, Wells JA. High-resolution epitope mapping of hGH-receptor interactions by alanine-scanning mutagenesis. *Science.* **1989**;244(4908):1081-5.

Dai J, Hyland EM, Yuan DS, Huang H, Bader JS, Boeke JD. Probing nucleosome function: a highly versatile library of synthetic histone H3 and H4 mutants. *Cell*. **2008**;134(6):1066-78.

Daujat S, Bauer UM, Shah V, Turner B, Berger S, Kouzarides T. Crosstalk between CARM1 methylation and CBP acetylation on histone H3. *Curr Biol*. **2002**;12(24):2090-7.

Dhalluin C, Carlson JE, Zeng L, He C, Aggarwal AK, Zhou MM. Structure and ligand of a histone acetyltransferase bromodomain. *Nature*. **1999**;399(6735):491-6.

Di Marcotullio L, Canettieri G, Infante P, Greco A, Gulino A. Protected from the inside: endogenous histone deacetylase inhibitors and the road to cancer. *Biochim Biophys Acta*. **2011**;1815(2):241-52.

Eberharter A, Sterner DE, Schieltz D, Hassan A, Yates JR 3rd, Berger SL, Workman JL. The ADA complex is a distinct histone acetyltransferase complex in *Saccharomyces cerevisiae*. *Mol Cell Biol*. **1999**;19(10):6621-31.

Edwards CR, Dang W, Berger SL. Histone H4 lysine 20 of *Saccharomyces cerevisiae* is monomethylated and functions in subtelomeric silencing. *Biochemistry*. **2011**;50(48):10473-83.

Egger G, Liang G, Aparicio A, Jones PA. Epigenetics in human disease and prospects for epigenetic therapy. *Nature.* **2004**;429(6990):457-63.

Felsenfeld G, McGhee JD. Structure of the 30 nm chromatin fiber. *Cell.* **1986**;44(3):375-7.

Feng Y, Wang J, Asher S, Hoang L, Guardiani C, Ivanov I, Zheng YG. Histone H4 acetylation differentially modulates arginine methylation by an in Cis mechanism. *J Biol Chem*. **2011**;286(23):20323-34.

Ferreira R, Eberharter A, Bonaldi T, Chioda M, Imhof A, Becker PB. Site-specific acetylation of ISWI by GCN5. *BMC Mol Biol*. **2007**;8:73.

Fischle W, Wang Y, Allis CD. Histone and chromatin cross-talk. *Curr Opin Cell Biol*. **2003**;15(2):172-83.

Fraga MF, Ballestar E, Villar-Garea A, Boix-Chornet M, Espada J, Schotta G, Bonaldi T, Haydon C, Ropero S, Petrie K, Iyer NG, Pérez-Rosado A, Calvo E, Lopez JA, Cano A, Calasanz MJ, Colomer D, Piris MA, Ahn N, Imhof A, Caldas C, Jenuwein T, Esteller M. Loss of acetylation at Lys16 and trimethylation at Lys20 of histone H4 is a common hallmark of human cancer. *Nat Genet*. **2005**;37(4):391-400.

Freidkin I, Katcoff DJ. Specific distribution of the *Saccharomyces cerevisiae* linker histone homolog HHO1p in the chromatin. *Nucleic Acids Res*. **2001**;29(19):4043-51.

Frisch SM, Mymryk JS. Adenovirus-5 E1A: paradox and paradigm. *Nat Rev Mol Cell Biol*. **2002**;3(6):441-52.

Fujita Y, Morinobu S, Takei S, Fuchikami M, Matsumoto T, Yamamoto S, Yamawaki S. Vorinostat, a histone deacetylase inhibitor, facilitates fear extinction and enhances expression of the hippocampal NR2B-containing NMDA receptor gene. *J Psychiatr Res*. **2012**;46(5):635-43.

Füllgrabe J, Kavanagh E, Joseph B. Histone onco-modifications. *Oncogene*. **2011**;30(31):3391-403.

Garcia BA, Hake SB, Diaz RL, Kauer M, Morris SA, Recht J, Shabanowitz J, Mishra N, Strahl BD, Allis CD, Hunt DF. Organismal differences in post-translational modifications in histones H3 and H4. *J Biol Chem*. **2007**;282(10):7641-55.

Gardner KE, Zhou L, Parra MA, Chen X, Strahl BD. Identification of lysine 37 of histone H2B as a novel site of methylation. *PLoS One*. **2011**;6(1):e16244.

Georgakopoulos T, Thireos G. Two distinct yeast transcriptional activators require the function of the GCN5 protein to promote normal levels of transcription. *EMBO J*. **1992**;11(11):4145-52.

Ghizzoni M, Haisma HJ, Maarsingh H, Dekker FJ. Histone acetyltransferases are crucial regulators in NF-κB mediated inflammation. *Drug Discov Today*. **2011**;16(11-12):504-11.

Glowczewski L, Yang P, Kalashnikova T, Santisteban MS, Smith MM. Histone-histone interactions and centromere function. *Mol Cell Biol*. **2000**;20(15):5700-11.

Godley LA, Le Beau MM. The histone code and treatments for acute myeloid leukemia. *N Engl J Med*. **2012**;366(10):960-1.

Goffrini P, Ferrero I, Donnini C. Respiration-dependent utilisation of sugars in yeasts: a determinant role for sugar transporters. *J Bacteriol*. **2002**;184(2):427-32.

Goldberg AD, Allis CD, Bernstein E. Epigenetics: a landscape takes shape. *Cell*. **2007**;128(4):635-8.

Govind CK, Zhang F, Qiu H, Hofmeyer K, Hinnebusch AG. Gcn5 promotes acetylation, eviction, and methylation of nucleosomes in transcribed coding regions. *Mol Cell*. **2007**;25(1):31-42.

Grant PA, Berger SL. Histone acetyltransferase complexes. *Semin Cell Dev Biol*. **1999**;10(2):169-77.

Grant PA, Duggan L, Côté J, Roberts SM, Brownell JE, Candau R, Ohba R, Owen-Hughes T, Allis CD, Winston F, Berger SL, Workman JL. Yeast Gcn5 functions in two multisubunit complexes to acetylate nucleosomal histones: characterization of an Ada complex and the SAGA (Spt/Ada) complex. *Genes Dev*. **1997**;11(13):1640-50.

Grant PA, Eberharter A, John S, Cook RG, Turner BM, Workman JL. Expanded lysine acetylation specificity of Gcn5 in native complexes. *J Biol Chem*. **1999**;274(9):5895-900.

Gregory PD, Schmid A, Zavari M, Lui L, Berger SL, Hörz W. Absence of Gcn5 HAT activity defines a novel state in the opening of chromatin at the PHO5 promoter in yeast. *Mol Cell*. **1998**;1(4):495-505.

Grunstein M. Histone acetylation in chromatin structure and transcription. *Nature*. **1997**;389(6649):349-52.

Guillemette B, Drogaris P, Lin HH, Armstrong H, Hiragami-Hamada K, Imhof A, Bonneil E, Thibault P, Verreault A, Festenstein RJ. H3 lysine 4 is acetylated at active gene promoters and is regulated by H3 lysine 4 methylation. *PLoS Genet*. **2011**;7(3):e1001354.

Hahn S, Young ET. Transcriptional regulation in *Saccharomyces cerevisiae*: transcription factor regulation and function, mechanisms of initiation, and roles of activators and coactivators. *Genetics*. **2011**;189(3):705-36.

Hall IM, Shankaranarayana GD, Noma K, Ayoub N, Cohen A, Grewal SI. Establishment and maintenance of a heterochromatin domain. *Science*. **2002**;297(5590):2232-7.

Hampsey M, Na JG, Pinto I, Ware DE, Berroteran RW. Extragenic suppressors of a translation initiation defect in the cyc1 gene of *Saccharomyces cerevisiae*. *Biochimie.* **1991**;73(12):1445-55.

Hampsey M. A review of phenotypes in *Saccharomyces cerevisiae*. *Yeast.* **1997**;13(12):1099-133.

Hanover JA, Krause MW, Love DC. Bittersweet memories: linking metabolism to epigenetics through O-GlcNAcylation. *Nat Rev Mol Cell Biol*. **2012**;13(5):312-21.

Haqqani AS, Kelly JF, Birnboim HC. Selective nitration of histone tyrosine residues in vivo in mutatect tumors. *J Biol Chem*. **2002**;277(5):3614-21.

Harashima S, Hinnebusch AG. Multiple GCD genes required for repression of GCN4, a transcriptional activator of amino acid biosynthetic genes in *Saccharomyces cerevisiae*. *Mol Cell Biol*. **1986**;6(11):3990-8.

Hargreaves DC, Crabtree GR. ATP-dependent chromatin remodeling: genetics, genomics and mechanisms. *Cell Res*. **2011**;21(3):396-420.

Haring M, Offermann S, Danker T, Horst I, Peterhansel C, Stam M. Chromatin immunoprecipitation: optimisation, quantitative analysis and data normalisation. *Plant Methods.* **2007**;3:11.

He H, Lehming N. Global effects of histone modifications. *Brief Funct Genomic Proteomic*. **2003**;2(3):234-43.

Hettmann C, Soldati D. Cloning and analysis of a *Toxoplasma gondii* histone acetyltransferase: a novel chromatin remodelling factor in Apicomplexan parasites. *Nucleic Acids Res*. **1999**;27(22):4344-52.

Hong L, Schroth GP, Matthews HR, Yau P, Bradbury EM. Studies of the DNA binding properties of histone H4 amino terminus. Thermal denaturation studies reveal that acetylation markedly reduces the binding constant of the H4 "tail" to DNA. *J Biol Chem*. **1993**;268(1):305-14.

Horn PJ, Peterson CL. Molecular biology. Chromatin higher order folding--wrapping up transcription. *Science*. **2002**;297(5588):1824-7.

Hou H, Yu H. Structural insights into histone lysine demethylation. *Curr Opin Struct Biol*. **2010**;20(6):739-48.

Howe L, Auston D, Grant P, John S, Cook RG, Workman JL, Pillus L. Histone H3 specific acetyltransferases are essential for cell cycle progression. *Genes Dev*. **2001**;15(23):3144-54.

Huang H, Maertens AM, Hyland EM, Dai J, Norris A, Boeke JD, Bader JS. HistoneHits: a database for histone mutations and their phenotypes. *Genome Res.* **2009**;19(4):674-81.

Huang S, Litt M, Felsenfeld G. Methylation of histone H4 by arginine methyltransferase PRMT1 is essential in vivo for many subsequent histone modifications. *Genes Dev.* **2005**;19(16):1885-93.

Huisinga KL, Pugh BF. A genome-wide housekeeping role for TFIID and a highly regulated stress-related role for SAGA in *Saccharomyces cerevisiae*. *Mol Cell*. **2004**;13(4):573-85.

Hunter T. The age of crosstalk: phosphorylation, ubiquitination, and beyond. *Mol Cell*. **2007**;28(5):730-8.

Iyer V, Struhl K. Poly(dA:dT), a ubiquitous promoter element that stimulates transcription via its intrinsic DNA structure. *EMBO J*. **1995**;14(11):2570-9.

Jacobson RH, Ladurner AG, King DS, Tjian R. Structure and function of a human TAFII250 double bromodomain module. *Science*. **2000**;288(5470):1422-5.

Jenuwein T, Allis CD. Translating the histone code. *Science*. **2001**;293(5532):1074-80.

Jenuwein T. Re-SET-ting heterochromatin by histone methyltransferases. *Trends Cell Biol*. **2001**;11(6):266-73.

Jin B, Li Y, Robertson KD. DNA methylation: superior or subordinate in the epigenetic hierarchy? *Genes Cancer.* **2011**;2(6):607-17.

Joo YJ, Kim JH, Kang UB, Yu MH, Kim J. Gcn4p-mediated transcriptional repression of ribosomal protein genes under amino-acid starvation. *EMBO J*. **2011**;30(5):859-72.

Kamakaka RT, Biggins S. Histone variants: deviants? *Genes Dev*. **2005**;19(3):295-310.

Kamieniarz K, Izzo A, Dundr M, Tropberger P, Ozretic L, Kirfel J, Scheer E, Tropel P, Wisniewski JR, Tora L, Viville S, Buettner R, Schneider R. A dual role of linker histone H1.4 Lys 34 acetylation in transcriptional activation. *Genes Dev*. **2012**;26(8):797-802.

Kawano A, Hayashi Y, Noguchi S, Handa H, Horikoshi M, Yamaguchi Y. Global analysis for functional residues of histone variant Htz1 using the comprehensive point mutant library. *Genes Cells*. **2011**;16(5):590-607.

Kawashima S, Nakabayashi Y, Matsubara K, Sano N, Enomoto T, Tanaka K, Seki M, Horikoshi M. Global analysis of core histones reveals nucleosomal surfaces required for chromosome bi-orientation. *EMBO J*. **2011**;30(16):3353-67.

Keppler BR, Archer TK. Chromatin-modifying enzymes as therapeutic targets--Part 1. *Expert Opin Ther Targets*. **2008a**;12(10):1301-12.

Keppler BR, Archer TK. Chromatin-modifying enzymes as therapeutic targets--Part 2. *Expert Opin Ther Targets*. **2008b**;12(11):1457-67.

Khavari DA, Sen GL, Rinn JL. DNA methylation and epigenetic control of cellular differentiation. *Cell Cycle.* **2010**;9(19):3880-3.

Khorasanizadeh S. The nucleosome: from genomic organization to genomic regulation. *Cell*. **2004**;116(2):259-72.

Kikuchi H, Takami Y, Nakayama T. GCN5: a supervisor in all-inclusive control of vertebrate cell cycle progression through transcription regulation of various cell cycle-related genes. *Gene*. **2005**;347(1):83-97.

Kim JH, Saraf A, Florens L, Washburn M, Workman JL. Gcn5 regulates the dissociation of SWI/SNF from chromatin by acetylation of Swi2/Snf2. *Genes Dev*. **2010**;24(24):2766-71.

Kornberg RD, Lorch Y. Twenty-five years of the nucleosome, fundamental particle of the eukaryote chromosome. *Cell*. **1999**;98(3):285-94.

Kouzarides T. Chromatin modifications and their function. *Cell*. **2007**;128(4):693-705.

Kozak ML, Chavez A, Dang W, Berger SL, Ashok A, Guo X, Johnson FB. Inactivation of the Sas2 histone acetyltransferase delays senescence driven by telomere dysfunction. *EMBO J*. **2010**;29(1):158-70.

Krebs AR, Karmodiya K, Lindahl-Allen M, Struhl K, Tora L. SAGA and ATAC histone acetyl transferase complexes regulate distinct sets of genes and ATAC defines a class of p300-independent enhancers. *Mol Cell*. **2011**;44(3):410-23.

Kulis M, Esteller M. DNA methylation and cancer. *Adv Genet.* **2010**;70:27-56.

Kuo MH, Allis CD. Roles of histone acetyltransferases and deacetylases in gene regulation. *Bioessays*. **1998**;20(8):615-26.

Kuo MH, Brownell JE, Sobel RE, Ranalli TA, Cook RG, Edmondson DG, Roth SY, Allis CD. Transcription-linked acetylation by Gcn5p of histones H3 and H4 at specific lysines. *Nature*. **1996**;383(6597):269-72.

Kuo MH, vom Baur E, Struhl K, Allis CD. Gcn4 activator targets Gcn5 histone acetyltransferase to specific promoters independently of transcription. *Mol Cell*. **2000**;6(6):1309-20.

Kuo MH, Zhou J, Jambeck P, Churchill ME, Allis CD. Histone acetyltransferase activity of yeast Gcn5p is required for the activation of target genes in vivo. *Genes Dev*. **1998**;12(5):627-39.

Kurdistani SK, Grunstein M. Histone acetylation and deacetylation in yeast. *Nat Rev Mol Cell Biol*. **2003**;4(4):276-84.

Kusch T, Florens L, Macdonald WH, Swanson SK, Glaser RL, Yates JR 3rd, Abmayr SM, Washburn MP, Workman JL. Acetylation by Tip60 is required for selective histone variant exchange at DNA lesions. *Science*. **2004**;306(5704):2084-7.

Lane AA, Chabner BA. Histone deacetylase inhibitors in cancer therapy. *J Clin Oncol*. **2009**;27(32):5459-68.

Lee SYL. (**2007**). *Suppressors of conditional histone H4 mutants*. Unpublished Honours thesis, Department of Biological Sciences, The National University of Singapore.

Lee TI, Causton HC, Holstege FC, Shen WC, Hannett N, Jennings EG, Winston F, Green MR, Young RA. Redundant roles for the TFIID and SAGA complexes in global transcription. *Nature*. **2000**;405(6787):701-4.

Lee TI, Young RA. Transcription of eukaryotic protein-coding genes. *Annu Rev Genet*. **2000**;34:77-137.

Lefèvre F, Rémy MH, Masson JM. Alanine-stretch scanning mutagenesis: a simple and efficient method to probe protein structure and function. *Nucleic Acids Res.* **1997**;25(2):447-8.

Li A, Yu Y, Lee SC, Ishibashi T, Lees-Miller SP, Ausió J. Phosphorylation of histone H2A.X by DNA-dependent protein kinase is not affected by core histone acetylation, but it alters nucleosome stability and histone H1 binding. *J Biol Chem*. **2010**;285(23):17778-88.

Li F, Lu J, Han Q, Zhang G, Huang B. The Elp3 subunit of human Elongator complex is functionally similar to its counterpart in yeast. *Mol Genet Genomics*. **2005**;273(3):264-72.

Li G, Reinberg D. Chromatin higher-order structures and gene regulation. *Curr Opin Genet Dev*. **2011**;21(2):175-86.

Li X, Wong J, Tsai SY, Tsai MJ, O'Malley BW. Progesterone and glucocorticoid receptors recruit distinct coactivator complexes and promote distinct patterns of local chromatin modification. *Mol Cell Biol*. **2003**;23(11):3763-73.

Liu Y, Xu X, Singh-Rodriguez S, Zhao Y, Kuo MH. Histone H3 Ser10 phosphorylation-independent function of Snf1 and Reg1 proteins rescues a gcn5-mutant in *HIS3* expression. *Mol Cell Biol*. **2005**;25(23):10566-79.

Ljungdahl PO, Daignan-Fornier B. Regulation of amino acid, nucleotide, and phosphate metabolism in *Saccharomyces cerevisiae*. *Genetics*. **2012**;190(3):885-929.

Lo WS, Trievel RC, Rojas JR, Duggan L, Hsu JY, Allis CD, Marmorstein R, Berger SL. Phosphorylation of serine 10 in histone H3 is functionally linked in vitro and in vivo to Gcn5-mediated acetylation at lysine 14. *Mol Cell*. **2000**;5(6):917-26.

Losa R, Omari S, Thoma F. Poly(dA).poly(dT) rich sequences are not sufficient to exclude nucleosome formation in a constitutive yeast promoter. *Nucleic Acids Res*. **1990**;18(12):3495-502.

Lu X, Simon MD, Chodaparambil JV, Hansen JC, Shokat KM, Luger K. The effect of H3K79 dimethylation and H4K20 trimethylation on nucleosome and chromatin structure. *Nat Struct Mol Biol*. **2008**;15(10):1122-4.

Luger K, Mäder AW, Richmond RK, Sargent DF, Richmond TJ. Crystal structure of the nucleosome core particle at 2.8 A resolution. *Nature.* **1997**;389(6648):251-60.

Lusser A, Kadonaga JT. Chromatin remodeling by ATP-dependent molecular machines. *Bioessays*. **2003**;25(12):1192-200.

Mai A, Rotili D, Tarantino D, Ornaghi P, Tosi F, Vicidomini C, Sbardella G, Nebbioso A, Miceli M, Altucci L, Filetici P. Small-molecule inhibitors of histone acetyltransferase activity: identification and biological properties. *J Med Chem*. **2006**;49(23):6897-907.

Mai X, Chou S, Struhl K. Preferential accessibility of the yeast his3 promoter is determined by a general property of the DNA sequence, not by specific elements. *Mol Cell Biol*. **2000**;20(18):6668-76.

Margueron R, Trojer P, Reinberg D. The key to development: interpreting the histone code? *Curr Opin Genet Dev.* **2005**;15(2):163-76.

Mariño-Ramírez L, Kann MG, Shoemaker BA, Landsman D. Histone structure and nucleosome stability. *Expert Rev Proteomics.* **2005**;2(5):719-29.

Marmorstein R, Roth SY. Histone acetyltransferases: function, structure, and catalysis. *Curr Opin Genet Dev*. **2001**;11(2):155-61.

Martens JA, Winston F. Recent advances in understanding chromatin remodeling by Swi/Snf complexes. *Curr Opin Genet Dev*. **2003**;13(2):136-42.

Martens JH, Stunnenberg HG, Logie C. The decade of the epigenomes? *Genes Cancer*. **2011**;2(6):680-7.

Martinato F, Cesaroni M, Amati B, Guccione E. Analysis of Myc-induced histone modifications on target chromatin. *PLoS One*. **2008**;3(11):e3650.

Matsubara K, Sano N, Umehara T, Horikoshi M. Global analysis of functional surfaces of core histones with comprehensive point mutants. *Genes Cells.* **2007**;12(1):13-33.

McCusker JH, Haber JE. crl mutants of *Saccharomyces cerevisiae* resemble both mutants affecting general control of amino acid biosynthesis and omnipotent translational suppressor mutants. *Genetics.* **1988**;119(2):317-27.

Meda F, Folci M, Baccarelli A, Selmi C. The epigenetics of autoimmunity. *Cell Mol Immunol*. **2011**;8(3):226-36.

Messner S, Altmeyer M, Zhao H, Pozivil A, Roschitzki B, Gehrig P, Rutishauser D, Huang D, Caflisch A, Hottiger MO. PARP1 ADP-ribosylates lysine residues of the core histone tails. *Nucleic Acids Res*. **2010**;38(19):6350-62.

Millar CB, Grunstein M. Genome-wide patterns of histone modifications in yeast. *Nat Rev Mol Cell Biol.* **2006**;7(9):657-66.

Morris KV. siRNA-mediated transcriptional gene silencing: the potential mechanism and a possible role in the histone code. *Cell Mol Life Sci.* **2005**;62(24):3057-66.

Muller S, Filippakopoulos P, Knapp S. Bromodomains as therapeutic targets. *Expert Rev Mol Med*. **2011**;13:e29.

Murr R. Interplay between different epigenetic modifications and mechanisms. *Adv Genet.* **2010**;70:101-41.

Narlikar GJ, Fan HY, Kingston RE. Cooperation between complexes that regulate chromatin structure and transcription. *Cell*. **2002**;108(4):475-87.

Nasmyth KA, Reed SI. Isolation of genes by complementation in yeast: molecular cloning of a cell-cycle gene. *Proc Natl Acad Sci U S A*. **1980**;77(4):2119-23.

Nelson CJ, Santos-Rosa H, Kouzarides T. Proline isomerization of histone H3 regulates lysine methylation and gene expression. *Cell*. **2006**;126(5):905-16.

Neuwald AF, Landsman D. GCN5-related histone N-acetyltransferases belong to a diverse superfamily that includes the yeast SPT10 protein. *Trends Biochem Sci*. **1997**;22(5):154-5.

Nishioka K, Rice JC, Sarma K, Erdjument-Bromage H, Werner J, Wang Y, Chuikov S, Valenzuela P, Tempst P, Steward R, Lis JT, Allis CD, Reinberg D. PR-Set7 is a nucleosome-specific methyltransferase that modifies lysine 20 of histone H4 and is associated with silent chromatin. *Mol Cell*. **2002**;9(6):1201-13.

North JA, Javaid S, Ferdinand MB, Chatterjee N, Picking JW, Shoffner M, Nakkula RJ, Bartholomew B, Ottesen JJ, Fishel R, Poirier MG. Phosphorylation of histone H3(T118) alters nucleosome dynamics and remodeling. *Nucleic Acids Res*. **2011**;39(15):6465-74.

Nowak SJ, Corces VG. Phosphorylation of histone H3: a balancing act between chromosome condensation and transcriptional activation. *Trends Genet*. **2004**;20(4):214-20.

Oettinger MA, Struhl K. Suppressors of *Saccharomyces cerevisiae* his3 promoter mutations lacking the upstream element. *Mol Cell Biol*. **1985**;5(8):1901-9.

O'Neill LP, Turner BM. Immunoprecipitation of native chromatin: NChIP. *Methods.* **2003**;31(1):76-82.

Otero G, Fellows J, Li Y, de Bizemont T, Dirac AM, Gustafsson CM, Erdjument-Bromage H, Tempst P, Svejstrup JQ. Elongator, a multisubunit component of a novel RNA polymerase II holoenzyme for transcriptional elongation. *Mol Cell*. **1999**;3(1):109-18.

Panzeter PL, Zweifel B, Malanga M, Waser SH, Richard M, Althaus FR. Targeting of histone tails by poly(ADP-ribose). *J Biol Chem*. **1993**;268(24):17662-4.

Paolinelli R, Mendoza-Maldonado R, Cereseto A, Giacca M. Acetylation by GCN5 regulates CDC6 phosphorylation in the S phase of the cell cycle. *Nat Struct Mol Biol*. **2009**;16(4):412-20.

Park S, Hanekamp T, Thorsness MK, Thorsness PE. Yme2p is a mediator of nucleoid structure and number in mitochondria of the yeast *Saccharomyces cerevisiae*. *Curr Genet.* **2006**;50(3):173-82.

Parthun MR. Hat1: the emerging cellular roles of a type B histone acetyltransferase. *Oncogene*. **2007**;26(37):5319-28.

Peng Z, Mizianty MJ, Xue B, Kurgan L, Uversky VN. More than just tails: intrinsic disorder in histone proteins. *Mol Biosyst*. **2012**;8(7):1886-901.

Pérez-Martín J, Johnson AD. Mutations in chromatin components suppress a defect of Gcn5 protein in *Saccharomyces cerevisiae*. *Mol Cell Biol*. **1998**;18(2):1049-54.

Peterson CL, Laniel MA. Histones and histone modifications. *Curr Biol.* **2004**;14(14):R546-51.

Petronis A. Epigenetics as a unifying principle in the aetiology of complex traits and diseases. *Nature*. **2010**;465(7299):721-7.

Phillips DM. The presence of acetyl groups of histones. *Biochem J*. **1963**;87:258-63.

Phizicky EM, Fields S. Protein-protein interactions: methods for detection and analysis. *Microbiol Rev.* **1995**;59(1):94-123.

Pokholok DK, Harbison CT, Levine S, Cole M, Hannett NM, Lee TI, Bell GW, Walker K, Rolfe PA, Herbolsheimer E, Zeitlinger J, Lewitter F, Gifford DK, Young RA. Genome-wide map of nucleosome acetylation and methylation in yeast. *Cell.* **2005**;122(4):517-27.

Pollard KJ, Peterson CL. Role for ADA/GCN5 products in antagonizing chromatin-mediated transcriptional repression. *Mol Cell Biol*. **1997**;17(11):6212-22.

Portela A, Esteller M. Epigenetic modifications and human disease. *Nat Biotechnol*. **2010**;28(10):1057-68.

Pray-Grant MG, Daniel JA, Schieltz D, Yates JR 3rd, Grant PA. Chd1 chromodomain links histone H3 methylation with SAGA- and SLIK-dependent acetylation. *Nature*. **2005**;433(7024):434-8.

Pray-Grant MG, Schieltz D, McMahon SJ, Wood JM, Kennedy EL, Cook RG, Workman JL, Yates JR 3rd, Grant PA. The novel SLIK histone acetyltransferase complex functions in the yeast retrograde response pathway. *Mol Cell Biol*. **2002**;22(24):8774-86.

Prelich G. Gene overexpression: uses, mechanisms, and interpretation. *Genetics*. **2012**;190(3):841-54.

Qian C, Zhou MM. SET domain protein lysine methyltransferases: Structure, specificity and catalysis. *Cell Mol Life Sci*. **2006**;63(23):2755-63.

Qiu H, Hu C, Zhang F, Hwang GJ, Swanson MJ, Boonchird C, Hinnebusch AG. Interdependent recruitment of SAGA and Srb mediator by transcriptional activator Gcn4p. *Mol Cell Biol*. **2005**;25(9):3461-74.

Ramachandran S, Vogel L, Strahl BD, Dokholyan NV. Thermodynamic stability of histone H3 is a necessary but not sufficient driving force for its evolutionary conservation. *PLoS Comput Biol*. **2011**;7(1):e1001042.

Rando OJ, Winston F. Chromatin and transcription in yeast. *Genetics*. **2012**;190(2):351-87.

Rea S, Eisenhaber F, O'Carroll D, Strahl BD, Sun ZW, Schmid M, Opravil S, Mechtler K, Ponting CP, Allis CD, Jenuwein T. Regulation of chromatin structure by site-specific histone H3 methyltransferases. *Nature*. **2000**;406(6796):593-9.

Recht J, Osley MA. Mutations in both the structured domain and N-terminus of histone H2B bypass the requirement for Swi-Snf in yeast. *EMBO J*. **1999**;18(1):229-40.

Reinke H, Hörz W. Histones are first hyperacetylated and then lose contact with the activated PHO5 promoter. *Mol Cell.* **2003**;11(6):1599-607.

Rice JC, Allis CD. Histone methylation versus histone acetylation: new insights into epigenetic regulation. *Curr Opin Cell Biol*. **2001**;13(3):263-73.

Robert F, Pokholok DK, Hannett NM, Rinaldi NJ, Chandy M, Rolfe A, Workman JL, Gifford DK, Young RA. Global position and recruitment of HATs and HDACs in the yeast genome. *Mol Cell*. **2004**;16(2):199-209.

Rosaleny LE, Ruiz-García AB, García-Martínez J, Pérez-Ortín JE, Tordera V. The Sas3p and Gcn5p histone acetyltransferases are recruited to similar genes. *Genome Biol*. **2007**;8(6):R119.

Ross CA, Shoulson I. Huntington disease: pathogenesis, biomarkers, and approaches to experimental therapeutics. *Parkinsonism Relat Disord*. **2009**;15 Suppl 3:S135-8.

Roth SY, Denu JM, Allis CD. Histone acetyltransferases. *Annu Rev Biochem*. **2001**;70:81-120.

Ruiz-García AB, Sendra R, Pamblanco M, Tordera V. Gcn5p is involved in the acetylation of histone H3 in nucleosomes. *FEBS Lett*. **1997**;403(2):186-90.

Sakamoto M, Noguchi S, Kawashima S, Okada Y, Enomoto T, Seki M, Horikoshi M. Global analysis of mutual interaction surfaces of nucleosomes with comprehensive point mutants. *Genes Cells*. **2009**;14(11):1271-330.

Sampley ML, Ozcan S. Regulation of insulin gene transcription by multiple histone acetyltransferases. *DNA Cell Biol*. **2012**;31(1):8-14.

Sansó M, Vargas-Pérez I, Quintales L, Antequera F, Ayté J, Hidalgo E. Gcn5 facilitates Pol II progression, rather than recruitment to nucleosome-depleted stress promoters, in *Schizosaccharomyces pombe*. *Nucleic Acids Res*. **2011**;39(15):6369-79.

Santisteban MS, Arents G, Moudrianakis EN, Smith MM. Histone octamer function in vivo: mutations in the dimer-tetramer interfaces disrupt both gene activation and repression. *EMBO J*. **1997**;16(9):2493-506.

Santisteban MS, Kalashnikova T, Smith MM. Histone H2A.Z regulates transcription and is partially redundant with nucleosome remodeling complexes. *Cell*. **2000**;103(3):411-22.

Santos-Rosa H, Schneider R, Bannister AJ, Sherriff J, Bernstein BE, Emre NC, Schreiber SL, Mellor J, Kouzarides T. Active genes are tri-methylated at K4 of histone H3. *Nature*. **2002**;419(6905):407-11.

Sarfstein R, Bruchim I, Fishman A, Werner H. The mechanism of action of the histone deacetylase inhibitor vorinostat involves interaction with the insulin-like growth factor signaling pathway. *PLoS One.* **2011**;6(9):e24468.

Sarg B, Helliger W, Talasz H, Koutzamani E, Lindner HH. Histone H4 hyperacetylation precludes histone H4 lysine 20 trimethylation. *J Biol Chem*. **2004**;279(51):53458-64.

Sato L, Noguchi S, Hayashi Y, Sakamoto M, Horikoshi M. Global analysis of functional relationships between histone point mutations and the effects of histone deacetylase inhibitors. *Genes Cells*. **2010**;15(6):553-94.

Sawan C, Herceg Z. Histone modifications and cancer. *Adv Genet*. **2010**;70:57-85.

Schiltz RL, Mizzen CA, Vassilev A, Cook RG, Allis CD, Nakatani Y. Overlapping but distinct patterns of histone acetylation by the human coactivators p300 and PCAF within nucleosomal substrates. *J Biol Chem*. **1999**;274(3):1189-92.

Selvi BR, Cassel JC, Kundu TK, Boutillier AL. Tuning acetylation levels with HAT activators: therapeutic strategy in neurodegenerative diseases. *Biochim Biophys Acta*. **2010**;1799(10-12):840-53.

Shahbazian MD, Zhang K, Grunstein M. Histone H2B ubiquitylation controls processive methylation but not monomethylation by Dot1 and Set1. *Mol Cell*. **2005**;19(2):271-7.

Shogren-Knaak M, Ishii H, Sun JM, Pazin MJ, Davie JR, Peterson CL. Histone H4-K16 acetylation controls chromatin structure and protein interactions. *Science*. **2006**;311(5762):844-7.

Shogren-Knaak M, Peterson CL. Switching on chromatin: mechanistic role of histone H4-K16 acetylation. *Cell Cycle*. **2006**;5(13):1361-5.

Singh RK, Gunjan A. Histone tyrosine phosphorylation comes of age. *Epigenetics*. **2011**;6(2):153-60.

Sinha SC, Chaudhuri BN, Burgner JW, Yakovleva G, Davisson VJ, Smith JL. Crystal structure of imidazole glycerol-phosphate dehydratase: duplication of an unusual fold. *J Biol Chem*. **2004**;279(15):15491-8.

Smith CM, Gafken PR, Zhang Z, Gottschling DE, Smith JB, Smith DL. Mass spectrometric quantification of acetylation at specific lysines within the amino-terminal tail of histone H4. *Anal Biochem*. **2003**;316(1):23-33.

Smith ER, Belote JM, Schiltz RL, Yang XJ, Moore PA, Berger SL, Nakatani Y, Allis CD. Cloning of Drosophila GCN5: conserved features among metazoan GCN5 family members. *Nucleic Acids Res*. **1998**;26(12):2948-54.

Smith ER, Pannuti A, Gu W, Steurnagel A, Cook RG, Allis CD, Lucchesi JC. The drosophila MSL complex acetylates histone H4 at lysine 16, a chromatin modification linked to dosage compensation. *Mol Cell Biol*. **2000**;20(1):312-8.

Smith MM, Santisteban MS. Genetic dissection of histone function. *Methods.* **1998**;15(4):269-81.

Spedale G, Timmers HT, Pijnappel WW. ATAC-king the complexity of SAGA during evolution. *Genes Dev*. **2012**;26(6):527-41.

Stebbing J, Bower M, Syed N, Smith P, Yu V, Crook T. Epigenetics: an emerging technology in the diagnosis and treatment of cancer. *Pharmacogenomics*. **2006**;7(5):747-57.

Sterner DE, Belotserkovskaya R, Berger SL. SALSA, a variant of yeast SAGA, contains truncated Spt7, which correlates with activated transcription. *Proc Natl Acad Sci U S A*. **2002a**;99(18):11622-7.

Sterner DE, Berger SL. Acetylation of histones and transcription-related factors. *Microbiol Mol Biol Rev*. **2000**;64(2):435-59.

Sterner DE, Grant PA, Roberts SM, Duggan LJ, Belotserkovskaya R, Pacella LA, Winston F, Workman JL, Berger SL. Functional organization of the yeast SAGA complex: distinct components involved in structural integrity, nucleosome acetylation, and TATA-binding protein interaction. *Mol Cell Biol*. **1999**;19(1):86-98.

Sterner DE, Nathan D, Reindle A, Johnson ES, Berger SL. Sumoylation of the yeast Gcn5 protein. *Biochemistry*. **2006**;45(3):1035-42.

Sterner DE, Wang X, Bloom MH, Simon GM, Berger SL. The SANT domain of Ada2 is required for normal acetylation of histones by the yeast SAGA complex. *J Biol Chem*. **2002b**;277(10):8178-86.

Strahl BD, Allis CD. The language of covalent histone modifications. *Nature*. **2000**;403(6765):41-5.

Struhl K. Constitutive and inducible *Saccharomyces cerevisiae* promoters: evidence for two distinct molecular mechanisms. *Mol Cell Biol*. **1986**;6(11):3847-53.

Struhl K. Nucleotide sequence and transcriptional mapping of the yeast pet56-his3-ded1 gene region. *Nucleic Acids Res*. **1985**;13(23):8587-601.

Sujatha S, Ishihama A, Chatterji D. Functional complementation between mutations at two distant positions in *Escherichia coli* RNA polymerase as revealed by second-site suppression. *Mol Gen Genet.* **2001**;264(5):531-8.

Suka N, Luo K, Grunstein M. Sir2p and Sas2p opposingly regulate acetylation of yeast histone H4 lysine16 and spreading of heterochromatin. *Nat Genet*. **2002**;32(3):378-83.

Suka N, Suka Y, Carmen AA, Wu J, Grunstein M. Highly specific antibodies determine histone acetylation site usage in yeast heterochromatin and euchromatin. *Mol Cell*. **2001**;8(2):473-9.

Sun WJ, Zhou X, Zheng JH, Lu MD, Nie JY, Yang XJ, Zheng ZQ. Histone acetyltransferases and deacetylases: molecular and clinical implications to gastrointestinal carcinogenesis. *Acta Biochim Biophys Sin (Shanghai)*. **2012**;44(1):80-91.

Sun ZW, Allis CD. Ubiquitination of histone H2B regulates H3 methylation and gene silencing in yeast. *Nature*. **2002**;418(6893):104-8.

Syntichaki P, Thireos G. The Gcn5.Ada complex potentiates the histone acetyltransferase activity of Gcn5. *J Biol Chem*. **1998**;273(38):24414-9.

Teo SHR. (**2008**). *Genetic analysis of histone mutants (Mechanisms of suppression of conditional histone alleles)*. Unpublished UROPS thesis, Department of Microbiology, The National University of Singapore.

Timmermann S, Lehrmann H, Polesskaya A, Harel-Bellan A. Histone acetylation and disease. *Cell Mol Life Sci*. **2001**;58(5-6):728-36.

Tsaprouni LG, Ito K, Powell JJ, Adcock IM, Punchard N. Differential patterns of histone acetylation in inflammatory bowel diseases. *J Inflamm (Lond)*. **2011**;8(1):1.

Tse C, Georgieva EI, Ruiz-García AB, Sendra R, Hansen JC. Gcn5p, a transcription-related histone acetyltransferase, acetylates nucleosomes and folded nucleosomal arrays in the absence of other protein subunits. *J Biol Chem*. **1998**;273(49):32388-92.

Turner BM, Birley AJ, Lavender J. Histone H4 isoforms acetylated at specific lysine residues define individual chromosomes and chromatin domains in Drosophila polytene nuclei. *Cell*. **199**2;69(2):375-84.

Turner BM. Defining an epigenetic code. *Nat Cell Biol*. **2007**;9(1):2-6.

Turner BM. Histone acetylation and an epigenetic code. *Bioessays*. **2000**;22(9):836-45.

Turner EL, Malo ME, Pisclevich MG, Dash MD, Davies GF, Arnason TG, Harkness TA. The *Saccharomyces cerevisiae* anaphase-promoting complex interacts with multiple histone-modifying enzymes to regulate cell cycle progression. *Eukaryot Cell*. **2010**;9(10):1418-31.

Urdinguio RG, Sanchez-Mut JV, Esteller M. Epigenetic mechanisms in neurological diseases: genes, syndromes, and therapies. *Lancet Neurol*. **2009**;8(11):1056-72.

Ushinsky SC, Bussey H, Ahmed AA, Wang Y, Friesen J, Williams BA, Storms RK. Histone H1 in *Saccharomyces cerevisiae*. *Yeast.* **1997**;13(2):151-61.

Vakoc CR, Mandat SA, Olenchock BA, Blobel GA. Histone H3 lysine 9 methylation and HP1gamma are associated with transcription elongation through mammalian chromatin. *Mol Cell*. **2005**;19(3):381-91.

van den Brink J, Akeroyd M, van der Hoeven R, Pronk JT, de Winde JH, Daran-Lapujade P. Energetic limits to metabolic flexibility: responses of Saccharomyces cerevisiae to glucose-galactose transitions. *Microbiology*. **2009**;155(Pt 4):1340-50.

Van Den Broeck A, Brambilla E, Moro-Sibilot D, Lantuejoul S, Brambilla C, Eymin B, Khochbin S, Gazzeri S. Loss of histone H4K20 trimethylation occurs in preneoplasia and influences prognosis of non-small cell lung cancer. *Clin Cancer Res*. **2008**;14(22):7237-45.

VanDemark AP, Kasten MM, Ferris E, Heroux A, Hill CP, Cairns BR. Autoregulation of the rsc4 tandem bromodomain by gcn5 acetylation. *Mol Cell*. **2007**;27(5):817-28.

Vaquero A, Sternglanz R, Reinberg D. NAD+-dependent deacetylation of H4 lysine 16 by class III HDACs. *Oncogene*. **2007**;26(37):5505-20.

Vernarecci S, Tosi F, Filetici P. Tuning acetylated chromatin with HAT inhibitors: a novel tool for therapy. *Epigenetics*. **2010**;5(2):105-11.

Villeneuve LM, Reddy MA, Natarajan R. Epigenetics: deciphering its role in diabetes and its chronic complications. *Clin Exp Pharmacol Physiol*. **2011**;38(7):451-9.

Waggoner D. Mechanisms of disease: epigenesis. *Semin Pediatr Neurol*. **2007**;14(1):7-14.

Waldmann T, Izzo A, Kamieniarz K, Richter F, Vogler C, Sarg B, Lindner H, Young NL, Mittler G, Garcia BA, Schneider R. Methylation of H2AR29 is a novel repressive PRMT6 target. *Epigenetics Chromatin*. **2011**;4:11.

Wang H, Cao R, Xia L, Erdjument-Bromage H, Borchers C, Tempst P, Zhang Y. Purification and functional characterization of a histone H3-lysine 4-specific methyltransferase. *Mol Cell*. **2001**;8(6):1207-17.

Winkler GS, Kristjuhan A, Erdjument-Bromage H, Tempst P, Svejstrup JQ. Elongator is a histone H3 and H4 acetyltransferase important for normal histone acetylation levels in vivo. *Proc Natl Acad Sci U S A*. **2002**;99(6):3517-22.

Winkler GS, Petrakis TG, Ethelberg S, Tokunaga M, Erdjument-Bromage H, Tempst P, Svejstrup JQ. RNA polymerase II elongator holoenzyme is composed of two discrete subcomplexes. *J Biol Chem*. **2001**;276(35):32743-9.

Wippo CJ, Krstulovic BS, Ertel F, Musladin S, Blaschke D, Stürzl S, Yuan GC, Hörz W, Korber P, Barbaric S. Differential cofactor requirements for histone eviction from two nucleosomes at the yeast PHO84 promoter are determined by intrinsic nucleosome stability. *Mol Cell Biol*. **2009**;29(11):2960-81.

Wittschieben BO, Fellows J, Du W, Stillman DJ, Svejstrup JQ. Overlapping roles for the histone acetyltransferase activities of SAGA and elongator in vivo. *EMBO J*. **2000**;19(12):3060-8.

Wittschieben BO, Otero G, de Bizemont T, Fellows J, Erdjument-Bromage H, Ohba R, Li Y, Allis CD, Tempst P, Svejstrup JQ. A novel histone acetyltransferase is an integral subunit of elongating RNA polymerase II holoenzyme. *Mol Cell*. **1999**;4(1):123-8.

Wolffe AP. Centromeric chromatin. Histone deviants. *Curr Biol*. **1995**;5(5):452-4.

Wood CM, Nicholson JM, Lambert SJ, Chantalat L, Reynolds CD, Baldwin JP. High-resolution structure of the native histone octamer. *Acta Crystallogr Sect F Struct Biol Cryst Commun*. **2005**;61(Pt 6):541-5.

Xu EY, Bi X, Holland MJ, Gottschling DE, Broach JR. Mutations in the nucleosome core enhance transcriptional silencing. *Mol Cell Biol*. **2005**;25(5):1846-59.

Xu K, Dai XL, Huang HC, Jiang ZF. Targeting HDACs: a promising therapy for Alzheimer's disease. *Oxid Med Cell Longev*. **2011**;2011:143269.

Xu W, Edmondson DG, Roth SY. Mammalian GCN5 and P/CAF acetyltransferases have homologous amino-terminal domains important for recognition of nucleosomal substrates. *Mol Cell Biol*. **1998**;18(10):5659-69.

Yang D, Arya G. Structure and binding of the H4 histone tail and the effects of lysine 16 acetylation. *Phys Chem Chem Phys*. **2011**;13(7):2911-21.

Yang X, Yu W, Shi L, Sun L, Liang J, Yi X, Li Q, Zhang Y, Yang F, Han X, Zhang D, Yang J, Yao Z, Shang Y. HAT4, a Golgi apparatus-anchored B-type histone acetyltransferase, acetylates free histone H4 and facilitates chromatin assembly. *Mol Cell*. **2011**;44(1):39-50.

Ye J, Ai X, Eugeni EE, Zhang L, Carpenter LR, Jelinek MA, Freitas MA, Parthun MR. Histone H4 lysine 91 acetylation a core domain modification associated with chromatin assembly. *Mol Cell*. **2005**;18(1):123-30.

Yu Q, Kuzmiak H, Zou Y, Olsen L, Defossez PA, Bi X. *Saccharomyces cerevisiae* linker histone Hho1p functionally interacts with core histone H4 and negatively

regulates the establishment of transcriptionally silent chromatin. *J Biol Chem*. **2009**;284(2):740-50.

Yu Q, Olsen L, Zhang X, Boeke JD, Bi X. Differential contributions of histone H3 and H4 residues to heterochromatin structure. *Genetics*. **2011b**;188(2):291-308.

Yu Y, Srinivasan M, Nakanishi S, Leatherwood J, Shilatifard A, Sternglanz R. A conserved patch near the C terminus of histone H4 is required for genome stability in budding yeast. *Mol Cell Biol*. **2011a**;31(11):2311-25.

Zegerman P, Canas B, Pappin D, Kouzarides T. Histone H3 lysine 4 methylation disrupts binding of nucleosome remodeling and deacetylase (NuRD) repressor complex. *J Biol Chem*. **2002**;277(14):11621-4.

Zhang H, Han J, Kang B, Burgess R, Zhang Z. Human histone acetyltransferase 1 protein preferentially acetylates H4 histone molecules in H3.1-H4 over H3.3-H4. *J Biol Chem*. **2012**;287(9):6573-81.

Zhang K, Sridhar VV, Zhu J, Kapoor A, Zhu JK. Distinctive core histone post-translational modification patterns in *Arabidopsis thaliana*. *PLoS One*. **2007**;2(11):e1210.

Zhang K, Williams KE, Huang L, Yau P, Siino JS, Bradbury EM, Jones PR, Minch MJ, Burlingame AL. Histone acetylation and deacetylation: identification of acetylation and methylation sites of HeLa histone H4 by mass spectrometry. *Mol Cell Proteomics*. **2002**;1(7):500-8.

Zhang W, Bone JR, Edmondson DG, Turner BM, Roth SY. Essential and redundant functions of histone acetylation revealed by mutation of target lysines and loss of the Gcn5p acetyltransferase. *EMBO J*. **1998**;17(11):3155-67.

Zhou Y, Grummt I. The PHD finger/bromodomain of NoRC interacts with acetylated histone H4K16 and is sufficient for rDNA silencing. *Curr Biol*. **2005**;15(15):1434-8.

Zhu B, Reinberg D. Epigenetic inheritance: uncontested? *Cell Res*. **2011**;21(3):435-41.

Zippo A, Serafini R, Rocchigiani M, Pennacchini S, Krepelova A, Oliviero S. Histone crosstalk between H3S10ph and H4K16ac generates a histone code that mediates transcription elongation. *Cell*. **2009**;138(6):1122-36.

Zweidler A. Role of individual histone tyrosines in the formation of the nucleosome complex. *Biochemistry*. **1992**;31(38):9205-11.

8. Appendices

8.1 Gene derivatives of Bank 13 (YEp13) tested in the phenotypic assay

Table 8.1 Gene derivatives of Bank 13 (YEp13)

Vector	Gene derivatives
YEp13	CCT6ΔC + YDR187C + YDR186CΔN
	CCT6ΔNΔC + YDR185C + ATC1 + YDR183C-A + PLP1
	HPA2ΔC
	SFG1
	SKI8
	SUF2
	YNL305C + MRPS18

8.2 Genes inserted into PactT424 and PactT424-HA tested in the phenotypic assay

Table 8.2 Genes inserted into PactT424 and PactT424-HA

Vector	Insert	Vector	Insert
PactT424	ESA1	PactT424-HA	ESA1
	GCN5		GCN5
	HAT1		HAT1
	HAT2		HAT2
	HPA1		HPA1
	HPA2		HPA2
	HPA3		HPA3
	RTT109		RTT109
	SAS2		SAS2
			HHF1 WT
			HHF1 Y98A
			HHF1 Y98D
			HHF1 Y98F

8.3 *HHF1* WT and mutant genes inserted into YCplac22 tested in the phenotypic assay

Table 8.3 *HHF1* WT and mutant genes inserted into YCplac22

Vector	*HHF1* Insert
YCplac22	HHF1 WT
	HHF1 Y51A
	HHF1 E53A
	HHF1 Y98A
	HHF1 K5A
	HHF1 K5A Y98A
	HHF1 K8A
	HHF1 K8A Y98A

Vector	*HHF1* Insert
	HHF1 K12A
	HHF1 K12A Y98A
	HHF1 K16A
	HHF1 K16A Y98A
	HHF1 K20A
	HHF1 K20A Y98A
	HHF1 K5,8,12A
	HHF1 K5,8,12A Y98A
	HHF1 K5,8,12,16A
	HHF1 K5,8,12,16A Y98A
	HHF1 K5,8,12,20A
	HHF1 K5,8,12,20A Y98A

8.4 *HHT1* WT and mutant genes inserted into YCplac111 tested in the phenotypic assay

Table 8.4 *HHT1* WT and mutant genes inserted into YCplac111

Vector	*HHT1* Insert
YCplac111	HHT1 WT
	HHT1 K4A
	HHT1 K14A
	HHT1 T32A
	HHT1 T118A

8.5 *HHF1* WT and mutant genes inserted into YCplac111 tested in the phenotypic assay

Table 8.5 *HHF1* WT and mutant genes inserted into YCplac111

Vector	*HHF1* Insert
YCplac111	HHF1 WT
	HHF1 Y51A
	HHF1 Y72A
	HHF1 Y88A
	HHF1 Y98A
	HHF1 Y98D
	HHF1 Y98F
	HHF1 K5A
	HHF1 K5A Y98A
	HHF1 K5R
	HHF1 K5R Y98A
	HHF1 K8A
	HHF1 K8A Y98A

Vector	*HHF1* Insert
	HHF1 K8R
	HHF1 K8R Y98A
	HHF1 K12A
	HHF1 K12A Y98A
	HHF1 K12R
	HHF1 K12R Y98A
	HHF1 K16A
	HHF1 K16A Y98A
	HHF1 K16R
	HHF1 K16R Y98A
	HHF1 K20A
	HHF1 K20A Y98A
	HHF1 K20R
	HHF1 K20R Y98A
	HHF1 K8,16R
	HHF1 K8,16R Y98A
	HHF1 K5,8,12A
	HHF1 K5,8,12A Y98A
	HHF1 K5,8,12,16A
	HHF1 K5,8,12,16A Y98A
	HHF1 K5,8,12,20A
	HHF1 K5,8,12,20A Y98A
	HHF1 K5 K8,12,16,20R
	HHF1 K5 K8,12,16,20R Y98A
	HHF1 K8 K5,12,16,20R
	HHF1 K8 K5,12,16,20R Y98A
	HHF1 K12 K5,8,16,20R
	HHF1 K12 K5,8,16,20R Y98A
	HHF1 K16 K5,8,12,20R
	HHF1 K16 K5,8,12,20R Y98A
	HHF1 K20 K5,8,12,16R
	HHF1 K20 K5,8,12,16R Y98A
	HHF1 K5,8,12,16,20R
	HHF1 K5,8,12,16,20R Y98A

8.6 Genes inserted into YEplac181 tested in the phenotypic assay

Table 8.6 Genes inserted into YEplac181

Vector	Insert
YEplac181	ATC1
	CSE4
	CSE4+ELM1
	ELM1
	HPA2
	HPA3

Vector	Insert
	KAR4
	MCK1
	SKI8
	SPS4
	YAP1
	YHR151C
	YHR177W

8.7 Primers used for amplification of candidate suppressor genes in one-step PCR

Table 8.7 Primers used for amplification of candidate suppressor genes in one-step PCR

Gene	Primer name	Sequence
ATC1	5'ATC1pro-EcoRI	GCCGAATTCTGTCTGGTGTTCCGAC
	3'ATC1ter-SalI	GCCGTCGACACATTCGAAATAAGAAAG
HPA2	5'HPA2pro-HindIII	GCCAAGCTTCCAACTACAAGTAATG
	3'HPA2ter-BamHI	TGGCACGCTGTTAGGATCCA
HPA3	5'HPA3pro-EcoRI	GCCGAATTCAGGTTAGCATGCCGT
	3'HPA3ter-SalI	GCCGTCGACAACCTCTTCAAATTC
MCK1	5'MCK1pro-HindIII	GCCAAGCTTCCCTCTTTCCCAATTCA
	3'MCK1ter-BamHI	CTTCGAGGATCCCGAATCTG
YAP1	5'YAP1pro-HindIII	GCCAAGTTTATCGGAAACGGCAG
	3'YAP1ter-BamHI	GGATCCCAAGGTAGTTACGATACTC
YHR151C	5'YHR151Cpro-HindIII	GCCAAGGGCTGACCTCCTAAAAAC
	3'YHR151Cter-BamHI	GGATCCCTTCTCGTGTCGTTAAG

8.8 Preparation of DH5α *E. coli*

1. Inoculate one colony of DH5α *E. coli* in 15 ml LB+300 µl 1 M magnesium sulphate ($MgSO_4$) and incubate at 37°C for more than 12 h at 200 rpm.
2. Inoculate 5 ml of culture in two sterile 2 L flasks containing 500 ml LB+10 ml 1 M $MgSO_4$ each and incubate at 37°C until OD_{600} = 0.5–0.7.
3. Transfer cultures into ice chilled 200 ml bottles and leave on ice for 5 min to stop cells from growing.
4. Centrifuge at 8000 rpm for 15 min at 4°C, remove supernatant and resuspend cells in cold TFBI solution (30 ml/bottle), then combine contents.
5. Centrifuge at 8000 rpm for 10 min at 4°C, remove supernatant and resuspend cells in cold TFBII solution (20 ml/bottle), then prepare aliquots as required.
6. Store DH5α *E. coli* at -80°C.

7. Incubate streaked cells on LB, LB+ampicillin and LB+chloramphenicol at 37°C for more than 12 h to check for contamination.

Table 8.8 Preparation of TFBI and TFBII solutions

TFBI solution (pH5.8)		**TFBII solution (pH6.5)**	
Constituent	**Amount**	**Constituent**	**Amount**
Potassium acetate (KOAc)	2.944 g	MOPS	1.047 g
Rubidium chloride (RbCl)	1.209 g	RbCl	0.605 g
Calcium chloride ($CaCl_2$)	1.47 g	$CaCl_2$	5.513 g
Manganese chloride ($MnCl_2$)	9.895 g	Deionised water	Top up to 300 ml
Deionised water	Top up to 600 ml	100 % Glycerol	75 ml
100 % Glycerol	150 ml	Deionised water	Top up to 450 ml
Deionised water	Top up to 850 ml	1 M Potassium hydroxide (KOH)	Adjust to pH6.5
1 M Acetic acid	Adjust to pH5.8	Deionised water	Top up to 500 ml
Deionised water	Top up to 1000 ml	Mix and autoclave	
Mix and autoclave			

8.9 Preparation of LB media

Table 8.9 Preparation of LB media

Constituent	**Amount**
Tryptone	10 g
Yeast extract	5 g
Sodium chloride (NaCl)	5 g
5 N Sodium hydroxide (NaOH)	Adjust to pH7.0

1. For broth, add deionised water to final volume of 1 L, stir till homogeneous and autoclave.
2. For plate, add deionised water to volume of 500 ml and stir till homogeneous. In a separate bottle, measure 15 g/L Bacto Agar and add deionised water to volume of 500 ml. Autoclave, cool at 55°C to prevent solidification of agar and mix the contents of both bottles.
3. For LB+ampicillin, add 2 ml Amp 1000X stock (2.5 g Amp in 50 ml sterile water) to autoclaved 1 L LB media.
4. For LB+chloramphenicol, add 4 ml Chl 500X stock (2.5 g Chl in 250 ml 100 % EtOH) to autoclaved 1 L LB media.

8.10 Preparation of DH10β *E. coli*

1. Inoculate one colony of DH10β *E. coli* in 10 ml LB and incubate at 37°C for more than 12 h at 200 rpm.
2. Inoculate 5 ml of culture in two sterile 2 L flasks containing 500 ml LB each and incubate at 37°C until OD_{600} = 0.5–0.7.
3. Transfer cultures into ice chilled 200 ml bottles and leave on ice for 15 min to stop cells from growing.
4. Centrifuge at 8000 rpm for 5 min at 4°C, remove supernatant and resuspend cells in 5 ml ice cold sterile water, then top up with 150 ml ice cold sterile water.
5. Centrifuge at 8000 rpm for 5 min at 4°C, remove supernatant and resuspend cells in 5 ml ice cold sterile water, then combine contents and top up with 150 ml ice cold sterile water.
6. Centrifuge at 8000 rpm for 5 min at 4°C, remove supernatant and resuspend cells in 100 ml ice cold 10 % glycerol.
7. Centrifuge at 8000 rpm for 5 min at 4°C, remove supernatant and resuspend cells in equal volume ice cold 10 % glycerol, then prepare aliquots as required.
8. Store DH10β *E. coli* at -80°C.
9. Incubate streaked cells on LB, LB+ampicillin and LB+chloramphenicol at 37°C for more than 12 h to check for contamination.

8.11 Preparation of miniprep solutions

Table 8.10 Preparation of miniprep solution I (cell suspension buffer)

Constituent	**Amount**
1 M Tris-HCl (pH7.5)	25 ml
0.5 M Ethylenediaminetetraacetic acid (EDTA) (pH8.0)	10 ml
Deionised water	465 ml
Mix and autoclave	
10 μg/ml RNase A	25 mg to be added after autoclaving

Table 8.11 Preparation of miniprep solution II (cell lysis buffer)

Constituent	**Amount**
Sterile water	430 ml
5 N NaOH	20 ml
10 % SDS	50 ml
Do not autoclave and add in the above order to prevent precipitation	

Table 8.12 Preparation of miniprep solution III (cell neutralisation buffer)

Constituent	Amount
KOAc	65 g
Deionised water	Top up to 200 ml
100 % Acetic acid	Adjust to pH4.8
Deionised water	Top up to 500 ml
Mix and autoclave	

8.12 Preparation of 10X loading dye

Table 8.13 Preparation of 10X loading dye

Constituent	Amount
100 % Glycerol	550 µl
0.5 M EDTA (pH8.0)	200 µl
1 % Bromophenol blue (BPB)	250 µl

8.13 Preparation of yeast extract peptone dextrose adenine (YPDA)

Table 8.14 Preparation of YPDA

Constituent	Amount
Yeast extract	10 g
Peptone	20 g
Glucose	20 g
Adenine	0.04 g

1. For broth, add deionised water to final volume of 1 L, stir till homogeneous and autoclave.
2. For plate, add deionised water to volume of 500 ml and stir till homogeneous. In a separate bottle, measure 15 g/L Bacto Agar and add deionised water to volume of 500 ml. Autoclave, cool at 55°C to prevent solidification of agar and mix the contents of both bottles.

8.14 Preparation of glucose/galactose complete or selective media

Table 8.15 Preparation of glucose/galactose media

Constituent	Amount
Glucose/galactose	20 g
Yeast nitrogen base	7 g
Amino acid premix (composition varies for different selective media)	0.7 g

1. For broth, add deionised water to final volume of 1 L, stir till homogeneous and autoclave.
2. For plate, add deionised water to volume of 500 ml and stir till homogeneous. In a separate bottle, measure 15 g/L Bacto Agar and add deionised water to volume of 500 ml. Autoclave, cool at 55°C to prevent solidification of agar and mix the contents of both bottles.
3. For media containing 5-fluoro-orotic acid (5-FOA), add 0.85 g 5-FOA per 1 L media and filter sterilise, instead of autoclaving.
4. For media containing 3-amino-1,2,4-triazole (3-AT, Sigma-Aldrich), add 3-AT powder as follows per 500 ml media and filter sterilise, instead of autoclaving.
    a. 10 mM AT: 0.420 g 3-AT powder
    b. 50 mM AT: 2.102 g 3-AT powder
    c. 100 mM AT: 4.204 g 3-AT powder
5. For media containing Antimycin A (AA, Merck), add 1 ml AA stock per 1 L media after autoclaving, where the AA stock is prepared by adding 1 mg AA to 1 ml 100 % ethanol.
6. For media containing copper sulphate ($CuSO_4$), add 1 ml 100 mM $CuSO_4$ stock per 1 L media after autoclaving.

8.15 Preparation of 0.1 M LiAc

Table 8.16 Preparation of 0.1 M LiAc

Constituent	**Amount**
1 M LiAc	5 ml
10X TE buffer	5 ml
Sterile water	40 ml

1. For 1 M LiAc stock, add 51 g LiAc to 500 ml deionised water and autoclave.
2. For 10X TE buffer stock, add 50 ml 1 M Tris-HCl (pH7.5) and 10 ml 0.5 M EDTA (pH8.0) to 440 ml deionised water and autoclave.

8.16 Preparation of 40 % PEG

Table 8.17 Preparation of 40 % PEG

Constituent	**Amount**
50 % PEG	40 ml
1 M LiAc	5 ml
10X TE Buffer	5 ml

1. For 50 % PEG stock, add 250 g PEG to 500 ml deionised water and autoclave.

8.17 Preparation of yeast breaking buffer

Table 8.18 Preparation of yeast breaking buffer

Constituent	**Amount**
Triton X-100	10 ml
10 % SDS	50 ml
5 M NaCl	10 ml
1 M Tris-HCl (pH8.0)	5 ml
0.5 M EDTA (pH8.0)	1 ml
Deionised water	Top up to 500 ml
Mix and autoclave	

8.18 Preparation of FA gel solutions

Table 8.19 Preparation of 10X FA gel buffer

Constituent	**Amount**
3-[N-morpholino]propanesulfonic acid (MOPS)	83.704 g
EDTA	2.9224 g
NaAc	8.203 g
RNase-free water	Top up to 1 L
Mix and dissolve completely	

Table 8.20 Preparation of 1X FA gel running buffer

Constituent	**Amount**
10X FA gel buffer	100 ml
37 % formaldehyde	20 ml
RNase-free water	880 ml

8.19 Preparation of SDS polyacrylamide denaturing gel

Table 8.21 Preparation of 4 % stacking gel

Constituent	**Amount for two gels**
Sterile water	4.5 ml
30 % Acrylamide/Bis-acrylamide, 29:1	1.0 ml
0.5 M Tris HCl (pH6.8)	1.875 ml
10 % SDS	75 µl
10 % ammonium persulphate (APS)	75 µl (added last to avoid premature solidification)
N,N,N',N'-tetramethyl-1,2-diaminoethane (TEMED)	7.5 µl (added last to avoid premature solidification)

Table 8.22 Preparation of resolving gels of varying percentages

Constituent	**Amount for two gels**		
	10 % gel	**12 % gel**	**18 % gel**
Sterile water	8.0 ml	6.6 ml	2.6 ml
30 % Acrylamide/Bis-acrylamide, 29:1	6.6 ml	8.0 ml	12.0 ml
1.5 M Tris HCl (pH8.8)	5.0 ml	5.0 ml	5.0 ml
10 % SDS	200 µl	200 µl	200 µl
10 % APS	200 µl	200 µl	200 µl
TEMED	8 µl	8 µl	8 µl

8.20 Preparation of 5X Western blot transfer buffer

Table 8.23 Preparation of 5X Western blot transfer buffer

Constituent	**Amount**
Tris	14.5 g
Glycine	72.5 g
10 % SDS	2.5 g
Sterile water	500 ml

8.21 Preparation of TBST

Table 8.24 Preparation of TBST

Constituent	**Amount**
1 M Tris-HCl (pH7.4)	100 ml
5 M NaCl	30 ml
10 % Tween-20	10 ml
Sterile water	860 ml
Mix and autoclave	

8.22 Preparation of Coomassie Blue staining solution and destaining solution

Table 8.25 Preparation of Coomassie Blue staining solution

Constituent	**Amount**
Sterile water	40 ml
Methanol	50 ml
Acetic acid	10 ml
Coomassie brilliant blue R-250	0.05 g

Table 8.26 Preparation of destaining solution

Constituent	**Amount**
Sterile water	225 ml
Methanol	225 ml
Acetic acid	50 ml

8.23 Preparation of yeast lysis buffer

Table 8.27 Preparation of yeast lysis buffer

Constituent	**Amount**
50 % NP40	1 ml
1 M KCl	25 ml
1 M Tris HCl (pH7.4)	50 ml
0.5 M EDTA (pH8.0)	1 ml
Deionised water	Top up to 500 ml
Mix and autoclave	

8.24 Preparation of pronase working buffer

Table 8.28 Preparation of pronase working buffer

Constituent	**Amount**
1 M Tris HCl (pH7.4)	5 ml
10 % SDS	2.5 ml
Sterile water	42.5 ml

8.25 Preparation of immunoprecipitation buffers

Table 8.29 Preparation of yeast lysis buffer with 0.5 M NaCl

Constituent	**Amount**
Yeast lysis buffer	45 ml
5 M NaCl	5 ml

Table 8.30 Preparation of ChIP wash buffer

Constituent	Amount
1 M Tris-HCl (pH7.5)	5 ml
1 M Lithium chloride (LiCl)	125 ml
50 % NP40	5 ml
50 % sodium deoxycholate	5 ml
Sterile water	360 ml

Table 8.31 Preparation of 1X TE buffer

Constituent	Amount
10X TE buffer	5 ml
Sterile water	45 ml

Table 8.32 Preparation of ChIP elution buffer

Constituent	Amount
1 M Tris-HCl (pH7.5)	25 ml
0.5 M EDTA (pH8.0)	10 ml
10 % SDS	50 ml
Sterile water	415 ml

8.26 Data for *HIS3* mRNA expression levels

Table 8.33 *HIS3* mRNA expression levels

Sample	*ACT1* average Ct	*HIS3* average Ct	ΔCt	$2^{(-\Delta Ct)}$	Sample:WT 0h	Standard deviation
WT 0h	20.90	24.32	3.42	0.09	1.00	0.00
WT 2h	20.43	21.85	1.41	0.38	4.03	-0.76
Y98A 0h	17.95	15.31	-2.64	6.22	0.97	-0.04
Y98A 2h	19.66	17.04	-2.63	6.18	0.97	-0.03
Y98A+Gcn5 0h	21.45	24.94	3.49	0.09	0.95	-0.43
Y98A+Gcn5 2h	22.03	24.01	1.98	0.25	2.72	0.62
Y98A+Hpa1 0h	21.10	24.04	2.94	0.13	1.40	0.23
Y98A+Hpa1 2h	20.49	23.15	2.66	0.16	1.70	-0.37
Y98A+Hpa2 0h	22.93	26.34	3.41	0.09	1.01	-1.28
Y98A+Hpa2 2h	25.09	27.65	2.56	0.17	1.82	-2.18
Y98A+Hpa3 0h	22.10	26.30	4.20	0.05	0.58	-0.27
Y98A+Hpa3 2h	20.90	24.15	3.26	0.10	1.12	0.69

8.27 Data for ImageJ quantification of the acetylation status of H4K8

Table 8.34 ImageJ quantification of the acetylation status of H4K8

Strain	H4K8	H4	H4K8:H4	Relative to WT 0h
WT 0h	14704.44	25406.87	0.58	1.00
WT 2h	20183.89	27883.77	0.72	1.25
Y98A 0h	17439.05	22156.97	0.79	1.36
Y98A 2h	20805.53	26513.14	0.78	1.36
Y98A+Gcn5 0h	17168.85	19707.21	0.87	1.51
Y98A+Gcn5 2h	21104.65	28462.42	0.74	1.28
Y98A+Gcn5 0h	29059.97	16250.39	1.79	3.09
Y98A+Gcn5 2h	33417.82	20567.92	1.62	2.81
Y98A+Hpa1 0h	28778.50	16236.39	1.77	3.06
Y98A+Hpa1 2h	27505.65	22223.05	1.24	2.14
Y98A+Hpa2 0h	30149.17	17703.87	1.70	2.94
Y98A+Hpa2 2h	27888.48	23496.84	1.19	2.05

8.28 Data for ImageJ quantification of the acetylation status of H4K16

Table 8.35 ImageJ quantification of the acetylation status of H4K16

Strain	H4K16	H4	H4K16:H4	Relative to WT 0h
WT 0h	7684.59	11150.49	0.69	1.00
WT 2h	9383.13	14595.85	0.64	0.93
Y98A 0h	7962.42	12121.95	0.66	0.95
Y98A 2h	1861.26	13820.56	0.13	0.20
Y98A+Gcn5 0h	9160.30	14820.02	0.62	0.90
Y98A+Gcn5 2h	7935.76	13870.68	0.57	0.83
Y98A+Gcn5 0h	22152.12	16545.68	1.34	1.94
Y98A+Gcn5 2h	22966.41	21957.41	1.05	1.52
Y98A+Hpa1 0h	19270.95	17053.22	1.13	1.64
Y98A+Hpa1 2h	21740.45	22986.05	0.95	1.37
Y98A+Hpa2 0h	23074.26	18250.87	1.26	1.83
Y98A+Hpa2 2h	22678.43	24592.97	0.92	1.34

8.29 Data for histone H4 occupancy at the *HIS3* locus

Table 8.36 Histone H4 occupancy at the *HIS3* promoter

Sample	Average input Ct	Average IP Ct	ΔCt	$2^{(\Delta Ct)}$	Input:IP	Percent IP	Percent $IP_{Antibody}$ − Percent $IP_{No\ antibody}$	Relative to WT 0h	Standard deviation
WT No-anti 0h	24.48583	34.21939	9.733552	851.3164	0.117465	0.002349			
WT No-anti 2h	22.31569	34.13365	11.81796	3610.446	0.027697	0.000554			
WT Anti-H4 0h	24.48583	20.14197	-4.34386	0.049246	2030.64	40.6128	40.61045	1	0
WT Anti-H4 2h	22.31569	20.10067	-2.21502	0.215383	464.2886	9.285771	9.285217	0.228641	-0.08435
Y98A No-anti 0h	21.22835	26.54073	5.312374	39.73598	2.516611	0.050332			
Y98A No-anti 2h	19.95098	26.12033	6.169351	71.97136	1.389442	0.027789			
Y98A Anti-H4 0h	21.22835	19.03168	-2.19667	0.21814	458.4202	9.168403	9.118071	0.224525	0.002244
Y98A Anti-H4 2h	19.95098	19.30529	-0.64568	0.639191	156.4478	3.128956	3.101167	0.076364	-0.00596
GCN5 No-anti 0h	17.22117	26.57127	9.350107	652.6235	0.153228	0.003065			
GCN5 No-anti 2h	16.95747	26.62518	9.667714	813.3395	0.12295	0.002459			
GCN5 Anti-H4 0h	17.22117	19.16543	1.944267	3.848422	25.98468	0.519694	0.516629	0.012722	-0.00461
GCN5 Anti-H4 2h	16.95747	19.19663	2.239166	4.721239	21.18088	0.423618	0.421159	0.010371	-0.00354

Table 8.37 Histone H4 occupancy at the *HIS3* ORF

Sample	Average input Ct	Average IP Ct	ΔCt	$2^{(\Delta Ct)}$	Input:IP	Percent IP	Percent $IP_{Antibody}$ − Percent $IP_{No\ antibody}$	Relative to WT 0h	Standard deviation
WT No-anti 0h	20.49403	30.28752	9.79349	887.4304	0.112685	0.002254			
WT No-anti 2h	19.84277	29.90104	10.05827	1066.207	0.09379	0.001876			
WT Anti-H4 0h	20.49403	20.06597	-0.42805	0.743263	134.5418	2.690837	2.688583	1	0
WT Anti-H4 2h	19.84277	19.72327	-0.1195	0.920506	108.6359	2.172718	2.170842	0.80743	-0.16289
Y98A No-anti 0h	21.49971	27.51937	6.019665	64.87833	1.541347	0.030827			
Y98A No-anti 2h	20.81645	26.45514	5.638699	49.82157	2.007163	0.040143			
Y98A Anti-H4 0h	21.49971	19.74371	-1.756	0.296068	337.7603	6.755207	6.72438	2.501087	0.075206
Y98A Anti-H4 2h	20.81645	19.59559	-1.22085	0.429029	233.0843	4.661686	4.621543	1.718951	-0.1669
GCN5 No-anti 0h	20.17221	27.38188	7.209668	148.0221	0.675575	0.013511			
GCN5 No-anti 2h	19.95154	27.6181	7.666557	203.1719	0.492194	0.009844			
GCN5 Anti-H4 0h	20.17221	20.46223	0.290023	1.222659	81.78893	1.635779	1.622267	0.603391	-0.13571
GCN5 Anti-H4 2h	19.95154	20.94799	0.996452	1.995088	50.1231	1.002462	0.992618	0.369198	-0.09283

8.30 Data for histone H4K16ac occupancy at the *HIS3* locus

Table 8.38 Histone H4K16ac occupancy at the *HIS3* promoter

Sample	Average input Ct	Average IP Ct	ΔCt	$2^{(\Delta Ct)}$	Input:IP	Percent IP	Percent $IP_{Antibody}$ − Percent $IP_{No\ antibody}$	Relative to WT 0h	Standard deviation
WT No-anti 0h	24.48583	34.21939	9.733552	851.3164	0.117465	0.002349			
WT No-anti 2h	22.31569	34.13365	11.81796	3610.446	0.027697	0.000554			
WT Anti-H4K16ac 0h	24.48583	21.64205	-2.84379	0.139295	717.902	14.35804	14.35569	1	0
WT Anti-H4K16ac 2h	22.31569	21.38774	-0.92795	0.525605	190.2569	3.805138	3.804584	0.265023	-0.08457
Y98A No-anti 0h	21.22835	26.54073	5.312374	39.73598	2.516611	0.050332			
Y98A No-anti 2h	19.95098	26.12033	6.169351	71.97136	1.389442	0.027789			
Y98A Anti-H4K16ac 0h	21.22835	17.54229	-3.68606	0.077694	1287.107	25.74214	25.69181	1.78966	-0.02616
Y98A Anti-H4K16ac 2h	19.95098	18.27348	-1.6775	0.312624	319.8728	6.397457	6.369668	0.443703	-0.02385
GCN5 No-anti 0h	17.22117	26.57127	9.350107	652.6235	0.153228	0.003065			
GCN5 No-anti 2h	16.95747	26.62518	9.667714	813.3395	0.12295	0.002459			
GCN5 Anti-H4K16ac 0h	17.22117	16.23812	-0.98305	0.505909	197.6639	3.953278	3.950213	0.275167	-0.07879
GCN5 Anti-H4K16ac 2h	16.95747	17.55092	0.593452	1.508853	66.27553	1.325511	1.323052	0.092162	-0.02175

Table 8.39 Histone H4K16ac occupancy at the *HIS3* ORF

Sample	Average input Ct	Average IP Ct	ΔCt	$2^{(\Delta Ct)}$	Input:IP	Percent IP	Percent $IP_{Antibody}$ – Percent $IP_{No\ antibody}$	Relative to WT 0h	Standard deviation
WT No-anti 0h	20.49403	30.28752	9.79349	887.4304	0.112685	0.002254			
WT No-anti 2h	19.84277	29.90104	10.05827	1066.207	0.09379	0.001876			
WT Anti-H4K16ac 0h	20.49403	19.1831	-1.31092	0.403063	248.1005	4.96201	4.959756	1	0
WT Anti-H4K16ac 2h	19.84277	18.78865	-1.05411	0.481593	207.6443	4.152885	4.151009	0.836938	-0.2138
Y98A No-anti 0h	21.49971	27.51937	6.019665	64.87833	1.541347	0.030827			
Y98A No-anti 2h	20.81645	26.45514	5.638699	49.82157	2.007163	0.040143			
Y98A Anti-H4K16ac 0h	21.49971	18.39311	-3.1066	0.116096	861.3528	17.22706	17.19623	3.467152	-0.11441
Y98A Anti-H4K16ac 2h	20.81645	18.68371	-2.13274	0.228025	438.549	8.77098	8.730837	1.760336	-0.12225
GCN5 No-anti 0h	20.17221	27.38188	7.209668	148.0221	0.675575	0.013511			
GCN5 No-anti 2h	19.95154	27.6181	7.666557	203.1719	0.492194	0.009844			
GCN5 Anti-H4K16ac 0h	20.17221	18.43269	-1.73952	0.299469	333.9244	6.678489	6.664977	1.343812	-0.26255
GCN5 Anti-H4K16ac 2h	19.95154	19.50031	-0.45123	0.73142	136.7204	2.734408	2.724564	0.549334	-0.12389

8.31 Data for Gcn5 occupancy at the *HIS3* locus

Table 8.40 Gcn5 occupancy at the *HIS3* promoter

Sample	Average input Ct	Average IP Ct	ΔCt	$2^{(\Delta Ct)}$	Input:IP	Percent IP	Percent $IP_{Antibody}$ − Percent $IP_{No\ antibody}$	Relative to WT 0h	Standard deviation
WT No-anti 0h	24.48583	34.21939	9.733552	851.3164	0.117465	0.002349			
WT No-anti 2h	22.31569	34.13365	11.81796	3610.446	0.027697	0.000554			
WT Anti-GCN5 0h	19.79887	25.86331	6.064439	66.92338	1.494246	0.029885	0.027536	1	0
WT Anti-GCN5 2h	18.93322	24.11087	5.177644	36.19313	2.762955	0.055259	0.054705	1.986705	0.370749
Y98A No-anti 0h	21.22835	26.54073	5.312374	39.73598	2.516611	0.050332			
Y98A No-anti 2h	19.95098	26.12033	6.169351	71.97136	1.389442	0.027789			
Y98A Anti-GCN5 0h	21.22835	23.85655	2.628202	6.182552	16.17455	0.323491	0.273159	9.920199	-3.63899
Y98A Anti-GCN5 2h	19.95098	23.99014	4.039164	16.44029	6.082619	0.121652	0.093864	3.408805	-0.88326
GCN5 No-anti 0h	17.22117	26.57127	9.350107	652.6235	0.153228	0.003065			
GCN5 No-anti 2h	16.95747	26.62518	9.667714	813.3395	0.12295	0.002459			
GCN5 Anti-GCN5 0h	17.22117	23.00379	5.782619	55.04805	1.816595	0.036332	0.033267	1.208157	-0.4688
GCN5 Anti-GCN5 2h	16.95747	22.47738	5.519915	45.88385	2.179416	0.043588	0.041129	1.493677	-0.36303

Table 8.41 Gcn5 occupancy at the *HIS3* ORF

Sample	Average input Ct	Average IP Ct	ΔCt	$2^{(\Delta Ct)}$	Input:IP	Percent IP	Percent $IP_{Antibody}$ – Percent $IP_{No\ antibody}$	Relative to WT 0h	Standard deviation
WT No-anti 0h	20.49403	30.28752	9.79349	887.4304	0.112685	0.002254			
WT No-anti 2h	19.84277	29.90104	10.05827	1066.207	0.09379	0.001876			
WT Anti-GCN5 0h	20.77447	26.87399	6.09952	68.57067	1.458349	0.029167	0.026913	1	0
WT Anti-GCN5 2h	20.3071	25.79346	5.486358	44.82893	2.230703	0.044614	0.042738	1.587998	0.187031
Y98A No-anti 0h	21.49971	27.51937	6.019665	64.87833	1.541347	0.030827			
Y98A No-anti 2h	20.81645	26.45514	5.638699	49.82157	2.007163	0.040143			
Y98A Anti-GCN5 0h	21.49971	25.65468	4.154966	17.81432	5.613461	0.112269	0.081442	3.026099	0.00052
Y98A Anti-GCN5 2h	20.81645	25.59816	4.781715	27.50678	3.635467	0.072709	0.032566	1.210037	0.060559
GCN5 No-anti 0h	20.17221	27.38188	7.209668	148.0221	0.675575	0.013511			
GCN5 No-anti 2h	19.95154	27.6181	7.666557	203.1719	0.492194	0.009844			
GCN5 Anti-GCN5 0h	20.17221	24.72523	4.553017	23.47441	4.259957	0.085199	0.071688	2.663652	-0.67955
GCN5 Anti-GCN5 2h	19.95154	24.91622	4.964678	31.22604	3.202455	0.064049	0.054205	2.014069	-0.44266